Technical Report CHL-99-21
December 1999

US Army Corps of Engineers
Engineer Research and Development Center

Use and Application of the Empirical Simulation Technique: User's Guide

by Norman W. Scheffner, James E. Clausner, Adele Militello, ERDC
Leon E. Borgman, University of Wyoming
Billy L. Edge, Texas A&M University
Peter J. Grace, Jacksonville District

Prepared for Headquarters, U.S. Army Corps of Engineers

The contents of this report are not to be used for advertising, publication, or promotional purposes. Citation of trade names does not constitute an official endorsement or approval of the use of such commercial products.

The findings of this report are not to be construed as an official Department of the Army position, unless so designated by other authorized documents.

Technical Report CHL-99-21
December 1999

Use and Application of the Empirical Simulation Technique: User's Guide

by Norman W. Scheffner, James E. Clausner, Adele Militello

Coastal and Hydraulics Laboratory
U.S. Army Engineer Research and Development Center
3909 Halls Ferry Road
Vicksburg, MS 39180-6199

Leon E. Borgman

University of Wyoming
Laramie, WY 32070

Billy L. Edge

Texas A&M University
College Station, TX 77843-3136

Peter J. Grace

U.S. Army Engineer District, Jacksonville
P.O. Box 4970
Jacksonville, FL 32202-0019

Final report

Prepared for U.S. Army Corps of Engineers
Washington, DC 20314-1000

Army Engineer Research and Development Center Cataloging-in-Publication Data

Use and application of the empirical simulation technique : user's guide / by Norman W. Scheffner ... [et. al] ; prepared for U.S. Army Corps of Engineers.
189 p. : ill. ; 28 cm. — (Technical report ; CHL-99-21)
Includes bibliographic references.
1. Simulation methods — Guidebooks. 2. Storm surges — Environmental aspects —Simulation methods. 3. Stochastic analysis. 4. Frequency spectra. I. Scheffner, Norman W. II. United States. Army. Corps of Engineers. III. U.S. Army Engineer Research and Development Center. IV. Coastal and Hydraulics Laboratory (U.S.) V. Series: ERDC/CHL TR ; 99-21.
TA7 E8 no.ERDC/CHL TR-99-21

Contents

List of Figures

List of Tables

Preface

The Empirical Simulation Technique (EST) described in this report was first developed for application to a storm-surge study for the U.S. Army Engineer District, Mobile. Enhancements to the methodology funded through the Dredging Research Program resulted in the application of the EST to a variety of reimbursable study applications. Although the EST has been extensively applied, no systematic verification of the model and its internal procedures had been conducted, and a user's manual describing theory and application had not been written. Completion of these two tasks has been made possible through authorization and funding under Work Unit 32971, "Frequency Analysis of Storm Processes" of the Coastal Navigation Hydrodynamics Research Program. This research program is sponsored by the Headquarters, U.S. Army Corps of Engineers. Administrative responsibility is assigned to the U.S. Army Engineer Research and Development Center (ERDC) Coastal and Hydraulics Laboratory (CHL), Vicksburg, MS.

General supervision was provided by Dr. James R. Houston and Mr. Charles C. Calhoun, Jr. (retired), Director and Assistant Director, respectively, of CHL. Direct supervision of the project was provided by Mr. H. Lee Butler (retired), Chief of the Research Division, Coastal Engineering Research Center (CERC). CERC and the Hydraulics Laboratory merged in October 1996 to form the CHL.

This report was written by Dr. Norman W. Scheffner, CHL, and Dr. Leon E. Borgman, University of Wyoming, Laramie, WY. Example applications were written by Mr. James E. Clausner, Dr. Adele Militello, and Dr. Scheffner, all of CHL; Dr. Billy L. Edge, Texas A&M University, College Station, TX; and Mr. Peter J. Grace, U.S. Army Engineer District, Jacksonville.

Additional information on this report and the supporting software can be obtained from Ms. Carolyn M. Holmes or Mr. Robert Ray Bottin, Program Managers of the Coastal Navigation Hydrodynamics Research Program, at 601-634-2025 or Dr. Norman W. Scheffner, Principal Investigator of Work Unit 32971, at 601-624-3220.

At the time of publication of this report, Dr. Lewis E. Link was Acting Director of ERDC, and COL Robin R. Cababa, EN, was Commander.

Summary

This report describes theory and implementation of the Empirical Simulation Technique (EST) procedure for simulating multiple life-cycle sequences of nondeterministic multiparameter systems such as storm events and their corresponding environmental impacts. The EST is based on a "Bootstrap" resampling-with-replacement, interpolation, and subsequent smoothing technique in which random sampling of a finite length database is used to generate a larger database. The only assumption is that future events will be statistically similar in magnitude and frequency to past events. The EST begins with an analysis of historical events that have impacted a specific locale. The selected database of events are then parameterized to define the characteristics of the event and the impacts of that event. Parameters that define the storm are referred to as input vectors. Response vectors define storm-related impacts such as surge elevation, inundation, shoreline/dune erosion, etc. These input and response vectors are then used as a basis for generating life-cycle simulations of storm-event activity with corresponding impacts.

Results of the multiple repetitions can be either directly input to an economics model or postprocessed to generate frequency-of-occurrence relationships. This report describes the latter, i.e., the postprocessing of multiple life-cycle simulations to compute frequency-of-occurrence relationships for storm effects such as coastal erosion and storm surge. Because multiple life-cycle scenarios are simulated through the EST, mean value frequencies are computed along with error estimates of deviation about the mean.

The EST is a generalized procedure applicable to any cyclic or frequency-related phenomena. However, this report describes only applications involving tropical and extratropical events as the source of periodic forcing. Because the approach is universally valid for any impact that can be related to periodic events (storm events in this case), five detailed examples are provided to describe application of the EST for various storm-related impacts. These include vertical erosion of subaqueous disposal mounds, dune and beach recession, maximum storm-surge elevation, combined storm surge and runup on beaches, and maximum velocities associated with bridge pier scour. Each example provides detailed descriptions of the construction of input and response vector space and provides a summary of EST application and study results.

1 Introduction

This report describes theory and implementation of the Empirical Simulation Technique (EST), a life-cycle approach to frequency and error associated risk analysis. The EST procedures were originally developed under contract by the Coastal Engineering Research Center (CERC), presently the Coastal and Hydraulics Laboratory (CHL) of the U.S. Army Engineer Research and Development Center, Vicksburg, MS, to Professor Leon E. Borgman of the University of Wyoming, Laramie, WY. Universal applicability of the EST has been demonstrated through implementation to projects located along all coasts of the United States to develop frequency-of-occurrence relationships for storm-related impacts such as storm-surge elevation, vertical erosion of dredged material mounds, and horizontal recession of coastal beaches and dunes. As a result of this demonstrated capability, the EST has been adopted by the Headquarters, U.S. Army Corps of Engineers, Washington, DC, as the recommended approach to developing risk-based design criteria.

This report is divided into six chapters. The first chapter provides a brief introduction and is followed by a description of the theory of the general approach to provide an awareness and appreciation of the strength of the EST and the general applicability of it to any nondeterministic cyclic physical process in the second chapter. The third chapter of the report describes some developmental history of the procedure and describes in detail the internal procedures of the model. The fourth chapter provides general guidance on implementation of the approach to any site-specific problem, to include necessary input and appropriate data sources. In Chapter 5, detailed case examples of model application are described to demonstrate typical case studies employing the methodology. Finally, a summary and conclusions are provided in Chapter 6.

2 Generalized Theory of the EST

The EST is a statistical procedure for simulating life-cycle time sequences of nondeterministic multiparameter systems. Any natural process for which some temporal cycle can be assigned is a candidate application of the EST. Potential examples extend from studies involving return periods of days to years, i.e., diurnal variability in surface elevation or temperature to variability of storm frequency and intensity. The primary application of the EST presented in this report deals with impacts of tropical and extratropical storm events. Although the forcing is primarily limited to storm events, the impacts can be any damage or effect caused by the passage of the storm. For example, studies have been conducted that address storm impacts such as subaqueous erosion of dredged material mounds, recession of coastal shorelines and dunes, and maximum surface elevations reached in back-bay regions as a result of storm overtopping of barrier islands. Recent applications have included rainfall-induced flooding associated with tropical- and extratropical-event-generated coastal surges.

In the following section, the basic principle of the EST is presented. In order to describe the advantages of the EST over other frequency analysis approaches, the EST is first contrasted to an alternative approach to frequency analysis, the Joint Probability Method (JPM). A comparison of the two approaches will be made for application to storm effects associated with hurricanes. This comparison is followed by a description of the EST.

Many past attempts to assign frequency relationships to periodic events are based on the assumption that the event can be parameterized and that the parameters are independent. Furthermore, it is often assumed that the probabilities of these underlying parameters can be modeled with empirical, or parametric, relationships. The joint probability of occurrence for a particular event is then computed as the product of the individual storm parameter probabilities via the assumed parametric relationships. This assumption is the primary basis of the JPM. An example application of the approach can be given for tropical storms. The assumption basic to the JPM is that the probability of occurrence of a given storm event can be written as the product of the probabilities corresponding to each storm parameter and, as stated above, that the probabilities for each parameter are independent. For example, tropical

storms are often described by five parameters. If the parameters are statistically independent, then the joint probability density function (pdf) for the five-dimensional set is the product of the individual pdfs, i.e.,

$$f = f_D\, f_R\, f_\theta\, f_v\, f_L \tag{1}$$

where f_D, f_R, etc., represent the pdf for the central pressure deficit D (far-field pressure p_n less central pressure p_0), radius to maximum winds R, azimuth of the storm track θ, forward speed of the eye of the storm V, and closest distance to landfall (with respect to some specified location) of the eye of the storm L.

The JPM has been widely used in the past for storm-surge analyses. However, the approach has two disadvantages. First, the method is based on a random combination of storm parameters that can produce hundreds of synthetic storm events. Each of these storm events is input to an appropriate storm model. Because hundreds of storms are involved in the convolution of storm parameters, the method requires a substantial amount of time and effort, i.e., a JPM analysis is time-consuming and costly.

A second disadvantage of the JPM is of a more basic nature; it assumes that storm parameters are independent (or partially dependent according to some parameterized relationship). This assumption is not entirely valid. For example, pressure deficit, maximum wind, and radius to maximum wind are not independent parameters. Therefore, a joint pdf based on assumed independence can lead to error in the computed joint pdf. The JPM also utilizes empirical relationships for specifying the pdf for each of the various storm parameters. These probability laws are specified with fixed formulas and, although the formulas are based on observations, are valid only in the average sense. Because many hurricane events do not behave according to the prescribed average relationships, synthetic storms may not act like actual storms and therefore may introduce a significant error in the intensity of the storm and therefore the corresponding probability of occurrence. For example, a hurricane with a large central pressure deficit and low maximum winds is not a realistic event because the two parameters are not independent.

EST Approach to Frequency Analysis

The EST was developed primarily to address the second disadvantage of the JPM because the parameters that describe tropical storm events are not independent, but are interrelated in some nonlinear sense. Because they are not independent, joint probability cannot be computed as the product of individual parameter probabilities. The EST utilizes observed and/or computed parameters associated with site-specific historical events as a basis for developing a methodology for generating multiple life-cycle simulations of storm activity and the effects associated with each simulated event. Contrary to the JPM, the technique does not rely on assumed parametric relationships but uses the joint probability relationships inherent in the local database. Therefore, in this approach, probabilities are site specific, do not depend on fixed parametric

relationships, and do not assume parameter independence. Thus, the EST is "distribution free" and nonparametric.

The EST is based on a "Bootstrap" resampling-with-replacement, interpolation, and subsequent smoothing technique in which a random sampling of a finite length database is used to generate a larger database. The only assumption is that future events will be statistically similar in magnitude and frequency to past events. The EST begins with an analysis of historical events that have impacted a specific locale. The selected database of events is then parameterized to define the characteristics of each event and the impacts of that event. Parameters that define the storm are referred to as input vectors. Response vectors define storm-related impacts such as inundation and shoreline/dune erosion. These input and response vectors are then used as a basis for generating life-cycle simulations of storm-event activity. Details of the approach follow.

Input vectors

Input vectors describe the physical characteristics of the storm event and the location of the event with respect to the area of interest. These values are defined as an N-dimensional vector space as follows:

$$\underline{v} = (v_1, v_2, v_3, \ldots\ldots, v_N) \tag{2}$$

For tropical events, appropriate vectors can include (a) the central pressure deficit, (b) the radius to maximum winds, (c) maximum wind velocity, (d) minimum distance from the eye of the storm to the location of interest, (e) forward speed of the eye, and (f) tidal phase during the event. Extratropical event input vectors can include (a) duration of event as measured by some threshold damage criteria, (b) associated wind wave heights and periods, and (c) tidal phase. It should be noted that input vectors are not limited to those described. Input vectors should be any physical attribute of the overall system that may affect the response of the system. For example, in some applications, rainfall and river stage should be included as input vectors since their values affect the computed distribution of high water within a basin. Examples given in Chapter 4 illustrate different applications of input vector space.

Response vectors

The second class of vectors describe any response that can be attributed to the passage of the storm. This M-dimensional space is defined as:

$$\underline{r} = (r_1, r_2, r_3, \ldots\ldots, r_M) \tag{3}$$

Tropical and extratropical responses can include parameters such as maximum surge elevation, shoreline erosion, and/or dune recession.

Although response vectors are related to input vectors

$$v \rightarrow r \tag{4}$$

the interrelationship is highly nonlinear and involves correlation relationships that cannot be directly defined, i.e., a nonparametric relationship. For example, in addition to storm input parameters, storm surge is a function of local bathymetry, shoreline slope and exposure, ocean currents, temperature, etc., as well as their spatial and temporal gradients. It is assumed, however, that these combined effects are reflected by the response vectors even though their individual contribution to the response is unknown.

Response vectors define storm effects such as maximum surge elevation, shoreline erosion, or dune recession. These parameters are usually not available from poststorm records at the spatial density required for a frequency analysis. Therefore, response vectors are generally computed via numerical models. For example, if the response of interest is maximum surge elevation, long-wave hydrodynamic models are coupled to tropical storm models or databases containing extratropical wind fields. If the damage of interest involves storm-related erosion, additional models are used that access the hydrodynamic model surge elevation and current hydrographs to compute, for example, berm/dune erosion. An example will subsequently be given for such a case.

The historical data for storms can be characterized as

$$[v_i ; i = 1, \ldots, I] \tag{5}$$

where I is the number of historical storm events. Events of the historical database v_i contain d_v-components such that

$$V_i = \Re^{d_v} \tag{6}$$

where $\Re^{d_v}$ denotes a d_v-dimensional space.

Ideally, there are an adequate number of historic event parameters to fill the d_v-dimensional vector space. An adequate number refers to both the number of events and the severity of events as measured by their descriptive parameters. If the number of historic events is sparse, then some event augmentation may be necessary. If the historic population contains redundant events, i.e., similar events with respect to input and response vector space, then some events may be omitted from the set of historic events. The methodology for developing a set of events for input to the EST is described below.

Introduce a "training set" of storm events to represent storms that have or could reasonably be expected to impact a particular location.

$$[v_j^* , j = 1, \ldots, J] \tag{7}$$

The set of v_j^* usually includes a representation of all historical events but may include storms that could have occurred—for example, a historical storm with a slightly altered path or increased/decreased radius to maximum wind. The propagation of each of these events will be modeled to compute event-specific response vectors.

EST Implementation

The goal of the EST is summarized as:

(1) given the following:
  (a) the historical data $[v_i \in \Re^{dv}; i = 1,...,I]$
  (b) the "training set" data $[v^*_j \in \Re^{dv}; j = 1,...,J]$ developed from the historic data set
  (c) the response vectors calculated from the training set $[r^*_j \in \Re^{dr}; j = 1,...,J]$

note: the EST has a capability to interpolate responses for any historical storms not in the training set computed from the responses of the training set $[r^*_k \in \Re^{dr}; k = 1,...,K]$

(2) produce N simulations of a T-year sequence of events, each with their associated input vectors $v^* \in \Re^{dv}$ and response vectors $r^* \in \Re^{dr}$.

Two criteria are required of the T-year sequence of events. The first criterion is that the individual events must be similar in behavior and magnitude to historical events, i.e., the interrelationships among the input and response vectors must be realistic. The second criterion is that the frequency of storm events in the future will remain the same as in the past. The following sections describe how these two criteria are preserved.

Storm consistency with past events

The first major assumption in the EST is that future events will be similar to past events. This criterion is maintained by ensuring that the input/response vectors for simulated events have similar values and joint probabilities to those of the training set of historical or historically based events. The simulation of realistic events is accounted for in the nearest neighbor interpolation, bootstrap, resampling technique developed by Borgman (Borgman et al. 1992). By using the training set as a basis for defining future events, unrealistic events are not included in the life cycle of events generated by the EST. Events that are output by the EST are similar to those in the training set with some degree of variability from the historic/historically based events. This variability is a function of the nearest neighbor; therefore, the deviation from historic conditions is limited to natural variability of the system.

The basic technique can be described in two dimensions as follows. Let X_1, X_2, X_3, ..., X_n be n independent, identically distributed random vectors (historic storm events), each having two components $[X_i = \{\underline{x}_i(1), \underline{x}_i(2)\}; i = 1,n]$. Each event X_i has a probability p_i as $1/n$; therefore, a cumulative probability relationship can be developed in which each storm event is assigned a segment of the total probability of 0 to 1. If each event has an equal probability, then each event is assigned a segment s_j such that $s_j \dashrightarrow X_j$. Therefore, each event occupies a fixed portion of the 0 to 1 probability space according to the total number of events in the training set as shown below.

$$\left[0 < s_1 \leq \frac{1}{n}\right]$$

.

$$\left[\frac{1}{n} < s_2 \leq \frac{2}{n}\right]$$

.

$$\left[\frac{2}{n} < s_3 \leq \frac{3}{n}\right]$$

. (8)

.

.

$$\left[\frac{n-1}{n} < s_n \leq .1\right]$$

A random number from 0 to 1 is selected to identify a storm event from the total storm population. The procedure is equivalent to drawing and replacing random samples from the full storm-event population.

The EST is not simply a resampling of historical events technique, but rather an approach intended to simulate the vector distribution contained in the training set database population. The EST approach is to select a sample storm based on a random number selection from 0 to 1 and then perform a random walk from the event X_i with x_1 and x_2 response vectors to/from the nearest neighbor vectors. The walk is based on independent uniform random numbers on (-1,1) and has the effect of simulating responses that are not identical to the historical events but are similar to events that have historically occurred.

The process can be summarized as follows. Select a specific storm event from the training set and proceed to the location in multidimensional input vector space corresponding to that event. From that location, perform a nearest neighbor random walk to define a new set of input vectors. This defines a new multidimensional input vector space that is different from that of the specific event initially selected but not substantially unlike it since it was developed from the random walk procedure starting from the selected event. This new input vector defines a new storm, similar to the original but with some variability in parameters. Finally, use this new input vector to interpolate a corresponding response.

Storm frequency

The second criterion to be satisfied is that the total number of storm events selected per year must be statistically similar to the number of historical events that have occurred at the area of concern. Given the mean frequency of storm events for a particular region, a Poisson distribution is used to determine the average number of expected events in a given year. For example, the Poisson distribution can be written in the following form:

$$Pr\ (s;\lambda) = \frac{\lambda^s\ e^{-\lambda}}{s!} \tag{9}$$

for $s = 0,1,2,3,...$ The probability $Pr(s;\lambda)$ defines the probability of having s events per year where λ is a measure of the historically based number of events per year.

Assume that for a particular location 32 tropical storms have occurred in a 100-year period. According to Equation 9, the frequency of events λ is 0.32. The random number selection of events begins by defining a Poisson distribution space from 0.0 to 1.0. For $\lambda = 0.32$, the number corresponding to $s = 0$ storms per year, $Pr(0,0.32)$ is 0.7261; thus, if a random number selection is greater than 0.0 and less than or equal to 0.7261, then no hurricanes would occur during that year of simulation. If the random number is between 0.7261 and 0.7261 + $Pr[1,0.32] = 0.7261 + 0.2324 = 0.9585$, one event is selected—two events for $0.9585 + 0.0372 = 0.9957$, etc. When one or more storms are indicated for a given year, they are randomly selected from the nearest neighbor interpolation technique described above.

Output of the EST program is multiple life-cycle simulations, i.e., N-repetitions of T-years of simulated storm-event responses. It is from these responses that frequency-of-occurrence relationships can be computed. Because EST output is of the form of multiple time-series simulations, postprocessing of output yields mean value frequency relationships with definable error estimates. The computational procedure followed is based on the generation of a cumulative distribution function corresponding to each of the T-year sequence of simulated data.

Risk-Based Frequency Analysis

The primary justification for applying the EST to a specific project is to generate risk-based frequency information relating the effectiveness and cost of the project with the level of protection provided. Construction in the past was based on design criteria for protection against the maximum probable event—a storm considered to be the most severe possible. As a result, structures were often overdesigned by a considerable amount and at a considerable cost because the design was based on a single storm with a negligible probability of occurrence. The design of coastal structures can no longer be based on some hypothetical "worst case" design event for which no frequency can be assigned because the approach is not economically viable. For example, cost/benefit ratios for probable maximum event-based designs are not often funded. Current practice is to evaluate design alternatives from an economics standpoint in which the probability of failure is considered for varying levels of protection.

The Corps of Engineers, as well as some local and Governmental agencies, have recognized the need to build structures that provide a realistic level of storm protection in order to make the project economically viable. Recently, the Corps has initiated the requirement for a risk-based analysis for evaluating all shore protection studies. Details of recent legislation can be found in Engineer Circular (EC) 1105-2-205 (U.S. Army Corps of Engineers (USACE) 1994). This requirement supersedes the design storm concept and requires a frequency analysis that not only provides mean value frequency estimates but also some measure of risk and uncertainty. The EST exactly satisfies this requirement and, for this reason, was specified as the approach to be applied for developing design criteria for shore protection structures.

The multiple life-cycle simulations produced by the EST can be used for developing design criteria in two approaches. In the first, the actual multiple time series are input to an economics model that computes coupled storm inundation, structure response, and associated economics. The model internally computes variability associated with the risk-based design. The other application, and the one described in detail by examples in this report, is the postprocessing of the multiple time series to generate single-response frequency relationships and associated variability. For the engineer, this analysis approach is generally used to assess the level of coastal protection afforded by some specific coastal design.

A detailed description of available economic models required of the first approach is not presented in this report. Instead, the methodology for postprocessing the life-cycle simulations to generate estimates of frequency and associated variability is presented. Therefore, in the following section, the procedures for computing mean value frequency-of-occurrence relationships from the N-repetitions of T-years of storm-event impact are presented along with an error analysis in the form of a standard deviation from the mean value. Finally, because coastal designs are often subject to both tropical and extratropical events, the mechanics for computing frequency relationships for combined storm types are presented.

Frequency-of-occurrence computations

Estimates of frequency of occurrence begin with a calculation of a cumulative distribution function (cdf) for the response vector of interest. Let $X_1, X_2, X_3, \ldots, X_n$ be n identically distributed random response variables with a cdf

$$F_x(x) = Pr[X \leq x] \tag{10}$$

where $Pr[\ ]$ represents the probability that the random variable X is less than or equal to some value x and $F_X(x)$ is the cumulative probability distribution function ranging from 0.0 to 1.0. The problem is to estimate the value of F_X without introducing some parametric relationship for probability. The following procedure is adopted because it makes use of the probability laws defined by the data and does not incorporate any prior assumptions concerning probability.

Assume a set of n observations of x data. The n values of x are first ranked in order of increasing size such that

$$x_{(1)} \leq x_{(2)} \leq x_{(3)} \leq \ldots \leq x_{(n)} \tag{11}$$

where the parentheses surrounding the subscript indicate that the data have been rank-ordered. The value $x_{(1)}$ is the smallest in the series and $x_{(n)}$ represents the largest. Let r denote the rank of the value $x_{(r)}$ such that rank 1 is the smallest and rank $r = n$ is the largest.

An empirical estimate of $F_X(x_{(r)})$, denoted by $\hat{F}_X(x_{(r)})$, is given by Gumbel (1954) (see also Borgman and Scheffner 1991 or Scheffner and Borgman 1992).

$$\hat{F}_x(x_{(r)}) = \frac{r}{(n+1)} \tag{12}$$

for $\{x_{(r)}, r = 1, 2, 3, \ldots, n\}$. This form of estimate allows for probabilities of future values of x to be less than the smallest observation $x_{(1)}$ with probability of $1/(n+1)$, and to be larger than the largest value $x_{(n)}$ also with probability $r/(n+1)$.

An example application of Equation 12 can be demonstrated for a set of 10 years of observed surface elevation data shown by year in Table 1. The rank ordered set of observations, the rank, and the cdf according to Equation 12 are shown in Table 2.

As can be seen in the table, this form of the cdf allows for values of x to be greater than the maximum or less than the minimum observed values in the historical database. A plot of the cumulative distribution function versus $x_{(r)}$ is shown in Figure 1. In the implementation of the EST, tail functions (Borgman and Scheffner 1991) are used to define the cdf for events larger than the largest

Table 1
Observed Yearly Data

Year	Elevation (ft), $x_{1,2,3,..10}$
1	3.2
2	3.5
3	8.0
4	1.0
5	10.5
6	5.9
7	8.6
8	4.1
9	2.3
10	7.5

Table 2
Rank Ordering, cdf Computation

$x_{(r)}$	Rank r	$F_X(x_{(r)})$
10.50	10	0.91
8.60	9	0.82
8.00	8	0.73
7.50	7	0.64
5.90	6	0.55
4.10	5	0.45
3.50	4	0.36
3.20	3	0.27
2.30	2	0.18
1.00	1	0.09

or smaller than the smallest observed event so that there is no discontinuity in the cdf.

The cdf as defined by Equation 12 and shown in Table 2 and Figure 1 is used to develop stage-frequency relationships in the following manner. Consider that the cdf for some storm impact corresponding to an n-year return period event can be determined from:

$$F\left(x_{(n)}\right) = 1 - \frac{1}{n} \tag{13}$$

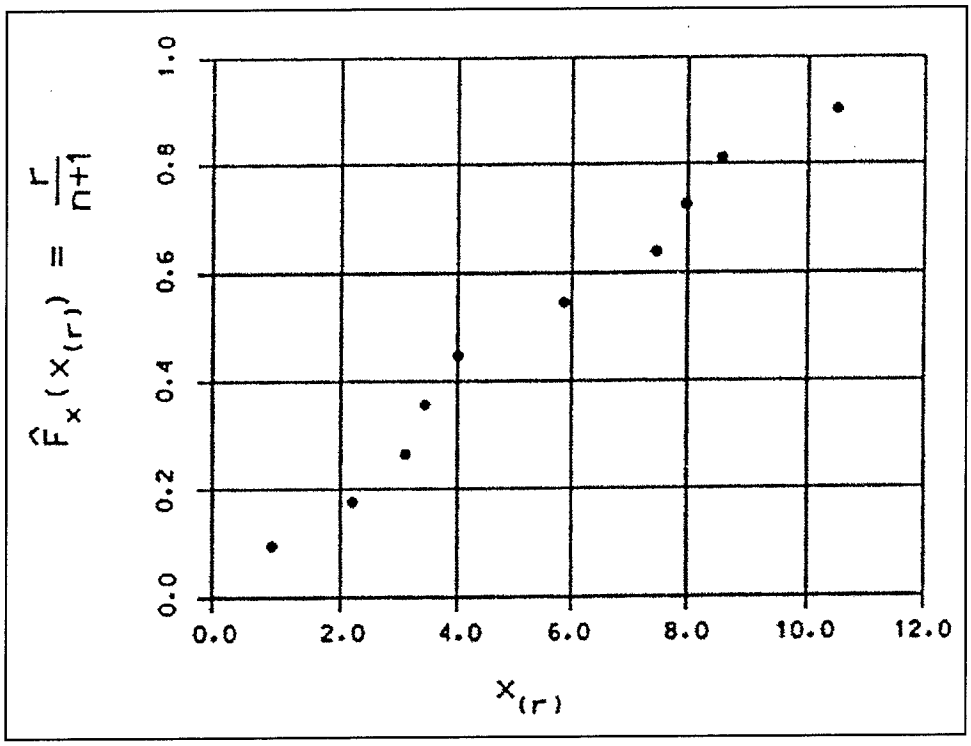

Figure 1. Cumulative distribution function, cdf

where $F(x_{(n)})$ is the simulated cdf for the n-year impact. Frequency-of-occurrence relationships are obtained by computing a simulated cdf for an n year event according to Equation 13 and, using that value for a cfd from Equation 12 and Table 2, linearly interpolating a stage. An example computation is shown in Table 3.

Table 3
Frequency-of-Occurrence Computation

n-year	$F(x_{(n)})$, n = 1,2,3,...10	$x_{(n)}$, n = 1,2,3,...10
1	0.00	-
2	0.50	5.00
3	0.67	7.67
4	0.75	8.13
5	0.80	8.47
6	0.83	8.81
7	0.86	9.44
8	0.88	9.87
9	0.89	10.08
10	0.90	10.29

Equations 12 and 13 are applied to each of the N-repetitions of T-years of storm events simulated via the EST. Therefore, there are N frequency-of-occurrence relationships generated. Then, for each return period year, a standard deviation, defined as:

$$\sigma = \sqrt{\left[(1/N) \sum_{n=1}^{n=N} (x_n - \bar{x})^2\right]} \tag{14}$$

(where bar x is the mean value), is computed to define an error band of ± one standard deviation corresponding to each mean value curve.

Combined tropical/extratropical frequency relationships

The calculation of frequency-of-occurrence relationships for combined tropical and extratropical events occurring within the same year begins with the assumption the tropical and extratropical events are independent. This relationship is made explicit by stating that the probability of both events occurring in a given year is equal to the product of the probability of each separate event occurring in the same year. For example,

$$F_{comb\ (x_{(n)})} = F_1\ (x_{(n)})\ F_2\ (x_{(n)}) \tag{15}$$

defines the probability of two independent n-year events occurring the same year.

Using the definition of Equation 13 for the cdf for an n-year event, Equation 15 can be written in terms of the return periods associated with either event as:

$$F_{comb} = F_1 F_2 = \left(1 - \frac{1}{R_1}\right)\left(1 - \frac{1}{R_2}\right) = 1 - \frac{1}{R_{comb}} \tag{16}$$

where $F_{comb}(x)$, $F_1(x)$, and $F_2(x)$ are the combined, tropical and extratropical event cdfs and $R_{comb}(x)$, $R_1(x)$, and $R_2(x)$ the respective return period in years.

Then the combined event return period $R_{comb}(x)$ for an n-year event can be written as

$$R_{comb}\ (x) = \frac{1}{\dfrac{1}{R_1(x)} + \dfrac{1}{R_2(x)} - \dfrac{1}{R_1(x)\ R_2(x)}} \tag{17}$$

where $R_{comb}(x)$ represents the return period associated with an n-year event, and the return period for an n-year tropical and extratropical event is R_1 and R_2.

Because the product of $R_1(x)$ and $R_2(x)$ is large with respect to R_1 or R_2, the relationship of Equation 17 can be approximated as

$$R_{comb}(x) = \frac{1}{\frac{1}{R_1(x)} + \frac{1}{R_2(x)}} \tag{18}$$

Frequency analysis summary

The procedures outlined above for a single response analysis for coastal designs have been applied to projects along all coasts of the United States and for a variety of applications. The approach has been shown to be accurate, easy to implement, and capable of generating design criteria not possible by conventional means. However, as with any numerical methodology, accurate results require accurate input. This section has described the general approach and philosophy of the EST, i.e., provide life-cycle simulations of periodic events based on historic or historically based data (input vectors) and associated impacts (response vectors). In the following section, a detailed description of the EST program is given. That section describes the specific parameters and procedures used to implement the generalized procedures described in this section.

3 Description of EST Implementation Mechanics

Empirical simulation is a computing technique that seeks to produce simulations of certain quantities directly from data of the same or related types without making assumptions concerning joint probability laws. The simulations are designed to imitate the real data in the sense that selected statistical properties are preserved. Insofar as possible, nonparametric (or distribution-free) statistical methods are used to avoid assumptions concerning joint probability law formulas and independence. The only exception to this in the EST program is that the storm events are taken as occurring as a Poisson process in the simulations.

Version 3.1 of the EST program largely uses kernel nonparametric regression procedures with the diameter of the kernel being based on the distance to a selected number of nearest neighbors in the vector space. The next version (4.1) will incorporate other options, including the Taylor-Thompson vector empirical simulation (Taylor 1989) and the MARS (multivariate adaptive regression splines) procedures (Friedman 1991). However, Version 3.1 is released now as a very much simplified and "cleaned up" version of the original program.

The original program (Version 1.1) was written under the pressure of deadlines for a particular immediate application. A number of possible options, such as stepwise linear regression, were written into the code but never tested and completed. The committee guiding the application decided that they did not wish to use those options, but also did not wish to take the time to clean up and remove the "fossil" code branches. The program worked quite well as long as only the well-tested options were designated. Also, it was felt desirable to let the program shake down, with each user inserting comments or improvements and modifications.

After the application was completed, Norman Scheffner at the Coastal Engineering Research Center (CERC), now part of the Coastal and Hydraulics Laboratory, incorporated a few significant improvements into the program (Version 2.1) and used it in a variety of applications. He developed substantial experience with successes (and a few defects) of the procedure. In 1993, CERC contracted with L. E. Borgman, Inc., through a subcontract with the University

of Wyoming (UW) for a very thorough 3-year study of the empirical simulation techniques and the creation of an improved and enhanced computer code. Three university faculty members (Leon Borgman, Richard Anderson-Sprecher, and Ken Gerow), together with Norman Scheffner from CERC, were involved in the 3-year study.

Version 3.1 is the code from the study at the middle of the third year. Version 4.1 will include recommended enhancements and a thorough examination of the methods within the context of statistical literature.

Frame of Reference

The original program was motivated by the need to simulate realistically various quantities, such as flooding and coastal damage, that might be caused by future hurricanes. Later, the method was extended to treat extratropical storms, and plans are underway to study the inclusion of hydrological data such as rainfall and streamflow.

The basic input data consist of a vector of descriptive quantities for each historical storm. Each of these historical storms is often "multiplied" by assuming that the historical storm might just as easily have happened at other levels of astronomical tide. Thus, one might input each historical storm five times, each with a different tide level from the tidal cycle. The probability of the single historical storm is now divided up equally among all of its versions. If there were originally 50 actual historical storms, and five different tide levels were used for each, then there would now be 250 storms that "might have occurred."

The various responses in terms of coastal flooding and damage need to be estimated. This usually involves a very time-consuming and expensive modeling effort incorporating oceanwide finite element grids. Even with large computers, it is typically not cost effective to run each and every storm in the input set.

It is much more cost effective to carefully select a subset of the total augmented historical storm set as a "training set." The modeling effort is applied carefully to this "training set," and then the responses are interpolated for the remaining storms not modeled. In Version 3.1, the interpolation is performed with nearest neighbor-scaled, Gaussian kernel, nonparametric degression. The procedure can be indicated by the block diagram in Figure 2.

Sensitivity studies are necessary in this whole process. The size of the training set is constrained by cost (encouraging a smaller size) and interpolation accuracy (pushing for as large a set as possible). It is usually desirable to run a small training set and a larger training set through the interpolation process to evaluate the incremental improvement of accuracy with size.

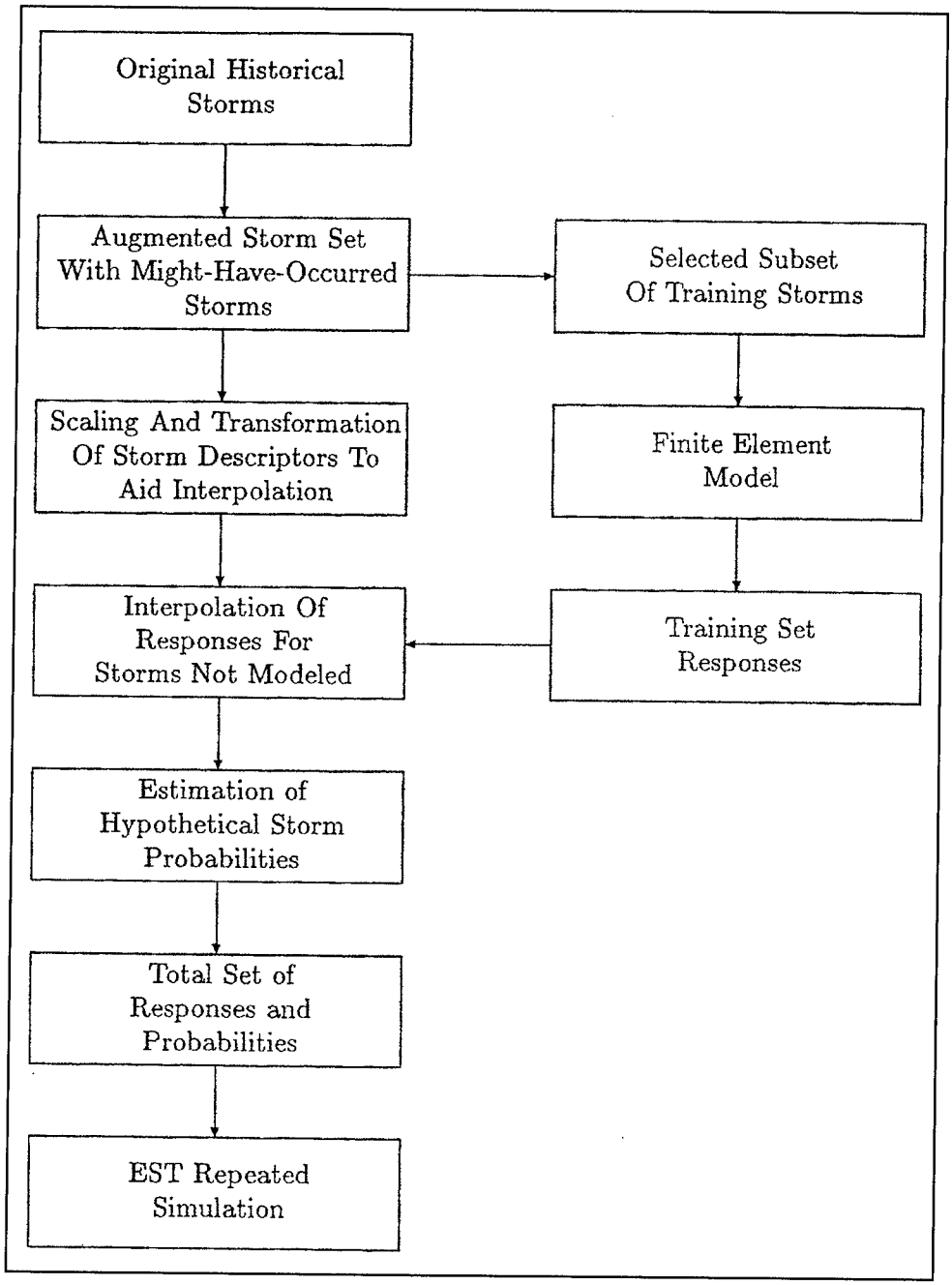

Figure 2. Overall procedure

Another useful procedure to estimate interpolation accuracy for a selected training set of storms is the "cross-validation" or "jackknife" method. In this technique, one storm (with model-computed responses) is selected out of the training set, and a new set of responses for it are interpolated from the responses of the remaining storms in the training set. The differences between the interpolated and model-based responses for that one storm are tabulated. Then, the process is repeated for each of the other storms in the training set. At termination, there is an error set for each of the training set storms that can be

interpreted as the error one would likely make in interpolating the nonmodeled storm responses.

Great accuracy of interpolation is not necessary for the simulations to preserve reasonably the statistical interrelationships of the original data. On the other hand, one does not want terribly "wild" responses to be produced. Version 4.1 will include the cross-validation as an option in the processing. Version 3.1 does not.

The scaling and transformation block in the last diagram has not been discussed up to now. It is often desirable to scale the input variables to have comparable magnitudes. A common technique used in factor analysis and principal component analysis is to subtract the variable mean from the variable and then divide the difference by the variable standard deviation. This is the method generally recommended for Version 3.1 of the program. (Please note that the responses are not scaled. Only the descriptors are treated this way.)

Occasionally, better interpolations are obtained if the logarithm of the variable is used instead of the value itself. This seems to happen when the variable is highly skewed in its range of values.

Another modification that seems to improve the interpolations sometimes is the insertion of entirely hypothetical storms that are not related to historical storms. The rationale here is that here may be "gaps" in the coverage of the vector space of storm descriptors where interpolations from far-away historical storms are questionable. A hypothetical storm could be placed into the "gap" and carried into the training set to "tie down" an intermediate response within the interpolation process.

The hypothetical storm does not have a natural probability of occurrence associated with it because of a historical history. If there are 250 storms augmented with tidal variation from 50 historical storms, it is natural to consider the probability of occurrence for each in the future as 1/250. If now two additional hypothetical storms are inserted, what should be assigned as their probability of occurrence? This is very close to the problem of how to estimate the probability density empirically from a data set. There is a great deal of study of density estimation in the statistical literature (Scott 1992). Kernel regression is the most common choice for use, although there is considerable discussion over the optimal shape for the kernel. In the absence of knowledge of the underlying probability model for the data, the Gaussian shape kernel is fairly successful. The width of the kernel is often adjusted by trial and error until the estimates appear reasonable. An alternative, which is used in Version 3.1 to estimate probabilities for hypothetical (nonhistorical) storms, is to base the width of the kernel on the distance of the domain location to the nearest three or four neighbors. This can proceed in a fairly automatic way without decisions by the software user.

Simple Example to Follow Through the Code

A very simple example will be followed through the flowchart shown in Figures 3, 4, and 5 to help the user gain an understanding of the process followed by the software. The example is intentionally smaller than desirable so that the steps and intermediate matrices can be printed into the text without using too much space. Table 4 gives the input data that will be used.

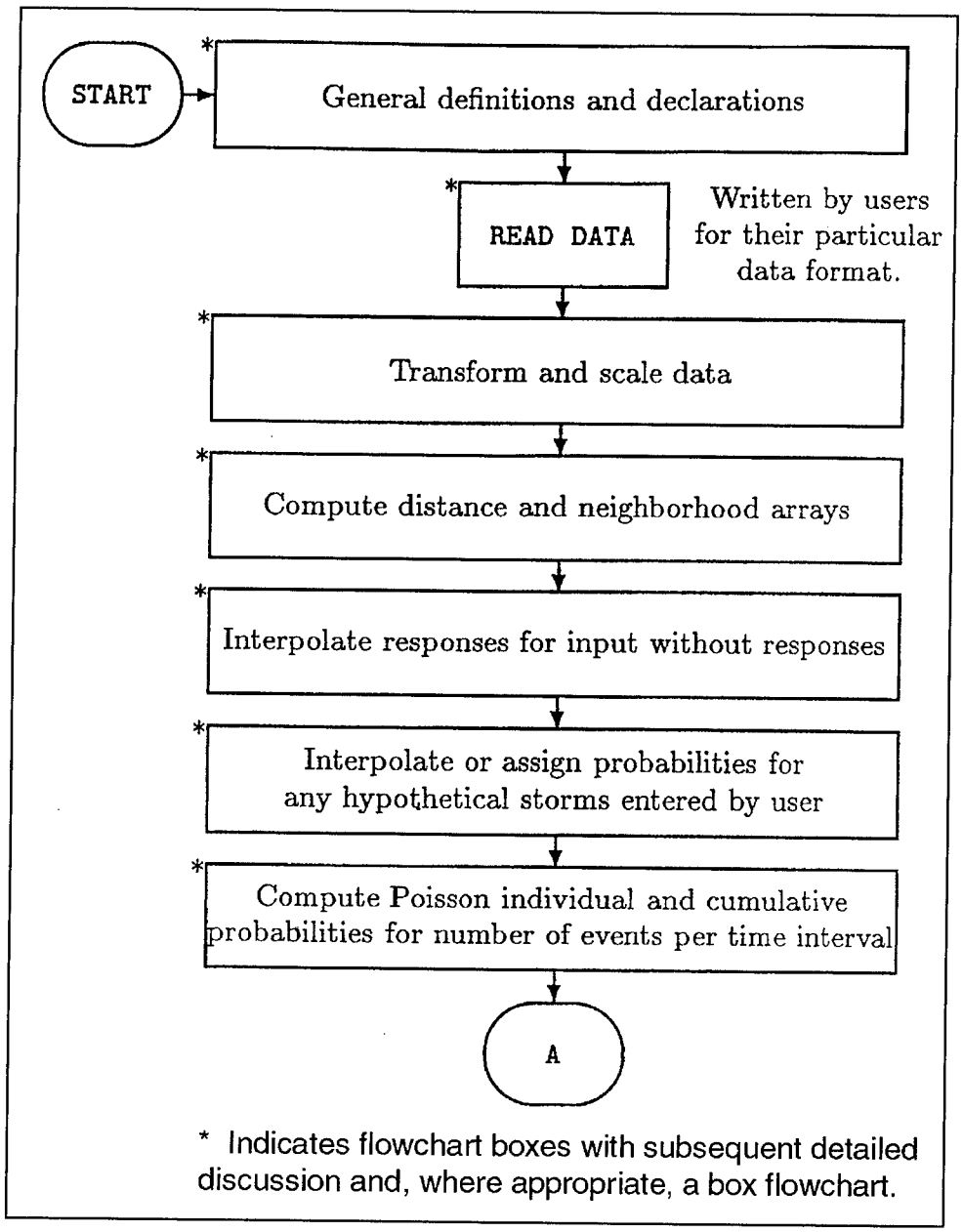

Figure 3. Preprocessing block

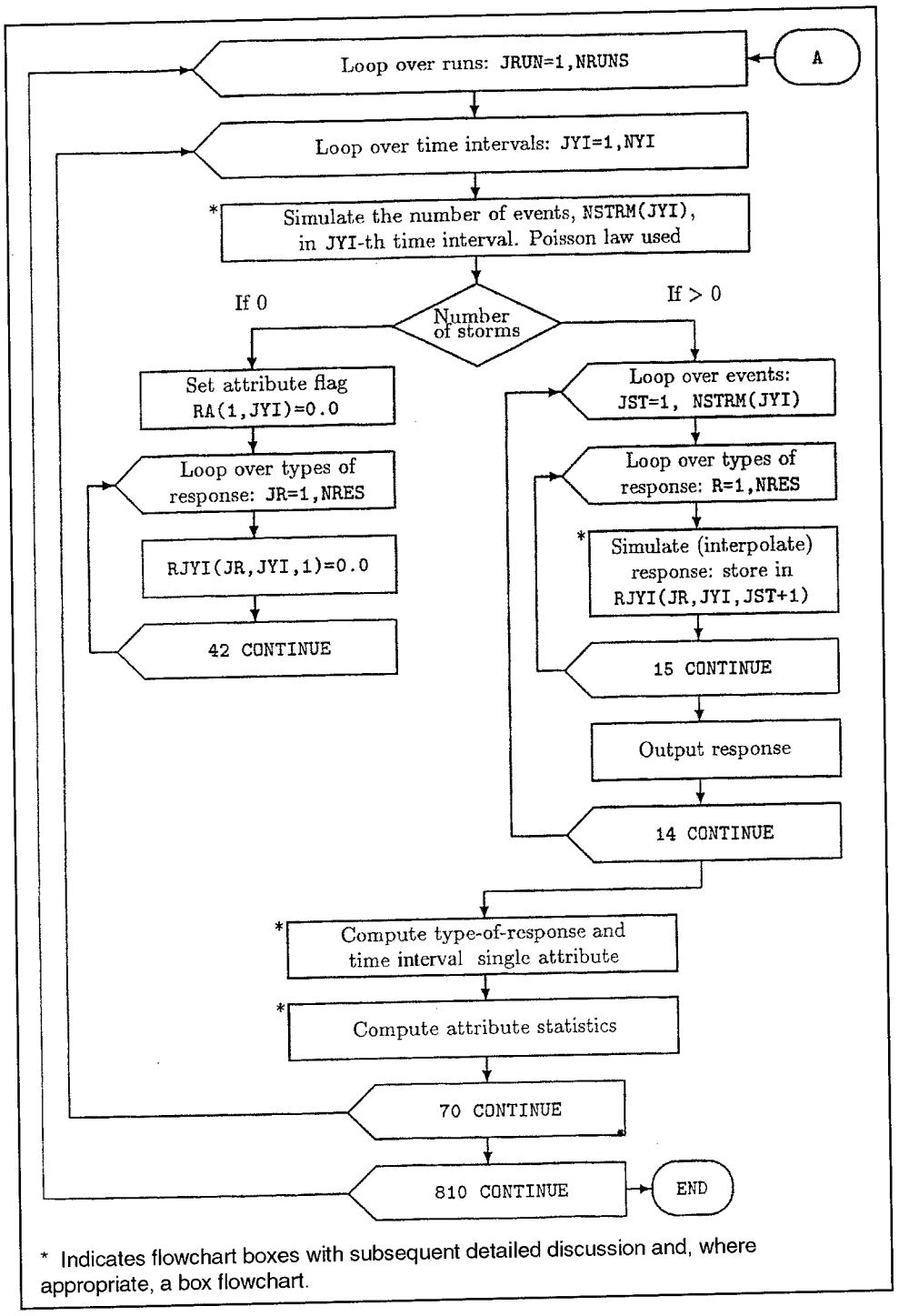

Figure 4. Simulation block

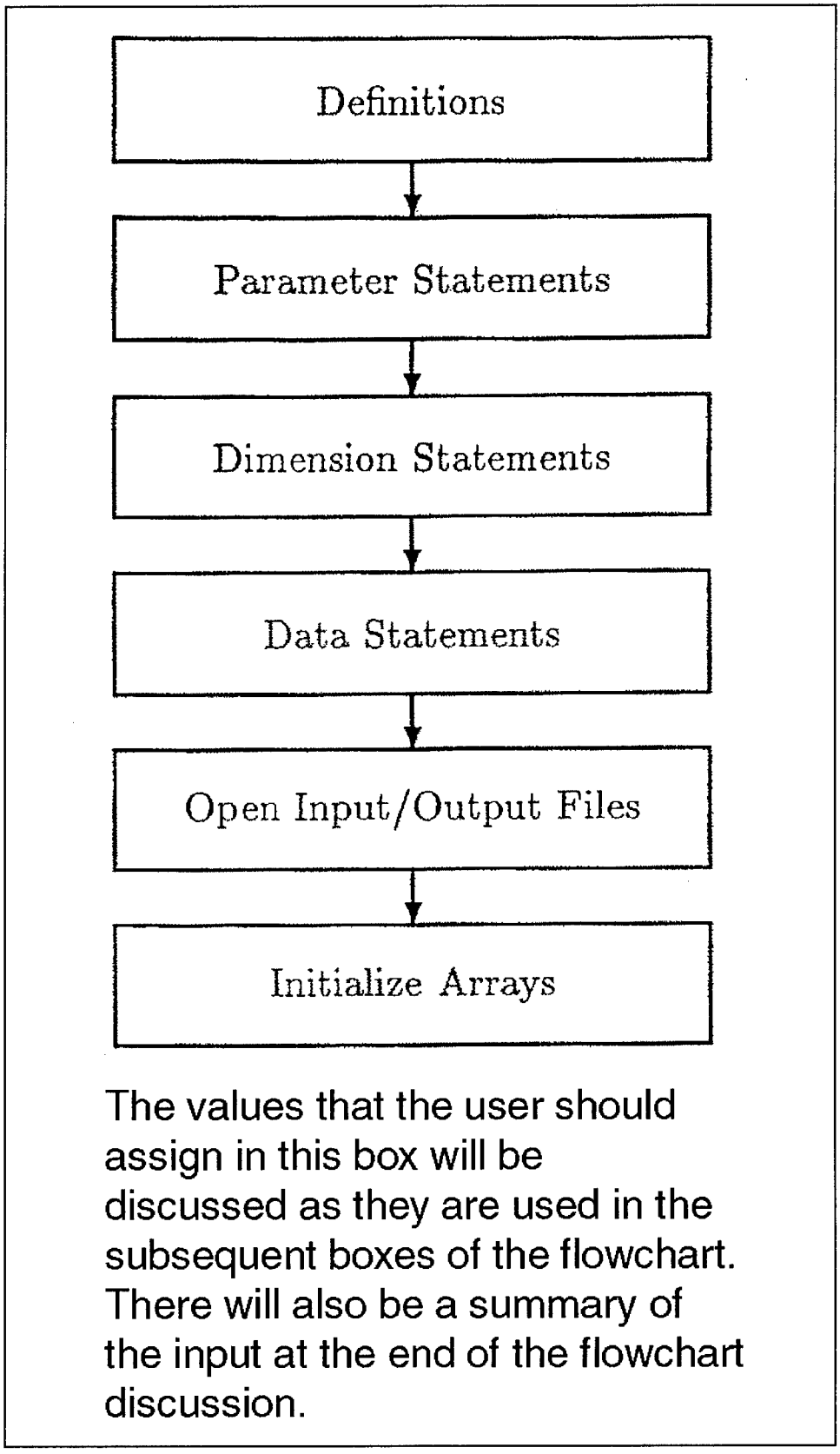

Figure 5. General definitions and declarations box

Table 4
Input Data for a Simple Example

IHIST	D1	D2	R
1.0000	337.5041	0.2443	3.5860
1.0000	412.5162	0.2663	11.4196
1.0000	372.8642	0.3415	7.2446
1.0000	62.2546	0.4558	-24.0012
1.0000	272.6218	0.0556	1.3265
1.0000	267.7060	0.1902	-3.1179
1.0000	331.7988	0.4123	3.7658
1.0000	248.8828	0.3582	-5.8324
0	299.7959	0.2729	-0.6269
0	460.6511	0.3414	16.6005
1.0000	384.7649	0.2022	
1.0000	326.8101	0.1979	
0	207.6511	0.3318	
0	292.9501	0.4516	
0	314.7981	0.3749	

In the table, the first column specifies whether the event is historical or not historical. Here there are 10 historical events in the subsequent computations; each of these events would be assigned an initial probability of 1/10. The five nonhistorical events will not have an initially assigned probability. In subsequent steps, the probabilities for both historical and nonhistorical storms will be readjusted so that all are assigned probabilities. The method for this will be discussed in later sections.

There are a few situations where nonhistorical events are treated and flagged as though they were historical storms. The most simple case for this would be the introduction of hypothetical storms (here storms are taken as the events), which are the same as the actual historical storm except that they are allowed to occur at alternate tide levels. If this is done for all historical storms for the same number of alternative tide levels for each storm, all the events, including the ones with alternate tides, can be flagged as IHIST=1.0, providing each tide level is believed to be equally likely to be associated with such a storm. If there are N original storms and k equally likely tide levels, including the tide level that actually occurred, then there would now be kN storms. These could be interpreted as being all equally likely to occur in the future so that the initial probability for each would be set at 1/(kN). This would happen automatically if IPFLAG is set to 1.0 for all of the storms, including the ones with the assigned

tide levels. If IPFLAG=2, the user is flagging the code that the probabilities for all storms were precomputed by the user and are read in with the other data as the vector PROB(I) for I=1,2,...,NSTOT. In this option, the value of IHIST can be anything, since the subsequent computations are unaffected by the value assigned. A full discussion of parameter settings and their effects on program control will be provided later.

The second and third columns, D1 and D2, are description variables (hereafter called descriptors). Only two descriptors are used for each event in this highly simplified problem. A more realistic problem would have 8 to 20 descriptors and, of course, a set of events much larger than 15.

The fourth column is a response variable that is regarded as being a function of the two descriptors. As the example shows, some historical and/or nonhistorical storms may not have precomputed values for the response.

In a real example, the computation of the response for a given event may involve a substantial amount of effort with finite element modeling. Considerable computer time may be required to obtain each response. Therefore, the code allows the response to be computed for a subset of all of the storms, called the "training set."

The training set is selected to span the domain space of descriptors as evenly as possible, so that the program can interpolate responses for the nontraining set events with reasonable accuracy. The basic interpolation method used here will be discussed later in connection with subroutine RTERP.

The example was restructured to a two-dimensional descriptor space so that graphical presentation of data and results would be possible. The responses are listed versus position in descriptor space in Figure 6. The events can be plotted in four classes:

a. Historical storms with responses *

b. Nonhistorical storms with responses +

c. Historical storms without responses x

d. Nonhistorical storms without responses o

The symbol used in Figure 6 for each class is given in the listing above. In the best possible situation, these would be a large enough list of historical storms so that hypothetical storms are unnecessary. It would also be possible to compute responses for every storm. Thus, all points in the figure would show * and all events would be historical with computed response.

In the real world of cost and time constraint, it is often impossible to compute a response for every storm. Also, for a given site, the historical storm data are very limited. Various tricks such as augmenting the real data with "might have

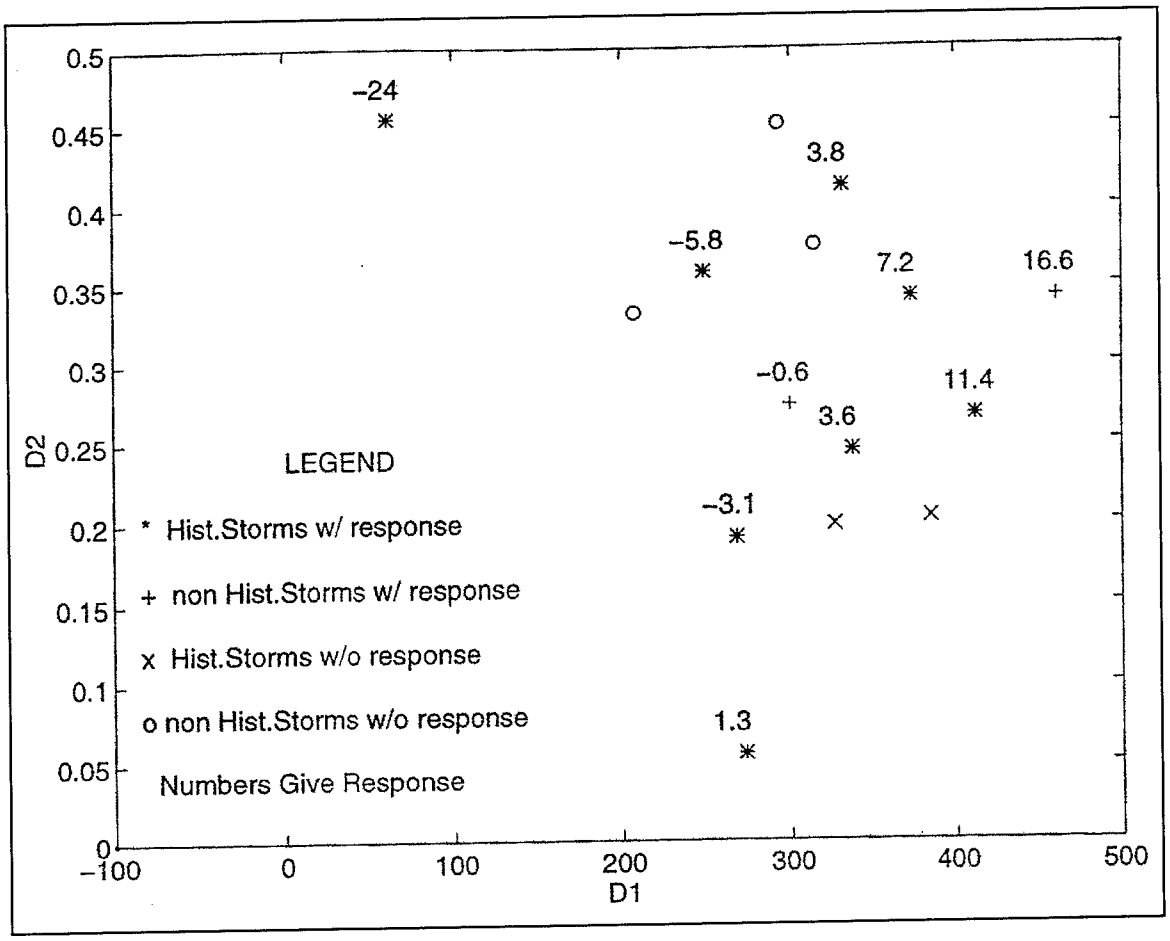

Figure 6. Responses listed versus position in descriptor space

occurred" artificial data at other tide levels, or introducing hypothetical storms to make the interpolation of responses more accurate, may be required.

A basic set of tasks for the computer code is to execute algorithms that reasonably interpolate responses from the training set responses and that establish estimates for the probabilities of hypothetical storms that are consistent with the real historical data.

In the following discussion, the steps in the code completing these tasks will be outlined. Following this, the steps in the actual empirical simulation (EST) will be specified and reviewed in some detail.

Input Parameters

A variety of parameters are input initially to control dimensioning of arrays and program logical flow. These are typically put in as PARAMETER statements before the dimensioning statements and after all the comment cards

specifying definitions at the beginning of the program. A concise table giving the definitions and the input parameter set used in the example is listed in Table 5.

Table 5: Parameter Definitions Listed from Software Code and Values Used in the Example

NTH	= NUMBER OF TRAINING SET HURRICANES
NTHD	= NSTOT-NTH, IF NSTOT IS GREATER THAN NTH = 1, IF NSTOT EQUALS NTH (THIS NUMBER IS ONLY USED FOR DIMENSIONING ARRAYS)
NSTOT	= TOTAL NUMBER OF STORMS IN THE LOGICAL UNION OF THE TRAINING SET AND THE HISTORICAL AND/OR HYPOTHETICAL SET OF STORMS
NSC	= NUMBER OF SCALARS IN THE CHARACTERIZATION OF EACH HURRICANE
NRES	= NUMBER OF RESPONSES COMPUTED FOR EACH STORM OF THE TRAINING SET
NY	= NUMBER OF YEARS PER INTERVAL
NYI	= NUMBER OF INTERVALS TO BE SIMULATED IN EACH SET
NRUNS	= NUMBER OF SETS OF SIMULATIONS
AVY	= AVERAGE NUMBER OF HURRICANES (ABOVE SEVERITY THRESHOLD) PER YEAR
NUMNAY	= NUMBER OF STORMS WHICH FORM A NEIGHBORHOOD
MAXNYI	= LARGEST NUMBER OF STORMS LIKELY TO OCCUR IN A NY-YEAR TIME INTERVAL (USED FOR DIMENSIONING). IF THERE ARE OVERFLOWS, THIS WILL BE INDICATED IN OUTPUT
ISED0	= STARTING SEED INTEGER FOR RANDOM NUMBER GENERATION
IPFLAG	= 1, IF ALL STORMS WITH IH(I) = 1 ARE TAKEN AS EQUALLY LIKELY = 2, IF PROBABILITIES FOR HISTORICAL OR RELATED STORMS ARE COMPUTED BY OTHER PROCEDURES AND PROB(I) FOR THOSE STORMS ARE READ IN AS INITIAL INPUT. UNDER THIS OPTION, STORMS WITH
IH(I)	= 1 DO NOT HAVE TO BE EQUALLY PROVABLE.
IHYP	= 0, HYPOTHETICAL STORMS NOT HISTORICAL OR EQUIVALENT HAVE THEIR PROB(I) SET TO ZERO, AND ARE NOT USED IN THE LATER EMPIRICAL SIMULATION = 1, HYPOTHETICAL STORMS NOT HISTORICAL OR EQUIVALENT [WITH IHIST(I)=1] HAVE THEIR PROB(I) COMPUTED TO PRESERVE KERNEL PROBABILITY DENSITY ESTIMATES, AND MAKE THE PROBABILITIES AS SMOOTH AS POSSIBLE OVER THE DOMAIN SPACE. THE HYPOTHETICAL STORMS ARE USED IN THE LAYER EMPIRICAL SIMULATION.

```
PRINC    = PROBABILITY INCREMENT USED IN ITERATION IN
           SUBR. PTERP5.  THE PROBABILITIES ARE CHANGED UP
           OR DOWN BY THE INCREMENT PRINC IN ADJUSTING
           THE PROBABILITY LIST TO MINIMIZE THE OBJECTIVE
           FUNCTION, OBJ.
ITERMX   = NUMBER OF OUTER LOOP ITERATIONS IN SUBR
           PTERP.  LOOP STOPS IF THE ABSOLUTE DIFFERENCE IN
           THE VARIABLE OBJ BETWEEN SUBSEQUENT ITERATION
           OF THE OUTPER LOOP IS LESS THAN PRINC/5.
ICMAX    = NUMBER OF INNER ITERATIONS IN SUBR PTERP5.
           THIS MANY ITERATIONS ARE DONE AS A BLOCK
           BETWEEN CHECKS FOR CONVERGENCE TO THE
           MINIMUM FOR OBJ.
WGTA     = WEIGHT USED FOR FIRST TERM OF THE OBJ
           VARIABLE AS COMPUTED ON SUBR OBJ.
WGTB     = WEIGHT USED FOR SECOND TERM OF THE OBJ
           VARIABLE AS COMPUTED ON SUBR OBJ.

C *** TEST INPUT PARAMETERS ***
  PARAMETER ( NTH   = 10   ) ! number of storms w response vectors
  PARAMETER ( NTHD  = 5    ) ! storms w/o response vectors
                               (min = 1)
  PARAMETER ( NSTOT = 15   ) ! total number of storms
  PARAMETER ( NCS   = 2    ) ! number of input vectors
  PARAMETER ( NRES  = 1    ) ! number of response vectors
  PARAMETER ( NY    = 1    ) ! number of years per interval
  PARAMETER ( NYI   = 50   ) ! number of intervals of years
  PARAMETER ( NRUNS = 2    ) ! number of sets of NYI simulations
  PARAMETER ( AVY   = 2.5  ) ! average number of storms per year
  PARAMETER ( NUMNAY= 4    ) ! size of neighborhood
  PARAMETER ( MAXNYI= 15   ) ! integer >= max num of storms in NY
                               yr.
  PARAMETER ( ISED0 = 345678) ! starting seed number

C *** PARAMETERS CONTROLLING SUBR. PTERP AND ITS
ITERATION
  PARAMETER ( IPFLAG= 1    ) ! flag for probability assignment
  PARAMETER ( IHYP  = 1    ) ! flag for hypothetical storm prob.
  PARAMETER ( PRINC = 0.000001 ) ! probability increment in PTERP5
  PARAMETER ( ITERMX= 100  ) ! number of PTERP5 outer iterations
  PARAMETER ( ICMAX = 20000 ) ! number of PTERP5 inner iterations
  PARAMETER ( WGTA  = 1000.0) ! weight for OBJA in subr. OBJFN
  PARAMETER ( WGTB  = 1.0  ) ! weight for OBJB in subr. OBJFN
```

The basic EST output consists of realistic simulations of responses for storms or events in a selected number of years. Thus, one might wish to produce 1,000 simulations of storm responses in a 50-year interval. In the parameter statements then, NY=50 and NYI=1000 would be assigned.

The parameter NRUNS specifies how many sets of 1,000, 50-year intervals are to be generated. For example, one might be interested in a two-dimensional (2-D) histogram for largest and second largest response in 50 years. Each of the 1,000, 50-year simulations would yield a pair of numbers giving the largest and second largest response in that 50-year period. There would be a thousand of these, and they could be processed outside the program to obtain the 2-D histogram using any convenient graphics package. The next natural question might be, "Are 1,000 repeats of the 50-year simulations adequate to reliably estimate the 2-D histogram?" This could be investigated by setting NRUNS=3, which would produce three replicates of the 1,000, 50-year results. The histograms from each of the three separate runs could be visually compared to see if dramatic differences are obvious.

In other applications, the user might wish to generate a storm record for each year. This could be achieved with NY=1, NYI=50, and NRUNS=1,000. This would produce 1,000, 50-year runs with the listing giving a year-by-year summary of the storms in that year. The example follows this mode of specification. Since this is purely an illustrative example, NRUNS is set to 2 rather than a more realistic 1,000 or so. The output can then be easily listed out for examination in a report table.

The parameters in Table 5 prior to NY describe the input data. The data table always consists of the training set with their responses, followed by the rest of the storms. NTH gives the number of storms in the training set. NTHD is the number of nontraining-set storms. NSTOT is the total number of storms.

Two saturations are possible here. The training set might consist of all the storms in the set. That is, the response can be computed for every storm listed. Then, NSTOT=NTH. For this situation, the parameter NTHD is actually zero. However, to keep the program from trying to dimension certain arrays with size zero, the parameter should be set to NTHD=1. The program will check whether NSTOT equals NTH, and if it does, the arrays dimensioned with NTHD will not be used. The other situation is where NSTOT is larger than NTH. That is the normal case, and for it the parameter NTHD is set to NSTOT-NTH.

The parameter NSC gives the number of scalar descriptors used to describe a storm. In the simpler example provided, NSC=2. The other parameter, NRES, states the number of responses for each storm. In the provided example, NRES is set to one since there is only one response.

The parameters following NRUNS serve various purposes. AVY lists the average number of storms per year from long-term climatology. It is used in the code to generate the number of storms in NY years according to a Poisson probability law. The Poisson law has no upper limit for the number of storms per the NY time interval. However, the probability of occurrence for that many storms gets infinitesimally small for large n. The arrays for storing the simulated responses in the NY years of time have to be dimensioned with a largest possible number. This parameter in the test example is set to MAXNYI=50. Since AVY=2.5 storms per year and NY=1 year, it is practically impossible that more

than 50 storms would occur in a given year. In fact, the Poisson probability for having 24 or more storms in a year for AVY=2.5 is $3.33\ (10)^{-16}$. Consequently, MAXNYI=50 is actually ridiculously conservative. However, it will certainly work for dimensioning purposes. The program will never fill such an array, unless a truly unbelievable situation develops within the numbers.

The parameter NUMNAY is the neighborhood size used in nearest neighbor interpolation and probability estimation. It is normally set to 3 or 4, although several runs can be made with different choices to see if it really makes much difference to the statistical outcome.

IDIST controls the type of scaling used to make descriptor variables comparable with each other. Currently, IDIST=1 is the only option available, although other scaling options may be introduced in later versions of the program. This whole topic will be discussed later in the report.

The parameter ISED0 is the starting seed integer for the random number generation. It normally is a 5 or 6-digit integer and should be changed from run to run of the program in order to get a different result each time. If the same seed integer is used, the same random numbers will be produced, and identical results will be tabulated by the program.

The parameters IPFLAG, IHYP, and PRINC all control the subroutine PTERP, which estimates probabilities for hypothetical storms introduced arbitrarily by the user. The meaning of these will be covered in much more detail in the discussion of PTERP later in the report.

Input Data Statements

Variable values often require various modifications and scalings before they are directly comparable with each other. Four options are available for this purpose and are controlled separately for each scalar in the input data table (D1 and D2 in the numerical example). The array TS(I,J) can be shifted in dimension, transformed, scaled, and weighted in that order.

The DIMFAC(J) vector of numerical multipliers is designed for changing dimensions. For example, if the J-th variable is in yards, and variables are desired in feet, then DIMFAC for that variable would be 3.0. The most common use for this factor is to effect a change from English to metric units.

The flag vector ITRANS(J) signals various functional transformations on the variables, such as using the logarithm of the data rather than the original values. Ordinarily, ITRANS(J)=0 designates no change of the variable.

The second flag vector, ISCALE(J), controls variable scales. If ISCALE(J)=0, no scaling is imposed and TSN(I,J)=TS(I,J). If ISCALE(J)=1, the TS(I,J) array is normed to

$$TSN(I,J) = \frac{TS(I,J)}{\sqrt{\sum_{K=1}^{NSTOT} \{TS(K,J)\}^2}} \tag{19}$$

That is, the data are adjusted to have a root-mean-square value equal to 1.0. If ISCALE(J)=2, the mean of each variable is subtracted from that variable, and the difference is divided by the root-mean-square of the differences for that variable. In mathematical formula,

$$\mu_J = \frac{1}{NSTOT} \sum_{I=1}^{NSTOT} TS(I,J)$$

$$\sigma_J = \sqrt{\frac{1}{NSTOT} \sum_{I=1}^{NSTOT} \{TS(I,J) - \mu_J\}} \tag{20}$$

$$TSN\ (I,J) = \frac{TS(I,J) - \mu_J}{\sigma_J}$$

The third flag vector is designed for the user's judgment in specifying the importance of each variable for the computation of distance between storms. The distance between storm I and storm J is computed in subroutine SDIST with the function

$$DSC(I,J) = \sqrt{\frac{\sum_{K=1}^{NSC} SWGT(K) * \{TSN(I,K) - TSN(J,K)\}^2}{\sum_{K=1}^{NSC} SWGT(K)}} \tag{21}$$

If SWGT(K) is made small relative to the other SWGT values, then the effect of the K-th normed scalar value in the distance computation is minimized. The SWGT(K) values are usually set to 1.0, which makes all normed scalar values equally important relative to distances. Definitions within the code describing the above parameters are shown in Table 6.

Table 6: Data Statements and Definitions from Program Comments

{ITRANS(J) ; J=1,NSC} = 0, IF J-TH SCALAR IS TO BE LEFT ALONE
= 1, IF J-TH SCALAR IS TO BE LOG TRANSFORMED
{ISCALE(J) ; j=1,NSC} = 0, IF J-TH SCALAR IS TO BE NOT NORMED

(COSINE AND SINES SHOULD ALWAYS BE IN THIS CATEGORY)
= 1, IF J-TH SCALAR IS TO BE RMS NORMED
= 2, IF J-TH SCALAR IS TO BE NORMED WITH ITS STD. DEV. AFTER SUBTRACTING ITS MEAN

{SWGT(I) ; I=1,NSC} = AVERAGING WEIGHTS OF SCALARS FORCOMPUTING DISTANCES IN EXTENDING HISTORICAL STORM EQUIPROBABILITY TO THE UNEQUAL PROBABILITIES ON THE TRAINING SET

{DIMFAC(J) ; J=1,NSC} = MULTIPLYING FACTORS FOR REDIMENSIONING (SET TO 1.0, IF NO CHANGE DESIRED)

*** TEST INPUT DATA STATEMENTS ***

```
DATA ITRANS/2*0/
DATA ISCALE/2*1/
DATA SWGT/2*1.0/
DATA DIMFAC/2*1.0/
```

Scaled Data for the Example

In the example, there is no change in dimensions (DIMFAC(J)=1 for J=1,2) and no transformations introduced (ITRAN(J)=0 for J=1,2). The type 2 scaling (ISCALE(J)=2 for J=1,2) is used for both variables, and the SWGT is set to 1.0 for both variables. Equation 20 gives the formula for the scaling computations. The resulting scaled values of D1 and D2 (DN1 and DN2, respectively) are listed in Table 7 and plotted with the associated responses in Figure 7. There is really no difference between Figures 6 and 7 except for the change in coordinate scaling.

Table 7: Normed Data for the Simple Example

DN1	DN2	R
0.3449	-0.5212	3.5860
1.1725	-0.3146	11.4196
0.7351	0.3917	7.2446
-2.6917	1.4652	-24.0012
-0.3709	-2.2934	1.3265
-0.4251	-1.0293	-3.1179
0.2820	1.0566	3.7658
-0.6328	0.5485	-5.8324
-0.0711	-0.2526	-0.6269
1.7035	0.3908	-6.6005
0.8663	-0.9166	
0.2270	-0.9570	
-1.0876	0.3006	
-0.1466	1.4257	
0.0943	0.7054	

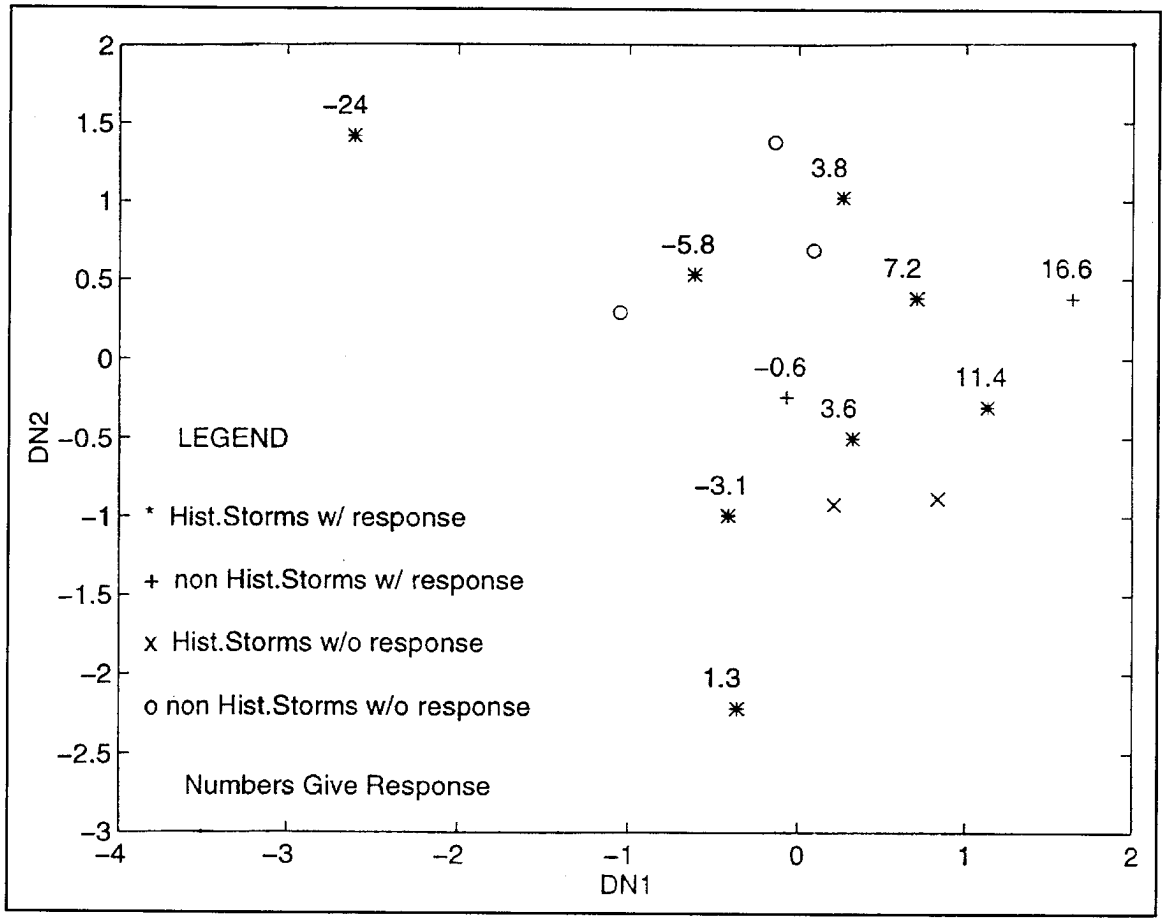

Figure 7. Responses listed versus position in descriptor space

Distance Array

The distances, in a mathematical sense, between the scalar descriptor vectors input are computed in subroutine SDIST. A weighted Euclidean distance is used. The input for the subroutine is the NSTOT by NSC matrix of TSN (normed TS values) and the user-assigned weights, SWGT, for each scalar component. The NSTOT by NSTOT matrix of distances between descriptor vectors is output from the subroutine as the matrix DSC. The (i,j) element of DSC is the distance between the i-th storm and the j-th storm as computed by Equation 21. If the SWGT weights are all 1.0, as they are in the illustrative example, the formula in Equation 21 reduces to the standard Euclidean distances,

$$DSC(I,J) = \sqrt{\frac{1}{NSC} \sum_{K=1}^{NSC} \{TSN(I,K) - TSN(J,K)\}^2} \qquad (22)$$

The assigned weights in SWGT allow the user to suppress selected scalar components if they are judged to be unreliably determined.

In the example, the TSN are given in Table 7, where TSN(I,1)=DN1(I) and TSN(I,2)=DN2(I). NSTOT=15 and NSC=2. Also, SWGT(I)=1.0, as set in the data statements previously. The DSC matrix resulting from these choices is given in Table 8.

Neighborhood Arrays

The nearest neighborhood methods used in much of the program are based on only using those "storms" or scalar descriptor vectors that are closest in the sense of the "distance" defined by Equation 21. A neighborhood size NUMNAY is given in the PARAMETER statements. In the example being followed, NUMNAY was set to 4. However, the user can select any integer size desired. Interpolations or empirical simulations are then developed using this "neighborhood" of nearest storms.

Two NSTOT by NUMNAY matrices of nearest neighbor specifiers are developed in the software. These are denoted by NEBOR and NEBOR2, as computed in subroutines NHOOD and NHOOD2, respectively. The concept will be illustrated with the NEBOR matrix for the example. Consider I=1 in Table 7. This gives

[TSN(1,1),TSN(1,2)] = [DN1,DN2] = [0.3449,-0.5212]

The distances of this vector to the list of total storms as taken from DSC in Table 8 are:

Storm No.	Distance From Storm No. 1
1	0.0000
2	0.6031
3	0.7020
4	2.5658
5	1.3515
6	0.6523
7	1.1166
8	1.0247
9	0.3502
10	1.1570
11	0.4627
12	0.3192
13	1.1678
14	1.4199
15	0.8852

Table 8
DSC Matrix for the Example

I \ J	1	2	3	4	5	6	7	8	9	10	11	12	13	14	15
1	0.0000	0.6031	0.7020	2.5658	1.3515	0.6523	1.1166	1.0247	0.3502	1.1570	0.4627	0.3192	1.1678	1.4199	0.8852
2	0.6031	0.0000	0.5874	3.0083	1.7745	1.2376	1.1561	1.4149	0.8804	0.6243	0.4776	0.8083	1.6563	1.5441	1.0495
3	0.7020	0.5874	0.0000	2.5392	2.0534	1.2971	0.5689	0.9735	0.7297	0.6848	0.9297	1.0191	1.2904	0.9609	0.5044
4	2.5658	3.0083	2.5392	0.0000	3.1235	2.3832	2.1225	1.5937	2.2157	3.1994	3.0276	2.6819	1.4016	1.7999	2.0420
5	1.3515	1.7745	2.0534	3.1235	0.0000	0.8947	2.4134	2.0181	1.4586	2.3987	1.3089	1.0352	1.9030	2.6346	2.1458
6	0.6523	1.2376	1.2971	2.3832	0.8947	0.0000	1.5574	1.1253	0.6036	1.8094	0.9167	0.4639	1.0506	1.7471	1.2804
7	1.1166	1.1561	0.5689	2.1225	2.4134	1.5574	0.0000	0.7399	0.9588	1.1100	1.4552	1.4243	1.1062	0.4000	0.2816
8	1.0247	1.4149	0.9735	1.5937	2.0181	1.1253	0.7399	0.0000	0.6918	1.6558	1.4822	1.2259	0.3663	0.7092	0.5260
9	0.3502	0.8804	0.7297	2.2157	1.4586	0.6036	0.9588	0.6918	0.0000	1.3348	0.8123	0.5408	0.8184	1.1879	0.6874
10	1.1570	0.6243	0.6848	3.1994	2.3987	1.8094	1.1100	1.6558	1.3348	0.0000	1.0977	1.4136	1.9747	1.4990	1.1594
11	0.4627	0.4776	0.9297	3.0276	1.3089	0.9167	1.4552	1.4822	0.8123	1.0977	0.0000	0.4530	1.6278	1.8045	1.2702
12	0.3192	0.8083	1.0191	2.6819	1.0352	0.4639	1.4243	1.2259	0.5408	1.4136	0.4530	0.0000	1.2864	1.7054	1.1792
13	1.1678	1.6563	1.2904	1.4016	1.9030	1.0506	1.1062	0.3663	0.8184	1.9747	1.6278	1.2864	0.0000	1.0372	0.8834
14	1.4199	1.5441	0.9609	1.7999	2.6346	1.7471	0.4000	0.7092	1.1879	1.4990	1.8045	1.7054	1.0372	0.000	0.5371
15	0.8852	1.0495	0.5044	2.0420	2.1458	1.2804	0.2816	0.5260	0.6874	1.1594	1.2702	1.1792	0.8834	0.5371	0.0000

If these are rearranged in order of ascending distance, the list becomes:

Distance From Storm No. 1	Storm No.
0.0000	1
0.3192	12
0.3502	9
0.4627	11
0.6031	2
0.6523	6
0.7020	3
0.8852	15
1.0247	8
1.1166	7
1.1570	10
1.1678	13
1.3515	5
1.4199	14
2.5658	4

Thus, Storm No. 12 is the closest storm to Storm No. 1. Next further away is Storm No. 9, then No. 11, and so forth. The neighborhood of storms of size 4, in order of closeness to Storm No. 1, are [12,9,11,2]. This list of I indices is made the first row of the matrix NEBOR shown in Table 9. The same thing is done for all the other storms in the list of NSTOT descriptor vectors.

Table 9: The Matrix NEBOR

I	Nearest Neighbor Indices Relative to I			
1	12	9	11	2
2	11	3	1	10
3	15	7	2	10
4	13	8	14	15
5	6	12	11	1
6	12	9	1	5
7	15	14	3	8
8	13	15	9	14
9	1	12	6	15
10	2	3	11	7
11	12	1	2	9
12	1	11	6	9
13	8	9	15	14
14	7	15	8	3
15	7	3	8	14

In the input data set (see Table 4), the first NTH rows list the storms with responses specified in the input. The rows for I=NTH+1 to NSTOT (11 through 15 in the example) give descriptor vectors [DN1 DN2] for which there is no

responses input. If NSTOT=NTH, then there are no data storms without specified input.

If NSTOT≠NTH, then responses for the storms for which no responses are provided must be interpolated from the available responses. In the example, Storms No. 11 through No. 15 need to have estimates made for their responses. Of course, it would be better to go back to the original mathematical modeling or techniques from which the tabled responses were obtained and get the additional responses by the same procedures. However, it is often very expensive in terms of time or expenditure to obtain a response for a given storm. For example, the response determination may require many hours of computer time on a supercomputer or many days of setup in a hydraulic basin for a physical model. Thus, it is often the case that only a certain number of responses can be determined if the project is going to stay within budget. The storms with these response determinations are called the "training set" and are listed as the first NTH rows of the TS(I,J) matrix.

As an admittedly imperfect determination, the remaining storms have their responses interpolated within the responses of the training set. It is desirable, if it can be afforded, to have NSTOT=NTH so that no interpolations are required. If that is impossible, the EST software computes a nearest neighbor interpolation for the unprovided responses. The procedure uses the nearest NUMNAY storms in the training set, as evaluated by Equation 21, to make a Gaussian kernel interpolation of the unknown responses. The exact procedure for this will be discussed in the section on subroutine RTERP later.

One of the inputs for RTERP is a NTHD by NSTOT matrix NEBOR2. Here NTHD=NSTOT-NTH, which is the number of storms with no responses. If NSTOT=NTH, then NTHD is set to one since it is used in dimensioning arrays and zero is unacceptable in FORTRAN 77 for such purposes. However, NEBOR2 is not computed if NSTOT=NTH, even though NTHD=1.

The computation of NEBOR2, as executed in subroutine NHOOD2, proceeds as before except that only neighbors from the training set are ranked, and this is done only for storms not in the training set. Thus, in the example, Storms No. 11 through No. 15 have no given responses. These must be estimated from Storms No. 1 through No. 10, which have responses specified. The matrix NEBOR2 is a 5 by 4 matrix (since NUMNAY=4, as before). It should be noted in passing, that NUMNAY cannot be larger than the size of the training set.

The distance data in DSC is used in the computation of NEBOR2. In the example, for Storm No. 11, the distances from the matrix DSC are:

Distance to Storm No.	Storm No. 11
1	0.4627
2	0.4776
3	0.9297
4	3.0276
5	1.3089

6	0.9167
7	1.4552
8	1.4822
9	0.8123
10	1.0977

If these are ranked in ascending order, the list becomes:

Distance to Storm No. 11	Storm No.
0.4627	1
0.4776	2
0.8123	9
0.9167	6
0.9297	3
1.0977	10
1.3089	5
1.4552	7
1.4822	8
3.0276	4

The NUMNAY=4 nearest neighbors to Storm No. 11 in the training set are Storms [1,2,9,6] in order of greater distance. This then constitutes the first row of the NEBOR2 matrix and gives the logical four storms to be used in interpolating a response for Storm No. 11. The corresponding computations are performed for the other storms that have no responses. The resulting NEBOR2 matrix is given in Table 10.

Table 10: The Matrix NEBOR2

I	Nearest Neighbor Indices in Training Set Relative to I			
11	1	2	9	6
12	1	6	9	2
13	8	9	6	7
14	7	8	3	9
15	7	3	8	9

The ranking of the distances in the EST program is made with a version of the "Quick Sort" algorithm written for FORTRAN. This is an extremely fast ranking method.

The nearest neighbor computations performed in subsequent steps of the software use the matrices DSC, NEBOR, and NEBOR2, so that these quantities are computed once only and stored for all later calculations.

Response Interpolation for Nontraining-Set Storms

The computation of responses for a given descriptor vector often involves substantial computer time and effort. Typically, an elaborate finite element model is required. Consequently, the EST software is set up so that responses may be computed only on a representative subset of the data called the "training set."

Ideally, the training set would consist of the complete data set so that all responses would be known. In any case, the training set should be as large as possible, consisting of most of the data.

A typical choice would be to include in the training set all of the most severe 50 percent of the data and also a substantial sampling of the least severe half of the data. In this way, the responses to be estimated by interpolation are restricted to the least severe storms, which have small effect on the long-term risk.

In the example computation shown in Table 4, the last five rows have no responses. These have to be interpolated. Since this is an artificial example, no attempt has been made to assess severity.

Several methods were considered for the multivariate interpolation. The original EST software included two schemes as options—kernel interpolation and stepwise regression. Subsequently, at the request of the users, the stepwise regression was deleted as requiring too much statistical background for accurate use by many engineers.

Accordingly, the EST program now only incorporates the nearest neighbor, kernel interpretation. This is a nonparametric method that is fairly robust. No interpolation scheme is perfect, however, and the kernel method has its faults also.

It is planned to include as an option in the next EST version a relatively new algorithm called MARS (multivariate adaptive regression splines).

The nearest neighbor kernel procedure is based on the following mathematics. Let v_o be a descriptor vector at which the response is to be interpolated. The neighborhood of nearest descriptor vectors within the training set was previously tabulated in matrix NEBOR2 (see Table 9). Let $v_1, v_2, \ldots, v_n$ be these nearest descriptor vectors in the training set. The interpolated response, R_o, is given by the formula

$$R_o = \frac{\sum_{j=1}^{n} w(v_j - v_o)\, R_j}{\sum_{j=1}^{n} w(v_j - v_o)} \qquad (23)$$

where R_j is the response associated with v_j, and

$$w(v) = e^{-\pi v^T v/(EW)} \tag{24}$$

The scalar EW is the effective radius of the kernel. The computation is performed in the software in the subroutine RTERP.

If it is assumed that the training set is selected to cover the descriptor space fairly evenly, a good selection for the effective radius of the kernel to interpolate R_o has been found to be

$$w(v) = e^{-\pi v^T v/(EW)} \tag{25}$$

Here, v_j are the descriptor vectors in the training set neighborhood of size n about v_o. This is incorporated into the EST software. The value of EW is stored in the vector EWW(I), which is computed in subroutine NHOOD2.

The present version of the EST uses a kernel that is isotropic. That is, it is the same in all directions. The next version of the EST program is planned to include an anisotropic kernel based on an ellipsoid fit to each neighborhood. As mentioned previously, it is also planned to include interpolation with the MARS algorithm as an additional option.

If the RTERP interpolations are applied to the simple example data, one obtains Table 11. It is more revealing to show the interpolations graphically. This is given in Figure 8. The interpolated values are listed above those descriptor vectors marked with the symbols × and ◦. The interpolated values appear visually to be a reasonable smooth variation from the training set responses. That is, the interpolations appear to be acceptable values that are not out of line and would appear to be about what one would get if the training set responses were contoured and the missing responses were then read from the contours.

Interpolation methods are generally "smoothers" and have trouble catching local peaks in the function if they are adequately reflected in the data. The kernel interpolation shares this defect.

Table 11: Interpolated Responses

I	D1	D2	DN1	DN2	R
					Training Set
1	337.5041	0.2443	0.3332	-0.5035	3.5860
2	412.5162	0.2663	1.1327	-0.3035	11.4196
3	372.8642	0.3415	0.7101	0.3787	7.2446
4	162.2546	0.4558	-2.6004	1.4153	-24.0012
5	272.6218	0.0556	-0.3583	-2.2157	1.3265
6	267.7060	0.1902	-0.4107	-0.9944	-3.1179

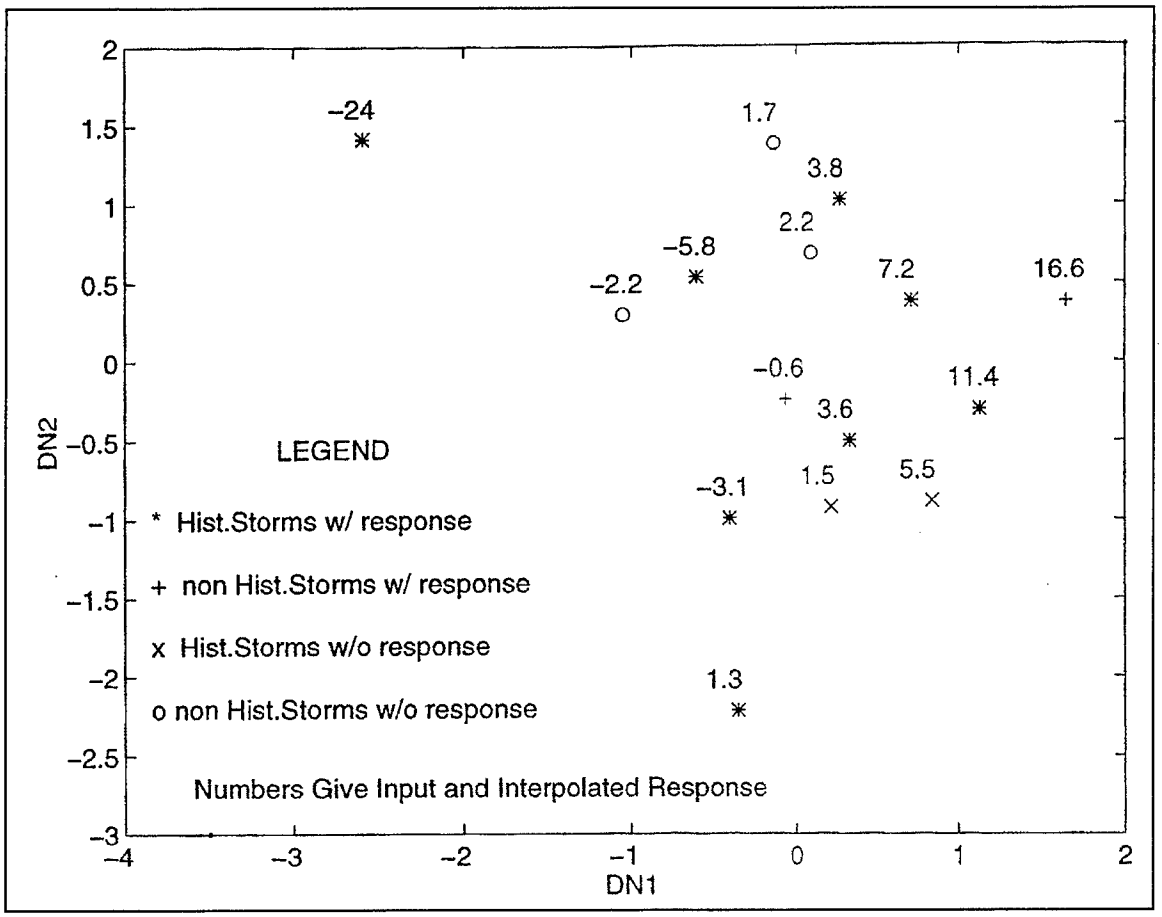

Figure 8. Input and interpolated responses

7	331.7988	0.4123	0.2724	1.0205	3.7658
8	248.8828	0.3582	-0.6113	0.5297	-5.8324
9	299.7959	0.2729	-0.0687	-0.2442	-0.6269
10	460.6511	0.3414	1.6458	0.3777	16.6005
					Interpolated
11	384.7649	0.2022	0.8370	-0.8852	5.5004
12	326.8101	0.1979	0.2193	-0.9248	1.4897
13	207.6511	0.3318	-1.0508	0.2902	-2.1674
14	292.9501	0.4516	-0.1416	1.3775	1.7393
15	314.7891	0.3749	0.0911	0.6819	2.2336

Estimation of Probabilities for Hypothetical Storms

The data set may include nonhistorical or hypothetical storms that did not actually occur but "might have occurred" in the judgment of the user. The main reason for including these is to provide a smoother coverage of the descriptor space so that the response interpolations or EST simulations can be more accurate.

The actually occurring historical data set may be augmented several ways within the EST software. Nonhistorical storms may be either equivalent storms or hypothetical storms. Equivalent storms are events that are the same as one of the historical storms except that a secondary property such as coastal crossing location or associated astronomical tide are varied slightly from that which actually occurred.

For example, the user may believe that a given historical storm could just as likely have crossed the coast 10 or 20 miles upcoast or downcoast from where it actually occurred. Then, four more storms just like the historical storm could be included in the data set with the only variation being the shift in path. The corresponding response for the distance of the reference site from the path could be directly read from the finite element model of responses over the area of the storm. The net effect of this is that the single historical storm now has four more "equivalent" versions. Suppose that there were originally 50 historical storms so that the probability for occurrence of each was 1/50. Then, a new probability of $1/[5(50)] = 0.02/5 = .004$ is attached both to the historical storm and its equivalents. One historical storm has been replaced with five storms that share the probability of the original historical storm.

A similar set of equivalent storms may be constructed around the astronomical tide that by accident may have been present when the storm occurred. The user may assemble a set of equally likely tide levels that could have been present. Then, the data set could be enlarged with a separate storm for each tide level. If the user chose four additional tide levels and four additional coastal crossings, then a given historical storm could be replaced with 25 equivalent storms, one of which actually happened. Again, the probability of the original storm is subdivided out equally to all of the equivalent storms.

A common choice in applications of the EST program is to replace each historical storm with the same number of equivalent storms. So if there were 50 original historical storms and 25 tide/coastal crossing equivalent storms were selected, then the training set would now incorporate 50(25)=1,250 storms. This enhancement could be carried out with little increase in effort in the finite element modeling provided that the response is related in a simple way to the astronomical tide and distance from the storm path. For example, if the response is the flood depth at a selected site, and the flooding is linear in the sense that the actual flood depth is the sum of the astronomical tide and the storm tide from the model computations, then the flood depth at the site is easily computed from the one model computation for each of the equivalent storms. This is not possible if nonlinear effects are present, such as barrier islands offshore from the site where substantial nonlinear variations in flooding are associated with island overtopping.

In the EST software, if all historical storms and their equivalents have been carefully selected so that they are equally likely, then the input integer IPFLAG is set to one, and computations in subroutine PTERP5 count the number of historical storms or equivalents and set the probability of each to one divided by the total number.

The above arrangement is not always possible or convenient. Suppose the historical storms near the site consist of some that cross the coast and some that travel parallel to the coast. The natural number of equivalent storms for those with coastal crossings may differ from those that do not cross the coast. In such cases, the variable IPFLAG is set to two, and the user is required to compute separately the probabilities and read them into the program as the array P(I) for all I with IHIST(I)=1. (IHIST is the flag that is set to one for historical storms or their equivalents in the data input.)

Completely hypothetical storms, not equivalent to any of the historical storms, may also be entered into the data set by the user. For example, finite element modeling might have been performed at considerable cost and effort for several "super" storms that meteorologically are believed possible for the region, but that are not actually in the historical data set. It seems a waste to not use them in the EST computations. Thus, they are included in the data set with IH=0 attached to them. If the responses were computed for them, they would be included also within the training set. Hypothetical storms may also be included in the nontraining set storms if the user desires.

The treatment of the hypothetical storms in the program is controlled by the input integer IHYP. If IHYP=0, the hypothetical storms are used in response interpolation if they are in the training set, but are not used in subsequent EST simulations. That is, the P(I) value for them is set to zero. This happens whether or not the hypothetical storms are in the training set.

If IHYP=1, an appropriate probability for the occurrence of the hypothetical storms is computed within subroutine PTERP5. This is, perhaps, a delicate point because probabilities are being manufactured for storms that have not actually occurred. It is very important that the probabilities for these be estimated in a way that is consistent with the historical data set.

The EST software in the current version tries to achieve this consistency by the following process. The historical data or their equivalents (everything flagged with IHIST=1) can be used to compute an estimate of the probability density over the descriptor space. The program uses a kernel procedure to make this estimate. (This procedure will be discussed in more detail later).

In the illustrative example, there are 10 storms with IHIST=1, and there are five hypothetical storms with IHIST=0. Initially then, the probability is 0.1 for each of the historical storms and zero for the hypothetical storms. This is shown graphically in Figure 9. The estimate of the probability density function from these 10 historical storms is contoured in the top graph of Figure 10.

The process for estimating probabilities for the hypothetical storms in the EST software seeks to preserve the density function and give a "smooth" set of probabilities. That is, the probability density function estimated from the enhanced set of probabilities should be about the same as the density function from the historical set only. Also, storms near each other in descriptor space

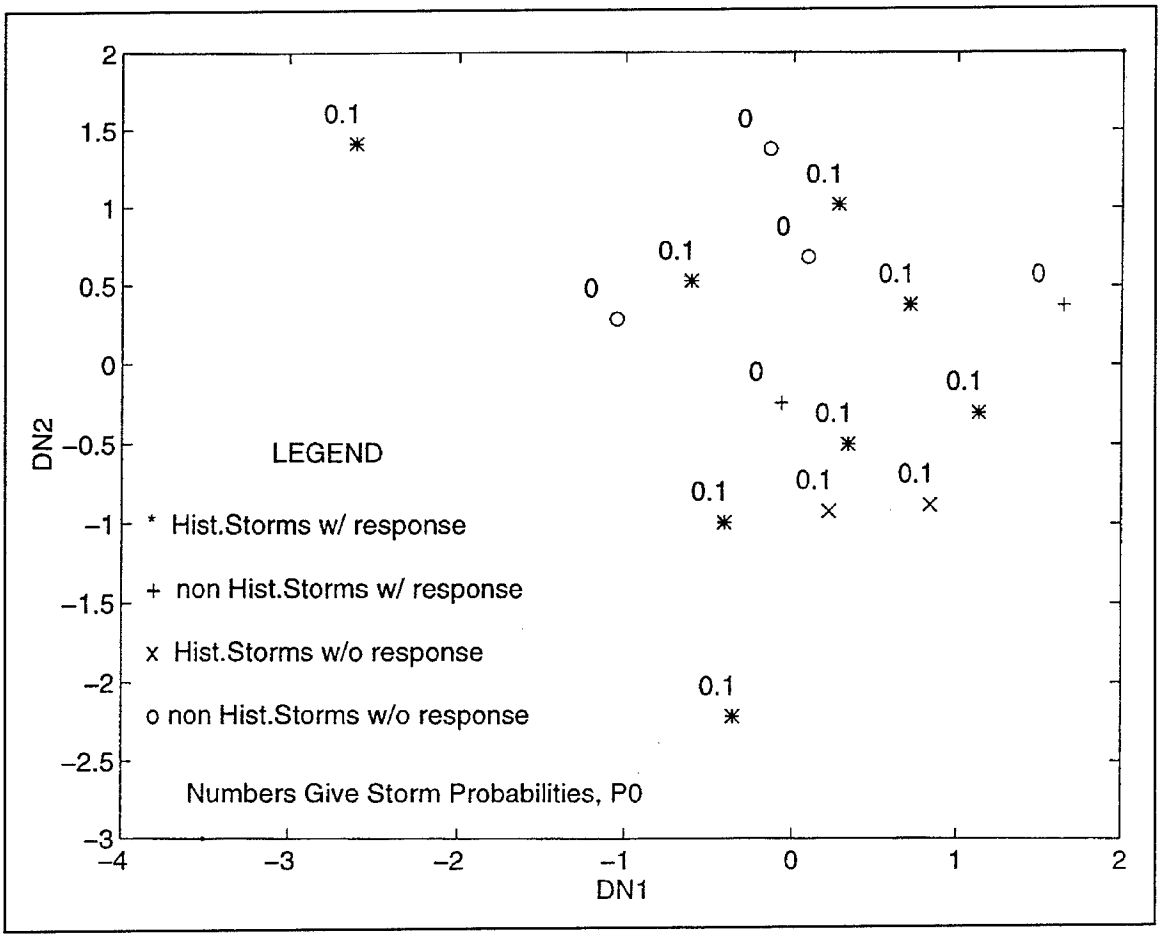

Figure 9. Initial probabilities for the example

should have about the same probabilities. An iterative process is used to produce probability estimates that match these criteria.

The methods incorporated into subroutine PTERP5 give estimates in the example as shown in Figure 9. The density function as estimated from these probabilities with the kernel computation is contoured in the bottom section of Figure 10.

Visually, the two contour graphs appear quite similar, and the algorithm used in subroutine PTERP5 satisfactorily achieves the estimation goals.

The methods discussed above are based on a kernel estimate of function proportional to the probability density defined as

$$f(v) = \sum_{j=1}^{n} w(v_j - v)p_j \qquad (26)$$

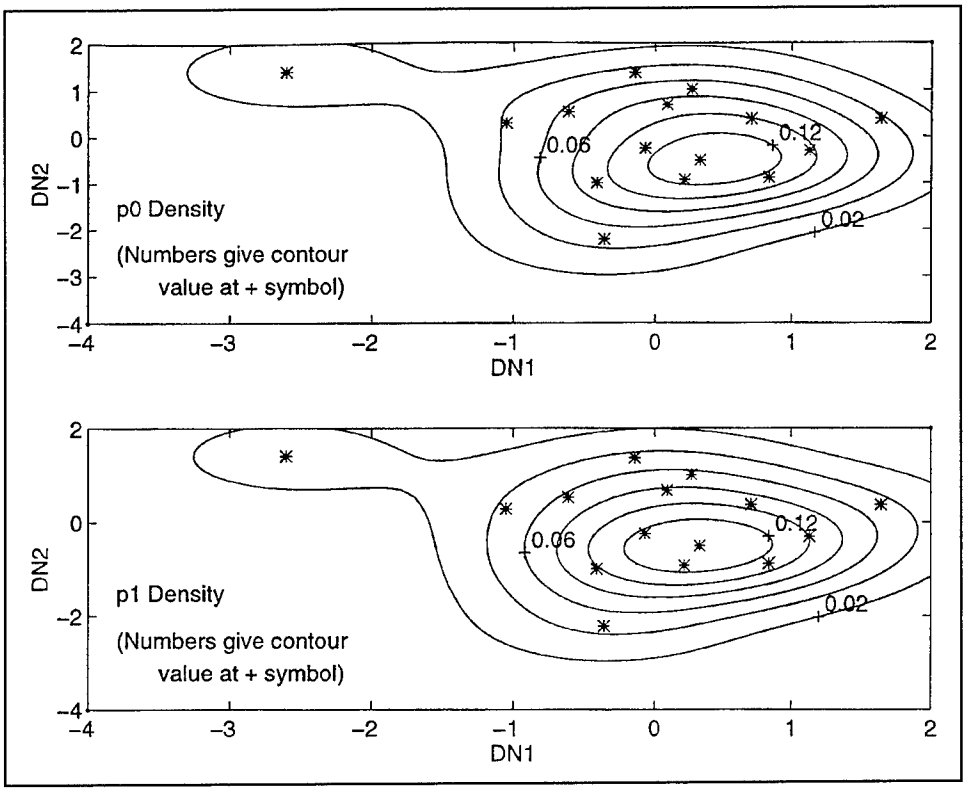

Figure 10. Density function estimates

where the notation from the previous section is used, and

$f(v)$ = probability density at v

p_j = probabilities assigned to each storm

$w(v_j - v) = e^{-\pi(v_j - v)^T (v_j - v)/c^2}$

c = maximum value of EW(I)

= EWMAX computed in subroutine NHOOD

The function $f(v)$, after norming so that it integrates to unity over the whole space, is what is contoured for the example in Figure 9. The norming is unnecessary for its use in subroutine PTERP5, so it is deleted in the code to simplify the mathematics.

Let p_{jo} be the probabilities assigned by the user to the historical storms of their equivalents (IHIST=1). For hypothetical storms (IHISTO=0), p_{jo} is set to zero. Now let p_j denote the estimates of probability to be made within which nonzero probabilities are assigned to the hypothetical storms. Define

$$f_o(v) = \sum_{j=1}^{n} w(v_j - v)p_{jo}$$

$$f(v) = \sum_{j=1}^{n} w(v_j - v)p_j \qquad (27)$$

It seems desirable that the assignment of probabilities to the hypothetical storms, with some corresponding adjustments of the probabilities on historical storms should not significantly change the probability density. In essence, $f_o(v)$ characterizes the probabilities for the historical storms. If the adjusted probabilities keep the same density, then the estimates are true to the original historical probabilities.

If p_j are selected to make Q_1 zero where

$$Q_1 = \sum_{k=1}^{n} \left[f_o(v_k) - \sum_{k=1}^{n} w(v_j - v_k)P_j \right]^2 \qquad (28)$$

then probability densities, at least at the storm locations, will remain the same. However, if $p_j \equiv p_{jo}$, the value of Q_1 will be exactly zero by definition of $f_o(v)$. Consequently, an additional criterion is needed. It seems reasonable to require that $f(v)$ be reasonably smooth over the v-space. That is, storms near each other should have similar p_j values. An objective function that forces this behavior when it is minimized is

$$Q_2 = \sum_{all\ neighborhoods} |\max(p_j) - \min(p_j)| \qquad (29)$$

A combined objective function whose minimization will achieve both goals is computed in subroutine OBJFN as

$$Q = a_1 Q_1 + a_2 Q_2 \qquad (30)$$

where

a_1 = WGTA in OBJFN

a_2 = WGTB in OBJFN

The values of a_1 and a_2 currently assigned in the program input parameters are

WGTA = 1,000

WGTA = 1

The values of Q_1 are substantially smaller than those of Q_2, so a larger weight is needed for Q_1. Also, the preservation of the historical density function as embodied in Q_1 is of primary importance, while the smoothness of the p_j over the descriptor space is of secondary importance.

An iterative scheme is set up in PTERP5 to converge to the p_j that minimize Q. The user may well need to adjust the values of WGTA and WGTB in the input to achieve a satisfactory convergence. Some trial and examination is required here.

After the probabilities have been assigned to all storms within subroutine PTERP5, the cumulative probabilities are computed as

$$CPROB\ (J) = \sum_{j=1}^{j} p_j \tag{31}$$

These will be used in the subsequent EST simulations for future storm activity.

Cumulative Poisson Probabilities

The number of storms per time interval is assumed to follow a Poisson probability law,

$$pr[N = n] = \frac{e^{-\lambda t}\,(\lambda t)^n}{n!} \tag{32}$$

where

t = number of years in the time interval

λ = average number of events (or storms) per year

The user is asked to input as initial parameters

MAXNYI = maximum number of storms possible per the interval

λ = AVY = average number per year

t = NY = number of years in the time interval

The value of MAXNYI should be selected so that the probabilities are zero for Pr[N $\geq$ MAXNYI]. A value of MAXNYI maybe 10 times λt should achieve this, although it is safer to examine a table of Poisson probabilities for that $\mu = \lambda t$ value, or alternatively to make some trial hand calculations. The Poisson probabilities are computed iteratively within the program as

$$Pr[N=0] = e^{-\lambda t}$$

$$p[N=1] = (\lambda t)\ Pr\ [N=0]$$

$$P[N=2] = \frac{(\lambda t)}{2}\ Pr\ [N=1]$$

$$P[N=3] = \frac{(\lambda t)}{3}\ Pr\ [N=2]$$

$$\vdots$$

$$P[N=n] = \frac{(\lambda t)}{n}\ Pr\ [N=n=1]$$

$$\vdots$$

$$P[N=MAXNYI] = \frac{(\lambda t)}{MAXNYI}\ Pr\ [N=MAXNYI\ -\ 1]$$

Finally, the cumulative Poisson probabilities are computed and saved in the software as

$$CPOI\ (I) = \sum_{J=0}^{I-1} p[N = j] \tag{33}$$

The user can print out and examine CPOI(I) in preliminary trial runs of the software to verify that MAXNYI was made large enough for the λ value specified.

Rapid Simulation of Discrete Random Variables

Let X be a discrete random variable taking on values $x_1, x_2, x_3, ..., x_N$ with probability $p_1, p_2, p_3, ..., p_N$. Simulations of X can be produced very rapidly with the use of a large vector NUM with the fraction p_k of the components of NUM equal to k. This is seen most easily by simple example. Suppose x_k and p_k are given by

k	x_k	p_k
1	0	.2
2	1	.4
3	2	.3
4	3	.1

A vector NUM that would match this is

$$NUM = \begin{bmatrix} 1 \\ 1 \\ 2 \\ 2 \\ 2 \\ 2 \\ 3 \\ 3 \\ 3 \\ 4 \end{bmatrix}.$$

There are 10 components. There are $p_1 = 0.2$ fraction of them equal to 1. Similarly, there are $p_2 = 0.4$ fraction of them equal to 2 = 1, and so forth.

A simulation of X can proceed by first generating a uniform random variable u with $0 < u < 1.0$. Here, N=10, so define

$$k = \{smallest\ integer \geq uN\} \tag{34}$$

Possible values of k are 1,2,3, ..., 10 for this case. Let the simulated value of X be $V(k)$. The simulation will automatically equal x_1 with probability p_1, x_2 with probability p_2, etc.

In the EST software, two discrete probability laws are involved in the simulations. These are (a) the probability law for the selection of a reference storm from the NSTOT storms (cumulative probability CPROB as computed in subroutine PTERP5) and (b) the Poisson probabilities for number of storms per time interval (cumulative probability CPOI as computed in the main program). The corresponding vector NUM for each is computed on the first call to subroutine RANCUM. The call to RANCUM is

CALL RANCUM (N, CUM, NUM, U, K, IFIRST)

The input arguments are N, CUM, and U. Here, CUM is the cumulative probability list for the random variable involved (CPROM or CPOI for EST). If IFIRST is zero, the vector NUM is computed before the random K corresponding to the uniform random number u is developed. If IFIRST $\neq$ 0, the subroutine assumes NUM has already been computed and proceeds directly with finding K for the given u.

After emerging from subroutine RANCUM, the simulation is $x(k)$, where x is the vector of realizations of X.

Fundamental EST Simulation

The simulation cycle starts with a loop over the number of separate runs desired (JRUNS=1, NRUNS). Each run consists of NYI time intervals, so the next loop is (JYI=1, NYI). For a given time interval, subroutine RANCUM is used to generate the number of storms that occur in the time interval. Then the number of storms is looped over (JST=1, NSTRM(JYI)), providing there is at least one storm in the time interval (NSTRM(JYI) ≥ 1). Finally, a response is simulated for each storm by a nearest neighbor random walk algorithm. This algorithm will be elaborated on in the next paragraph.

For a given storm, subroutine RANCUM is used to select one of the NSTOT storms from the data set according to the probabilities generated in subroutine PTERP5. The index for this storm is denoted by IREF. Let $R_1, R_2, R_3, \ldots,$ R_{NUMNAY} be the responses for the storms in the neighborhood about the reference storm with response R_{IREF}. Let U_j be independent uniform random numbers from the interval ($-BASE/2 < U_j < BASE/2$) for $j = 1,2,3, \ldots,$ NUMNAY, where currently BASE = 1/NUMNAY. The empirical simulation is given by

$$R = R_{IREF} + \sum_{j=1}^{NUMNAY} U_j \, [R_j - R_{IREF}] \qquad (35)$$

The user can adjust the variable BASE to force the variance of the simulations to be about the same as the input variances. This variable also controls the simulations on the edge of the data cluster so that they do not leap too far out beyond existing data.

A substantial study was made of this and other proposed algorithms by Park, Borgman, and Anderson-Sprecher (1996). Further study is also underway currently (Ravindra, in preparation). Substantial improvements to the above algorithm have been developed. These will be included in the next version of the program and provided to users after appropriate testing.

EST Simulation Process

A detailed listing of the output for the example is given in Table 12 on the following pages. The starting seed number is listed at the beginning of each run. The change in seed number after the first call to the random number subroutine is listed immediately below to the left. Then the results are listed for each time interval (here, 1 year). After the 50 time intervals for the run, a summary chart of selected statistics is given.

A subroutine named ATRIB is available to the user to compute any attribute of the responses within each time interval that the user wishes to examine. Currently, subroutine ATRIB computes the maximum response within the

interval. The lower quartile, median, and upper quartile of the attribute over all the time intervals in the run are listed in a summary table in the output.

Table 12: Detailed Output

```
 Run Number 1:
 -------------

 ******************************************
 SIMULATION NUMBER =    1  SEED NUMBER:        345678
    16471
 INTERVAL   1, NUMBER OF STORMS   0
 INTERVAL   2, NUMBER OF STORMS   2
 STORM RESPONSES, (1ST IS FLOATED INTEGER GIVING NUMBER OF STORMS
PRESENT)
    1  2.00
    2 -2.59
    3  6.68
 INTERVAL   3, NUMBER OF STORMS   2
 STORM RESPONSES, (1ST IS FLOATED INTEGER GIVING NUMBER OF STORMS
PRESENT)
    1  2.00
    2  0.12
    3  2.58
 INTERVAL   4, NUMBER OF STORMS   3
 STORM RESPONSES, (1ST IS FLOATED INTEGER GIVING NUMBER OF STORMS
PRESENT)
    1  3.00
    2 13.60
    3  4.28
    4 11.51
 INTERVAL   5, NUMBER OF STORMS   2
 STORM RESPONSES, (1ST IS FLOATED INTEGER GIVING NUMBER OF STORMS
PRESENT)
    1  2.00
    2 -5.87
    3  5.12

 INTERVAL   6, NUMBER OF STORMS   4
 STORM RESPONSES, (1ST IS FLOATED INTEGER GIVING NUMBER OF STORMS
PRESENT)
    1  4.00
    2 -29.28
    3 -1.06
    4 -2.56
    5 -2.87
 INTERVAL   7, NUMBER OF STORMS   2
 STORM RESPONSES, (1ST IS FLOATED INTEGER GIVING NUMBER OF STORMS
PRESENT)
    1  2.00
    2  1.07
    3 -5.50
 INTERVAL   8, NUMBER OF STORMS   2
 STORM RESPONSES, (1ST IS FLOATED INTEGER GIVING NUMBER OF STORMS
PRESENT)
    1  2.00
    2  7.78
    3  1.43
 INTERVAL   9, NUMBER OF STORMS   2
 STORM RESPONSES, (1ST IS FLOATED INTEGER GIVING NUMBER OF STORMS
PRESENT)
    1  2.00
```

```
   2  6.26
   3  1.38
 INTERVAL  10, NUMBER OF STORMS   4
 STORM RESPONSES, (1ST IS FLOATED INTEGER GIVING NUMBER OF STORMS
PRESENT)
   1  4.00
   2  3.55
   3 -18.53
   4 -1.38
   5 -0.27
 INTERVAL  11, NUMBER OF STORMS   1
 STORM RESPONSES, (1ST IS FLOATED INTEGER GIVING NUMBER OF STORMS
PRESENT)
   1  1.00
   2 -2.37
 INTERVAL  12, NUMBER OF STORMS   1
 STORM RESPONSES, (1ST IS FLOATED INTEGER GIVING NUMBER OF STORMS
PRESENT)
   1  1.00
   2  1.05
 INTERVAL  13, NUMBER OF STORMS   1
 STORM RESPONSES, (1ST IS FLOATED INTEGER GIVING NUMBER OF STORMS
PRESENT)
   1  1.00
   2  10.15

 INTERVAL  14, NUMBER OF STORMS   7
 STORM RESPONSES, (1ST IS FLOATED INTEGER GIVING NUMBER OF STORMS
PRESENT)
   1  7.00
   2  3.32
   3  2.26
   4  3.61
   5  9.98
   6 -3.64
   7  1.64
   8  6.10
 INTERVAL  15, NUMBER OF STORMS   5
 STORM RESPONSES, (1ST IS FLOATED INTEGER GIVING NUMBER OF STORMS
PRESENT)
   1  5.00
   2  3.43
   3  12.15
   4  9.36
   5  15.76
   6  1.94
 INTERVAL  16, NUMBER OF STORMS   3
 STORM RESPONSES, (1ST IS FLOATED INTEGER GIVING NUMBER OF STORMS
PRESENT)
   1  3.00
   2 -5.99
   3  4.71
   4  3.06
 INTERVAL  17, NUMBER OF STORMS   1
 STORM RESPONSES, (1ST IS FLOATED INTEGER GIVING NUMBER OF STORMS
PRESENT)
   1  1.00
   2 -26.01
 INTERVAL  18, NUMBER OF STORMS   1
 STORM RESPONSES, (1ST IS FLOATED INTEGER GIVING NUMBER OF STORMS
PRESENT)
   1  1.00
```

```
   2 16.74
 INTERVAL  19, NUMBER OF STORMS   3
 STORM RESPONSES, (1ST IS FLOATED INTEGER GIVING NUMBER OF STORMS
PRESENT)
   1  3.00
   2 12.00
   3  5.53
   4  1.35
 INTERVAL  20, NUMBER OF STORMS   2
 STORM RESPONSES, (1ST IS FLOATED INTEGER GIVING NUMBER OF STORMS
PRESENT)
   1  2.00
   2  8.32
   3 -1.09
 INTERVAL  21, NUMBER OF STORMS   6
 STORM RESPONSES, (1ST IS FLOATED INTEGER GIVING NUMBER OF STORMS
PRESENT)
   1  6.00
   2 12.00
   3  4.33
   4  1.61
   5 -6.02
   6  5.35
   7 16.59
 INTERVAL  22, NUMBER OF STORMS   0
 INTERVAL  23, NUMBER OF STORMS   1
 STORM RESPONSES, (1ST IS FLOATED INTEGER GIVING NUMBER OF STORMS
PRESENT)
   1  1.00
   2  1.36
 INTERVAL  24, NUMBER OF STORMS   4
 STORM RESPONSES, (1ST IS FLOATED INTEGER GIVING NUMBER OF STORMS
PRESENT)
   1  4.00
   2  2.36
   3 -3.56
   4  2.12
   5 12.30
 INTERVAL  25, NUMBER OF STORMS   3
 STORM RESPONSES, (1ST IS FLOATED INTEGER GIVING NUMBER OF STORMS
PRESENT)
   1  3.00
   2  0.73
   3 12.47
   4  2.01
 INTERVAL  26, NUMBER OF STORMS   2
 STORM RESPONSES, (1ST IS FLOATED INTEGER GIVING NUMBER OF STORMS
PRESENT)
   1  2.00
   2  5.28
   3 10.71
 INTERVAL  27, NUMBER OF STORMS   0
 INTERVAL  28, NUMBER OF STORMS   2
 STORM RESPONSES, (1ST IS FLOATED INTEGER GIVING NUMBER OF STORMS
PRESENT)
   1  2.00
   2  1.68
   3  0.41
 INTERVAL  29, NUMBER OF STORMS   3
 STORM RESPONSES, (1ST IS FLOATED INTEGER GIVING NUMBER OF STORMS
PRESENT)
   1  3.00
   2  5.95
```

```
   3  7.52
   4 -23.07
 INTERVAL  30, NUMBER OF STORMS   0
 INTERVAL  31, NUMBER OF STORMS   3
 STORM RESPONSES, (1ST IS FLOATED INTEGER GIVING NUMBER OF STORMS
PRESENT)
   1  3.00
   2  13.95
   3  2.92
   4  2.11
 INTERVAL  32, NUMBER OF STORMS   5
 STORM RESPONSES, (1ST IS FLOATED INTEGER GIVING NUMBER OF STORMS
PRESENT)
   1  5.00
   2  2.53
   3  10.39
   4  1.14
   5  4.79
   6  5.99
 INTERVAL  33, NUMBER OF STORMS   6
 STORM RESPONSES, (1ST IS FLOATED INTEGER GIVING NUMBER OF STORMS
PRESENT)
   1  6.00
   2  4.76
   3  7.90
   4 -1.65
   5  0.89
   6  3.51
   7 -3.36
 INTERVAL  34, NUMBER OF STORMS   1
 STORM RESPONSES, (1ST IS FLOATED INTEGER GIVING NUMBER OF STORMS
PRESENT)
   1  1.00
   2  11.42
 INTERVAL  35, NUMBER OF STORMS   3
 STORM RESPONSES, (1ST IS FLOATED INTEGER GIVING NUMBER OF STORMS
PRESENT)
   1  3.00
   2 -3.18
   3  6.19
   4  6.67
 INTERVAL  36, NUMBER OF STORMS   1
 STORM RESPONSES, (1ST IS FLOATED INTEGER GIVING NUMBER OF STORMS
PRESENT)
   1  1.00
   2  5.73
 INTERVAL  37, NUMBER OF STORMS   1
 STORM RESPONSES, (1ST IS FLOATED INTEGER GIVING NUMBER OF STORMS
PRESENT)
   1  1.00
   2 -21.23
 INTERVAL  38, NUMBER OF STORMS   5
 STORM RESPONSES, (1ST IS FLOATED INTEGER GIVING NUMBER OF STORMS
PRESENT)
   1  5.00
   2  1.53
   3  6.24
   4  1.32
   5  0.37
   6  5.88

 INTERVAL  39, NUMBER OF STORMS   3
```

```
 STORM RESPONSES, (1ST IS FLOATED INTEGER GIVING NUMBER OF STORMS
PRESENT)
   1  3.00
   2 -25.27
   3 -24.14
   4 -24.05
 INTERVAL  40, NUMBER OF STORMS   1
 STORM RESPONSES, (1ST IS FLOATED INTEGER GIVING NUMBER OF STORMS
PRESENT)
   1  1.00
   2 -25.68
 INTERVAL  41, NUMBER OF STORMS   4
 STORM RESPONSES, (1ST IS FLOATED INTEGER GIVING NUMBER OF STORMS
PRESENT)
   1  4.00
   2  1.63
   3  5.69
   4  8.53
   5  5.53
 INTERVAL  42, NUMBER OF STORMS   1
 STORM RESPONSES, (1ST IS FLOATED INTEGER GIVING NUMBER OF STORMS
PRESENT)
   1  1.00
   2 -4.21
 INTERVAL  43, NUMBER OF STORMS   1
 STORM RESPONSES, (1ST IS FLOATED INTEGER GIVING NUMBER OF STORMS
PRESENT)
   1  1.00
   2  1.30
 INTERVAL  44, NUMBER OF STORMS   2
 STORM RESPONSES, (1ST IS FLOATED INTEGER GIVING NUMBER OF STORMS
PRESENT)
   1  2.00
   2 -20.10
   3 -3.23
 INTERVAL  45, NUMBER OF STORMS   4
 STORM RESPONSES, (1ST IS FLOATED INTEGER GIVING NUMBER OF STORMS
PRESENT)
   1  4.00
   2 -25.37
   3  3.45
   4  11.45
   5 -0.34
 INTERVAL  46, NUMBER OF STORMS   4
 STORM RESPONSES, (1ST IS FLOATED INTEGER GIVING NUMBER OF STORMS
PRESENT)
   1  4.00
   2  1.25
   3  11.08
   4  1.58
   5 -21.15
 INTERVAL  47, NUMBER OF STORMS   0

 INTERVAL  48, NUMBER OF STORMS   3
 STORM RESPONSES, (1ST IS FLOATED INTEGER GIVING NUMBER OF STORMS
PRESENT)
   1  3.00
   2 -2.94
   3 -2.86
   4  4.71
 INTERVAL  49, NUMBER OF STORMS   1
 STORM RESPONSES, (1ST IS FLOATED INTEGER GIVING NUMBER OF STORMS
PRESENT)
```

```
   1  1.00
   2  16.73
 INTERVAL   50, NUMBER OF STORMS    4
 STORM RESPONSES, (1ST IS FLOATED INTEGER GIVING NUMBER OF STORMS
PRESENT)
   1  4.00
   2  12.29
   3  12.23
   4  3.15
   5  4.67

 Run Number 2:
 ------------
 ********************************************
 SIMULATION NUMBER =     2  SEED NUMBER:          1438
   42951
 INTERVAL    1, NUMBER OF STORMS    3
 STORM RESPONSES, (1ST IS FLOATED INTEGER GIVING NUMBER OF STORMS
PRESENT)
   1  3.00
   2  -0.33
   3  13.83
   4 -27.86
 INTERVAL    2, NUMBER OF STORMS    3
 STORM RESPONSES, (1ST IS FLOATED INTEGER GIVING NUMBER OF STORMS
PRESENT)
   1  3.00
   2  5.50
   3  12.23
   4  2.91
 INTERVAL    3, NUMBER OF STORMS    2
 STORM RESPONSES, (1ST IS FLOATED INTEGER GIVING NUMBER OF STORMS
PRESENT)
   1  2.00
   2  -0.35
   3  6.70
 INTERVAL    4, NUMBER OF STORMS    2
 STORM RESPONSES, (1ST IS FLOATED INTEGER GIVING NUMBER OF STORMS
PRESENT)
   1  2.00
   2  -2.99
   3 -20.92

 INTERVAL    5, NUMBER OF STORMS    7
 STORM RESPONSES, (1ST IS FLOATED INTEGER GIVING NUMBER OF STORMS
PRESENT)
   1  7.00
   2  1.59
   3  -2.08
   4  -4.14
   5  11.99
   6  3.78
   7  1.29
   8  4.37
 INTERVAL    6, NUMBER OF STORMS    2
 STORM RESPONSES, (1ST IS FLOATED INTEGER GIVING NUMBER OF STORMS
PRESENT)
   1  2.00
   2  2.28
   3  -6.33
 INTERVAL    7, NUMBER OF STORMS    3
```

```
 STORM RESPONSES, (1ST IS FLOATED INTEGER GIVING NUMBER OF STORMS
PRESENT)
   1  3.00
   2  2.99
   3 -3.74
   4 -22.85
 INTERVAL   8, NUMBER OF STORMS   2
 STORM RESPONSES, (1ST IS FLOATED INTEGER GIVING NUMBER OF STORMS
PRESENT)
   1  2.00
   2 -2.58
   3 -2.68
 INTERVAL   9, NUMBER OF STORMS   2
 STORM RESPONSES, (1ST IS FLOATED INTEGER GIVING NUMBER OF STORMS
PRESENT)
   1  2.00
   2 -1.30
   3 12.25
 INTERVAL  10, NUMBER OF STORMS   2
 STORM RESPONSES, (1ST IS FLOATED INTEGER GIVING NUMBER OF STORMS
PRESENT)
   1  2.00
   2  2.78
   3 10.89
 INTERVAL  11, NUMBER OF STORMS   0
 INTERVAL  12, NUMBER OF STORMS   1
 STORM RESPONSES, (1ST IS FLOATED INTEGER GIVING NUMBER OF STORMS
PRESENT)
   1  1.00
   2 -3.93
 INTERVAL  13, NUMBER OF STORMS   3
 STORM RESPONSES, (1ST IS FLOATED INTEGER GIVING NUMBER OF STORMS
PRESENT)
   1  3.00
   2  2.02
   3 10.95
   4  3.28

 INTERVAL  14, NUMBER OF STORMS   6
 STORM RESPONSES, (1ST IS FLOATED INTEGER GIVING NUMBER OF STORMS
PRESENT)
   1  6.00
   2  2.38
   3 -5.91
   4  3.52
   5  1.68
   6 -1.43
   7  5.61
 INTERVAL  15, NUMBER OF STORMS   1
 STORM RESPONSES, (1ST IS FLOATED INTEGER GIVING NUMBER OF STORMS
PRESENT)
   1  1.00
   2  0.95
 INTERVAL  16, NUMBER OF STORMS   5
 STORM RESPONSES, (1ST IS FLOATED INTEGER GIVING NUMBER OF STORMS
PRESENT)
   1  5.00
   2  1.75
   3  4.13
   4  1.79
   5  2.16
   6 -0.70
 INTERVAL  17, NUMBER OF STORMS   4
```

```
 STORM RESPONSES, (1ST IS FLOATED INTEGER GIVING NUMBER OF STORMS
PRESENT)
   1  4.00
   2  4.88
   3  1.44
   4 -0.28
   5  3.72
 INTERVAL  18, NUMBER OF STORMS   3
 STORM RESPONSES, (1ST IS FLOATED INTEGER GIVING NUMBER OF STORMS
PRESENT)
   1  3.00
   2  8.15
   3 -1.52
   4  5.01
 INTERVAL  19, NUMBER OF STORMS   2
 STORM RESPONSES, (1ST IS FLOATED INTEGER GIVING NUMBER OF STORMS
PRESENT)
   1  2.00
   2 -0.49
   3 -0.99
 INTERVAL  20, NUMBER OF STORMS   0
 INTERVAL  21, NUMBER OF STORMS   2
 STORM RESPONSES, (1ST IS FLOATED INTEGER GIVING NUMBER OF STORMS
PRESENT)
   1  2.00
   2 -2.53
   3 -0.92

 INTERVAL  22, NUMBER OF STORMS   3
 STORM RESPONSES, (1ST IS FLOATED INTEGER GIVING NUMBER OF STORMS
PRESENT)
   1  3.00
   2  2.46
   3 -24.48
   4  5.48
 INTERVAL  23, NUMBER OF STORMS   2
 STORM RESPONSES, (1ST IS FLOATED INTEGER GIVING NUMBER OF STORMS
PRESENT)
   1  2.00
   2 10.92
   3 -27.65
 INTERVAL  24, NUMBER OF STORMS   2
 STORM RESPONSES, (1ST IS FLOATED INTEGER GIVING NUMBER OF STORMS
PRESENT)
   1  2.00
   2  1.96
   3  4.14
 INTERVAL  25, NUMBER OF STORMS   3
 STORM RESPONSES, (1ST IS FLOATED INTEGER GIVING NUMBER OF STORMS
PRESENT)
   1  3.00
   2 -21.57
   3  4.65
   4  2.87
 INTERVAL  26, NUMBER OF STORMS   5
 STORM RESPONSES, (1ST IS FLOATED INTEGER GIVING NUMBER OF STORMS
PRESENT)
   1  5.00
   2 17.59
   3  2.29
   4  0.98
   5 15.43
```

```
   6  10.42
 INTERVAL   27, NUMBER OF STORMS    2
 STORM RESPONSES, (1ST IS FLOATED INTEGER GIVING NUMBER OF STORMS
PRESENT)
   1   2.00
   2   2.17
   3  -3.34
 INTERVAL   28, NUMBER OF STORMS    3
 STORM RESPONSES, (1ST IS FLOATED INTEGER GIVING NUMBER OF STORMS
PRESENT)
   1   3.00
   2  11.49
   3  12.70
   4   0.79
 INTERVAL   29, NUMBER OF STORMS    3
 STORM RESPONSES, (1ST IS FLOATED INTEGER GIVING NUMBER OF STORMS
PRESENT)
   1   3.00
   2  -6.33
   3   7.95
   4   1.18

 INTERVAL   30, NUMBER OF STORMS    3
 STORM RESPONSES, (1ST IS FLOATED INTEGER GIVING NUMBER OF STORMS
PRESENT)
   1   3.00
   2  -2.77
   3  -5.08
   4   1.31
 INTERVAL   31, NUMBER OF STORMS    3
 STORM RESPONSES, (1ST IS FLOATED INTEGER GIVING NUMBER OF STORMS
PRESENT)
   1   3.00
   2   3.80
   3  11.89
   4 -21.67
 INTERVAL   32, NUMBER OF STORMS    0
 INTERVAL   33, NUMBER OF STORMS    4
 STORM RESPONSES, (1ST IS FLOATED INTEGER GIVING NUMBER OF STORMS
PRESENT)
   1   4.00
   2   1.28
   3   5.47
   4   1.93
   5   7.55
 INTERVAL   34, NUMBER OF STORMS    4
 STORM RESPONSES, (1ST IS FLOATED INTEGER GIVING NUMBER OF STORMS
PRESENT)
   1   4.00
   2   2.07
   3  -2.35
   4   1.40
   5  -4.25
 INTERVAL   35, NUMBER OF STORMS    1
 STORM RESPONSES, (1ST IS FLOATED INTEGER GIVING NUMBER OF STORMS
PRESENT)
   1   1.00
   2  -0.83
 INTERVAL   36, NUMBER OF STORMS    3
 STORM RESPONSES, (1ST IS FLOATED INTEGER GIVING NUMBER OF STORMS
PRESENT)
   1   3.00
   2  12.93
```

```
   3 -0.91
   4 10.33
 INTERVAL  37, NUMBER OF STORMS   4
 STORM RESPONSES, (1ST IS FLOATED INTEGER GIVING NUMBER OF STORMS
PRESENT)
   1  4.00
   2 -18.52
   3  8.39
   4 -18.41
   5  1.02

 INTERVAL  38, NUMBER OF STORMS   3
 STORM RESPONSES, (1ST IS FLOATED INTEGER GIVING NUMBER OF STORMS
PRESENT)
   1  3.00
   2  1.63
   3  5.47
   4  11.94
 INTERVAL  39, NUMBER OF STORMS   2
 STORM RESPONSES, (1ST IS FLOATED INTEGER GIVING NUMBER OF STORMS
PRESENT)
   1  2.00
   2 -3.01
   3 -0.80
 INTERVAL  40, NUMBER OF STORMS   3
 STORM RESPONSES, (1ST IS FLOATED INTEGER GIVING NUMBER OF STORMS
PRESENT)
   1  3.00
   2  1.65
   3 -3.38
   4  6.01
 INTERVAL  41, NUMBER OF STORMS   4
 STORM RESPONSES, (1ST IS FLOATED INTEGER GIVING NUMBER OF STORMS
PRESENT)
   1  4.00
   2  1.43
   3  2.27
   4  1.68
   5  4.72
 INTERVAL  42, NUMBER OF STORMS   2
 STORM RESPONSES, (1ST IS FLOATED INTEGER GIVING NUMBER OF STORMS
PRESENT)
   1  2.00
   2 -28.12
   3 -4.39
 INTERVAL  43, NUMBER OF STORMS   1
 STORM RESPONSES, (1ST IS FLOATED INTEGER GIVING NUMBER OF STORMS
PRESENT)
   1  1.00
   2 -25.52
 INTERVAL  44, NUMBER OF STORMS   3
 STORM RESPONSES, (1ST IS FLOATED INTEGER GIVING NUMBER OF STORMS
PRESENT)
   1  3.00
   2  4.25
   3  3.12
   4 -0.31
 INTERVAL  45, NUMBER OF STORMS   1
 STORM RESPONSES, (1ST IS FLOATED INTEGER GIVING NUMBER OF STORMS
PRESENT)
   1  1.00
   2  0.67
```

```
 INTERVAL  46, NUMBER OF STORMS   1
 STORM RESPONSES, (1ST IS FLOATED INTEGER GIVING NUMBER OF STORMS
PRESENT)
   1  1.00
   2 -2.62


 INTERVAL  47, NUMBER OF STORMS   3
 STORM RESPONSES, (1ST IS FLOATED INTEGER GIVING NUMBER OF STORMS
PRESENT)
   1  3.00
   2 -16.98
   3 -5.43
   4 -2.98
 INTERVAL  48, NUMBER OF STORMS   1
 STORM RESPONSES, (1ST IS FLOATED INTEGER GIVING NUMBER OF STORMS
PRESENT)
   1  1.00
   2  16.31
 INTERVAL  49, NUMBER OF STORMS   1
 STORM RESPONSES, (1ST IS FLOATED INTEGER GIVING NUMBER OF STORMS
PRESENT)
   1  1.00
   2 -3.32
 INTERVAL  50, NUMBER OF STORMS   2
 STORM RESPONSES, (1ST IS FLOATED INTEGER GIVING NUMBER OF STORMS
PRESENT)
   1  2.00
   2  5.66
   3 -1.45
```

An array {RJYI(I,J,K); I=1, NRES; J=1, NYI; K=MAXNYI+1} is available within the code at the end of each run. This can be saved to an output file for further processing at the discretion of the user. A listing of RJYI (restricted to I=1) for the example is shown in Table 13 on the following pages, along with some summary statistics. The first column of RJYI contains a floated integer giving the number of storms in the interval tabulated on the row. Subsequent columns give the responses. The number of columns in the array is MAXNYI+1=16, but only the first eight columns are tabled since the maximum number of storms in all runs is seven for this data set.

Table 13: RJYI for the Example

```
Run Number 1:
-------------
0.00      0.00      0.00      0.00      0.00      0.00      0.00      0.00
2.00     -2.59      6.68      0.00      0.00      0.00      0.00      0.00
2.00      0.12      2.58      0.00      0.00      0.00      0.00      0.00
3.00     13.60      4.28     11.51      0.00      0.00      0.00      0.00
2.00     -5.87      5.12      0.00      0.00      0.00      0.00      0.00
4.00    -29.28     -1.06     -2.56     -2.87      0.00      0.00      0.00
2.00      1.07     -5.50      0.00      0.00      0.00      0.00      0.00
2.00      7.78      1.43      0.00      0.00      0.00      0.00      0.00
2.00      6.26      1.38      0.00      0.00      0.00      0.00      0.00
4.00      3.55    -18.53     -1.38     -0.27      0.00      0.00      0.00
1.00     -2.37      0.00      0.00      0.00      0.00      0.00      0.00
1.00      1.05      0.00      0.00      0.00      0.00      0.00      0.00
1.00     10.15      0.00      0.00      0.00      0.00      0.00      0.00
7.00      3.32      2.26      3.61      9.98     -3.64      1.64      6.10
5.00      3.43     12.15      9.36     15.76      1.94      0.00      0.00
```

```
3.00    -5.99     4.71     3.06     0.00     0.00     0.00     0.00
1.00   -26.01     0.00     0.00     0.00     0.00     0.00     0.00
1.00    16.74     0.00     0.00     0.00     0.00     0.00     0.00
3.00    12.00     5.53     1.35     0.00     0.00     0.00     0.00
2.00     8.32    -1.09     0.00     0.00     0.00     0.00     0.00
6.00    12.00     4.33     1.61    -6.02     5.35    16.59     0.00
0.00     0.00     0.00     0.00     0.00     0.00     0.00     0.00
1.00     1.36     0.00     0.00     0.00     0.00     0.00     0.00
4.00     2.36    -3.56     2.12    12.30     0.00     0.00     0.00
3.00     0.73    12.47     2.01     0.00     0.00     0.00     0.00
2.00     5.28    10.71     0.00     0.00     0.00     0.00     0.00
0.00     0.00     0.00     0.00     0.00     0.00     0.00     0.00
2.00     1.68     0.41     0.00     0.00     0.00     0.00     0.00
3.00     5.95     7.52   -23.07     0.00     0.00     0.00     0.00
0.00     0.00     0.00     0.00     0.00     0.00     0.00     0.00
3.00    13.95     2.92     2.11     0.00     0.00     0.00     0.00
5.00     2.53    10.39     1.14     4.79     5.99     0.00     0.00
6.00     4.76     7.90    -1.65     0.89     3.51    -3.36     0.00
1.00    11.42     0.00     0.00     0.00     0.00     0.00     0.00
3.00    -3.18     6.19     6.67     0.00     0.00     0.00     0.00
1.00     5.73     0.00     0.00     0.00     0.00     0.00     0.00
1.00   -21.23     0.00     0.00     0.00     0.00     0.00     0.00
5.00     1.53     6.24     1.32     0.37     5.88     0.00     0.00
3.00   -25.27   -24.14   -24.05     0.00     0.00     0.00     0.00
1.00   -25.68     0.00     0.00     0.00     0.00     0.00     0.00
4.00     1.63     5.69     8.53     5.53     0.00     0.00     0.00
1.00    -4.21     0.00     0.00     0.00     0.00     0.00     0.00
1.00     1.30     0.00     0.00     0.00     0.00     0.00     0.00
2.00   -20.10    -3.23     0.00     0.00     0.00     0.00     0.00
4.00   -25.37     3.45    11.45    -0.34     0.00     0.00     0.00
4.00     1.25    11.08     1.58   -21.15     0.00     0.00     0.00
0.00     0.00     0.00     0.00     0.00     0.00     0.00     0.00
3.00    -2.94    -2.86     4.71     0.00     0.00     0.00     0.00
1.00    16.73     0.00     0.00     0.00     0.00     0.00     0.00
4.00    12.29    12.23     3.15     4.67     0.00     0.00     0.00
MINIMUM RESPONSE PER RUN =    -29.27754
MAXIMUM RESPONSE PER RUN =     16.73644
MEAN RESPONSE PER RUN =       1.34144
ST.DEV. RESPONSE PER RUN =     9.78985

Run Number 2:
-------------
3.00    -0.33    13.83   -27.86     0.00     0.00     0.00     0.00
3.00     5.50    12.23     2.91     0.00     0.00     0.00     0.00
2.00    -0.35     6.70     0.00     0.00     0.00     0.00     0.00
2.00    -2.99   -20.92    11.51     0.00     0.00     0.00     0.00
7.00     1.59    -2.08    -4.14    11.99     3.78     1.29     4.37
2.00     2.28    -6.33    -2.56    -2.87     0.00     0.00     0.00
3.00     2.99    -3.74   -22.85     0.00     0.00     0.00     0.00
2.00    -2.58    -2.68     0.00     0.00     0.00     0.00     0.00
2.00    -1.30    12.25     0.00     0.00     0.00     0.00     0.00
2.00     2.78    10.89    -1.38    -0.27     0.00     0.00     0.00
0.00    -2.37     0.00     0.00     0.00     0.00     0.00     0.00
1.00    -3.93     0.00     0.00     0.00     0.00     0.00     0.00
3.00     2.02    10.95     3.28     0.00     0.00     0.00     0.00
6.00     2.38    -5.91     3.52     1.68    -1.43     5.61     6.10
1.00     0.95    12.15     9.36    15.76     1.94     0.00     0.00
5.00     1.75     4.13     1.79     2.16    -0.70     0.00     0.00
4.00     4.88     1.44    -0.28     3.72     0.00     0.00     0.00
3.00     8.15    -1.52     5.01     0.00     0.00     0.00     0.00
2.00    -0.49    -0.99     1.35     0.00     0.00     0.00     0.00
0.00     8.32    -1.09     0.00     0.00     0.00     0.00     0.00
2.00    -2.53    -0.92     1.61    -6.02     5.35    16.59     0.00
3.00     2.46   -24.48     5.48     0.00     0.00     0.00     0.00
2.00    10.92   -27.65     0.00     0.00     0.00     0.00     0.00
2.00     1.96     4.14     2.12    12.30     0.00     0.00     0.00
```

```
3.00   -21.57     4.65     2.87     0.00     0.00     0.00     0.00
5.00    17.59     2.29     0.98    15.43    10.42     0.00     0.00
2.00     2.17    -3.34     0.00     0.00     0.00     0.00     0.00
3.00    11.49    12.70     0.79     0.00     0.00     0.00     0.00
3.00    -6.33     7.95     1.18     0.00     0.00     0.00     0.00
3.00    -2.77    -5.08     1.31     0.00     0.00     0.00     0.00
3.00     3.80    11.89   -21.67     0.00     0.00     0.00     0.00
0.00     2.53    10.39     1.14     4.79     5.99     0.00     0.00
4.00     1.28     5.47     1.93     7.55     3.51    -3.36     0.00
4.00     2.07    -2.35     1.40    -4.25     0.00     0.00     0.00
1.00    -0.83     6.19     6.67     0.00     0.00     0.00     0.00
3.00    12.93    -0.91    10.33     0.00     0.00     0.00     0.00
4.00   -18.52     8.39   -18.41     1.02     0.00     0.00     0.00
3.00     1.63     5.47    11.94     0.37     5.88     0.00     0.00
2.00    -3.01    -0.80   -24.05     0.00     0.00     0.00     0.00
3.00     1.65    -3.38     6.01     0.00     0.00     0.00     0.00
4.00     1.43     2.27     1.68     4.72     0.00     0.00     0.00
2.00   -28.12    -4.39     0.00     0.00     0.00     0.00     0.00
1.00   -25.52     0.00     0.00     0.00     0.00     0.00     0.00
3.00     4.25     3.12    -0.31     0.00     0.00     0.00     0.00
1.00     0.67     3.45    11.45    -0.34     0.00     0.00     0.00
1.00    -2.62    11.08     1.58   -21.15     0.00     0.00     0.00
3.00   -16.98    -5.43    -2.98     0.00     0.00     0.00     0.00
1.00    16.31    -2.86     4.71     0.00     0.00     0.00     0.00
1.00    -3.32     0.00     0.00     0.00     0.00     0.00     0.00
2.00     5.66    -1.45     3.15     4.67     0.00     0.00     0.00
MINIMUM RESPONSE PER RUN =    -28.11612
MAXIMUM RESPONSE PER RUN =     17.59286
MEAN RESPONSE PER RUN =       0.29264
ST.DEV. RESPONSE PER RUN =     9.11051
```

Discussion of the Example Output

Although the example is way too small and quite artificial, it is interesting to compare the data from Table 11 with the simulation. The mean and standard deviation of the response, *R*, after incorporating the probabilities shown in Figure 11 are

Input Data Average = 0.6097

Input Data Standard Deviation = 9.3211

The simulation responses in Table 13 when both runs are combined give

Simulation Average = 1.3032

Simulation Standard Deviation = 9.9967

This is quite good agreement between data and simulation.

Another comparison is given in Figure 12, where the input Poisson probabilities with mean = 2.5 are shown above, and the frequency histogram of simulated number of storms per time interval (1 year) are graphed below. The curves compare visually quite well.

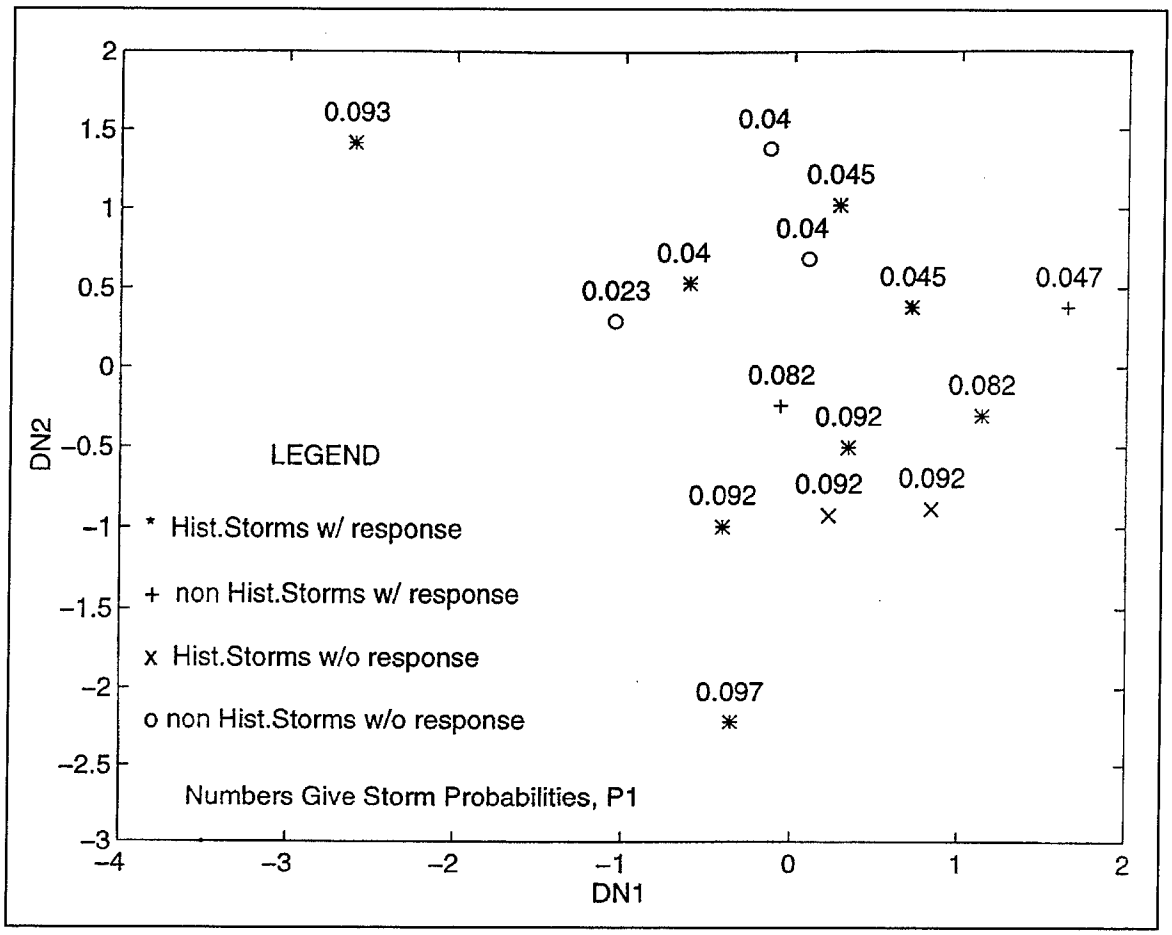

Figure 11. Enhanced probabilities

Many such comparisons could be developed. However, considering the simplistic nature of the example, it does not seem desirable to carry these much further. Also, the present computer is an interim version that almost immediately will be upgraded with many enhancements to EST Version 4.1.

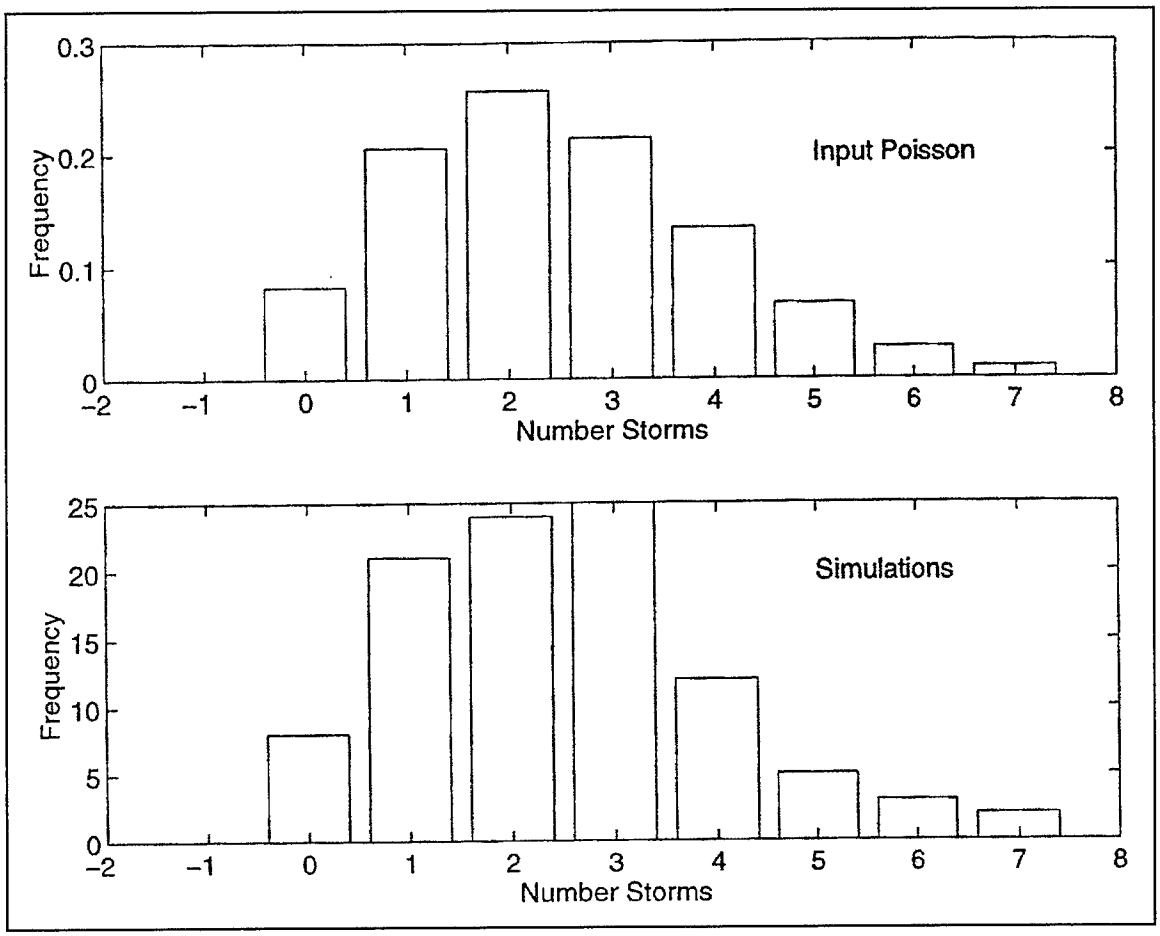

Figure 12. Comparison of number of storms for input and simulations

4 EST Implementation

Implementation of the EST requires the user to define specific input and response vectors particular to the project and the associated boundary conditions. Input vectors are generally obtained through analysis of storm track data, the Wave Information Study (WIS) hindcast, the National Weather Service (NWS), the United States Geological Survey (USGS), the National Ocean Survey (NOS), and other similar sources of environmental boundary conditions. Response vectors, as stated above, reflect the impacts of each specific event at each specific location. In most cases, response vectors are generated through application of numerical models; however, if archived data are available for historic events for an adequate length of time, these data can be used directly. In the following sections, specific input and response vectors are described and possible sources are presented.

Input Vectors

Input vectors are specific to the event type (i.e., tropical or extratropical surge, flooding, other) and the primary mechanism of effect (i.e., wave dominated, surge dominated, rainfall dominated, etc.). In the following tables (Tables 14 and 15), input vectors that have been used for specific projects are listed under event types. These lists are not necessarily complete, and some vectors should not be used for certain applications, as will be noted later in the applications section.

Table 14 Tropical Event Input Vectors

1. DST: Some measure of distance of the eye of the hurricane to the location of interest. The distance has been defined as the minimum distance between the eye and station during the propagation of the storm.

2. P0: Central pressure of the storm, usually measured at the DST location of the storm.

3. VEL: Forward velocity of the eye of the storm at DST.

4. ANG: Angle of propagation of the eye of the storm measured from DST.

5. R0: Radius to maximum wind of the hurricane measured at DST.

6. TIDE: Some measure of the tide with which the surge has been combined or has occurred in conjunction with. For example, in some cases the surge can be linearly added to the primary tidal constituent (M_2) amplitude to give a surge at high tide. Usually, the above vectors are specified for four phases of the tide so that each event yields four sets of input vectors corresponding to high tide, mean tide at peak ebb, low tide, and mean tide at peak flood.

7. Q: Discharge or stage of possible inflow tributaries if they significantly contribute to the response vector of interest, flood stage for example.

8. RF: Rainfall over the basin during the event if rainfall represents a significant contribution to the response vector.

9. H,T: Deepwater wave height and period define nearshore wave-induced setup. In many applications, setup can represent a significant contribution to the total surface elevation. Additionally, subaqueous sediment transport is a function of both surge-induced currents and wave-orbital velocities. Therefore, in some applications, wave conditions should be represented in input vector space.

Extratropical events cannot be readily parameterized in a manner similar to tropical storms. This is primarily due to their large area of influence and the fact that waves, pressure deficit, and maximum winds are not extreme; they just persist for long periods of time. Therefore, extratropical input vectors need to be carefully selected to represent components of the specific study. Table 15 lists some vectors specified in recent investigations. As with tropical events, the list is not intended to be complete but to provide guidance for input vector selection.

Table 15 Extratropical Event Input Vectors

1. TIDE: Extratropical events typically occur over several diurnal or semidiurnal tide cycles. Therefore, in order to account for tide/surge interaction, four-phase amplitudes associated with the spring/neap cycle have been used. Then, as with the tropical events, the surge can be linearly added to spring/neap amplitude to indicate total surface elevation at four phases of the lunar cycle.

2. DUR: Impact from extratropical events is primarily due to the duration of the storm, not the magnitude of the surge. Therefore, some measure of storm duration above some threshold value should be specified as an input vector. One choice is the number of hours during which the surge is greater than 0.3 m.

3. Q: Discharge or stage of possible inflow tributaries if they significantly contribute to the response vector of interest, flood stage for example.

4. RF: Rainfall over the basin during the event if rainfall represents a significant contribution to the response vector.

5. H,T: Deepwater wave height and period define nearshore wave-induced setup. In many applications, setup can represent a significant contribution to the total surface elevation. Additionally, subaqueous sediment transport is a function of both surge-induced currents and wave-orbital velocities. Therefore, in some applications, wave conditions should be represented in input vector space.

6. VMAX: The maximum depth-averaged current has been specified as an indication of peak sediment transport. Although this parameter can easily occur at negative surge (drawdown), it is a primary factor in subaqueous erosion.

The above tables represent tropical and extratropical event input vectors used in past and present applications. Future applications may require additional vectors. For example, if the grain size of a beach fill disposal mound is being evaluated for response to storm surge, then grain size D_0 should be included as an input vector. In many cases, a sensitivity analysis of the input vector space should be conducted to determine the appropriateness of the specified vector space. If the defined space is not well posed such that the response vector is not well correlated with the input vectors, the standard deviations of the resulting frequency relationships will be excessive. In this case, some of the input vectors may need to be eliminated or more descriptive vectors added.

Response Vectors

Response vectors represent some measure of impact from the passage of the storm. These vectors are used to define the variable for which response versus frequency-of-occurrence relationships are generated. These frequency relationships provide a measure of design effectiveness for storm events of some measurable intensity. For example, an X-ft-high levee provides protection against the N-year event or a dredged disposal cap X ft thick will not be eroded in 30 ft of water by a N-year event. These measures of effectiveness and the corresponding uncertainty analysis provide the necessary input for selecting cost-effective coastal designs.

Typical response vectors, and their corresponding frequency-of-occurrence relationships, specified in recent or anticipated studies include the following:

a. Maximum water surface elevations have been used to evaluate the effectiveness of existing and proposed dune heights to reduce back-bay flooding. Surface elevations are also used to optimize levee heights and locations in low-elevation river deltas. An additional application is to determine realistic stage-frequency relationships for areas at which

insufficient prototype data are available to compute frequency relationships. Applications of this nature can be used to define frequency-indexed inundation maps for use in developing evacuation criteria.

b. Maximum shoreline/dune recession values are routinely used to provide frequency-indexed design criteria to evaluate various beach renourishment templates. Recession data can also provide information on the erodibility of beaches and dunes renourished with material of differing grain size.

c. Vertical erosion of subaqueous disposed dredged material mounds have been used to develop frequency criteria to provide guidance for designing, locating, and/or optimizing Offshore Dredged Material Disposal Sites (ODMDS). For example, vertical erosion values are used for developing design criteria for capped disposal mounds. These computations can be used to optimize mound location, height, and cap thickness to withstand the 100-year event.

d. Salinity/water quality intrusion estimates can be used to optimize channel deepening. Locations at which an N-year event results in salinity or various water quality magnitudes that exceed some prescribed threshold can be used to optimize various channel or inlet modifications. These applications can also be used to evaluate future conditions by analyzing both the mean value distribution and the upper/lower spread of EST simulations to investigate the effect of wet or dry years on the system.

e. Sediment transport/deposition patterns can be used to estimate future patterns of erosion and deposition. These life-cycle simulations can be used to evaluate the effectiveness of inlet dredging or other modifications such as jetties or optimizing jetty length.

f. Current velocities as a function of storm surge in the vicinity of bridge piers can be frequency indexed and used to determine some measure of bridge scour.

Unfortunately, response vectors generally require numerical modeling efforts in order to develop a matrix of responses for a training set of storm events spanning a sufficient period of time for which a computed frequency relationship is meaningful. For example, although tropical event track data are available for the east coast of the United States, Gulf of Mexico, and Caribbean Sea since 1886, the distribution of surge elevations are only available at a few locations and then only for the last 20-30 years. In order to perform an EST-based frequency analysis, the surge elevations for all storms of the 112-year period of record that impacted the specific location of interest need to be available.

Fortunately, as will be discussed below, databases are available that contain much of this information for nearshore open-coast locations along the east coast,

Gulf of Mexico, and Caribbean Sea. In addition, tidal constituent databases are available for all coasts of the United States. These databases were developed for use as boundary conditions for models and can be directly used to develop open-coast stage-frequency relationships or used as input for external shoreline/dune recession models, subaqueous erosion models, or other appropriate response models. Listed below are databases available to the user to develop or partially develop EST input and response vector space.

Databases

The Coastal and Hydraulics Laboratory (CHL) of the U.S. Army Engineer Research and Development Center maintains a data archival system referred to as CEDARS (Coastal Engineering Data Retrieval System). CEDARS contains a considerable amount of information and data. A complete description of the contents can be accessed through the CHL homepage:

http://chl.wes.army.mil/

Data that may be directly used for developing input or response vectors or provide input to models that generate response vectors are summarized below.

Waves

The Wave Information Studies (WIS) hindcast database provides hindcast wave height, period, and direction data for specific locations along the Atlantic and Pacific oceans, the Gulf of Mexico, and the Great Lakes. For the Atlantic and Pacific oceans, the time series is from the WIS Phase II hindcast for the 20-year period of 1956-1975. The Gulf of Mexico Phase I hindcast is for the 20-year period of 1956-1975, and the Great Lakes Phase I are for the 32-year period of 1956-1987. The new Atlantic and Gulf of Mexico hindcast is now available for the 20-year period of 1976-1995. Hindcast data are provided at discrete open-ocean and nearshore stations at 3-hr increments. WIS hindcast information provides input to models such as SBEACH (Storm Induced BEAch CHange) for estimating shoreline/dune recession and LTFATE (Long Term FATE) for estimating subaqueous erosion.

Tidal constituent database

The Advanced CIRCulation (ADCIRC, Luettich, Westerink, and Scheffner 1992) model was used to generate tidal constituent databases for the east coast, Gulf of Mexico, and Caribbean Sea as well as for the eastern North Pacific Ocean. These databases were developed through the Dredging Research Program (DRP) of the U.S. Army Corps of Engineers. Each database contains constituent amplitudes and Greenwich epochs for both depth-averaged currents and surface elevations. The east coast database (Westerink, Luettich, and

Scheffner 1993) contains eight diurnal and semidiurnal astronomical constituents (K_1, O_1, P_1, Q_1, M_2, S_2, N_2, and K_2), while the Pacific database (Hench et al. 1994) contains five (K_1, O_1, M_2, S_2, and N_2). Both references given above contain co-tidal charts and summaries of comparison stations/error analysis. The tidal databases provide a user capability to generate a forecast/hindcast tidal time series at any location within the computational domain via interpolation between the nearest three nodes. The tidal databases can be used to generate time-series boundary forcing for other models or provide constituent input for the input vector space of surge studies.

Tropical storm-event database

A tropical storm database for the east and Gulf of Mexico coasts of the United States (Scheffner et al. 1994) was generated by reconstructing 134 historically based storm events selected from the National Oceanic and Atmospheric Administration (NOAA) National Hurricane Center's HURricane DATabase (HURDAT) of tropical storm events (Jarvinen, Neumann, and Davis 1988). These data were used to develop input to a Planetary Boundary Layer hurricane wind model that generates the spatial and temporal distribution of wind and pressure corresponding to each tropical event. These wind and pressure boundary condition data are input to the ADCIRC hydrodynamic model to compute nearshore surge elevation and current hydrographs corresponding to 486 discrete nearshore locations along the east coast and U.S. portion of the Gulf of Mexico. Tidal phase was not included in the storm-surge computations. Each hydrograph is contained in a database that can be accessed for subsequent use in any coastal study requiring tropical storm-surge data.

The east coast and Gulf of Mexico tropical event database was generated through the DRP. The report referenced above summarizes results of a numerical storm-surge study conducted for the east and Gulf of Mexico coasts of the United States. The report describes a database of surge elevations and currents produced from the numerical simulation of 134 historically based tropical storm events and their maximum water-level surge impact at 486 discrete locations along the east and Gulf coasts and Puerto Rico. A visual indication of the spatial distribution of peak surge elevation is provided in the form of an atlas of storm track and maximum storm surges corresponding to a 246-station nearshore subset of the 486-location database. The report contains cross reference tables of stations impacted by each event and the events impacting each station.

Software are provided with the EST program to access the HURDAT database and write a partial input vector file for each station computed at the point when the hurricane eye is closest to that station. Additional input vectors, such as wave height and period, tidal phase, peak velocity, sediment grain size, etc., as well as the response vector must be added by the user. A program that generates EST input files is provided as an example program for combining input and response vectors into a common EST input file. The example is used in the first of five example applications of the EST provided in the next chapter.

Extratropical storm database

An extratropical storm-event database was generated by using the U.S. Navy Fleet Numerical Meteorology and Oceanography Center's database of winds for the 16-year winter storm period (defined as September through March) of 1977 through 1993. These data are provided at 6-hr intervals on a 2.5° latitude and longitude grid. Those values were then interpolated onto the ADCIRC computational grid to compute an extratropical storm database consisting of surface elevation and current hydrographs at each of the 486 stations described above. The extratropical event database, also generated through the DRP, contains all severe events occurring during the 16-year sequence of winter months; however, unlike tropical events that are clearly distinguishable, identification of individual extratropical events within the records requires some additional analysis.

5 EST Applications

This section is provided to present some generalized steps that should be considered in any frequency analysis. For this report, the frequency analysis refers to tropical and extratropical storm events and their associated effects. Alternate applications to seasonal or epochal phenomena such as rainfall/runoff flood/drought, etc., will require alternate steps; however, the methodology is equally applicable. Although some of the following steps may prove to be unnecessary for a particular application, they provide a list of considerations to alert the user of potential data sources that may be necessary for conducting a study. The general guidelines are followed by detailed example studies that have been conducted using the EST approach. The examples illustrate the broad applicability of the approach to a variety of problems associated with storm-related effects. The examples also demonstrate that the study can be highly complex or made relatively simple. For example, the Fire Island study of Example 3 and the Samoa frequency analysis of Example 4 utilize mainframe computer facilities to generate the response vector data set. Examples 1 and 2 utilize existing databases of storm events and apply PC models to generate response vectors. In each example, however, the general step format is followed, although in some cases they are shown not to be necessary and their omission is noted.

Generalized Procedures

In all applications, several specific steps have to be performed, or at least considered, by the investigator in order to define the environmental forcings that affect the particular system. These necessarily precede the generation of frequency-of-occurrence relationships for the selected responses. These steps include the following:

Storm-event selection

Storms that have impacted the study area have to be identified from some database. In most applications, the HURDAT database for the Atlantic Ocean, Gulf of Mexico, and Caribbean Sea is ideal for the selection of tropical events.

Similar databases exist for subregions in the Pacific Ocean and Indian Ocean. The WIS databases can be used to identify periods of extratropical storm activity. For the east coast domain, tropical and extratropical storm hydrographs have been archived in CEDARS and can be directly downloaded.

Tidal conditions

In most applications, the phase and magnitude of the tidal contribution needs to be accounted for. The tidal constituent databases in CEDARS for the east and west coasts provide this information.

Wave conditions

Many applications require some specification of wave conditions. As in the tidal component, this information is available through the CEDARS databases. In some applications, other approaches can be used as will be demonstrated in the first example.

Storm-event hydrograph input

Finally, the storm event, tide, and wave conditions need to be used to generate input for models that generate response vectors for the problem of interest. In the simplest applications, the surge, tide, and wave conditions are combined to generate a site-specific hydrograph for each storm event of the tropical and extratropical event training set. Examples for developing these hydrographs are given in the first two examples.

In more complex applications, the storms identified in the first step and the tidal forcings identified in the second step are used to define wind field/pressure forcing input to the ADCIRC model (or other appropriate hydrodynamic model) to generate site-specific responses. Wave conditions, if necessary, are then separately defined at each computational node.

Response vector generation

The time-series input generated by either combining surge, tide, and wave conditions or identifying storms and using wave/pressure forcing are used to generate response vectors. For the first two examples, response models are used directly to generate response vectors from the time-series databases of the CEDARS. The last three examples use the ADCIRC model results to generate response vectors of maximum surge elevation as a function of historic events identified from the CEDARS. In all cases, response vectors are generated that correspond to the input vector set for each station and for each storm event.

EST life-cycle simulations

One final phase of the analysis is to generate multiple life-cycle time series of tropical and extratropical events. For alternate applications, water years, El Niño cycles, etc., can be generated. In the example applications provided below, tropical and extratropical events represent the cyclic pattern, and 100 repetitions of a 200-year sequence of events are simulated via the EST. This step involves construction of input files for the EST and specification of event frequency. For some applications, the generation of multiple life-cycle simulations is the desired product of the EST.

Frequency-of-occurrence computations

If the required product of the analysis is a frequency-of-occurrence relationship, the final step of the project is postprocessing of the life-cycle simulated EST output files to generate separate frequency-of-occurrence relationships for tropical and extratropical events. These two relationships can then be combined to produce a combined event frequency relationship and associated error estimate that can be used to define design criteria. The following examples provide typical applications of the EST to design problems.

Example 1: Mud Dump Dredged Material Disposal Site Analysis

The first example presented is a frequency-of-erosion study performed for the U.S. Army Engineer District, New York, as part of a site capacity study for the Mud Dump Disposal site located offshore of Sandy Hook, NJ. The Mud Dump Disposal site was the designated open-water dredged material disposal site for the Port of New York and New Jersey (NYNJ) when this study was conducted. Critical to the management of dredged material removed from the Port of NYNJ was the remaining capacity within the Mud Dump site. The procedures described in this example were used to determine mound heights and corresponding minimum water depths in which capped mounds can be placed without experiencing unacceptable amounts of vertical erosion. These computations directly influence the ultimate capacity of the Mud Dump site to contain contaminated dredged material.

At the time of this study, the Mud Dump Disposal site was virtually the only authorized site for open-water placement of dredged material from the Port of NYNJ. The site is a 1.12 by 2 nautical mile rectangle located approximately 6 nautical miles east of Sandy Hook, NJ (Figure 13), in an area known as the New York Bight. Water depths at the site range from less than 50 ft to over 90 ft. As of October 1994, up to 65 M yd^3 of dredged material (based on scow logs) have been placed in the site. Because the Mud Dump was the only available disposal site for fine-grained dredged material from the Port of NYNJ, the remaining capacity was an extremely important issue in the overall plan for

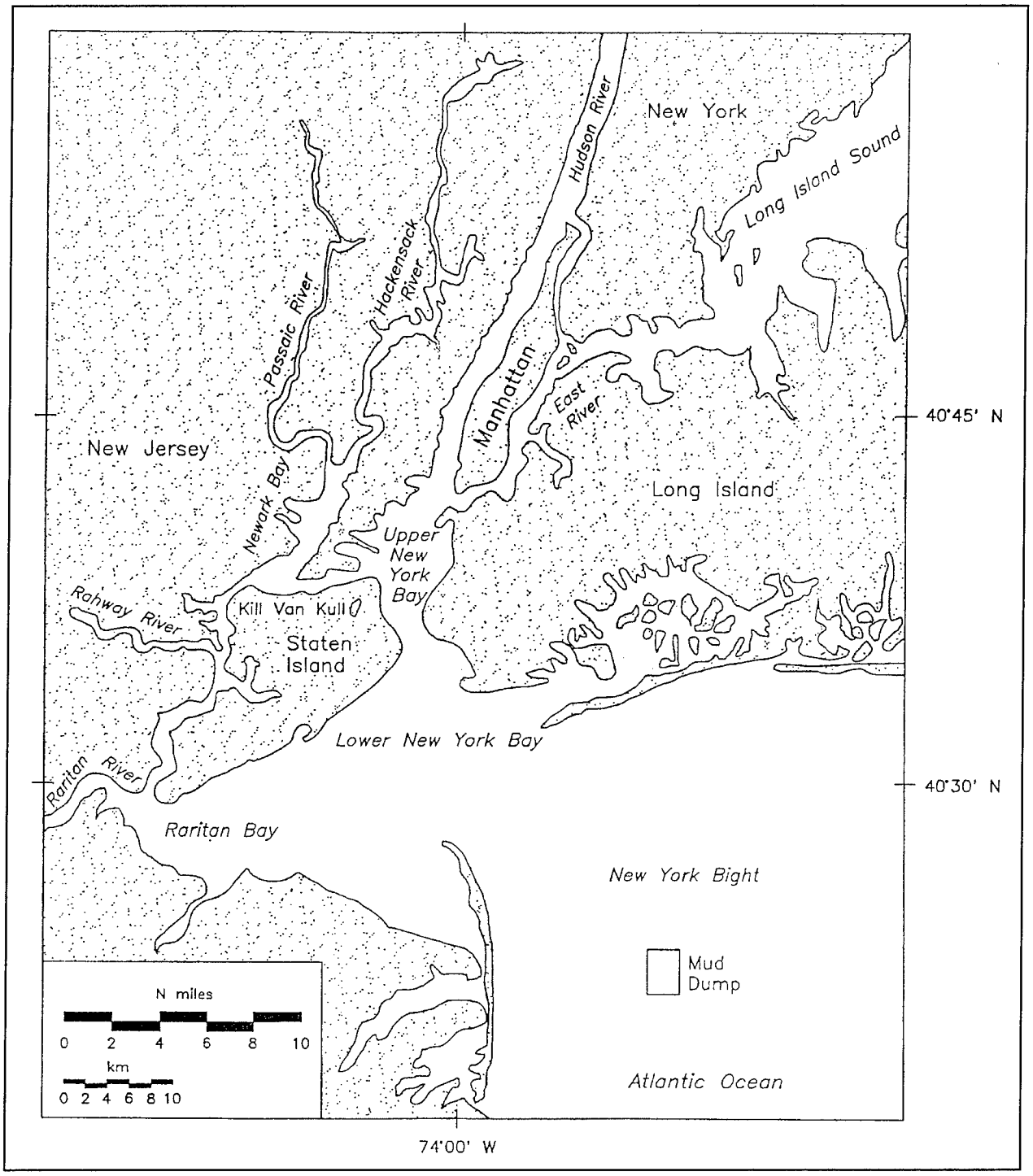

Figure 13. Mud Dump Disposal site location

managing dredging and disposal for the Port. Because of the large volume of contaminated material inside the port, the remaining capacity of the Mud Dump site for Category II (requiring special handling, i.e., capping for open-water

placement) dredged material (USEPA/USACE 1991) was critical in the sediment management process for the New York District and the Port of NYNJ.

At the request of the New York District, the U.S. Army Engineer Research and Development Center Coastal Engineering Research Center (CERC), presently part of the Coastal Hydraulics Laboratory, conducted a study to define the Mud Dump site capacity as well as other issues related to capping (Clausner, Scheffner, and Allison 1995). The most critical part of this effort was studies to compute the frequency-of-occurrence of vertical erosion for mounds of various elevations in the Mud Dump site. Previous studies have shown erosion of fine-grained materials from mound flanks as a result of severe northeasters (McDowell 1993; McDowell, May, and Pabst 1994). At the request of the New York District, mounds with cap elevations ranging from 50 to 75 ft were modeled, with ambient depths of 60 to 83 ft. The following sections detail the procedures implemented for the EST analysis.

Storm-event selection

The first step in a frequency-of-erosion study is to identify storms that have impacted the site of interest. For sites on the east coast, particularly the northeast coast, both tropical storms (hurricanes) and extratropical storms (northeasters) have to be included in the analysis. While the tropical storms often have higher winds, waves, and surge, the longer duration of the extratropical storms can produce vertical erosion of equal or greater magnitude than hurricanes. The following two subsections demonstrate the process for selecting appropriate storm events for use in erosion modeling of disposal mounds.

Tropical-storm selection. Tropical-event selection begins with locating the DRP data archive station nearest the disposal site of interest from the tropical-event summary report (Scheffner et al. 1994). Station 304 is nearest to the Mud Dump site; therefore, storm events impacting this location were selected for the frequency analysis. Figure 14 shows the spatial distribution of the archived data locations from the summary report and the location of the Mud Dump site.

Sixteen storm events were identified from the database report that impacted Station 304. An example event is shown for Hurricane Gloria in Figure 15. All 16 events are shown in Table 16. Tracks of all 16 events and their spatial distribution of maximum storm-surge elevation for the nearshore stations in decimeters (meter/10.) can be found in the tropical-storm database report (Scheffner et al. 1994).

Extratropical event selection. The full 16-season database of extratropical events for DRP Station 304 was extracted from the archived database. Unlike tropical events, extratropical events are not well defined. For example, surface elevation and current hydrographs for Station 304 for the 1977-78 winter season are shown in Figure 16. As shown, these first-order parameters do not immediately isolate specific extratropical storm events of interest.

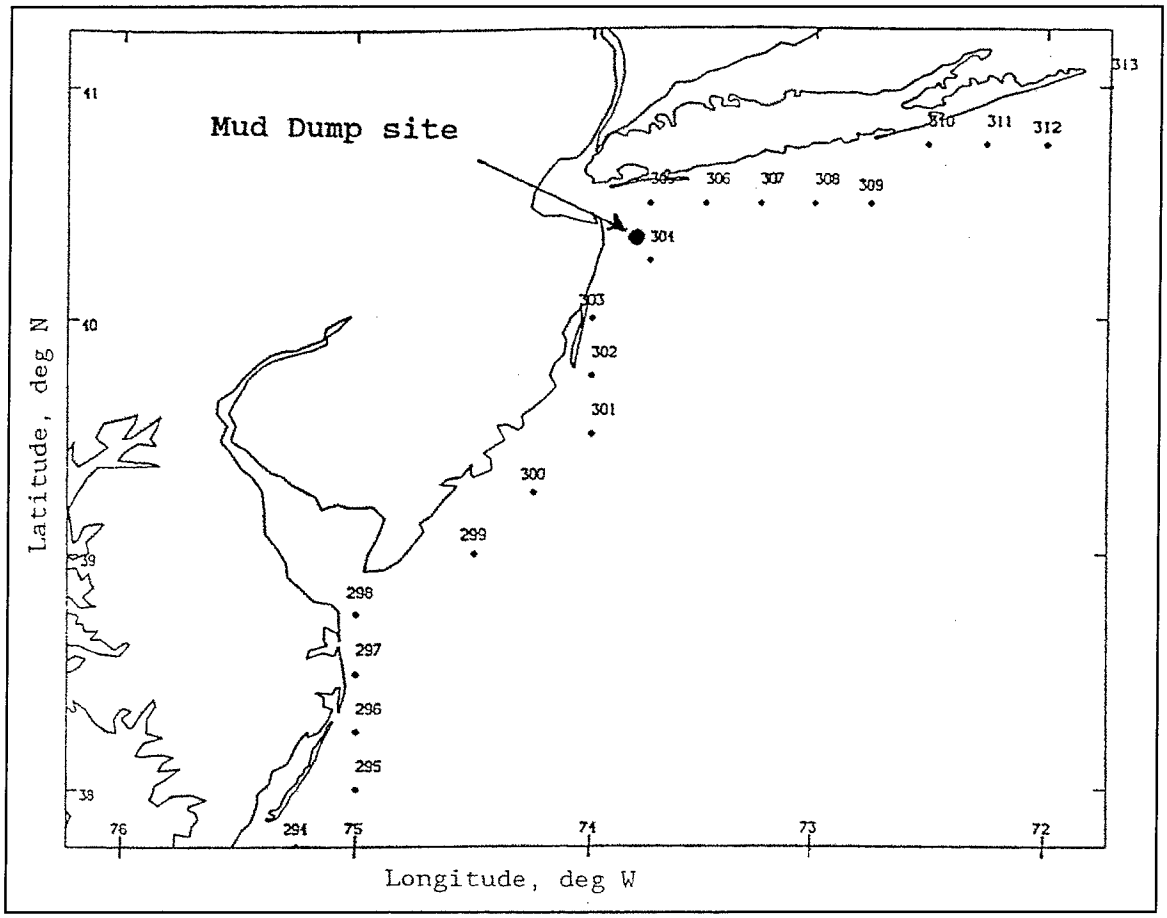

Figure 14. Location of Mud Dump site and DRP Station 304

The primary reason for the difficulty in identifying extratropical storms for this specific application of subaqueous erosion is the fact that the currents accompanying each event are relatively small (i.e., on the order of 20-30 cm/sec at the Mud Dump site), and their effects have to be considered with respect to other environmental factors occurring at the time of the storm. These factors include the local depth, the orbital velocities of the wave field, the duration of the event, and the phase of the tide. Therefore, in order to isolate significant events from each 7-month record, a more quantitative approach to event parameterization was developed and implemented for the Mud Dump study.

Developing a systematic procedure to identify and subsequently separate significant storm events from the extratropical storm database required an analysis of combinations of individual first-order parameter components that may provide an indication of disposal-site impact. Because the storm effect of interest for this application is vertical erosion of a disposal mound, a methodology for identifying storms with measurable erosional impact was developed by combining available storm-event information into a second-order parameter, one that represents some combination of first-order parameters such as surge, tide, wave height, etc. This parameter was chosen to be the

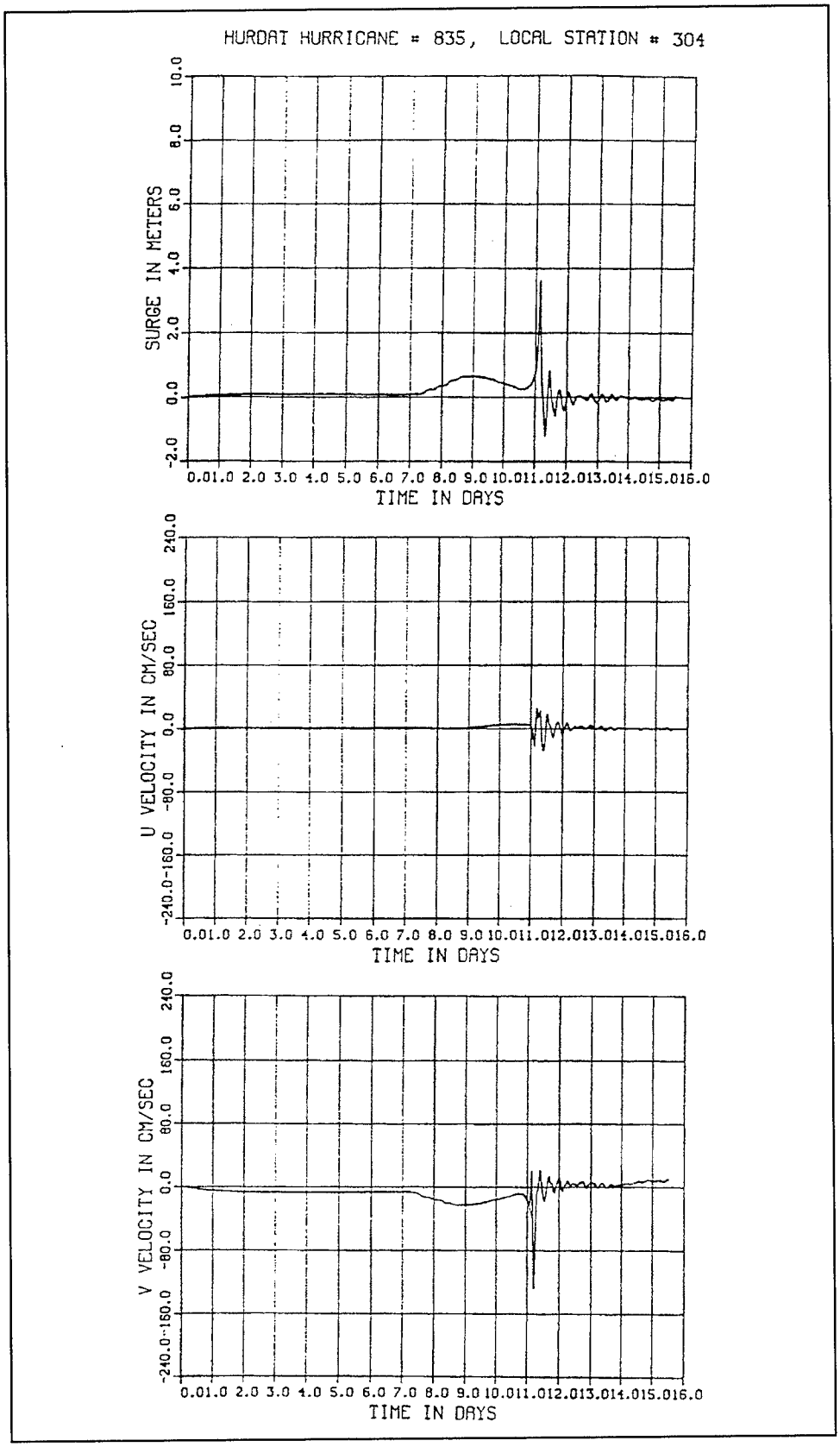

Figure 15. Surge hydrograph for Hurricane Gloria

Table 16
Tropical Events Impacting the Mud Dump Site

HURDAT Storm No.	Given Name	Date (month/day/year)
296	Not named	09/22/1929
327	Not named	08/17/1933
332	Not named	09/08/1933
353	Not named	08/29/1935
370	Not named	09/08/1936
386	Not named	09/10/1938
436	Not named	09/09/1944
535	Carol	08/25/1954
541	Hazel	10/05/1954
545	Connie	08/03/1955
597	Donna	08/29/1960
657	Doria	09/08/1967
702	Doria	08/20/1971
712	Agnes	06/14/1972
748	Belle	08/06/1976
835	Gloria	09/16/1985

instantaneous sediment-transport magnitude, computed as a function of the storm-induced surge elevation and current, the maximum M_2 tidal amplitude and maximum and M_2 tidal velocity magnitude, the wave height and period, grain size of the disposal mound cap, and ambient depth.

The transport relationships used were the Ackers-White (1973) total load, noncohesive sediment-transport equations with a modification for the presence of waves suggested by Bijker (1967). These relationships form the basis of the noncohesive transport computations in the LTFATE model. The result is a transport magnitude hydrograph computed as a function of surge and tidal currents, wave climate, depth, and grain size. For the Mud Dump site example, the mean depth was specified as 83 ft and mean grain size set at 0.40 mm. The 83-ft depth was specified as the base depth area within the Mud Dump site considered for capping, and 0.40-mm sand was the suggested cap material.

The sediment-transport hydrograph for the 1977-78 storm season is shown in Figure 17. As evident in the figure, distinct events are now clearly visible in the time series. This approach to event identification represents a significant improvement over use of first-order parameters such as those shown in Figure 16.

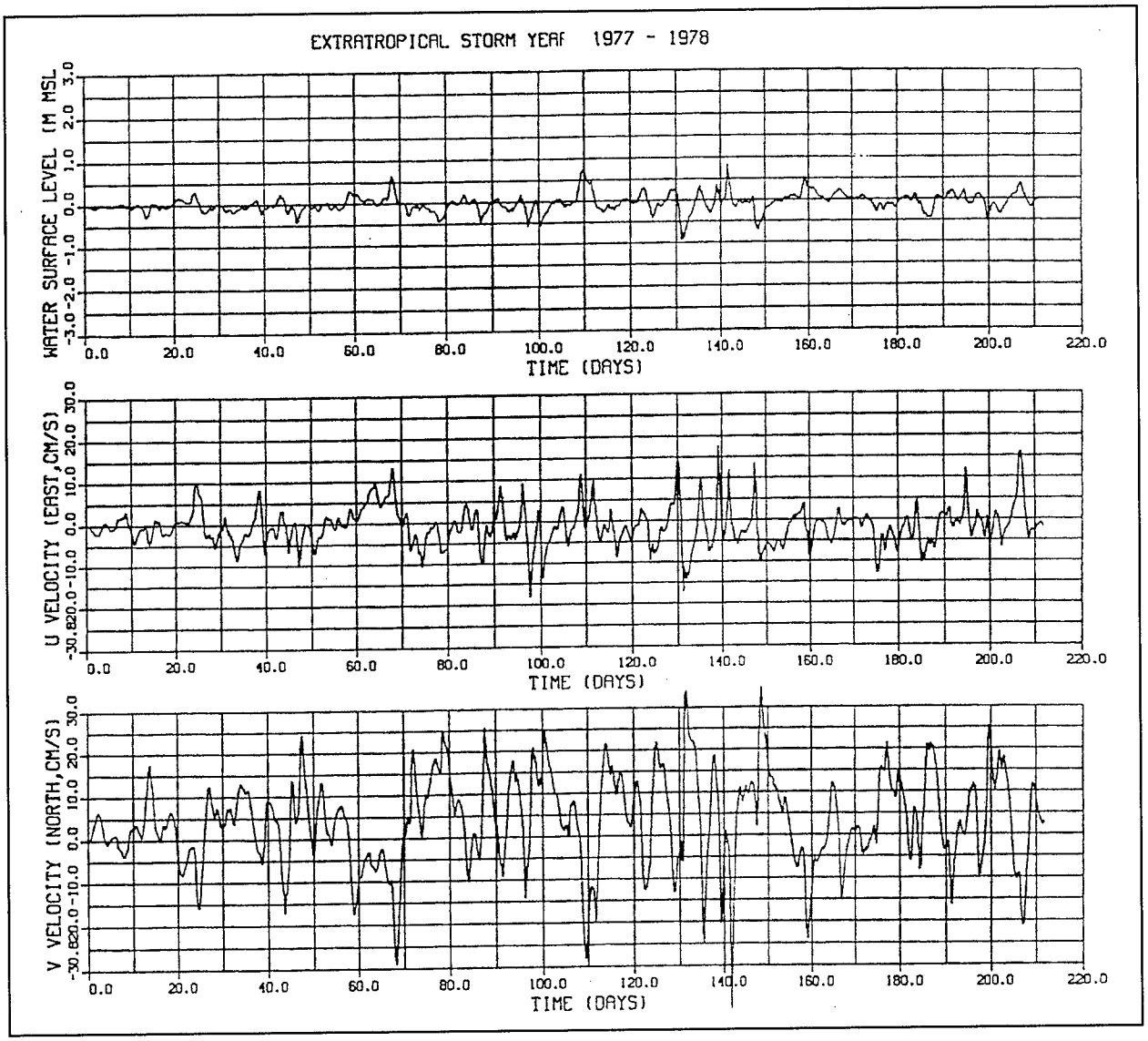

Figure 16. Extratropical storm hydrograph for 1977-78 season

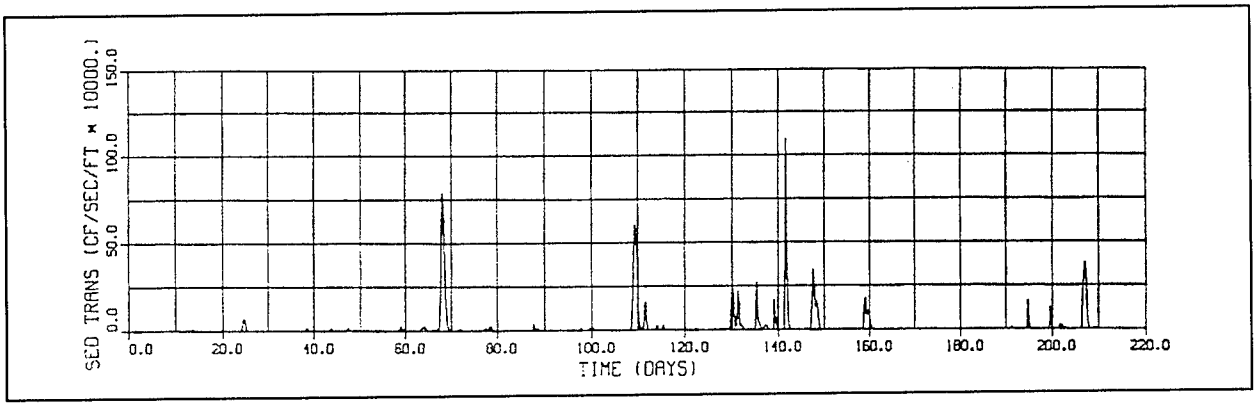

Figure 17. Sediment-transport hydrograph for 1977-78 season

Table 17
Summary of Storm Events by Day of Season/Maximum Transport Magnitude in $ft^3/sec/ft\text{-}width \times 10^{-4}$

YEAR	1	2	3	4	5	TOTAL
77-78	68/80	110/65	142/110	207/35	-	4
78-79	146/190	171/50	193/50	205/50	-	4
79-80	132/35	138/35	195/50	-	-	3
80-81	55/125	154/70	163/105	210/30	-	4
81-82	-	-	-	-	-	0
82-83	55/70	164/50	199/50	-	-	3
83-84	41/35	102/110	180/45	210/165	-	4
84-85	43/85	165/180	-	-	-	2
85-86	27/160	65/125	160/30	191/30	200/70	5
86-87	93/190	115/40	123/40	-	-	3
87-88	-	-	-	-	-	0
88-89	-	-	-	-	-	0
89-90	49/(33)	-	-	-	-	1
90-91	-	-	-	-	-	0
91-92	126/40	-	-	-	-	1
92-93	101/150	165/30	185/120	194/155	-	4

Analysis of the 16 seasonal transport hydrographs resulted in the adoption of a threshold value of 30.0×10^{-4} $ft^3/sec/ft\text{-}width$ as the basis for selecting events that may cause erosion to the Mud Dump site. Table 17 presents a summary of the analysis for the 1977-1993 storm years in the form of the approximate day (measured from 1 September) of occurrence and the magnitude of the peak transport value. The total number of events per season is also tabulated. According to these criteria, the computed average number of events per year that impact the Mud Dump site is 38 events/16 seasons = 2.375 events/year.

The purpose for selecting specific storms is to develop a training set of events for the EST simulations. The specific effect of interest clearly has a direct bearing on the selection of appropriate storm events. For example, the 10 storm events that cause the most shoreline erosion at a particular location are not necessarily the same 10 events that cause the most vertical erosion of a capped mound in the same area. A separate storm analysis would be required to identify events that cause shoreline/dune recession. However, this second-order parameter approach to storm isolation has been found to be successful in identifying events that cause erosion to a disposal mound. By defining the appropriate parameter, the approach is equally applicable to shoreline processes analyses.

Because vertical erosion is the impact of interest, the transport hydrographs for all 16 seasons were used to identify 38 specific events with a peak transport magnitude greater than the threshold value of 30.0×10^{-4} ft^3/sec/ft-width at the Mud Dump site. These events are listed in Table 17. For each identified event, hydrographs of total water surface elevation (storm plus tide), total U and V current (storm plus tide), and wave height and period were generated.

Hydrographs for each of the 38 time periods identified in the table were constructed to be 6 days in duration, centered on the day indicated in Table 17.

Tidal conditions

Station 304 is located at 73.75° west longitude and 40.25° north latitude. The CEDARS tidal constituent database yields the eight constituent amplitude and epoch arguments shown in Table 18.

Table 18
Tidal Constituents for DRP-WIS Station 304

Const	h-amp, m	h-κ, deg	U-amp m/sec	U-κ, deg	V-amp m/sec	V-κ, deg
K_1	0.0867	95.2	0.0049	194.3	0.0061	27.1
O_1	0.0589	100.4	0.0028	193.3	0.0042	43.5
P_1	0.0359	91.0	0.0020	193.5	0.0028	19.7
Q_1	0.0111	98.3	0.0006	202.4	0.0007	19.2
N_2	0.1704	195.6	0.0181	295.6	0.0226	116.0
M_2	0.7744	215.3	0.0837	313.8	0.1012	133.8
S_2	0.1507	254.6	0.0169	355.4	0.0213	173.4
K_2	0.0482	246.6	0.0054	347.2	0.0068	164.9

Tropical and extratropical surge simulations did not include tides at the time of the event, i.e., they were modeled with respect to a constant and zero Mean Sea Level (MSL). Because tide elevation and currents are a factor in mound erosion, their impact on the current must be included in the analysis. When tidal phase is accounted for, each storm event has an equal probability of occurring at any time during the tidal cycle. For simplicity, four tidal phases were considered in this analysis: (a) high tide, (b) MSL during peak flood, (c) low tide, and (d) MSL during peak ebb. These four phases are designated as phases 0, 90, 180, and 270 deg, respectively.

At the Mud Dump site, the M_2 semidiurnal tidal constituent accounts for over 90 percent of the tidal energy (based on the eight-constituent database) as can be seen in the listing of constituent amplitude and local epochs κ shown in Table 18. Therefore, to account for the four tidal phases, M_2 amplitude A and local epoch phase data κ for elevation (h = 0.7744 m, κ = 215.3°) and current (U:

A = 0.0837 m/sec, κ = 313.8°; V: A = 0.1012 m/sec, κ = 133.8°) were extracted from the DRP database and used to expand the 16 tropical storms and 38 extratropical season database of storms without tides to a 64 tropical storm database with tides and a 152 extratropical storm database with tides. This expanded set of hydrographs represents a combination of the surge hydrograph with the tidal hydrographs generated for the four phases of the tide based on the M_2 tidal constituent.

Wave conditions

The wave field input for the extratropical database of events was obtained from the WIS and available in the CEDARS database. An example time series is the WIS wave height and period time series for DRP Station 304 for the winter 1977-78 season shown in Figure 18.

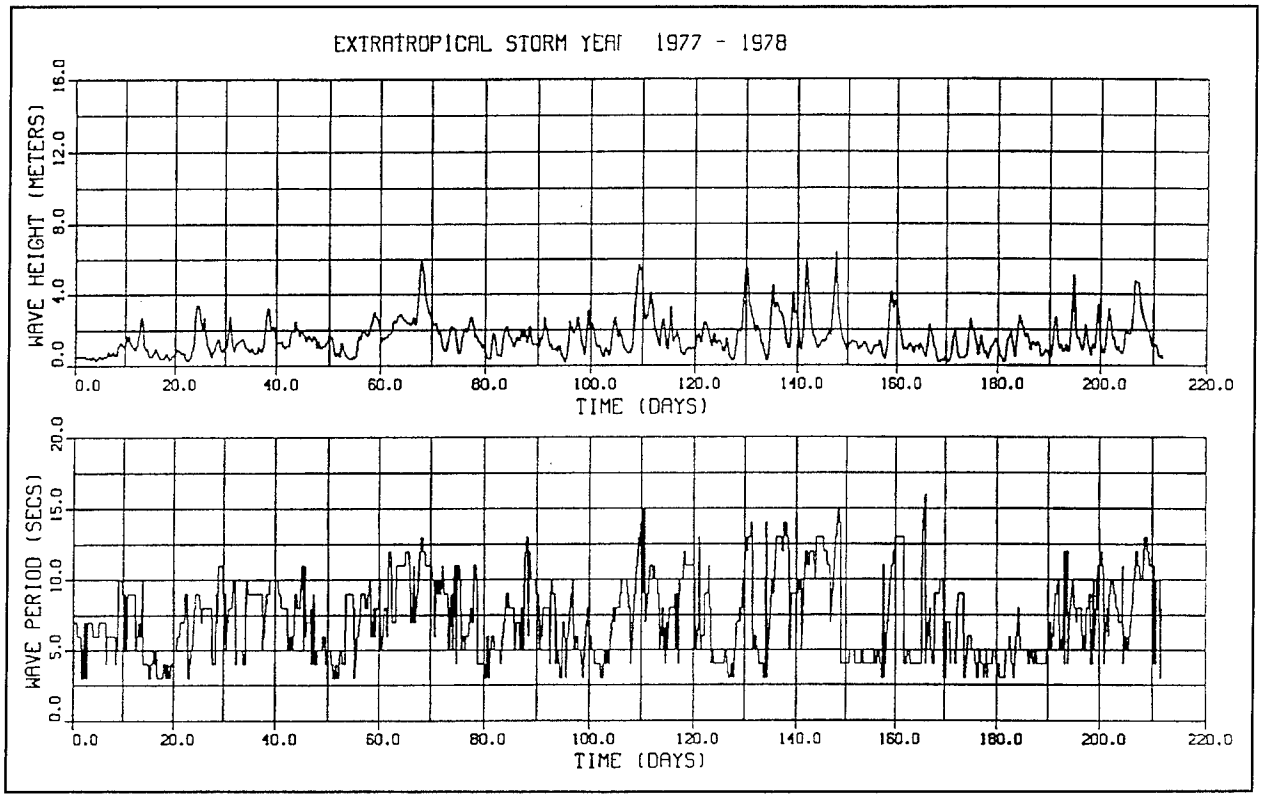

Figure 18. WIS wave height and period time series for 1977-78

Wave conditions corresponding to all selected tropical events are not available in the CEDARS database; therefore, some form of approximation is required. A methodology presented in the *Shore Protection Manual* (SPM 1984) was selected for this study. This approximation gives an estimate of the deepwater significant wave height and period at the point of maximum wind for

a slowly moving hurricane. The wave height and period are given by the following formulae:

$$H_o = 16.5\ e^{\frac{R\Delta p}{100}} \left[1 + \frac{0.208\alpha V^F}{\sqrt{U_R}}\right] \tag{36}$$

and

$$T_s = 8.6\ e^{\frac{R\Delta p}{200}} \left[1 + \frac{0.204\alpha V^F}{\sqrt{U_R}}\right] \tag{37}$$

where

H_o = deepwater significant wave height in feet

T_s = corresponding significant wave period in seconds

R = radius to maximum wind in nautical miles

$\Delta p = p_n - p_o$, where p_n is the normal pressure of 29.93 in. of mercury and p_o is the central pressure of the hurricane

V_F = forward speed of the hurricane in knots

U_R = maximum sustained wind speed in knots calculated 33 ft above MSL at radius R

α = a coefficient depending on the speed of the hurricane. The suggested value is 1.0 for a slowly moving hurricane

All of the above variables contained in Equations 36 and 37 are contained in or can be calculated from the HURDAT database.

A reduction in wave height as a function of the radial distance to maximum significant wave (taken as the distance to maximum wind) and the radial distance to the point of interest is given in the SPM (p 3-85, SPM 1984). Once this reduction factor is applied to the maximum wave height computed according to Equation 36 above, the corresponding approximate wave period can be computed from the following:

$$T = 12.1\sqrt{\frac{H_o}{g}} \tag{38}$$

where T is the wave period in seconds and g is the acceleration of gravity (32.2 ft/sec^2).

Maximum wave heights should be limited by the breaking wave criteria of H_b=0.65*depth based on measurements indicating that storm-generated waves in open water are limited to approximately 0.6-0.7 times the local depth.[1] Design scenarios, to be described below, include mound configurations located at three depths, the minimum of which was 63.0 ft. In order to prescribe wave field boundary conditions that are consistent for all simulations, the minimum depth was used to define maximum wave criteria. Therefore, maximum allowable waves were limited to 0.65*63.0 = 40.95 ft = 12.48 m. This criterion was used for all simulation scenarios.

Wave heights and periods described by the SPM approach described above approach zero when the hurricane is far removed from the location of interest. Therefore, minimum values were specified based on summary tables provided by WIS (Hubertz et al. 1993) for the WIS station closest to DRP Station 304. In this example, WIS Station 72 exactly corresponds to DRP 304. The average direction of travel for the 16 tropical events was computed to be approximately 11° clockwise from true north (an azimuth of 191° by WIS convention). According to Hubertz et al. (1993), the largest number of waves at an azimuth of 180° were in the 5.0- to 6.9-sec band. Therefore, a minimum period of 6.0 sec was selected for the storm-event hydrographs. Maximum mean wave conditions for the months of September and October were reported to be 1.2 and 1.3 m, respectively; therefore, a minimum wave condition was selected to be 1.25 m.

Storm-event hydrographs input

Each of the 16 tropical-event hydrographs represents the full storm history, from beginning to end, often a week or more in duration. Because only the erosional effect of the specific event on the site is of interest, each tropical-event hydrograph was constructed to be 99-hr in duration, measured as 48 hr before the 3-hr duration peak and 48 hr after the peak. The time of peak is computed as the time when the eye of the storm is closest to the site of interest. The time-step of the hydrographs was selected to be 3 hr and archived for input to the LTFATE model.

Each of the 38 extratropical event hydrographs were combined with hydrographs corresponding to four tidal phases (each lagged by 90°). The WIS wave field was superimposed on the centered storm that was constructed to be 6 days in duration, centered on the day indicated in Table 17. All hydrographs were generated at a 3-hr time-step and archived for input to the LTFATE model.

---

[1] Personal Communication, 1994, Donald T. Resio, U.S. Army Engineer Research and Development Center, Vicksburg, MS.

The depth at Station 304, contained in the summary report, is approximately 108 ft. Because the depth at the Mud Dump site is shallower than that of Station 304, the surge velocities were increased by assuming that the surge current values can be approximated as proportional to the relative depths at the two sites. A mean depth for the Mud Dump site in the area of interest was determined to be approximately 83 ft; therefore, the DRP-generated surge current hydrographs were adjusted according to the criteria that Q=VA=Const; therefore, $V_{Mud} = V_{304}*108./83$. This proportionality was applied to both tropical- and extratropical-storm current hydrographs.

Response vector generation - the LTFATE model

After the selected storms were constructed, the LTFATE model was used to compute the maximum amount of vertical erosion resulting from each storm for each of the disposal-site configurations of interest. For this Mud Dump site application, six combinations of ambient depth, mound height, and crest depth were tested. These combinations of design scenarios are tabulated in Table 19. All mound configurations had side slopes of 1:50, and the cap material was specified to be noncohesive sand with a d_{50} of 0.40 mm.

Table 19
Mud Dump Mound Configurations

Test Number	Ambient Depth, ft	Mound Height, ft	Crest Depth, ft
1	63	13	50
2	63	8	55
3	73	13	60
4	73	8	65
5	83	13	70
6	83	8	75

The surge, tidal, and wave field time series must be placed into a format compatible with LTFATE input requirements. An example LTFATE input file for hurricane No. 835 is shown in Table 20. For the Mud Dump study, storm-event input files representing the 99-hr time sequences for each of the 64 tropical storm events and the 144-hr time sequences for each of the 152 extratropical storm events were input to LTFATE to evaluate the erosion potential of the configurations shown in Table 20. For all six design configurations and for each storm, the maximum vertical erosion experienced at any location on the mound during each of the simulations was archived for input to the EST to develop life-cycle scenarios from which the desired vertical erosion versus frequency-of-occurrence relationships were computed.

Table 20
Example LTFATE Input File

	Wave height-m	Wave period-sec	U-cm/sec	V-cm/sec	Surge-m
Hurricane: 835 WIS Station: 304					
219.00	1.250	6.000	9.251	-38.308	1.164
222.00	1.250	6.000	11.406	-39.243	0.071
225.00	1.250	6.000	-3.124	-20.060	0.049
228.00	1.250	6.000	-5.420	-15.662	1.71
231.00	1.250	6.000	9.419	-30.920	1.172
234.00	1.250	6.000	15.334	-35.614	0.077
237.00	1.250	6.000	1.519	-16.542	-0.207
240.00	1.250	6.000	-4.056	-7.843	0.794
243.00	1.250	6.000	9.616	-22.601	1.095
246.00	1.250	6.000	17.646	-30.015	0.074
249.00	1.250	6.000	5.436	-13.767	-0.424
252.00	1.250	6.000	-3.789	-0.846	0.462
255.00	1.748	6.000	7.207	-12.689	1.008
258.00	4.787	6.000	17.136	-24.358	0.165
261.00	9.829	9.460	6.573	-13.044	-0.361
264.00	12.485	14.567	-7.198	-8.491	0.750
267.00	12.485	15.433	-31.538	20.684	3.775
270.00	12.485	14.567	30.319	-121.682	0.077
273.00	9.829	9.460	-28.224	13.077	-1.510
276.00	4.787	6.000	6.797	-4.497	0.262
279.00	1.748	6.000	-0.205	8.166	0.201
282.0	1.250	6.000	5.546	-6.199	0.412
285.00	1.250	6.000	13.366	-12.180	-1.050
288.00	1.250	6.000	-18.947	27.948	-0.298
291.00	1.250	6.000	2.285	1.164	0.663
294.00	1.250	6.000	5.566	-1.685	0.223
297.00	1.250	6.000	9.583	-6.201	-0.647
300.00	1.250	6.000	-6.529	13.946	-0.438
303.00	1.250	6.000	-4.978	15.048	0.544
306.00	1.250	6.000	7.271	0.057	0.589
309.00	1.250	6.000	13.559	-10.128	-0.625
312.00	1.250	6.000	-7.279	14.726	-0.672
315.00	1.250	6.000	-9.291	15.761	0.606

EST life-cycle simulations

As noted earlier, the EST is a procedure that uses a limited database of historical occurrences to generate multiple simulated event scenarios. These simulations require both input and response vectors to define the intensity and effects of past storm events as well as a parameter to define the frequency of events. The following subsections summarize the tropical and extratropical EST input file development.

Tropical storm vectors. For tropical events, input vectors were defined as (a) tidal phase, (b) closest distance from the eye to the location of interest, (c) direction of propagation at closest proximity, (d) central pressure deficit, (e) forward velocity of the eye, (f) maximum velocity of hurricane winds, and (g) radius to maximum winds. Response for the Mud Dump is defined as the maximum erosion occurring at any location on the mound as a result of the passage of the single storm. Input and response vectors for hurricane Nos. 296, 327, 332, 353, 370, and 386 for the site scenario of a 13-ft mound located in 73 ft of water are shown in Table 21.

Table 21
EST Input for Tropical Events

			(a)	(b)	(c)	(d)	(e)	(f)	(g)	Max Erosion
Mud Dump Eros-Freq Anal., 73 13, 1:50										
1	296	1	1.00	84.85	29.35	25.83	30.68	18.39	43.42	0.50
2	296	1	0.00	84.85	29.35	25.83	30.68	18.39	43.42	0.60
3	296	1	-1.00	84.85	29.35	25.83	30.68	18.39	43.42	0.50
4	296	1	0.00	84.85	29.35	25.83	30.68	18.39	43.42	0.60
5	327	1	1.00	172.26	10.41	35.31	45.00	20.19	43.42	0.50
6	327	1	0.00	172.26	10.41	35.31	45.00	20.19	43.42	0.70
7	327	1	-1.00	172.26	10.41	35.31	45.00	20.19	43.42	.060
8	327	1	0.00	172.26	10.41	35.31	45.00	20.19	43.42	0.70
9	332	1	1.00	127.87	47.98	47.81	70.00	15.86	36.60	0.60
10	332	1	0.00	127.87	47.98	47.81	70.00	15.86	36.60	0.80
11	332	1	-1.00	127.87	47.98	47.81	70.00	15.86	36.60	0.70
12	332	1	0.00	127.87	47.98	47.81	70.00	15.86	36.60	0.80
13	353	1	1.00	179.15	69.69	68.20	71.66	40.08	43.42	0.60
14	353	1	0.00	179.15	69.69	68.20	71.66	40.08	43.42	0.50
15	353	1	-1.00	179.15	69.69	68.20	71.66	40.08	43.42	0.60
16	353	1	0.00	179.15	69.69	68.20	71.66	40.08	43.42	0.50
17	370	1	1.00	62.34	45.70	42.07	81.35	23.34	8.68	0.20
18	370	1	0.00	62.34	45.70	42.07	81.35	23.34	8.68	0.20
19	370	1	-1.00	62.34	45.70	42.07	81.35	23.34	8.68	0.20
20	370	1	0.00	62.34	45.70	42.07	81.35	23.34	8.68	0.20
21	386	1	1.00	42.14	358.37	66.07	80.65	47.77	43.42	1.10
22	386	1	0.00	42.14	358.37	66.07	80.65	47.77	43.42	1.10
23	386	1	-1.00	42.14	358.37	66.07	80.65	47.77	43.42	1.00
24	386	1	0.00	42.14	358.37	66.07	80.65	47.77	43.42	1.10

Frequency of events is ensured through specification of the parameter Λ. For tropical events, 16 storms were found to have impacted the area in 104 years. Therefore, Λ for tropical events is 0.15385 events per year or 1 event every 6.5 years.

Extratropical storm vectors. Input vectors for extratropical events were defined as (a) tidal phase, (b) duration of the event defined as the number of hours during which the computed transport magnitude exceeds 10.0×10^{-4} ft^3/sec/ft-width, (c) maximum transport magnitude computed during the storm event, (d) wave height, (e) wave period, and (f) maximum depth-averaged velocity magnitude associated with the maximum transport value. The response vector was defined as above. Input and response vectors for the first seven events of the 1977-93 seasons for the site scenario of a 13-ft mound located in 73 ft of water are shown in Table 22. The frequency of events are specified with $\Lambda = 2.375$ computed from 38 events in 16 seasons.

The EST program generates a 200-year tabulation consisting of the number of storm events that occurred each year and the vertical erosion corresponding to each event. The total summation of erosion magnitudes per year was selected as the design parameter of interest. For example, if three storm events were simulated during the first year, the sum of the three vertical erosions would be used to define the parameter for which frequency-of-occurrence relationships would be computed.

Frequency-of-occurrence computations

To most effectively use the results from the EST simulations for cap erosion layer thickness design, frequency of vertical erosion curves and tables were generated for each design scenario based on the life-cycle simulations. For the Mud Dump site example, vertical erosion versus frequency-of-occurrence relationships were generated for each of the 100 simulations described above for each of the six-depth/mound-height configurations for both tropical and extratropical storms. A summary of the results is given below.

Tropical storms. In the analysis of the 100 frequency relationships, an average vertical erosion magnitude is computed relative to each return period. From the EST simulations of tropical storms, an example plot of the 100 recurrence relationships and mean value (indicated by O) for the 8-ft mound located at an 83-ft depth is shown in Figure 19. Note that the spread of data points about the mean demonstrates a reasonable degree of variability, as would be expected of a stochastic process.

Finally, the standard deviation of the 100 events relative to the mean is computed as a measure of variability. Output for design purposes contains only the mean frequency-of-occurrence relationship with a ± one standard deviation band. An example of this output is shown in Figure 20 for the 8-ft mound at the 83-ft depth shown in Figure 19. Table 23 summarizes the frequency-of-occurrence of vertical erosion from tropical storms for all six mound

Table 22
EST Input for Extratropical Events

			(a)	(b)	(c)	(d)	(e)	(f)	Max Erosion
Extratropical Storm Year 1977 - 1993 7313									
1	1	1	1.00	21.00	67.94	5.90	12.00	51.84	0.40
2	1	1	0.00	18.00	64.44	5.90	12.00	50.30	0.40
3	1	1	-1.00	27.00	63.87	5.70	13.00	51.43	0.40
4	1	1	0.00	24.00	68.02	5.70	13.00	53.28	0.40
5	2	1	1.00	21.00	57.56	5.60	12.00	50.81	0.40
6	2	1	0.00	21.00	54.58	5.70	11.00	49.91	0.40
7	2	1	-1.00	30.00	49.01	5.50	13.00	46.74	0.40
8	2	1	0.00	33.00	52.04	5.40	13.00	49.54	0.40
9	3	1	1.00	18.00	50.41	5.60	10.00	51.81	0.30
10	3	1	0.00	18.00	82.83	5.70	12.00	60.61	0.40
11	3	1	-1.00	15.00	97.55	6.00	11.00	64.28	0.40
12	3	1	0.00	15.00	93.77	6.00	11.00	62.89	0.40
13	4	1	1.00	15.00	35.30	4.70	12.00	49.52	0.20
14	4	1	0.00	15.00	37.15	4.70	12.00	50.76	0.20
15	4	1	-1.00	9.00	32.33	4.70	11.00	48.90	0.20
16	4	1	0.00	12.00	32.10	4.60	12.00	48.57	0.20
1	1	1	1.00	18.00	231.38	7.30	13.00	78.79	0.60
2	1	1	0.00	21.00	258.78	7.30	13.00	84.31	0.70
3	1	1	-1.00	18.00	249.12	7.20	12.00	85.46	0.60
4	1	1	0.00	18.00	146.77	7.20	12.00	61.79	0.60
5	2	1	1.00	9.00	35.46	5.40	12.00	41.26	0.20
6	2	1	0.00	9.00	44.12	5.40	12.00	46.29	0.20
7	2	1	-1.00	9.00	44.65	5.40	11.00	48.23	0.20
8	2	1	0.00	15.00	24.61	5.20	12.00	36.25	0.20
9	3	1	1.00	6.00	43.27	5.50	11.00	46.27	0.20
10	3	1	0.00	9.00	30.97	5.20	10.00	44.52	0.20
11	3	1	-1.00	12.00	17.42	4.70	9.00	42.20	0.20
12	3	1	0.00	6.00	29.30	5.50	11.00	37.80	0.20

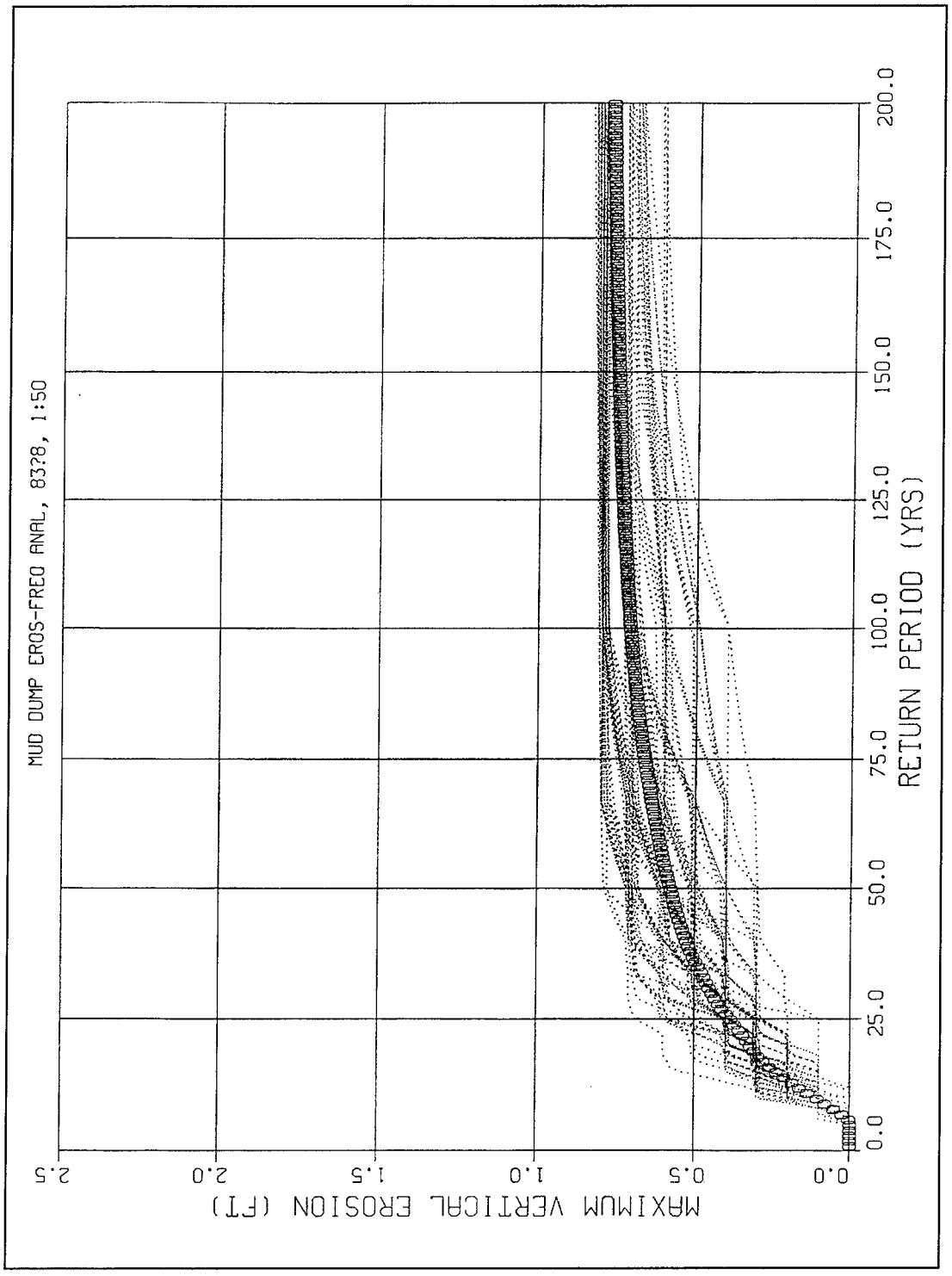

Figure 19. Tropical event frequency relationships for 8-ft mound at 83-ft depth

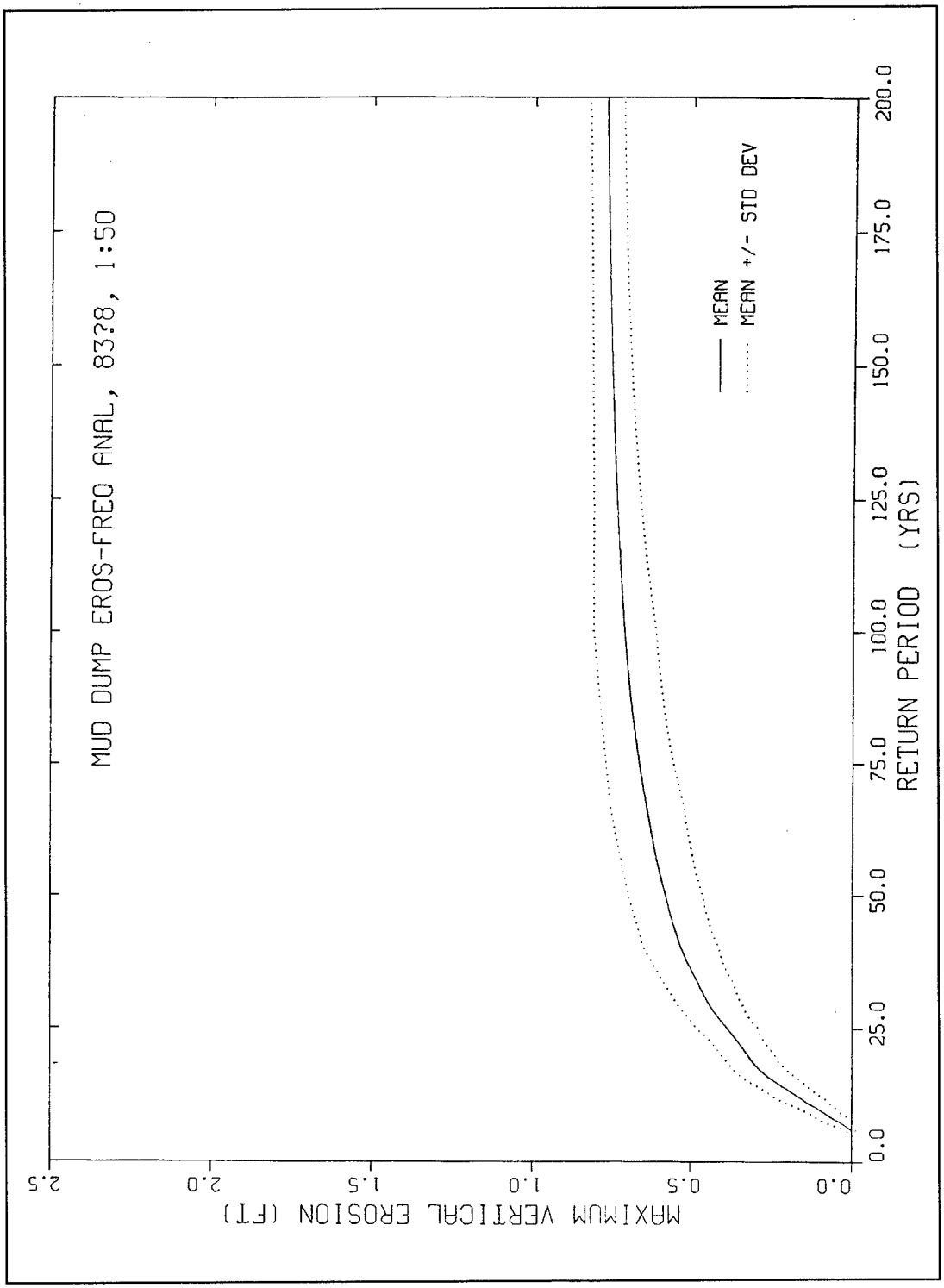

Figure 20. Tropical event mean value/standard deviation frequency relationships for 8-ft mound at 83-ft depth

Table 23
Mean Value of Vertical Erosion/Frequency-of-Occurrence for Tropical Storms at the Mud Dump Site

Test Number/Ambient Depth-Mound Height/Crest Depth, ft	25-Year Mean (± sd), ft	50-Year Mean (± sd), ft	100-Year Mean (± sd), ft
1/(63-13)/50	1.202 (0.228)	1.560 (0.232)	1.857 (0.259)
2/(63-8)/55	0.907 (0.191)	1.275 (0.225)	1.516 (0.187)
3/(73-13)/60	0.805 (0.175)	1.166 (0.219)	1.422 (0.195)
4/(73-8)/65	0.575 (0.130)	0.837 (0.166)	1.046 (0.157)
5/(83-13)/70	0.524 (0.120)	0.761 (0.141)	0.949 (0.151)
6/(83-8)/75	0.384 (0.096)	0.578 (0.117)	0.710 (0.100)

configurations in the form of a mean value and ± standard deviation error that can be added to or subtracted from the mean value.

Extratropical storm. An analysis identical to that for tropical storms was conducted for extratropical events. From the Mud Dump site analysis, an example plot of the 100 recurrence relationships and mean value (indicated by O) for the 8-ft mound located at an 83-ft depth is shown in Figure 21. As for the tropical storms, the spread of data points about the mean demonstrates a reasonable degree of variability, as would be expected of any stochastic process. An example of the mean frequency-of-occurrence relationship with a ± one standard deviation band is shown in Figure 22 for the 8-ft mound at the 83-ft depth. Table 24 summarizes the frequency-of-occurrence of vertical erosion from extratropical storms for all six mound configurations in the form of a mean value and ± standard deviation error that can be added to or subtracted from the mean value.

Combined tropical and extratropical storms. The erosion versus frequency-of-occurrence relationships for tropical and extratropical events were combined to generate a single curve and table of frequencies for each of the design configurations. The combined frequency-of-occurrence is computed by adding the frequencies associated with tropical and extratropical events for a given magnitude of erosion. For example, consider the 8-ft mound located in 83 ft of water. An erosion of 1.0 ft corresponds to a return period of 83 years for hurricanes but only 10 years for extratropical events. The combined frequency is equal to 1/83 + 1/10 or 0.11, corresponding to a return period of just 9 years. A comparison of the combined event in Table 25, shown below, and Tables 23 and 24 shows that extratropical events are the dominant storm type in the New York Bight. This dominance is evidenced by the fact that the combined event frequency relationships are very similar to the extratropical relationships. This is not surprising considering that on the average 15 extratropical storms occur for every hurricane. Also, vertical erosion because of extratropical events is generally more severe than for tropical events because of the longer duration of extratropical storms.

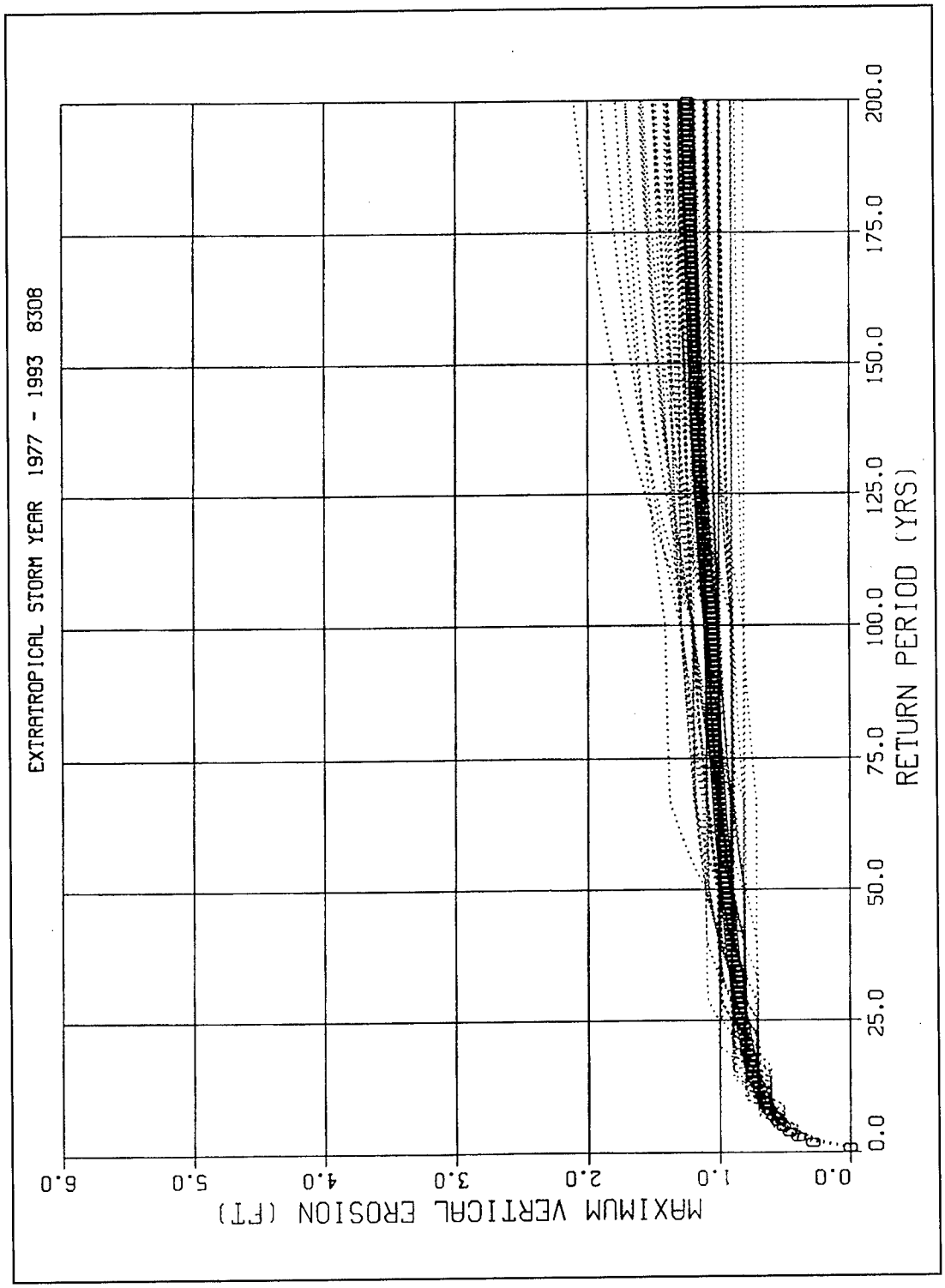

Figure 21. Extratropical event frequency relationships for 8-ft mound at 83-ft depth

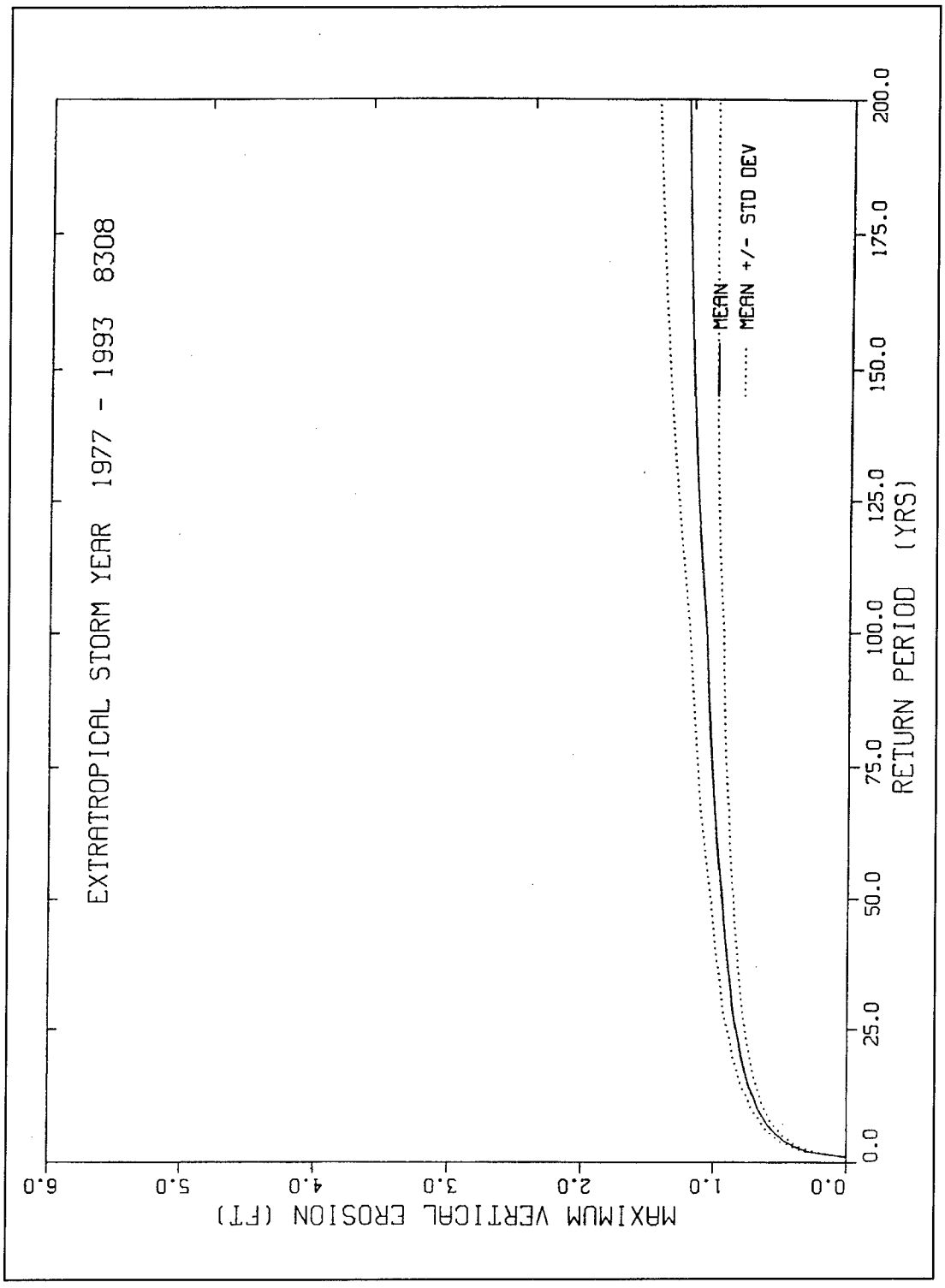

Figure 22. Extratropical event mean value/standard deviation frequency relationships for 8-ft mound at 83-ft depth

Table 24
Mean Value Erosion/Frequency-of-Occurrence for Extratropical Storms at the Mud Dump Site

Test Number/Ambient Depth-Mound Height/Crest Depth, ft	25-Year Mean (± sd), ft	50-Year Mean (± sd), ft	100-Year Mean (± sd), ft
1/(63-13)/50	2.996 (0.215)	3.425 (0.299)	3.875 (0.417)
2/(63-8)/55	2.134 (0.145)	2.268 (0.200)	2.568 (0.285)
3/(73-13)/60	1.766 (0.126)	2.016 (0.166)	2.280 (0.257)
4/(73-8)/65	1.256 (0.100)	1.431 (0.129)	1.626 (0.183)
5/(83-13)/70	1.148 (0.086)	1.312 (0.118)	1.490 (0.157)
6/(83-8)/75	0.830 (0.070)	0.941 (0.086)	1.069 (0.126)

Table 25
Vertical Erosion Frequency-of-Occurrence

	Combined Hurricane/Northeaster Single-Year Erosion Frequency, ft			
Base Depth/ Mound Height/ Crest Depth, ft	10 Years	25 Years	50 Years	100 Years
63/13/50	2.4	3.0	3.4	3.9
63/08/55	1.6	2.0	2.3	2.6
73/13/60	1.5	1.8	2.0	2.3
73/08/65	1.0	1.3	1.5	1.7
83/13/70	0.9	1.2	1.3	1.6
83/08/75	0.7	0.8	0.9	1.1

A summary of results, shown in Table 25, was prepared to provide both episodic and cumulative erosion estimates for each design option. The episodic values are provided at return periods of 10, 25, 50, and 100 years. Cumulative erosion, computed as described earlier, is provided for a 1-, 5-, and 10-year total.

Summary

The storm-surge frequency analyses described in this example made extensive use of the DRP databases and the EST. The approach required the generation of a database of storm responses that, for this analysis, were selected to be vertical erosion. In conclusion, vertical erosion versus

frequency-of-occurrence relationships generated through the techniques described in this report were used as a basis for designing a capped disposal mound.

Example 2: Brevard County, Florida, Dune/Beach Recession Analysis

The second example describes the methods employed for establishing frequency-of-occurrence relationships for storm-induced horizontal recession of beaches and dunes in Brevard County, Florida. Those relationships were required as input to the economic analysis of storm damages in a feasibility phase study of the Brevard County Shore Protection Project performed by the Jacksonville District of the U.S. Army Corps of Engineers. The project shoreline extends for approximately 22 miles along the Atlantic coast of Florida, just south of Cape Canaveral. The study area is depicted in Figure 23.

Proposed shore protection measures must be subjected to a benefit-cost analysis, to assess whether Federal participation in the project is appropriate. Primary benefits are typically quantified in terms of the reduction of storm-induced damages to existing property and/or structures. In order to quantify those benefits, one must estimate (a) the damage potential that exists without the proposed protection measures (i.e., for existing conditions), and (b) the damage potential that exists with measures in place. Benefits are expressed as the reduction in storm-induced damages resulting from the presence of the shore protection measure.

This example documents efforts to quantify damage potential of the existing conditions. In order to account for risks and uncertainties inherent to the analysis procedure, methods were selected to express storm damages in a probabilistic manner. In other words, the results were required in the form of recession versus frequency-of-occurrence relationships. The EST was selected as the tool of choice to establish those relationships. The overall beach recession analysis procedure requires execution of steps similar to those previously described for the dump site application. The following sections describe each of those major tasks.

Storm-event selection

Because of the Atlantic coast location of the project site, the shoreline in question is subjected to both tropical and extratropical storms. The procedure for identification of storms that have impacted project beaches is very similar to that of the first example.

Tropical-storm selection. The tropical-storm database summary report indicated that data archive Station 433 was nearest the project site. The location

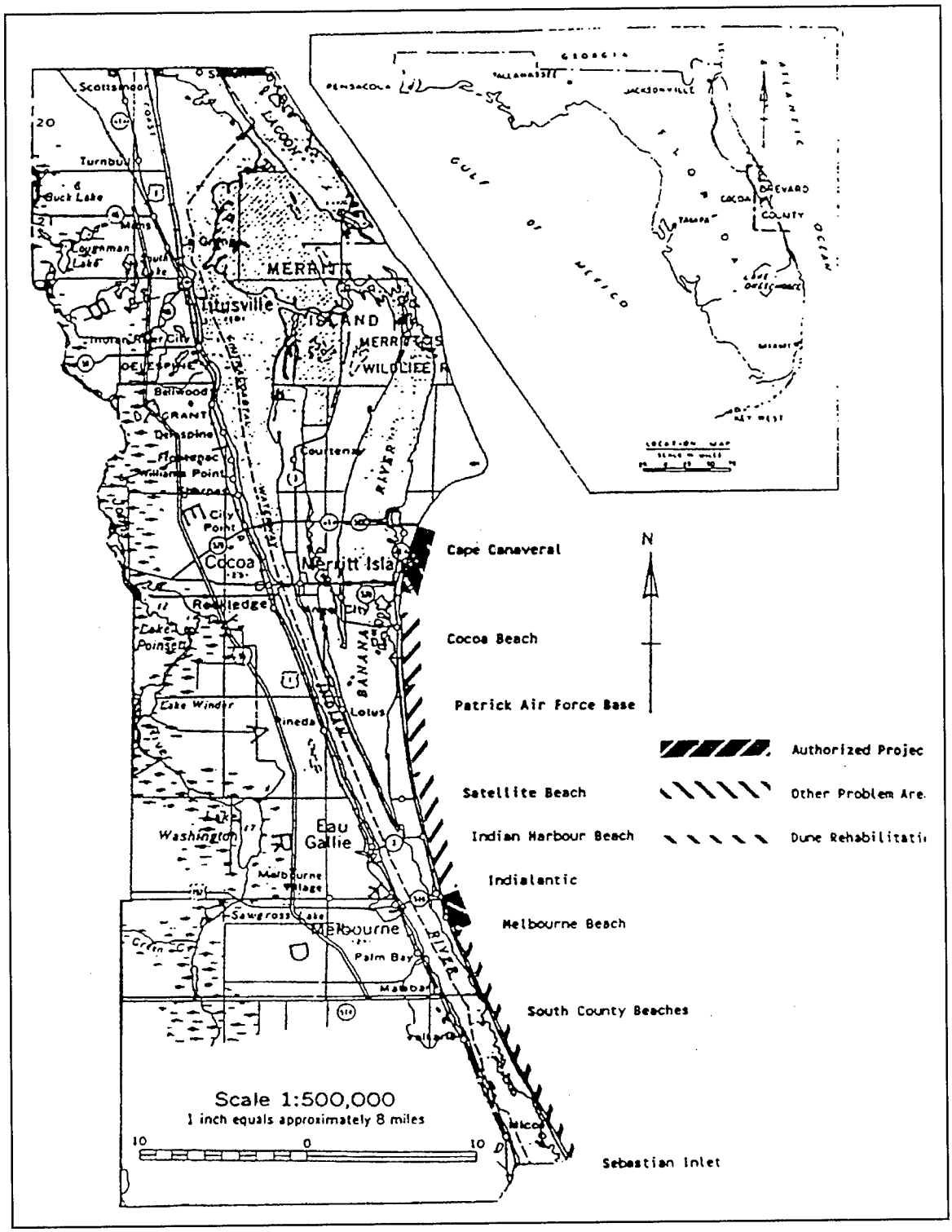

Figure 23. Brevard County study area

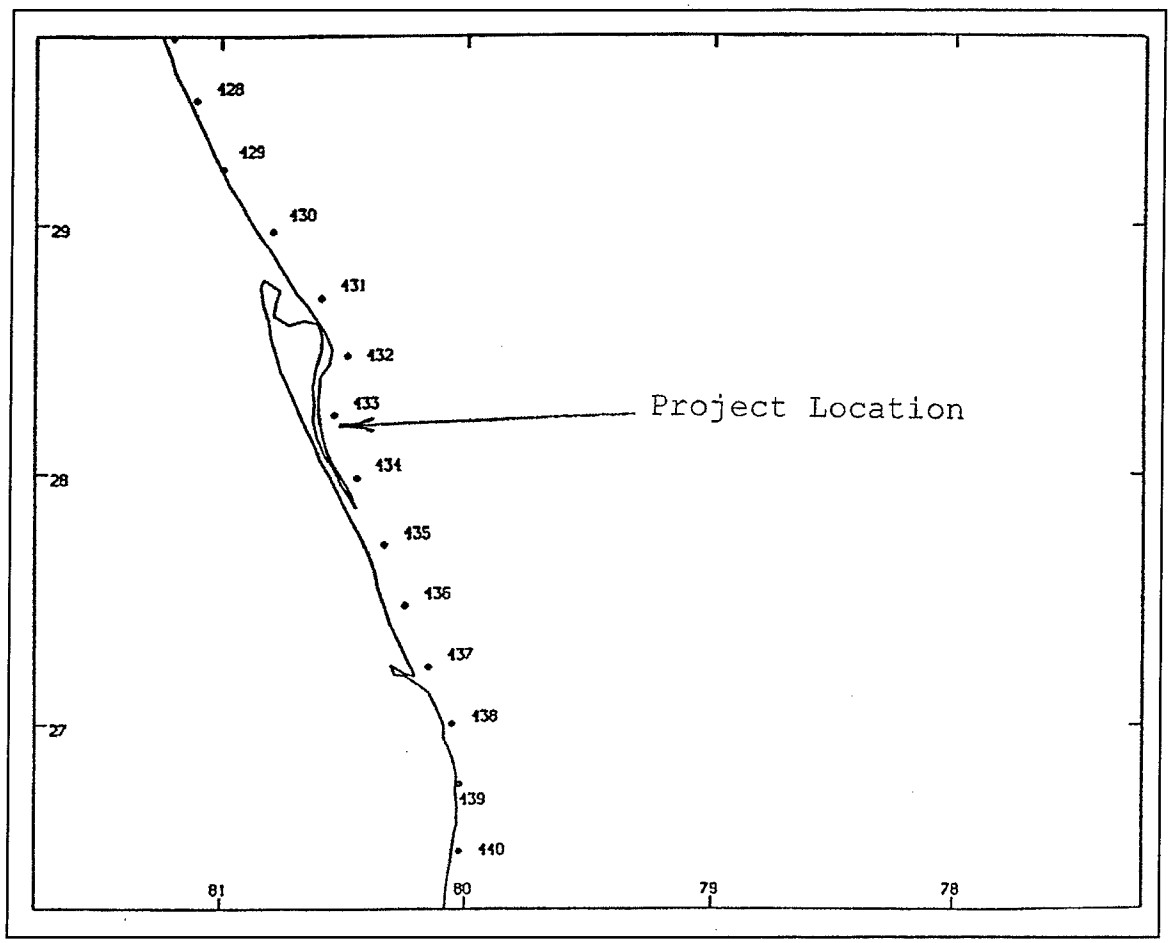

Figure 24. Location of project beaches and Station 433

of Station 433 is shown in Figure 24. The storm-surge database yielded 20 tropical storms that have significantly influenced the area represented by Station 433. In this case, a significant influence implies the storm resulted in a surge of at least 1.0 ft at the site in question. The 20 storms identified for Brevard County are listed in Table 26. Individual storm tracks and maximum surge elevations at all nearshore stations are available in the tropical-storm database summary report (Scheffner et al. 1994). An estimate of the frequency of occurrence of tropical storms that impact the project shores can be computed as 20 events/104 seasons = 0.192 events per year.

Extratropical-storm selection. Tropical storms that have influenced the project shores were readily identified by inspection of storm-surge elevations; however, the identification of influential extratropical storms was not as straightforward. As noted previously, the extratropical-storm database contains 16 winter seasons of storm surge and current hydrographs. An initial assumption was that inspection of hindcasted wave-height hydrographs corresponding to each season would reveal individual storms; however, that assumption was incorrect. An alternative for identifying individual storms involved inspection of

Table 26
Tropical Events Impacting Project Beaches

HURDAT Storm No.	Given Name	Date (month/day/year)
112	Not named	08/03/1899
127	Not named	08/04/1901
194	Not named	10/09/1910
271	Not named	07/22/1926
276	Not named	09/11/1926
289	Not named	08/03/1928
292	Not named	09/06/1928
296	Not named	09/22/1929
331	Not named	08/31/1933
353	Not named	08/29/1935
357	Not named	10/30/1935
440	Not named	10/12/1944
461	Not named	09/04/1947
473	Not named	09/18/1948
477	Not named	08/23/1949
499	King	10/13/1950
530	Hazel	10/07/1953
629	Cleo	08/20/1964
662	Abby	06/01/1968
777	David	08/25/1979

storm-surge elevation and current hydrographs available from the 16-season extratropical database. Those hydrographs for Station 433 during the 1977-78 season are shown in Figure 25. However, as the figure indicates, conclusive identification of storm periods was not possible based on inspection of these first-order parameters. One might expect storm surge to be an effective indicator of storm activity; however, the project shores are not typically subjected to extreme surge elevations, in part because of bathymetry, sheltering by Cape Canaveral, and typical forcing characteristics of extratropical weather systems. Therefore, the first-order storm-surge elevation was not an acceptable storm-identifying parameter for the Brevard County project.

Experience gained during analysis of the Mud Dump Disposal site (i.e., Example 1) indicated that an appropriate second-order parameter could be a more effective identifier of individual extratropical storms. Past recession analyses have shown that beach response to storms is particularly sensitive to the magnitude and duration of the surge; therefore, as a third alternative for

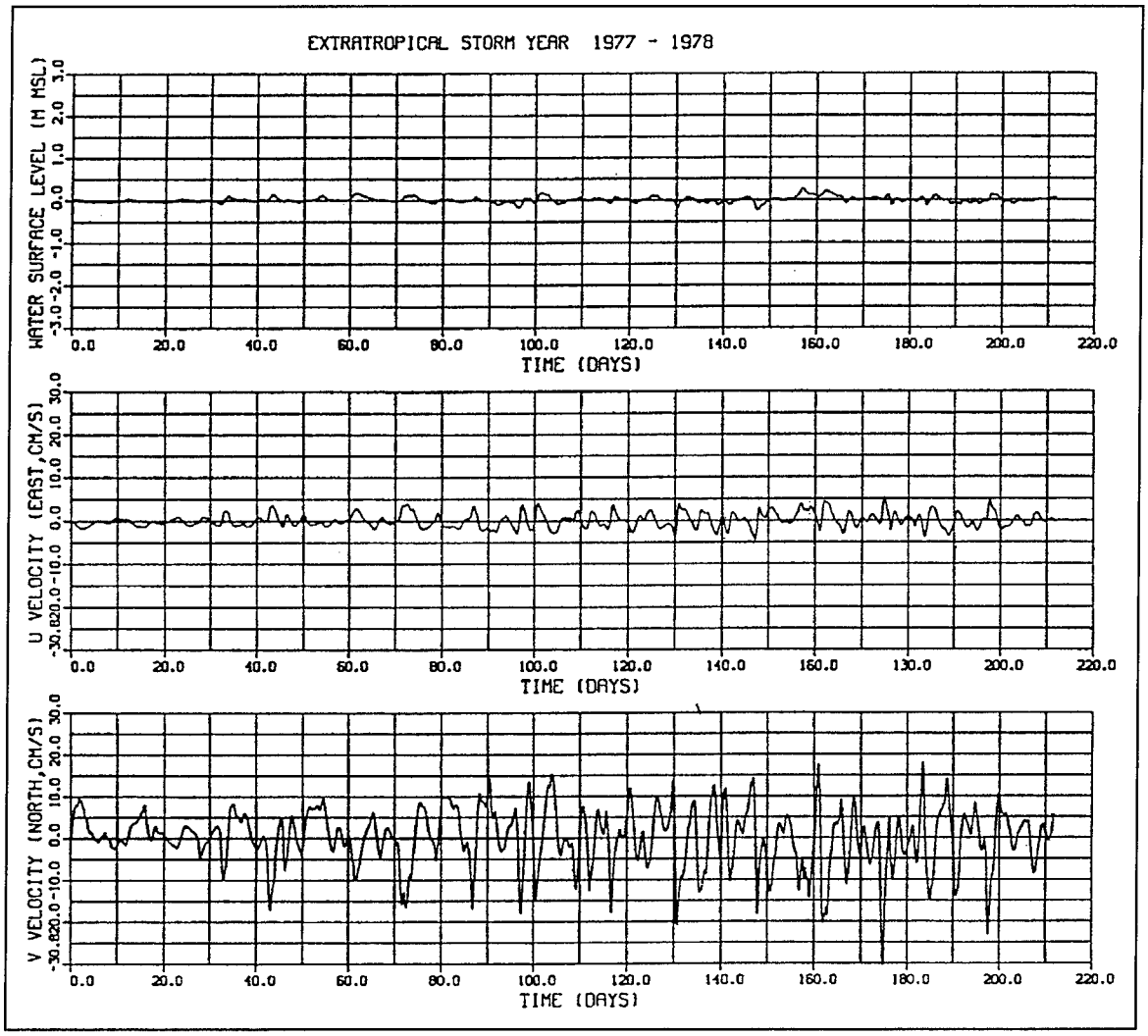

Figure 25. Storm-surge elevation and current data, 1977-78 extratropical season

identifying individual storms, investigators chose to inspect hydrographs of the surge magnitude squared, which is directly proportional to the energy in the long period storm-surge wave. An example, again reflecting the 1977-78 season, is provided in Figure 26.

The resulting hydrograph is obviously a more effective tool for assisting in the identification of individual storms. Inspection of surge-squared hydrographs for the other 15 seasons, a general estimation of the frequency of extratropical storms along the east coast of Florida, and knowledge concerning the more prominent storms, such as the November 1994 Thanksgiving Day Storm, resulted in a 0.5-ft^2 threshold magnitude of the second-order surge parameter. Therefore, individual extratropical storms were identified as those events characterized by surge-squared values that equaled or exceeded 0.5 ft^2. As an example, Figure 27 indicates that one extratropical storm, which occurred in February, influenced the Brevard County shores during the 1977-78 season.

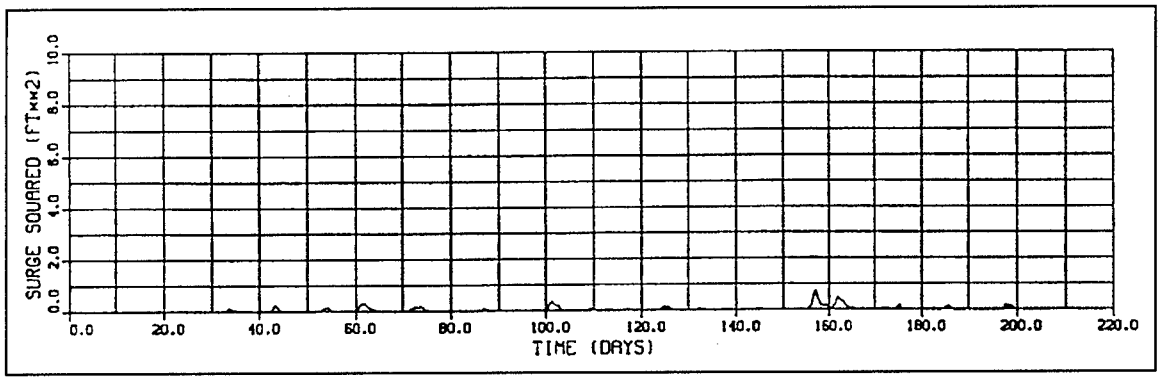

Figure 26. Surge-squared hydrograph, 1977-78 extratropical season

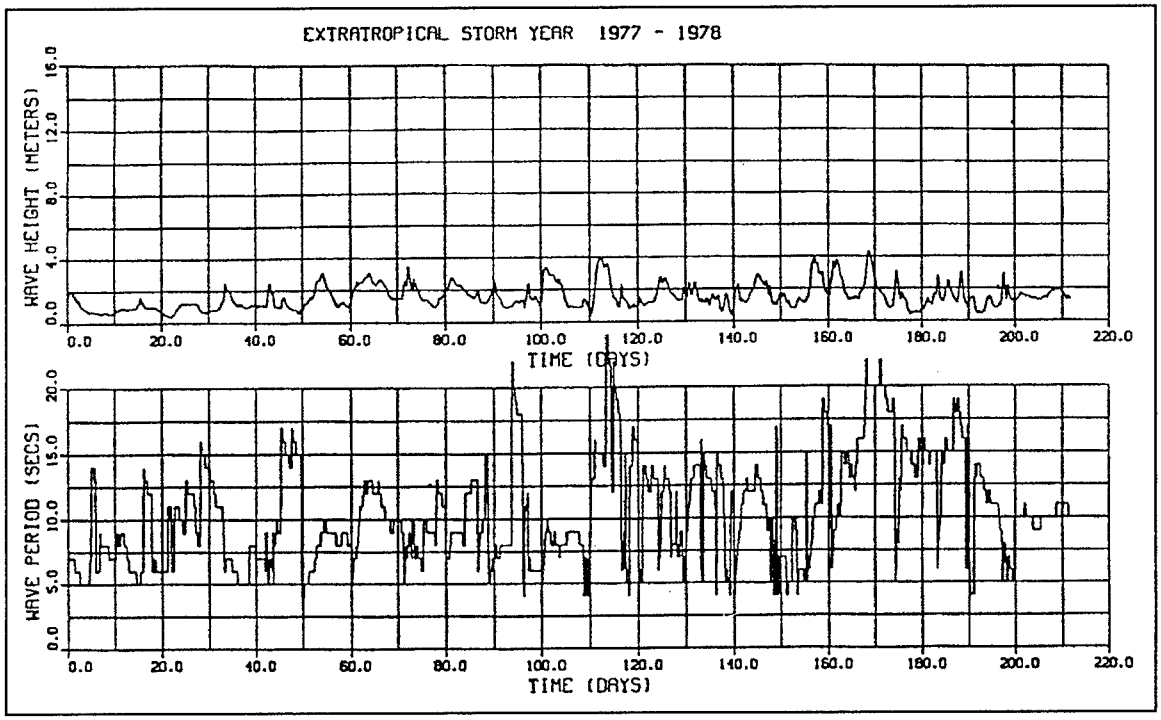

Figure 27. WIS wave data, 1977-78 extratropical season

Analysis of all 16 extratropical storm seasons resulted in a compilation of the storms listed in Table 27. This table indicates that 22 storms influenced the Brevard County beaches during the extratropical seasons from 1977 through 1993. It also identifies the approximate day of occurrence (measured from 1 September) and magnitude of the second-order surge parameter. An estimate of the frequency of occurrence of extratropical storms that impact the project site can be computed as 22 events/16 seasons = 1.375 events per year.

In summary, the procedure for selection of storm events resulted in the identification of 20 tropical storms and 22 extratropical storms that have influenced the Brevard County beaches. The tropical-storm database

Table 27
Summary of Storm Events by Day of Maximum Surge Squared

Year	1	2	3	4	5	Total
77-78	157/0.7	-	-	-	-	1
78-79	47/0.7	119/1.0	170/0.8	-	-	3
79-80	65/0.6	-	-	-	-	1
80-81	112/0.8	166/1.0	-	-	-	2
81-82	-	-	-	-	-	0
82-83	-	-	-	-	-	0
83-84	115/0.8	122/1.5	143/0.8	-	-	3
84-85	84/1.5	-	-	-	-	1
85-86	14/0.7	130/1.0	203/0.6	-	-	3
86-87	48/0.7	75/0.9	96/0.5	128/1.6	-	4
87-88	-	-	-	-	-	0
88-89	144/0.5	-	-	-	-	1
89-90	-	-	-	-	-	0
90-91	-	-	-	-	-	0
91-92	-	-	-	-	-	0
92-93	148/1.0	199/1.1	-	-	-	2

encompasses those storms that occurred during the 104-year period from 1886 through 1989. The extratropical-storm database includes 16 years of data, from 1977 through 1993. Estimated frequencies of occurrence for tropical and extratropical storms that influence the Brevard County beaches are 0.192 and 1.375 storms per year, respectively.

Tidal conditions

The total storm-induced surge elevation (prior to inclusion of wave and wind setup) can be divided into two major components, storm surge and astronomical tide. The tropical and extratropical simulations that generated the storm-surge characteristics contained in the DRP database did not include consideration of tides at the time of the storm event. Storm-surge modeling was performed with respect to mean sea level; however, total surge elevation and corresponding beach recession estimates can be significantly influenced by the magnitude and phasing of the tidal component. Tidal influence was accounted for by assuming that each storm event has an equal probability of occurring at any time during the tidal cycle.

For this analysis, investigators simplified that assumption by allowing the onset of the storm conditions to coincide with four individual tidal phases.

Those phases were designated as 0 deg (high tide), 90 deg (MSL during peak flood), 180 deg (low tide), and 270 deg (MSL during peak ebb). Tidal constituents characteristic of the project site were obtained from the DRP database for computation of tidal elevations. The result of combining storm surge and tidal components of the total surge elevation is a fourfold increase in the number of individual storms in the tropical and extratropical databases. For example, each individual storm in the original 20-storm tropical database was represented by four storms that differ solely with regard to tidal phasing; therefore, the tropical-storm database was expanded from 20 to 80 storms, and the extratropical-storm database was expanded from 22 to 88 storms.

It should also be noted that time histories of the storms in question were limited in duration to the periods in which the storms were influencing the project beaches. The appropriate hydrograph durations for extratropical and tropical storms were determined to be 150 and 42 hr, respectively. Extratropical-storm hydrographs were generated with a 3-hr time-step to accomplish compatibility with the hindcasted wave data. Tropical-storm hydrographs were generated with a 1-hr time-step.

Wave conditions

The WIS database available in the CEDARS was used as the source of extratropical wave information. WIS Station 18 was identified as the wave hindcast station nearest the project site. An example of the resulting data is provided in Figure 27, which depicts the wave height and period hydrographs for the 1977-78 winter season. Those wave height and period hydrographs represented deepwater wave conditions at WIS Station 18. Wave transformation to reflect nearshore wave conditions was accomplished during execution of the beach recession model. As the figure indicates, visual inspection of wave height and period time series were not an effective method for identifying individual extratropical storms and the reason for developing an energy approach to storm identification.

Wave conditions corresponding to tropical storms were computed in accordance with the procedures described in Example 1. Storm track direction and minimum height and period values were specified based on information from the WIS summary tables (Hubertz et al. 1993) for Station 18.

Storm-event hydrograph input

The previous three steps now need to be combined to develop input hydrographs for the SBEACH program. Since this application involves beach recession as the response vector, the influencing parameters include storm-surge elevation, wave height, and wave period. Typical examples of constructed hydrographs reflecting extratropical and tropical conditions are presented in Figure 28.

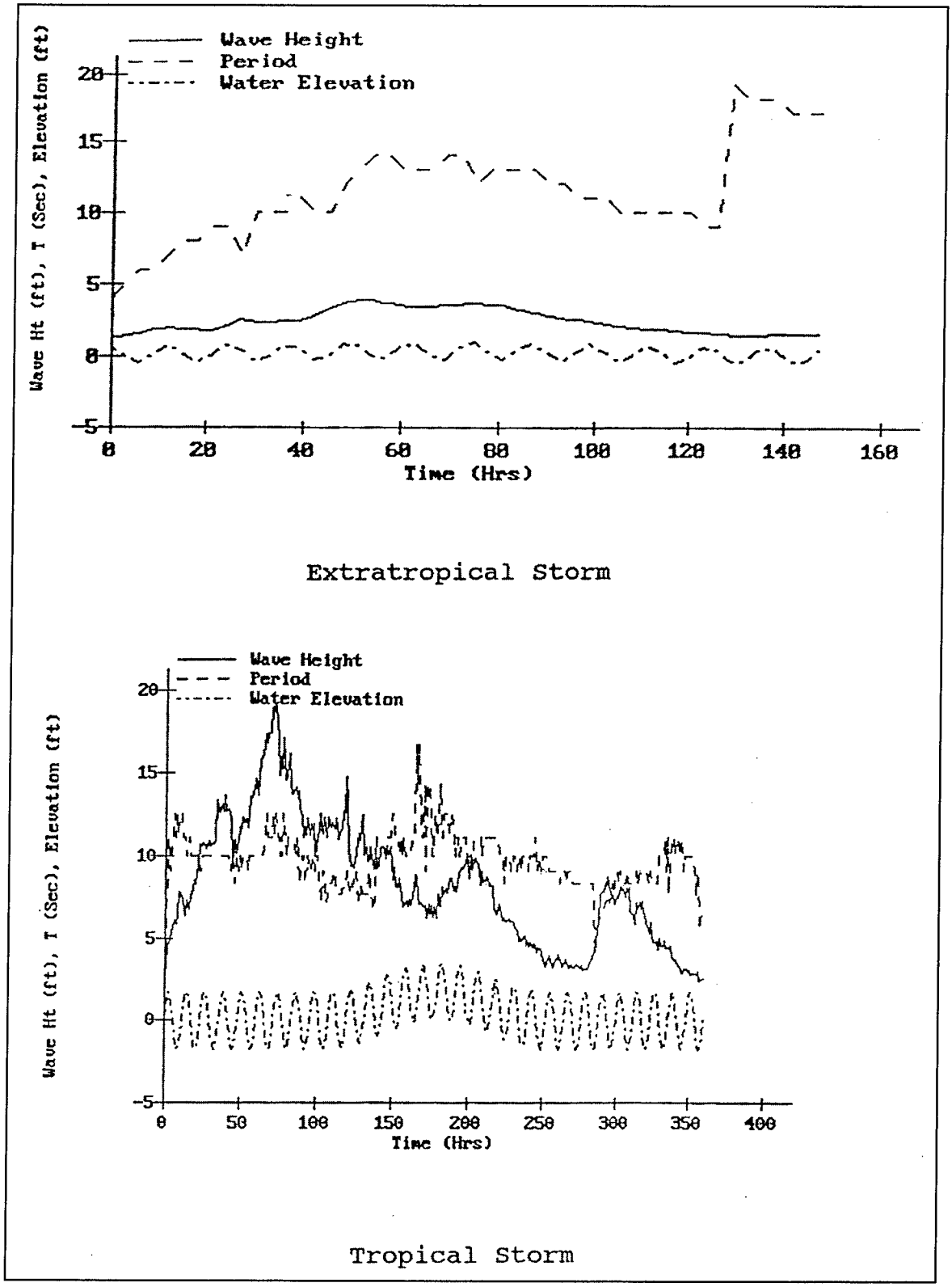

Figure 28. Typical wave and surge conditions

Response vector generation - the SBEACH model

In this example, the damages of concern are related to beach recession, which may be estimated with models such as SBEACH (Larson and Kraus 1989; Larson, Kraus, and Byrnes 1990). The SBEACH model was developed to simulate beach-profile changes that result from varying storm waves and water levels. These profile changes include the formation and movement of major morphological features such as longshore bars, troughs, and berms. SBEACH is a two-dimensional model that considers only cross-shore sediment transport, i.e., the model assumes that simulated profile changes are produced only by cross-shore processes. SBEACH is an empirically based numerical model that was formulated using both field data and the results of large-scale physical model tests. Input data required by SBEACH describe (a) the storm being simulated and (b) the beach of interest. Basic requirements include time histories of wave height, wave period, and storm-surge elevation, beach-profile surveys, and median-sediment grain size. For this investigation, recession was defined as the horizontal distance from the mean high-water mark on the prestorm profile to the most landward point where the vertical difference in prestorm and poststorm profiles equals 0.5 ft. Figure 29 depicts an example computed storm-induced recession of about 150 ft.

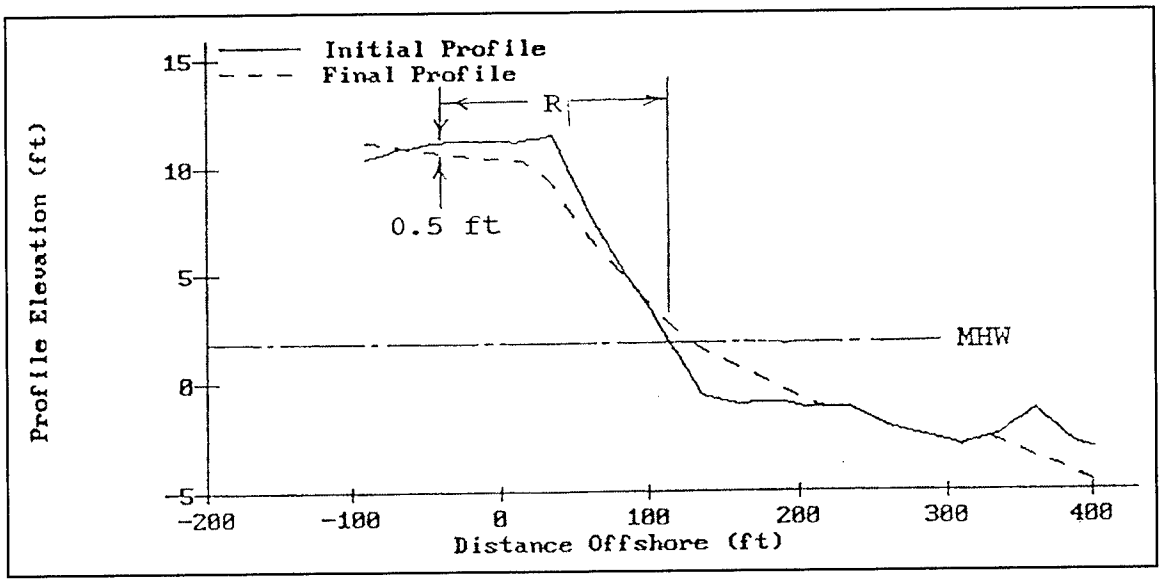

Figure 29. Storm-induced recession defined

For each storm simulation, the initial step in the SBEACH modeling procedure was transformation of the deepwater wave conditions to the finite water depth corresponding to the seaward extent of the beach profile. For this application, profiles extended approximately 900 m offshore where depths ranged from 8 to 10 m. Wave transformations were performed using the methods developed for the Shoreline Modeling System (Gravens 1992).

A comparative analysis of beach-profile surveys indicated that the project shoreline could be divided into three reaches. Each reach was represented by a composite profile generated with the Beach Morphology Analysis Package (Sommerfeld et al. 1993). SBEACH simulations of the 88 extratropical storms and 80 tropical storms were then performed for each reach. The estimated beach recession corresponding to each of those storms was archived for input to the EST analysis.

EST life-cycle simulations

The final step in the empirical simulation/frequency analysis involves preparation of the EST input files, simulation of life-cycle time series, and postprocessing of EST output. Input to the EST represents files containing input vectors and response vectors. The values of the input parameters reflect storm intensity. The response vector, in this application, quantifies the beach recession resulting from a given storm; and the storm-frequency parameters are used to dictate the occurrence of extratropical and tropical storms throughout the multiyear life-cycle analysis.

The goal of this phase of the frequency analysis is to generate multiple repetitions of multiyear scenarios in which storm events may occur. For this application, 100 repetitive simulations of a 200-year period of storm activity were performed. Simulations of extratropical and tropical storm histories were performed separately. For each simulation, a 200-year tabulation was generated that included the number of storms that occurred each year and the beach recession corresponding to each storm. This information provides the basis for calculation of return periods associated with various degrees of beach recession.

Tropical-storm vectors. The characteristics of individual tropical storms were defined as (a) tidal phase, (b) closest distance from the eye to the project site, (c) direction of propagation at time of closest proximity, (d) central-pressure deficit, (e) forward velocity of the eye, (f) maximum wind speed, and (g) radius to maximum winds. As noted previously, the response to each storm was defined as the horizontal distance from the mean high-water mark on the prestorm profile to the most landward point where the vertical difference in prestorm and poststorm profiles equals 0.5 ft. Input and response vectors for several tropical events are presented in Table 28. The frequency of occurrence of tropical storms that impact the project beaches was previously estimated as 0.192 events per year. This corresponds to one storm event every 5.2 years.

Extratropical-storm vectors. Input vectors describing extratropical storms were defined as (a) tidal phase, (b) storm duration, (c) maximum surge elevation, (d) wave height, and (e) wave period. The response vector was beach recession, as defined previously. Typical extratropical-storm vectors are presented in Table 29, which includes input and response vectors corresponding to the three storms that influenced Brevard County shores during the 1983-84 season.

Table 28
EST Input for Tropical Storms

Storm Number	Tidal Phase	Brevard County, FL - Tropical - Reach 1					Radius to Maximum Winds, nmi	Beach Recession, ft
		Eye to Project Distance, nmi	Track Direction, deg	Central Pressure Deficit, mbars	Maximum Wind Speed, knots	Forward Speed, knots		
72	1	28.97	340.71	27.81	101.95	11.8	8.68	25
72	0	28.97	340.71	27.81	101.95	11.8	8.68	28
72	-1	28.97	340.71	27.81	101.95	11.8	8.68	38
72	0	28.97	340.71	27.81	101.95	11.8	8.68	112
112	1	71.37	9.39	54.84	105	6.66	8.68	118
112	0	71.37	9.39	54.84	105	6.66	8.68	79
112	-1	71.37	9.39	54.84	105	6.66	8.68	82
112	0	71.37	9.39	54.84	105	6.66	8.68	143
127	1	196.12	278.76	30.39	36.46	5.28	43.42	110
127	0	196.12	278.76	30.39	36.46	5.28	43.42	118
127	-1	196.12	278.76	30.39	36.46	5.28	43.42	143
127	0	196.12	278.76	30.39	36.46	5.28	43.42	113
194	1	45.28	7.54	59.49	60.02	8.92	43.42	207
194	0	45.28	7.54	59.49	60.02	8.92	43.42	203
194	-1	45.28	7.54	59.49	60.02	8.92	43.42	203
194	0	45.28	7.54	59.49	60.02	8.92	43.42	203
249	1	54.06	75.08	55.35	80	10.65	34.46	203
249	0	54.06	75.08	55.35	80	10.65	34.46	161
249	-1	54.06	75.08	55.35	80	10.65	34.46	203
249	0	54.06	75.08	55.35	80	10.65	34.46	203
271	1	29.81	320.53	37.02	60.11	9.24	31.33	194
271	0	29.81	320.53	37.02	60.11	9.24	31.33	203
271	-1	29.81	320.53	37.02	60.11	9.24	31.33	203
271	0	29.81	320.53	37.02	60.11	9.24	31.33	197

The frequency of occurrence of extratropical storms that impact the project beaches was previously estimated as 1.375 events per year.

Frequency-of-occurrence computations. The primary objective of this application of the EST is the generation of damage versus frequency-of-occurrence relationships. For this project, curves (and corresponding tables) reflecting the frequency of beach recession were generated for each of the three Brevard County shoreline reaches. For the purposes of this example, the

Table 29
EST Input for Extratropical Storms

Brevard County, FL - Extratropical - Reach 1						
Storm Number	Tidal Phase	Duration, hr	Maximum Surge Ht, m	Maximum Wave Ht, m	Peak Wave per sec	Beach Recession, ft
1	1	42	0.41	3.3	9	108
1	0	42	0.50	3.9	11	110
1	-1	42	0.48	3.9	10	118
1	0	42	0.45	3.8	9	100
2	1	36	0.54	4.7	12	130
2	0	36	0.65	4.9	11	143
2	-1	36	0.57	4.7	10	116
2	0	36	0.43	4.3	12	113
3	1	39	0.45	4.4	9	130
3	0	39	0.37	3.7	16	116
3	-1	39	0.40	3.9	16	118
3	0	39	0.43	4.3	10	116
4	1	66	0.68	5.8	14	153
4	0	66	0.68	5.4	14	153
4	-1	66	0.62	5.2	13	156
4	0	66	0.68	6.1	14	149

discussion of results will be limited to only one reach. A summary of the Reach 2 results is provided below.

Tropical storms. As noted above, 100 repetitive simulations of a 200-year period of tropical-storm activity were performed. Each of those simulations yielded a recession-recurrence relationship, as shown in Figure 30. For each return period, a mean recession value was computed. Those values are represented by the broad curve of Figure 30. The data spread or scatter relative to the mean values indicates a reasonable degree of variability, as would be expected. This variability is quantified through computation of the standard deviation for each return period. For use in economic analyses or project design, the probabilistic recession data may be displayed as shown in Figure 31. This provides the mean frequency-of-occurrence relationship with upper and lower confidence limits defined by the standard deviation value. Table 30 summarizes the frequency-of-occurrence relationships for tropical-storm-induced beach recession at Reach 2.

Extratropical storms. The statistical procedure described above was also used for analysis of the extratropical-storm-induced recession data. Comprehensive results of the 100 repetitive simulations of a 200-year period of

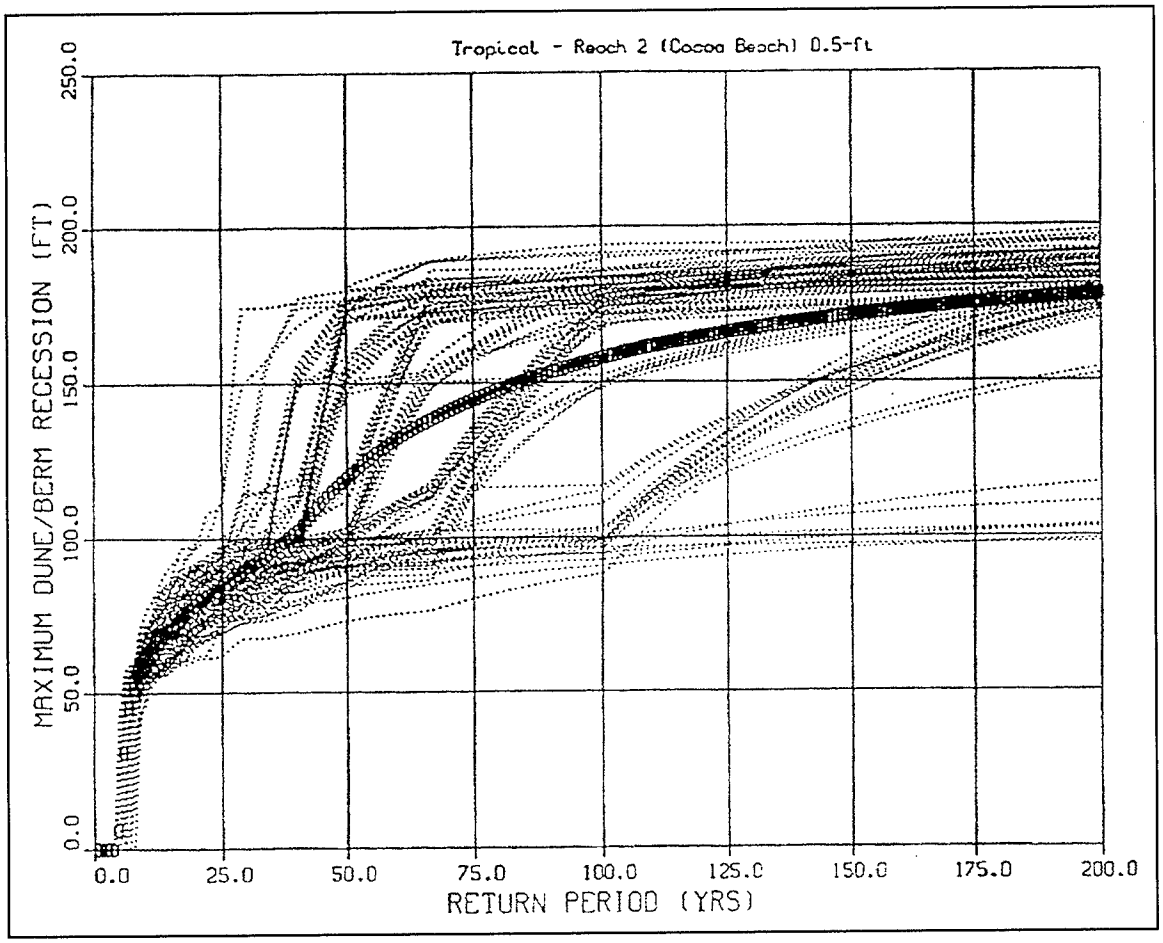

Figure 30. Tropical-storm recession-frequency relationships

tropical-storm activity are presented in Figure 32. The mean frequency-of-occurrence relationship with upper and lower confidence limits defined by the standard deviation value is shown in Figure 33. Table 31 summarizes the frequency-of-occurrence relationships for extratropical-storm-induced beach recession at Reach 2.

Combined tropical and extratropical storms. For the Brevard County application, the frequency analysis is to be used in an economic evaluation of the impacts of beach recession; therefore, the frequency-of-occurrence versus recession relationships served as input to an economic model. The economic model estimates beach-recession-related costs that will be incurred over a multi-year period if no project improvements are constructed. Economic models such as this are often modified to maximize their effectiveness for particular applications; therefore, the models used by individual agencies may vary considerably. Users must ensure that the recession/frequency relationships are developed properly so that the EST results are suitable for use in the selected economic model. For example, the economic model used in this application required recession/frequency relationships in which the frequency of occurrence

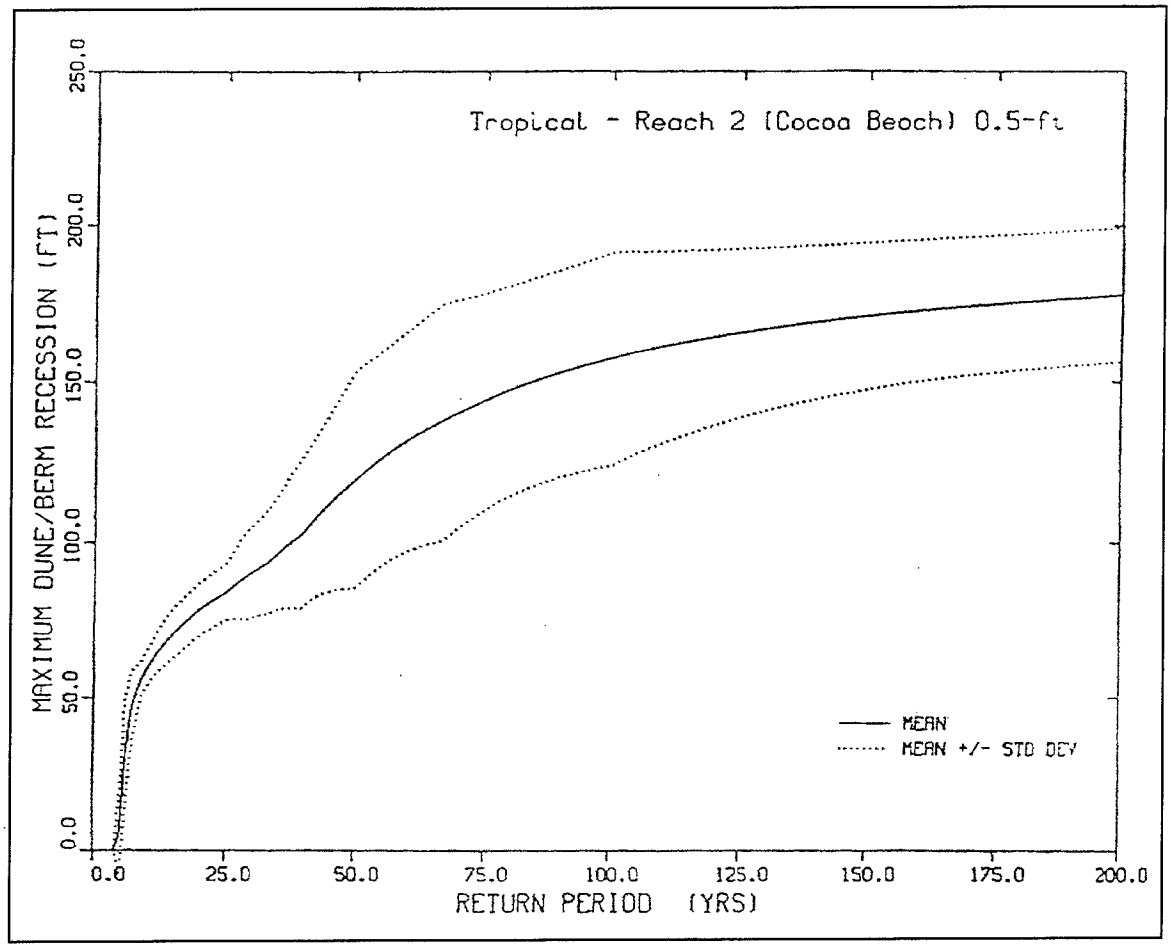

Figure 31. Tropical-storm recession-frequency relationships (mean values ± one standard deviation)

Table 30
Tropical Storm Recession Return Periods, Reach 2 - Cocoa Beach

Return Period, years	Beach Recession, ft	Standard Deviation, ft
1	0	0
2	0	0
5	6	14
10	59	6
25	84	9
50	119	34
75	144	34
100	158	34
150	171	23
200	178	22

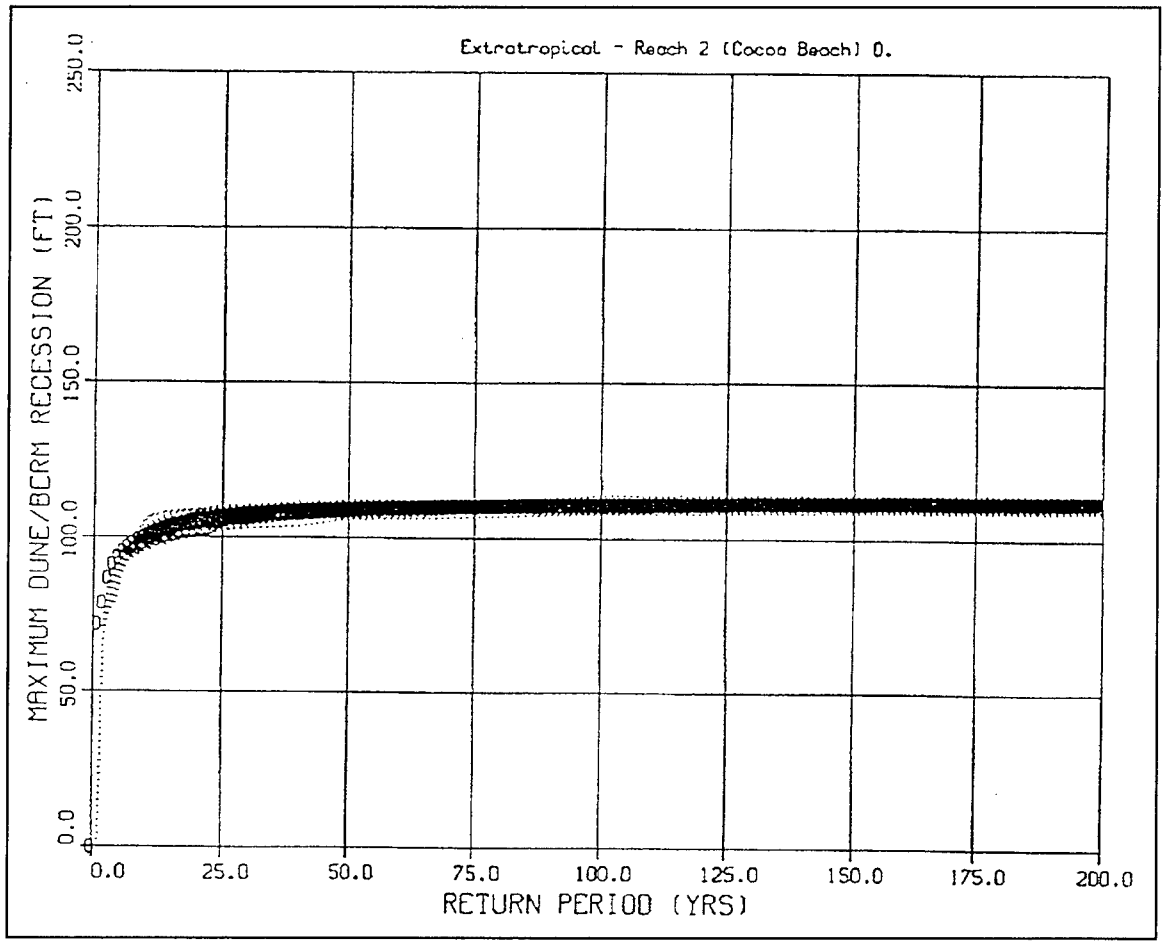

Figure 32. Extratropical-storm recession-frequency relationships

corresponded to individual storms (i.e., episodic recession). Other economic models may consider cumulative recession, with partial beach recovery, when more than one storm occurs in a season. For those models, the recession/frequency relationships should reflect cumulative recession, and frequency of occurrence should refer to storm seasons, not individual storms.

In the Brevard County application, no distinction was made between extratropical and tropical storms in the economic model; therefore, for compatibility with the economic model, the two sets of EST results were merged according to the methodology presented in the first section of this report. For example, the following algorithm was used to accomplish this combination of extratropical and tropical results:

For a given recession value: $R_c = (1/R_t + 1/R_e)^{-1}$ (39)

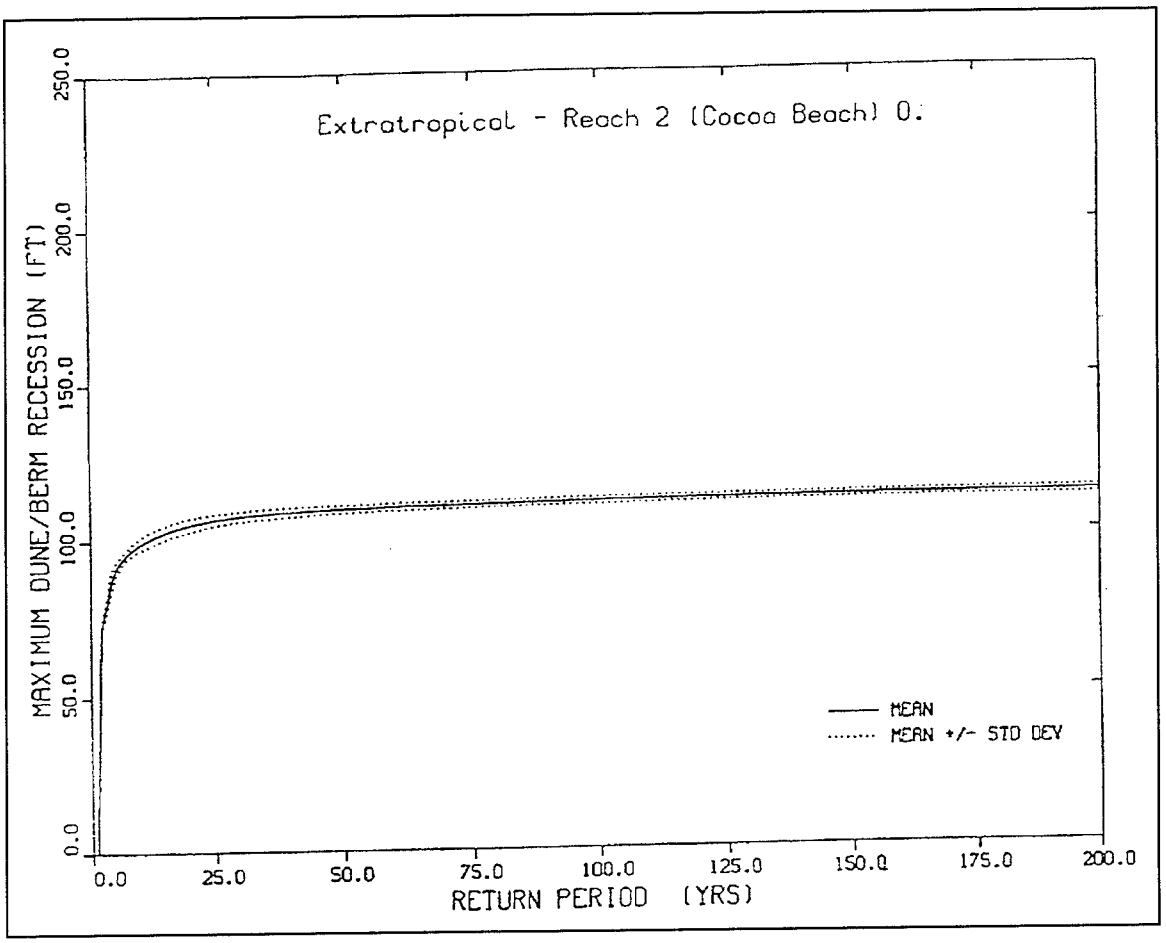

Figure 33. Extratropical recession-frequency relationships (mean values ± one standard deviation)

Table 31
Extratropical Storm Recession Return Periods, Reach 2 - Cocoa Beach

Return Period, years	Beach Recession, ft	Standard Deviation, ft
1	16	0
2	72	2
5	91	2
10	99	2
25	106	2
50	109	1
75	110	1
100	111	1
150	112	1
200	112	1

where

R_c = combined return period corresponding to the chosen recession

R_t = tropical-storm return period corresponding to the chosen recession

R_e = extratropical-storm return period corresponding to the chosen recession

The resulting curve is depicted by the solid line in Figure 34. The hashed curves represent the mean recession curves corresponding to extratropical and tropical storms. The figure indicates, as expected, that extratropical storms (because of their greater frequency of occurrence) dominate the results corresponding to lower return periods. The greatest recession values were characteristic of severe tropical storms, as indicated in the figure. Return periods associated with levels of combined storm recession are provided in Table 32.

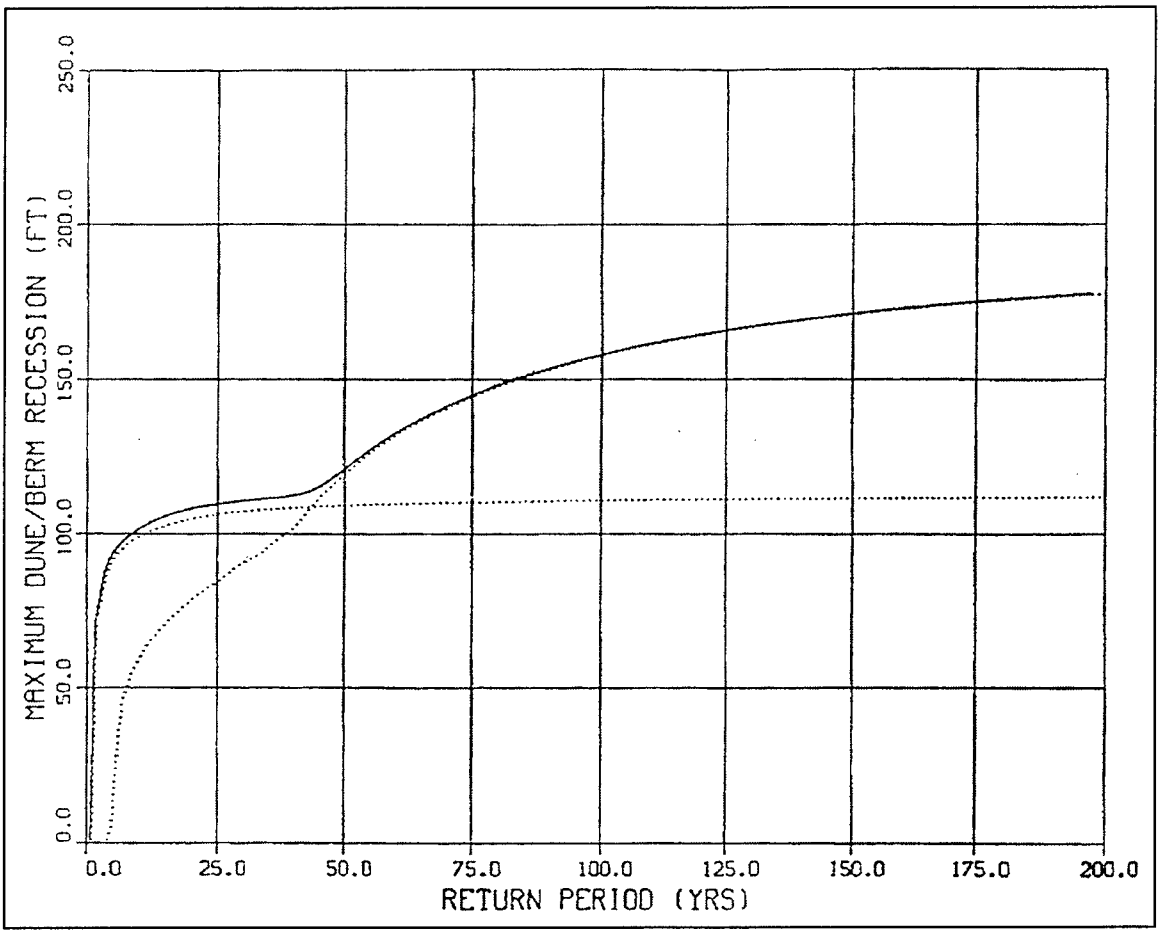

Figure 34. Combined extratropical/tropical beach recession versus frequency-of-occurrence relationship

Table 32
Combined Storm Recession Return Periods, Reach 2 - Cocoa Beach

Return Period, years	Beach Recession, ft	Standard Deviation, ft
1	16	2
2	74	2
5	93	2
10	102	6
25	110	9
50	121	34
75	145	34
100	158	34
150	171	23
200	178	22

Figures 33 and 34 indicate that beach-recession values corresponding to extratropical storms approach their maximum at relatively low return periods, i.e., 10 to 15 years. Then for greater return periods, there is little increase in recession, as indicated by the flat portion of the recession/frequency curve. This uniformity of extratropical recession results is due, in part, to the relatively minor extratropical storm surges characteristic of the project site. Since storm-surge influence is minor, the forcing parameters that dominate the recession calculations are wave height and period; however, the waves are typically depth limited; therefore, even for significantly different deepwater wave conditions, there is little wave height variation after transformation to the nearshore zone.

Summary

The preceding information provides an additional example of how the EST procedure may be applied to engineering problems that require probabilistic analyses. This application generated frequency-of-occurrence relationships for storm-induced beach recession. Those relationships were then utilized as input to an economic model for quantification of recession-related damages.

Example 3: Reformulated Fire Island to Montauk Point Storm-Surge Study

The Fire Island to Montauk Point (FIMP) study was initiated in 1981 to develop storm-surge elevation frequency-of-occurrence relationships along the coast and within the bays of southern Long Island, NY. Results of the FIMP

study, completed in 1983, were utilized for the development of storm-surge protection criteria. The southern shore of Long Island, NY, has experienced significant erosion in the past two decades because of seasonal storms. This erosion has affected the elevation of the protective dune system as well as shoreline orientation, nearshore and back-bay bathymetry, and inlet orientation and cross-sectional geometry. Because these alterations to the physical system can affect the propagation of a storm surge and the subsequent possibility of overtopping, breaching, and back-bay flooding, a new study, titled the Reformulated Fire Island to Montauk Point (REFIMP) study, was initiated in 1995. This revisit of the FIMP study provided an opportunity to apply state-of-the-art numerical and stochastic modeling techniques.

The study requested by the New York District requires evaluation of the impact of storm events on both open-coasts and back-bay areas protected by barrier islands. The specific study area of interest extends from Fire Island Inlet to Moriches Inlet, to Shinnecock Inlet, and includes Great South Bay, Moriches Bay, and Shinnecock Bay as shown in Figure 35. Study goals therefore require high-resolution modeling of both tropical and extratropical events. Because the CEDARS databases do not contain surge or circulation data to support this study, surge computations are made using the ADCIRC long-wave hydrodynamic model.

A problem often encountered in the modeling of nearshore flow dynamics is that the computational boundaries of the model are not well removed from the area of interest. For example, the continental shelf can substantially affect the amplitude and phase of a storm surge propagating from open water onto the shelf. A major advantage of unstructured grids is the ability of having sparse resolution in areas of deep bathymetry and high resolution in shallow areas of interest. The 20,000-node computational domain used in the generation of the DRP east coast, Gulf of Mexico, and Caribbean Sea databases formed the initial grid for the REFIMP grid. Because high resolution was to be placed in the study area, the initial grid was truncated at south Florida. The final grid for the REFIMP study is shown in Figure 36. In this grid, the offshore boundary to the east is placed at 60° west longitude, while the southern boundary is placed at approximately 26° north latitude. An example of grid flexibility is shown in Figures 37 and 38, which represents an enlargement of the study area. Figure 37 is the computational grid in which the barrier islands (shaded) are included in the grid in order to allow for wetting/drying and overtopping. Figure 38 shows the high-resolution capability of the model by detailing the entrance to Fire Island Inlet.

The CEDARS time-series databases are inappropriate for applications requiring high spatial resolution; however, the specific storms that have historically impacted the area were identified from the tropical-storm summary report generated through the DRP (Scheffner et al. 1994). The following sections summarize the selection of the training set of events and the use of these events to generate storm surge versus frequency-of-occurrence relationships. This example represents a more rigorous development of input and response vectors requiring that ADCIRC simulations be verified by demonstrating that the

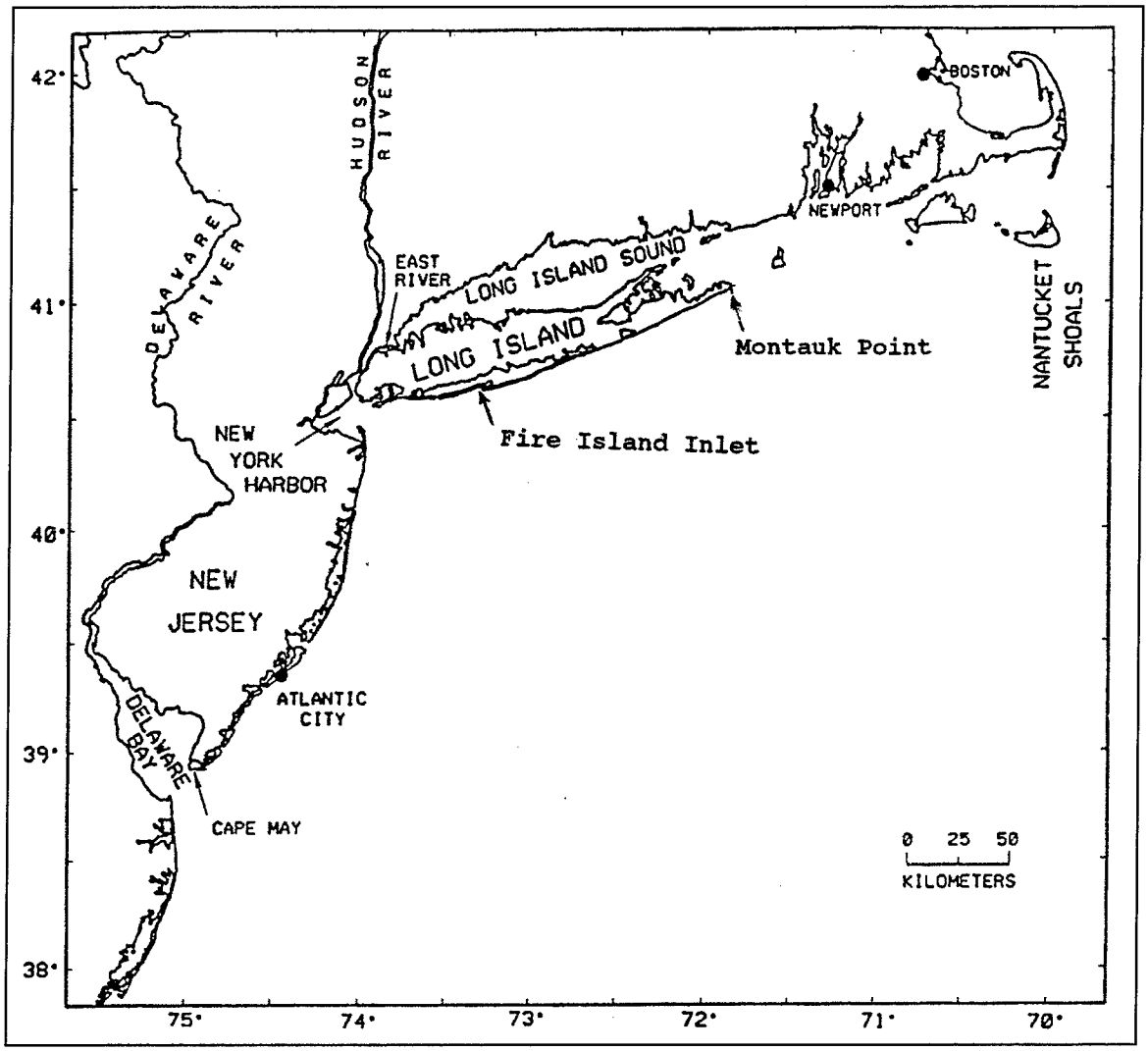

Figure 35. FIMP study-site location

model is capable of acceptably reproducing tides and tropical and extratropical storms in the study area. Therefore, the example description section on storm-event hydrograph input is replaced by a section of model verification. In this manner, the input hydrographs of tide, wind, and pressure forcing are demonstrated to be correct. With this exception, the same general steps detailed in the previous examples are applicable here.

Storm-event selection

As reported in previous examples, the study begins with selecting specific tropical and extratropical events to populate the EST training set. Each event of the training set must be a realistic event for the area, either a historic event or a hypothetical event based on a historic event with a slightly altered path or radius to maximum wind. Site specificity is then ensured because the joint

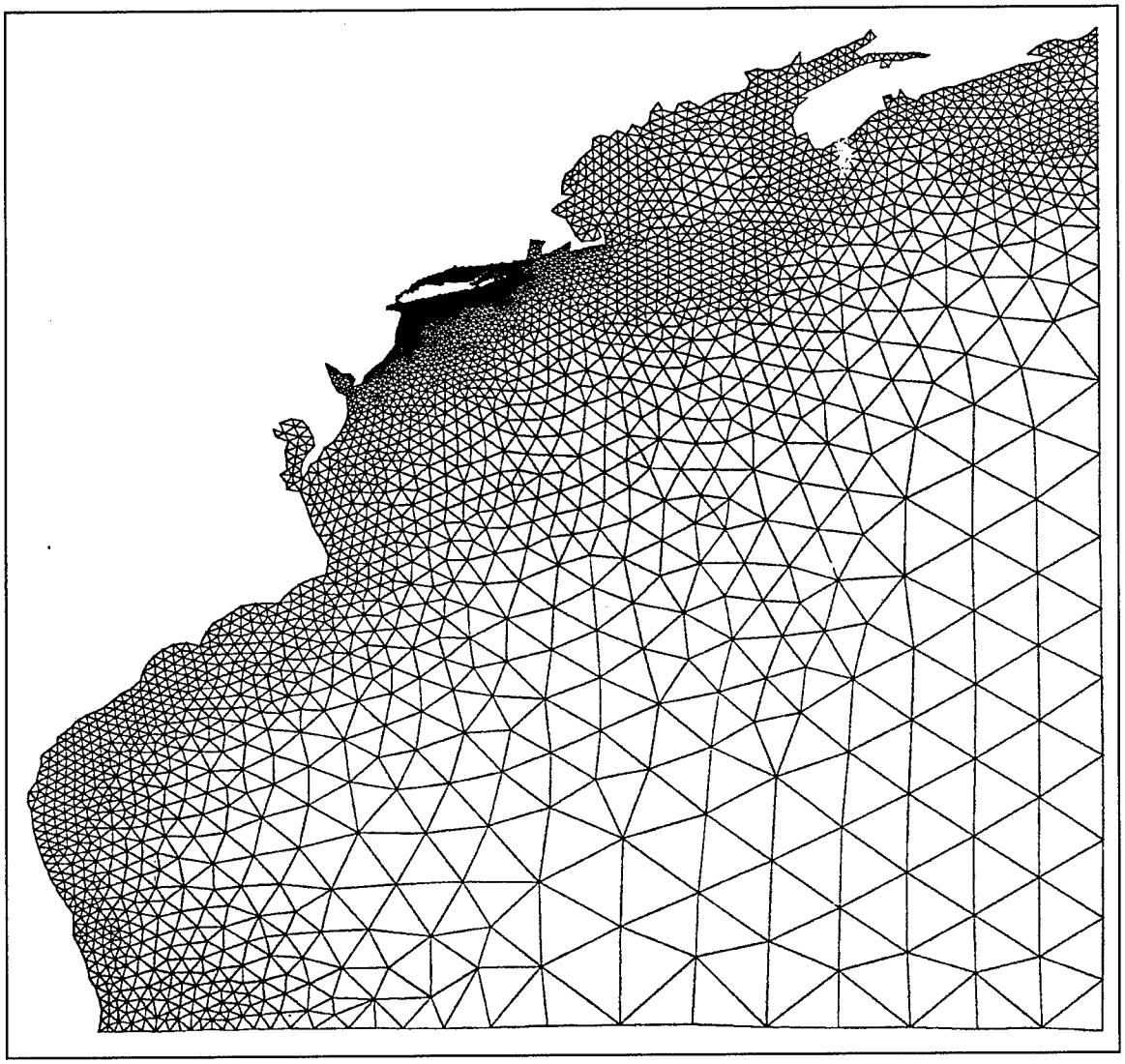

Figure 36. REFIMP computational grid

probabilities among the various input/response vectors reflect the joint probabilities inherent in parameters descriptive of actual events (or some slight variation of) that are site specific. The following two sections describe the construction of the tropical and extratropical training sets.

Tropical events. The tropical-storm database (Scheffner et al. 1994) previously described was used to define an initial training set of historical tropical events. Ideally, historical events represent the full range of possible event intensities. For extratropical events, this is generally the case because extratropical events occur often, cover extremely large areas, and persist for long periods of time (i.e., days). However, with tropical events, the worst case tropical-event scenario may be a historic event with a slightly shifted path or larger/smaller radius to maximum wind. Because the accuracy of the EST is dependent upon a full training set, some augmentation of the historic events is

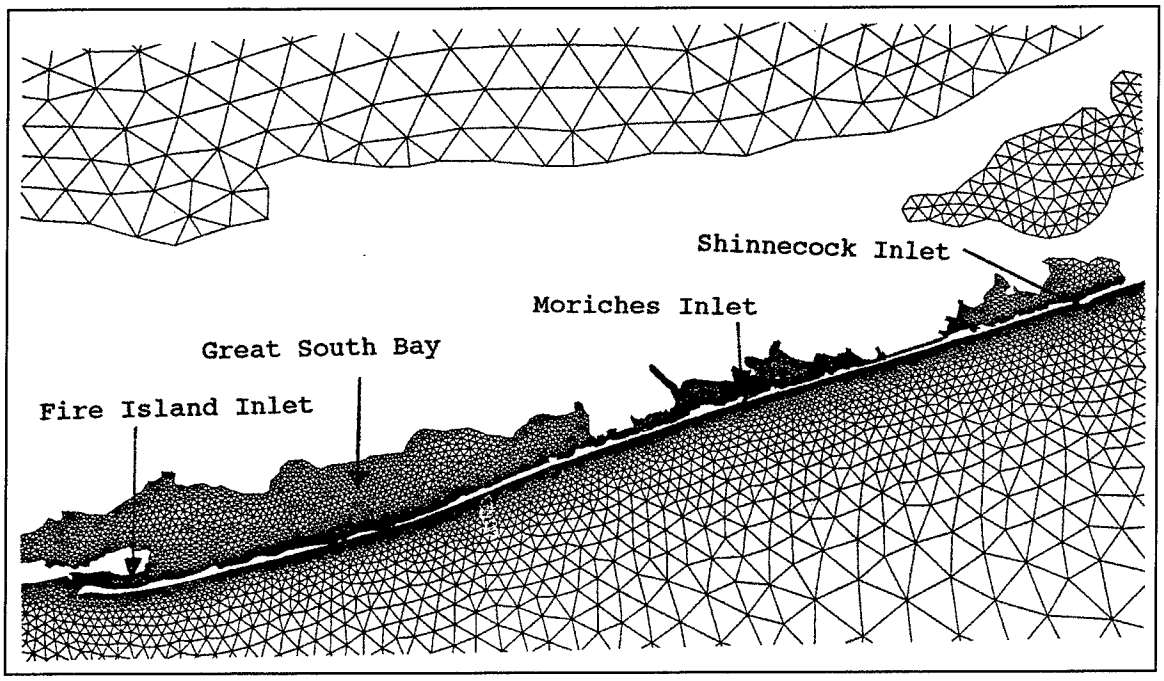

Figure 37. Barrier islands of REFIMP study

often necessary. This was found to be necessary for the REFIMP study because station locations of interest span over 50 miles, from Fire Island Inlet to east of Shinnecock Inlet, and typical radius to maximum winds are of this magnitude. Therefore, a storm or record in the eastern portion of the study area may not severely impact the western regions. An example follows.

Although severe events have occurred in the study area, i.e., the 1938 storm and Hurricane Gloria in 1985, they do not impact all stations equally. For example, the 1938 hurricane made landfall at the eastern side of Great South Bay, generating a 5.0-ft surge (without tide) in the vicinity of Fire Island Inlet. If, however, the 1938 event had made landfall 40 miles to the west, near Jones Inlet, the maximum storm surge near Fire Island Inlet would have been on the order of 11.0 ft. Therefore, although the 1938 event may represent a storm of record for some locations, it does not for other locations within the study area.

In order to supplement the training set so that all stations within the study experience a (hopefully) maximum intensity event, and thereby fill the vector space with events ranging from nominal to intense, four additional storm events were added to the initial training set. These events were developed as perturbations of the two most intense events of record, the 1938 event and Hurricane Gloria. These four combinations produced maximum surges throughout the study area. The final training set consisted of 20 events, 16 historical and 4 representing perturbations of the two most severe events of record. The full training set is shown in Table 33.

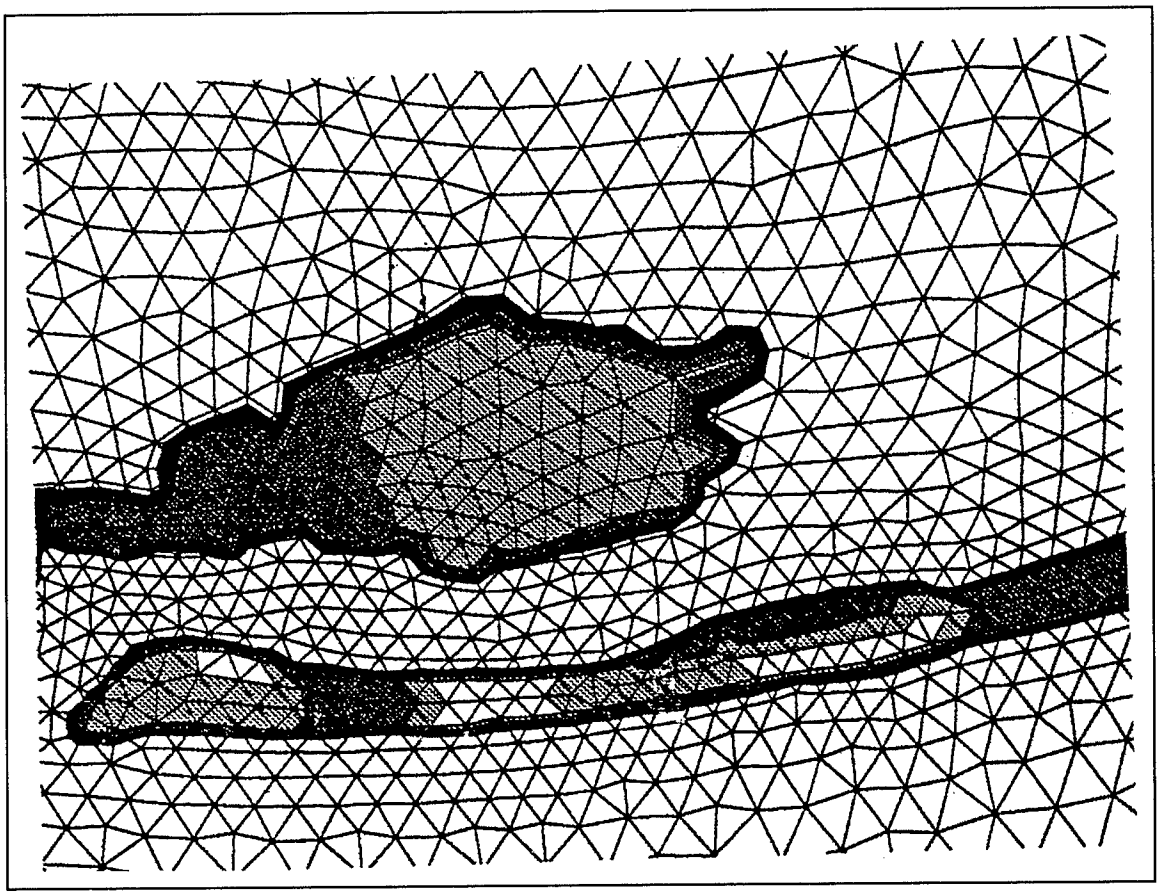

Figure 38. Fire Island Inlet representation of REFIMP grid

Extratropical events. In a similar manner to the tropical-event database described above, the CEDARS 16-year time-series databases at specific locations were inadequate for the needs of this study. However, the database was used to identify specific event periods that impacted the study area. These data contain severe events occurring during the 16-year sequence of winter months; however, as in the previously presented examples, identification of individual extratropical events within the records requires some additional analysis of the records. Time-series surface-elevation plots corresponding to an archived station near the center of the study area were analyzed. Each time series represented surge with no tide. Nine events were selected from the 1977-1993 winter season data base. The starting time for each of the nine events is shown in Table 34.

The storm events of Tables 33 and 34 represent the range of intensities of tropical and extratropical events that impact the study area. These events have historically occurred or have a reasonable potential for occurring based on past storm activity.

Table 33
Tropical Events Impacting the REFIMP Study Area

HURDAT Storm No.	Given Name	Date (month/day/year)
1. 296	Not named	09/22/1929
2. 327	Not named	08/17/1933
3. 332	Not named	09/08/1933
4. 353	Not named	08/29/1935
3. 370	Not named	09/08/1936
6. 386	Not named	09/10/1938
7. 436	Not named	09/09/1944
8. 535	Carol	08/25/1954
9. 541	Hazel	10/05/1954
10. 545	Connie	08/03/1955
11. 597	Donna	08/29/1960
12. 657	Doria	09/08/1967
13. 702	Doria	08/20/1971
14. 712	Agnes	06/14/1972
15. 748	Belle	08/06/1976
16. 835	Gloria	09/16/1985
17. 386a	1938_a	-
18. 386b	1938_b	-
19. 835a	Gloria_a	-
20. 835b	Gloria_b	-

Table 34
Extratropical Events Impacting the REFIMP Study Area

Events	Starting Date
1.	16 January 1978
2.	20 January 1979
3.	23 October 1980
4.	10 December 1983
5.	27 March 1984
6.	10 February 1985
7.	1 December 1986
8.	8 December 1992
9.	11 March 1993

Tidal conditions

The ADCIRC model has already been verified to tides with the generation of an eight-constituent tidal database over the full east coast, Gulf of Mexico, and Caribbean Sea domain from which the present computational grid shown in Figure 36 was extracted. Because the grid of the REFIMP study is truncated, a limited tidal verification was performed to demonstrate that tides were not affected by the truncation. As described above, only the M_2 tidal constituent is used in this study; therefore, verification is limited to the M_2.

Wave conditions

The application of the EST presented in this example was for storm surge only; therefore, no wave component was included. For some studies, however, a wave component is a necessary modeling task. For example, a study of total water-surface elevation-frequency relationships for the Samoan Islands requires consideration of wave ponding behind the reef system, wave setup, and wave runup. A summary of this study will be presented in the following example.

Model verification

Execution of the REFIMP study first requires that the ADCIRC model be calibrated and verified to demonstrate that results are consistent with known prototype response. This verification has to be made separately for tides, tropical storms, and extratropical events. Following the verification process, model simulations directly provide response vectors that can be considered accurate. The following three sections briefly describe the verification process for tides, tropical events, and extratropical events.

Tidal verification. Tidal propagation is simulated with the ADCIRC model by specifying a surface-elevation time series on the eastern and southern boundary of the computational grid. This elevation time series is computed from specified amplitudes and Greenwich epoch values that are available in the CEDARS database. The ADCIRC model has an internal harmonic analysis option such that amplitudes and epochs are computed at user-specified locations. Verification of the M_2 constituent was then made by comparing ADCIRC-computed amplitudes and Greenwich epochs to those for locations for which harmonic constituent data were available. Stations within the study area were shown to be reproduced in both phase and amplitude. These comparisons are made in Table 35.

Tropical-storm verification. Two efforts of verification of tropical-event propagation were made. In the first, simulated surge only (no tide) elevations at Sandy Hook and the Battery were compared with observed data reported by Harris (1963) and Jarvinen and Gebert (1986). These data are available at only a few locations, none of which are directly within the study area. As a result, the initial comparisons were made to adjust storm parameters to produce the most

Table 35
Tidal Verification of ADCIRC

Station Location	ADCIRC amp-ft	Harm. amp-ft	ADCIRC G-deg	Harm. G-deg
Atlantic City, NJ	1.845	1.914	0.36	354.14
Sandy Hook, NJ	2.074	2.151	11.04	7.12
The Battery, NY	1.877	2.104	27.08	22.54
Bridgeport, CN	2.835	3.185	103.41	107.96
Willits Point, NY	3.068	3.711	117.50	118.16
Montauk Point, NY	1.237	0.945	50.09	46.32
New London, CT	1.527	1.166	50.70	57.80
Newport, RI	1.678	1.684	14.78	1.26
East Rockaway Inlet	2.045	1.980	356.93	346.32
Jones Inlet - outside	1.943	1.830	357.18	349.54
East Bay	1.350	1.330	28.64	25.88
Fire Island CGS[1]	0.878	0.880	9.44	24.94
Heckshire State Park	0.443	0.417	95.89	96.98
Smith Point	0.495	0.500	93.20	81.66
Moriches CGS	1.182	0.870	25.76	13.70
Shinnecock CGS[2]	1.527	1.260	355.85	1.04

[1] Fire Island Coast Guard Station (CGS) Harmonic analysis compared with ADCIRC station Fire Island Bridge.
[2] Shinnecock CGS Harmonic analysis compared with ADCIRC station Shinnecock Inlet outside.

realistic event possible. Results of the ADCIRC/prototype comparisons were considered to be very good, as demonstrated in Table 36.

The second phase of verification was a detailed comparison of ADCIRC results to storm-surge elevation data collected/archived during the FIMP study. These data represented historical surge-elevation data within the study area for the 1938 hurricane and Hurricanes Carol and Donna. Results of the comparison led to the conclusion that the ADCIRC model was verified to tropical events.

Extratropical-storm propagation. A previous study for the New York District involved verification of two extratropical events that impacted the Bight. These two events were the March 1984 and December 1992 northeasters. Both events generated a documented surge at Sandy Hook of approximately 4.0 ft MSL. Therefore, the goal of the extratropical verification was to use the DRP wind-field database and reproduce peak surge elevations at Sandy Hook.

Simulations of the two events resulted in surges at Sandy Hook of 3.74 ft for March 1984 and 3.87 ft for December 1992. Detailed analysis of surge

Table 36
Comparisons of Maximum Surge Elevation (ft) of Harris (1963) and ADCIRC

Storm HURDAT Number (Name)	Sandy Hook Harris/ADCIRC	The Battery Harris/ADCIRC
296 (not named)	-	2.8/2.3
327 (not named)	2.1/1.2	2.3/1.7
332 (not named)	1.4/1.2	1.3/1.1
370 (not named)	1.9/2.4	2.4/2.1
386 (not named)	3.2/3.3	4.1/4.3
436 (not named)	5.3/4.8	5.0/4.2
535 (Carol)	3.2/2.7	3.1/2.7
541 (Hazel)	2.1/2.6	2.7/3.3
545 (Connie)	2.7/1.3	3.1/1.7
597 (Donna)	5.2/3.7	5.3/3.4
835 (Gloria)[1]	7.5/7.7	-

[1] Data of Jarvinen and Gebert (1986).

distribution in the study area was not perused because the ADCIRC results have been shown to be accurate in both the tidal and tropical storm-surge analysis. Therefore, reproduction of the two above events was considered sufficient for verification of ADCIRC to extratropical events.

Response vector generation - the ADCIRC model

Although ADCIRC has been verified for tides and storms, the accuracy of the frequency-of-occurrence relationships depends on two factors. First, the number of historic and hypothetical events must represent a realistic representation of possible events for the study area. Secondly, the frequency of sampling according to the Poisson criteria must be correct. The following sections summarize how the final training set was selected that resulted in the generation of a tropical- and extratropical-response vector set.

Tropical events. The original intent of the construction of the training set was to combine the 16 historical events and 4 hypothetical events with the four phases of the tide. This practice resulted in the creation of an 80-event training set. Preliminary results, however, showed that the surge elevations with return periods on the order of 50 years were too low. Evaluation of the training set showed that many low-intensity events, when combined with low tide, resulted in a negative surge. Therefore, these events were removed from the training set. The final training set therefore consisted of 66 events, with the following HURDAT events represented at only high tide and two MSL values: 296, 327,

332, 353, 370, 436, 535, 541, 545, 597, 657, 702, 712, and 748. The remaining events of Table 33 were represented by all four phases of the tide.

Verification of adequacy of the training set was made by plotting the location of the storm of record on the stage versus frequency-of-occurrence relationship generated via the EST and the 66-member training set. It is assumed that the worst event in 104 years of HURDAT data should represent an event with a return period of approximately 100 years. The event of record for the western half of the study area is Hurricane Gloria; the 1938 event represents the storm of record for the eastern half. The four relationships shown in Figure 39 represent the four near-coast stations of Jones Inlet outside (No. 10), Fire Island Mouth (No. 18), Moriches Inlet (No. 27), and Shinnecock CGS (No. 33). For each plot, the mean value frequency relationship is shown with the ± one standard deviation limits and the hurricane of record plotted at its respective location on the plot. In all cases, the storm of record is near the mean value and within the plotted error bounds. Through these comparisons, the tropical event training set was determined to be sufficiently populated to produce accurate frequency-of-occurrence relationships.

Extratropical events. The procedures used in the FIMP study were similar to those used in the REFIMP study, but with an alternate time period used in the analysis. The FIMP study paid a considerable amount of attention to matching historical databased frequency relationship. Therefore, the approach to verification of the extratropical training set was to generate frequency relationships at open locations that best matched the FIMP results. If the generated training set was adequate to accomplish this goal, it was considered adequate for generating frequency relationships at all sites in the study area.

Unlike tropical events, extratropical events of low intensity occur at least once a year. Although only nine events were used in the construction of the training set, those events represent severe storms and were selected to populate the upper extremes of surge. However, some criteria had to be established to determine a lower bound that reflects a small event occurring during spring tide. Therefore two criteria were defined in the creation of the training set, one for the minimum value and one for the timing of the event with respect to tidal spring/neap phase.

Extratropical events generally persist for more than one tidal cycle. Therefore, defining a phasing relationship with respect to the semidiurnal tide similar to the tropical-event procedure is unrealistic. A more realistic approach is to consider that the event will occur somewhere within the spring-neap lunar cycle. For example, the event has an equal probability of occurring (a) at spring tide, (b) between spring and neap, (c) at neap tide, and (d) between neap and spring. Because the harmonic analyses for each gage location were for M_2 only, a scaling factor was developed from the full NOAA harmonic constituent data for Sandy Hook, NY. The M_2 amplitude for Sandy Hook is 2.151 ft. The sum of the major constituents of the NOAA harmonic analysis is approximately 4.5 ft. Division by the M_2 amplitude yields a spring tide scaling factor of approximately 2.0. A typical neap tide for Sandy Hook is on the order of 1.5 ft;

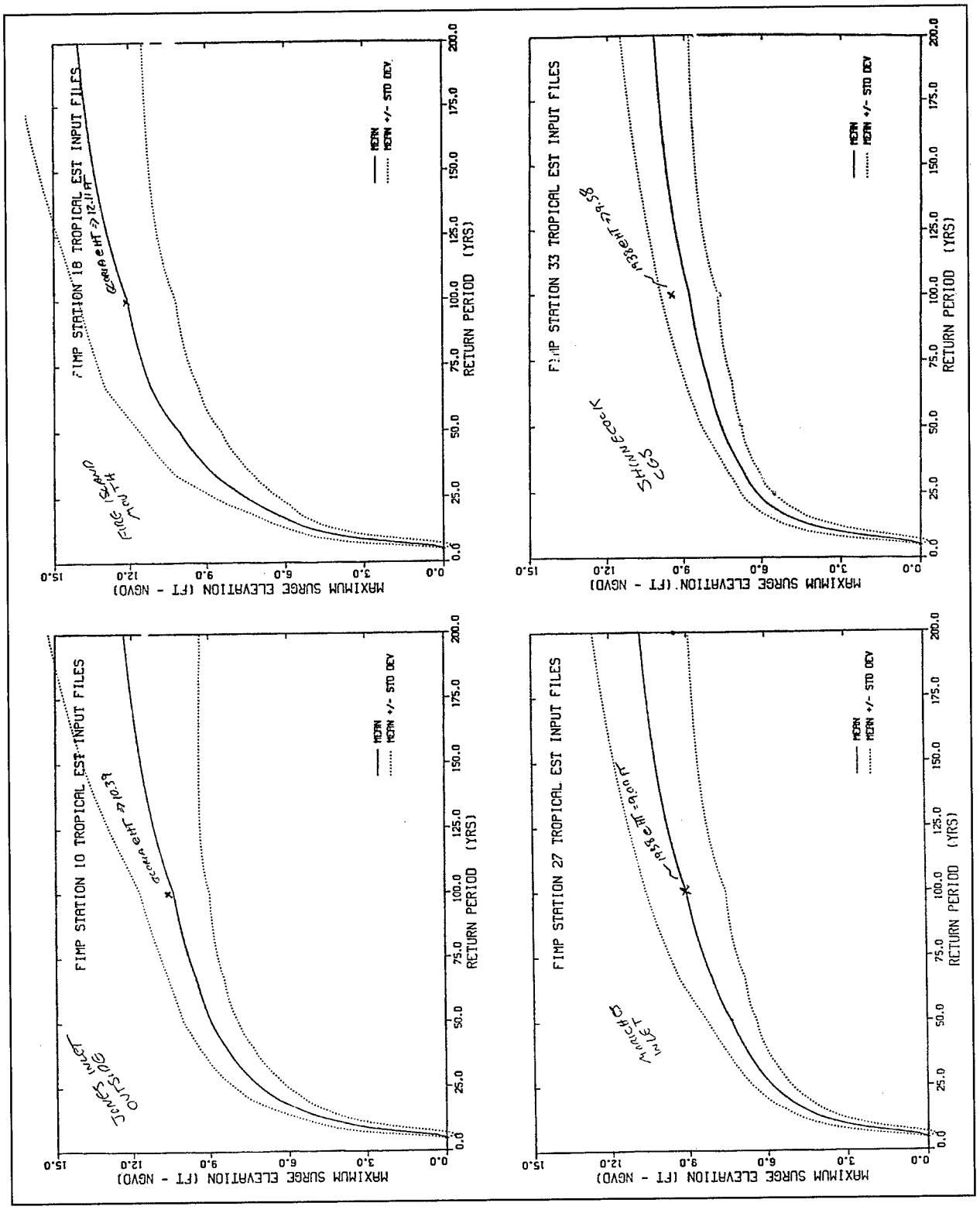

Figure 39. Tropical-event frequency relationships for FIMP Stations 10, 18, 27, and 33

therefore, the neap scaling factor was set at 0.7. Finally, a typical intermediate tide is 2.5 ft, producing a midcycle factor of approximately 1.15. Therefore, the multiplication factors for the M_2 amplitudes were 2.0, 1.15, 0.70, and 1.15 corresponding to spring, spring/neap, neap, and neap/spring. The mean value surface elevation computed as a product of the M_2 harmonic analysis was finally added to the final total surface elevation.

Although the tidal phase and surge information is accounted for through the process described above, a minimum tidal elevation was set in order to ensure that small surge events are at least greater than those accompanying normal yearly tidal cycles. This minimum was defined as a maximum spring tide plus a low-frequency perturbation component defined as 0.75 ft. The low-frequency component has been observed in all tidal records in the Bight and was described by Scheffner et al. (1994). The maximum spring tide was defined according to a multiplier computed as the sum of all 37 NOAA tidal constituents divided by the M_2 amplitude. The resulting multiplication factor was 2.28. As in the previous computation, the minimum value includes the local station mean value obtained from the M_2 analysis.

Each of the events of the training set were first simulated without tides. The training set was then constructed by adding the surge elevation, the computed mean surface elevation (computed from the M_2 harmonic analysis), and the M_2 amplitude multiplied by the spring-to-neap adjustment factor. These simulations did not include the effects of breaching. In order to account for elevated surge values associated with overtopping and breaching when severe events occur (usually) near spring tide, an additional set of simulations was made. For the four most severe events of the training set (March 1994, February 1985, December 1992, and March 1993), the storm was phased to coincide with peak M_2 flood and substituted for spring modified (2.0 multiplier) M_2 plus surge. Breaching was then included in each simulation.

Results of the frequency simulations were compared with the FIMP results at the open-coast locations used for the tropical-event comparisons. Results, shown in Figure 40, are comparable with the FIMP results. Therefore, the training set was considered acceptable for use in all simulations.

EST life-cycle simulations

Input vectors describe the magnitude of the storm event and the location of the event with respect to the area of interest. For tropical events, five vectors were defined as follows:

a. Tidal phase during the event, with 1.0 corresponding to high-water slack, 0.0 for MSL at maximum ebb, -1.0 low-water slack, and 0.0 MSL at maximum flood.

b. Minimum distance from the eye of the storm to the location of interest in statute miles.

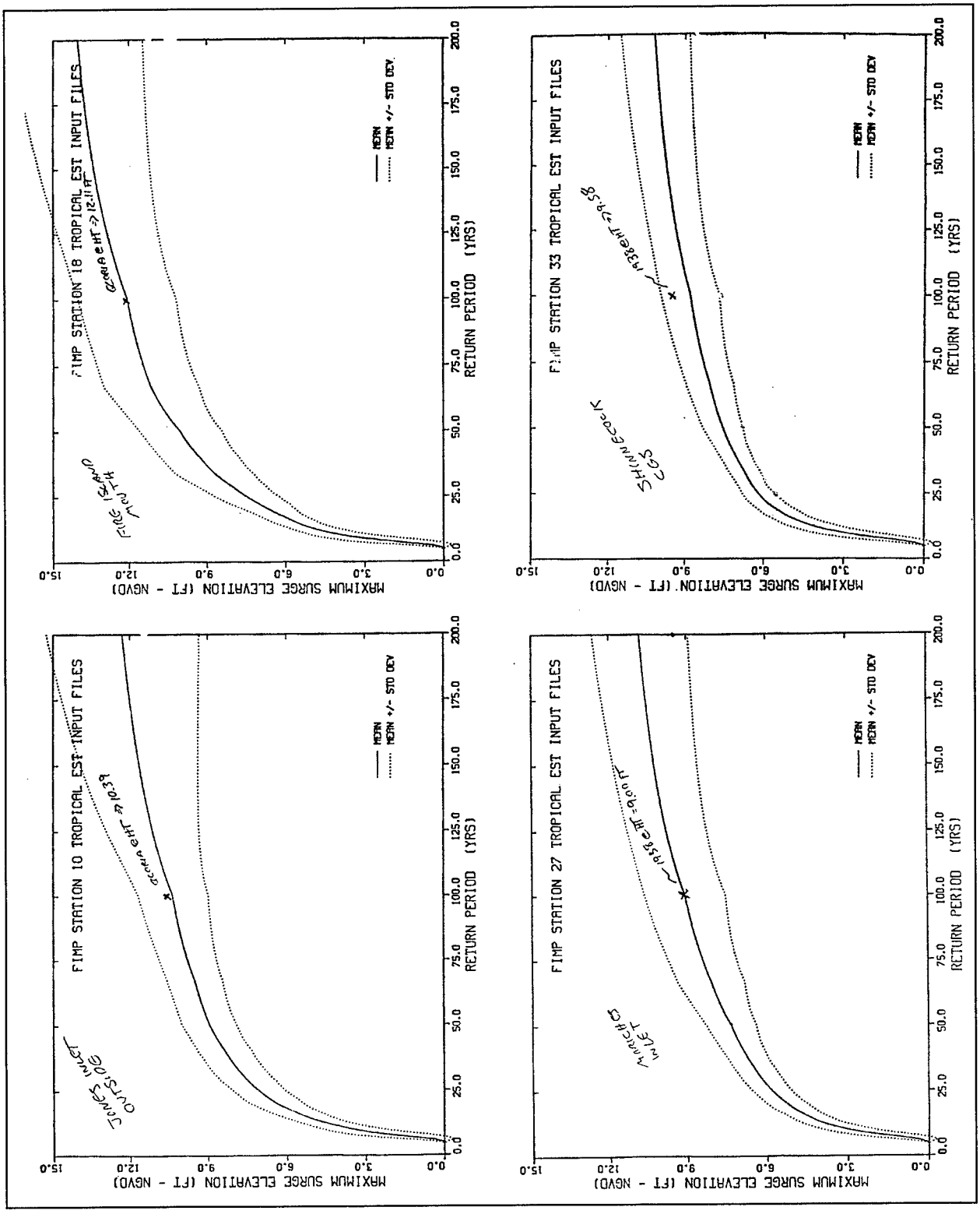

Figure 40. Extratropical-event frequency relationships for FIMP Stations 10, 18, 27, and 33

c. Central pressure deficit of the hurricane eye in millibars.

d. Maximum winds in the hurricane, measured in knots.

e. Forward speed of the eye of the hurricane, measured in statute miles per hour.

The radius to maximum winds and the angle of propagation were not used as input vectors in this study because of vector space discontinuities when the station location was inside/outside the radius to maximum and when the angle of propagation was slightly more or less that 0.0°. The five vectors selected were determined by optimizing vector space with respect to the spread of data in the error analysis of the frequency computations, i.e., as measured by the computed ± standard deviation. An example tropical event input/response vector input for Station 18, Fire Island Inlet mouth, is shown in Table 37. Where a, b, d, e, and f correspond to the variables listed on page 87. Note that in this application, direction of propagation and radius to maximum are not used.

Extratropical event input vectors were defined as follows:

a. Tidal phase during the event, with 0.7 corresponding to neap tide, 1.13 for midway between neap tide and spring tide, and 2.0 for spring tide. Each multiplier is applied to the M_2 tidal constituent at each station location.

b. Surge elevation with no tidal contribution measured in feet.

c. M_2 tidal constituent amplitude at each tidal phase measured in feet.

Because extratropical events cannot be parameterized in the same manner as tropical events, the above input vectors were found to produce good results in the EST formulation. An example extratropical event input/response vector input for Station 18, Fire Island Inlet mouth, is shown in Table 38.

Frequency-of-occurrence computations

Frequency-of-occurrence relationships for tropical, extratropical, and combined events were generated for all stations in the study area. Computations were based on 100 repetitions of a 200-year sequence of events. An example plot for Station 18 for the 100 frequency relationships and mean value relationships as well as the mean value and ± one standard deviation are given in Figures 41 and 42 for the tropical and Figures 43 and 44 for extratropical events. The combined curve is given in Figure 45. A summary table for Station 18 giving mean value and standard deviations is given in Table 39.

Table 37
Tropical Event EST Input

FIMP Station 18 - Base, Fire Island Mouth

			(a)	(b)	(d)	(e)	(f)	Surge
18	296	1	1.00	91.68	25.48	30.00	18.59	2.96
18	296	1	0.00	91.68	25.48	30.00	18.59	1.20
18	296	1	0.00	91.68	25.48	30.00	18.59	1.20
18	327	1	1.00	188.00	34.56	43.94	19.56	3.05
18	327	1	0.00	188.00	34.56	43.94	19.56	1.28
18	327	1	0.00	188.00	34.56	43.94	19.56	1.28
18	332	1	1.00	131.26	47.13	70.41	19.12	3.12
18	332	1	0.00	131.26	47.13	70.41	19.12	1.35
18	332	1	0.00	131.26	47.13	70.41	19.12	1.35
18	353	1	1.00	195.85	67.60	73.40	42.17	3.02
18	353	1	0.00	195.85	67.60	73.40	42.17	1.26
18	353	1	0.00	195.85	67.60	73.40	42.17	1.26
18	370	1	1.00	64.49	41.88	80.54	24.41	3.65
18	370	1	0.00	64.49	41.88	80.54	24.41	1.89
18	370	1	0.00	64.49	41.88	80.54	24.41	1.89
18	386	1	1.00	12.21	66.07	80.65	47.77	7.57
18	386	1	0.00	12.21	66.07	80.65	47.77	5.80
18	386	1	-1.00	12.21	66.07	80.65	47.77	4.04
18	386	1	0.00	12.21	66.07	80.65	47.77	5.80
18	436	1	1.00	29.61	48.90	74.02	25.59	5.74
18	436	1	0.00	29.61	48.90	74.02	25.59	3.98
18	436	1	0.00	29.61	48.90	74.02	25.59	3.98
18	535	1	1.00	31.32	36.56	84.11	29.43	4.44
18	535	1	0.00	31.32	36.56	84.11	29.43	2.68
18	535	1	0.00	31.32	36.56	84.11	29.43	2.68
18	541	1	1.00	214.92	40.27	70.00	42.25	3.81
18	541	1	0.00	214.92	40.27	70.00	42.25	2.05
18	541	1	0.00	214.92	40.27	70.00	42.25	2.05
18	545	1	1.00	189.10	28.79	43.59	16.40	3.00
18	545	1	0.00	189.10	28.79	43.59	16.40	1.24
18	545	1	0.00	189.10	28.79	43.59	16.40	1.24

Table 38
Extratropical Event EST Input

FIMP Station 18 - Base, Fire Island Mouth

			(1)	(2)	(3)	Surge
18	1	1	2.37	1.11	4.18	5.29
18	1	1	2.37	1.11	4.18	5.29
18	1	1	2.37	1.11	4.18	5.29
18	1	1	2.37	1.11	4.18	5.29
18	2	1	2.35	1.15	4.14	5.29
18	2	1	2.35	1.15	4.14	5.29
18	2	1	2.35	1.15	4.14	5.29
18	2	1	2.35	1.15	4.14	5.29
18	3	1	1.66	2.36	2.93	5.29
18	3	1	1.66	2.36	2.93	5.29
18	3	1	1.66	2.36	2.93	5.29
18	3	1	2.00	2.36	3.53	6.41
18	4	1	1.74	2.22	3.07	5.29
18	4	1	1.74	2.22	3.07	5.29
18	4	1	1.74	2.22	3.07	5.29
18	4	1	2.00	2.22	3.53	6.27
18	5	1	1.47	2.70	2.59	5.29
18	5	1	1.47	2.70	2.59	5.29
18	5	1	1.47	2.70	2.59	5.29
18	5	1	2.00	2.70	3.53	7.14
18	6	1	1.43	2.77	2.52	5.29
18	6	1	1.43	2.77	2.52	5.29
18	6	1	1.43	2.77	2.52	5.29
18	6	1	2.00	2.77	3.53	6.53
18	7	1	1.66	2.37	2.93	5.29
18	7	1	1.66	2.37	2.93	5.29
18	7	1	1.66	2.37	2.93	5.29
18	7	1	2.00	2.37	3.53	6.42
18	8	1	1.51	2.62	2.67	5.29
18	8	1	1.51	2.62	2.67	5.29
18	8	1	1.51	2.62	2.67	5.29
18	8	1	2.00	2.62	3.53	6.66
18	9	1	0.70	3.85	1.23	5.61
18	9	1	1.13	3.85	1.99	6.37
18	9	1	1.13	3.85	1.99	6.37
18	9	1	2.00	3.85	3.53	7.61

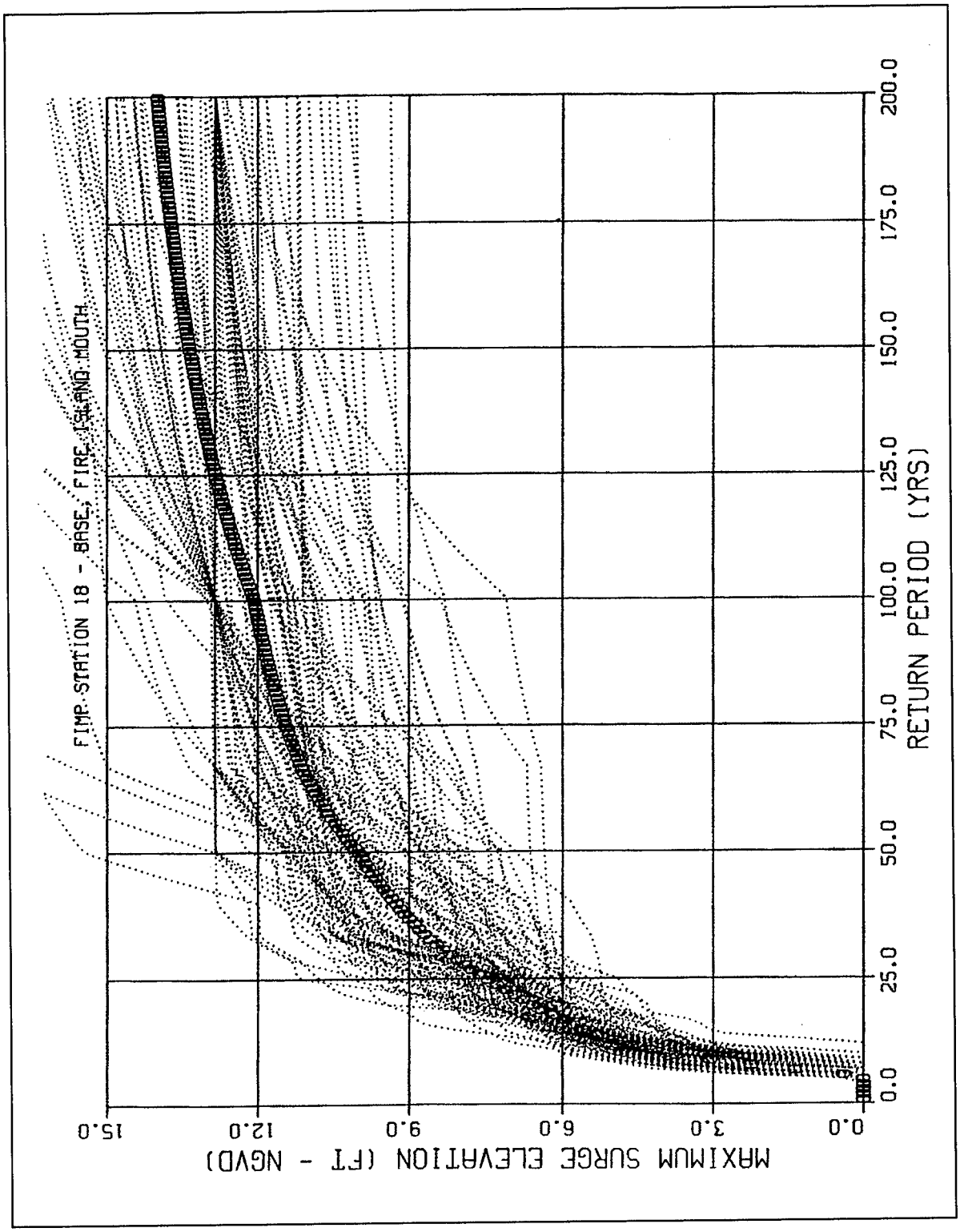

Figure 41. Tropical frequency relationships for Station 18

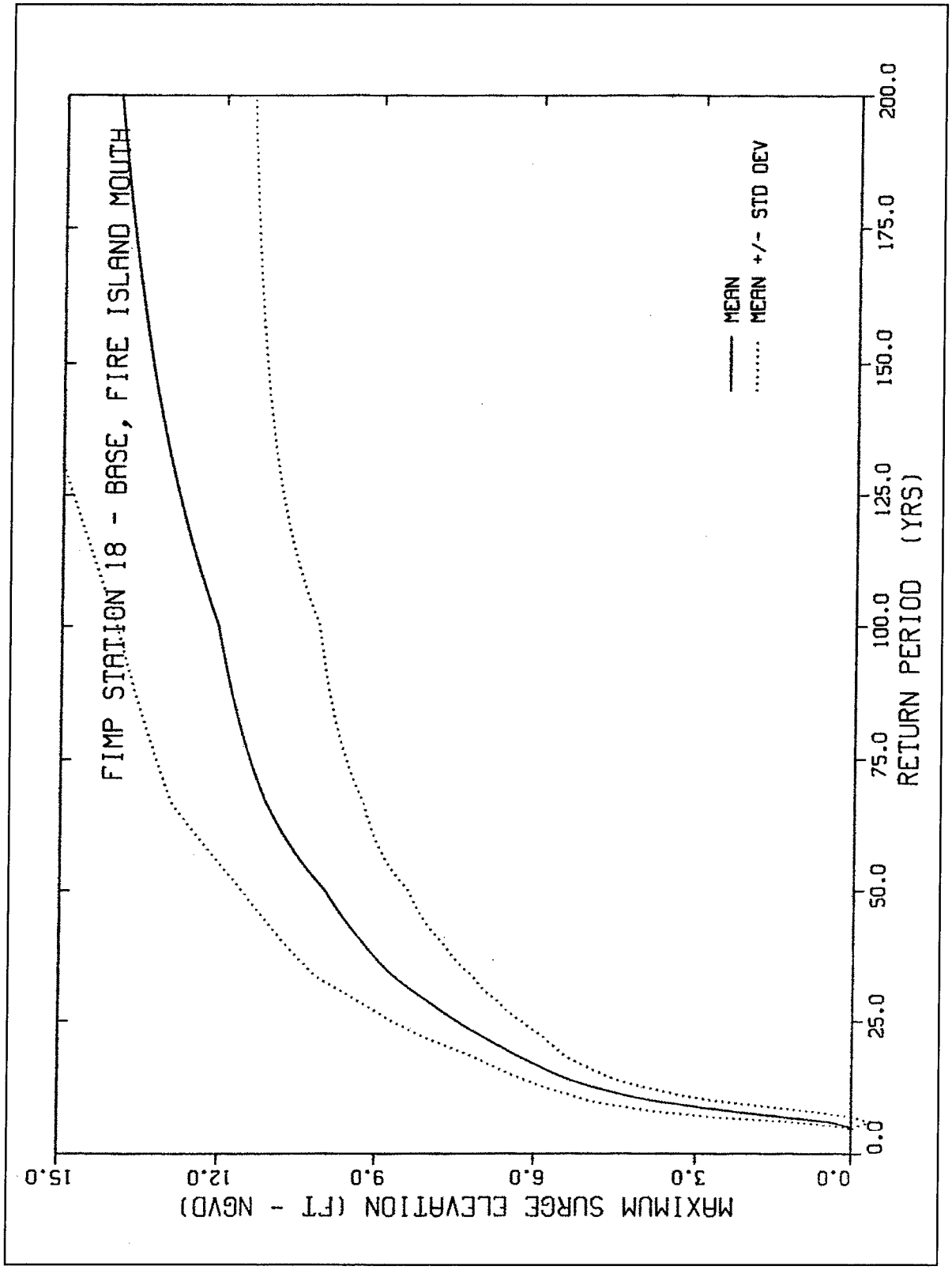

Figure 42. Tropical mean value and SD for Station 18

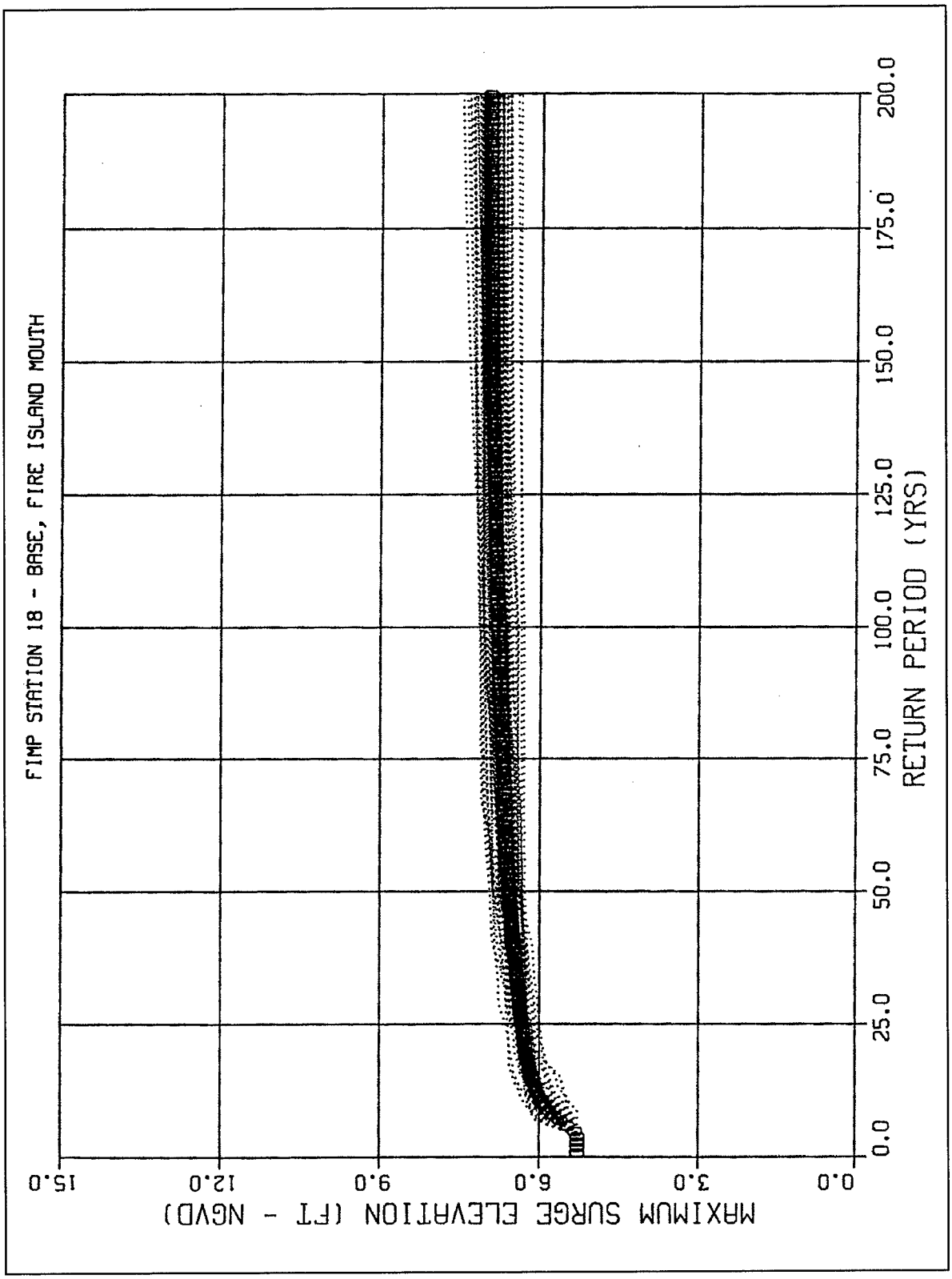

Figure 43. Extratropical frequency relationships for Station 18

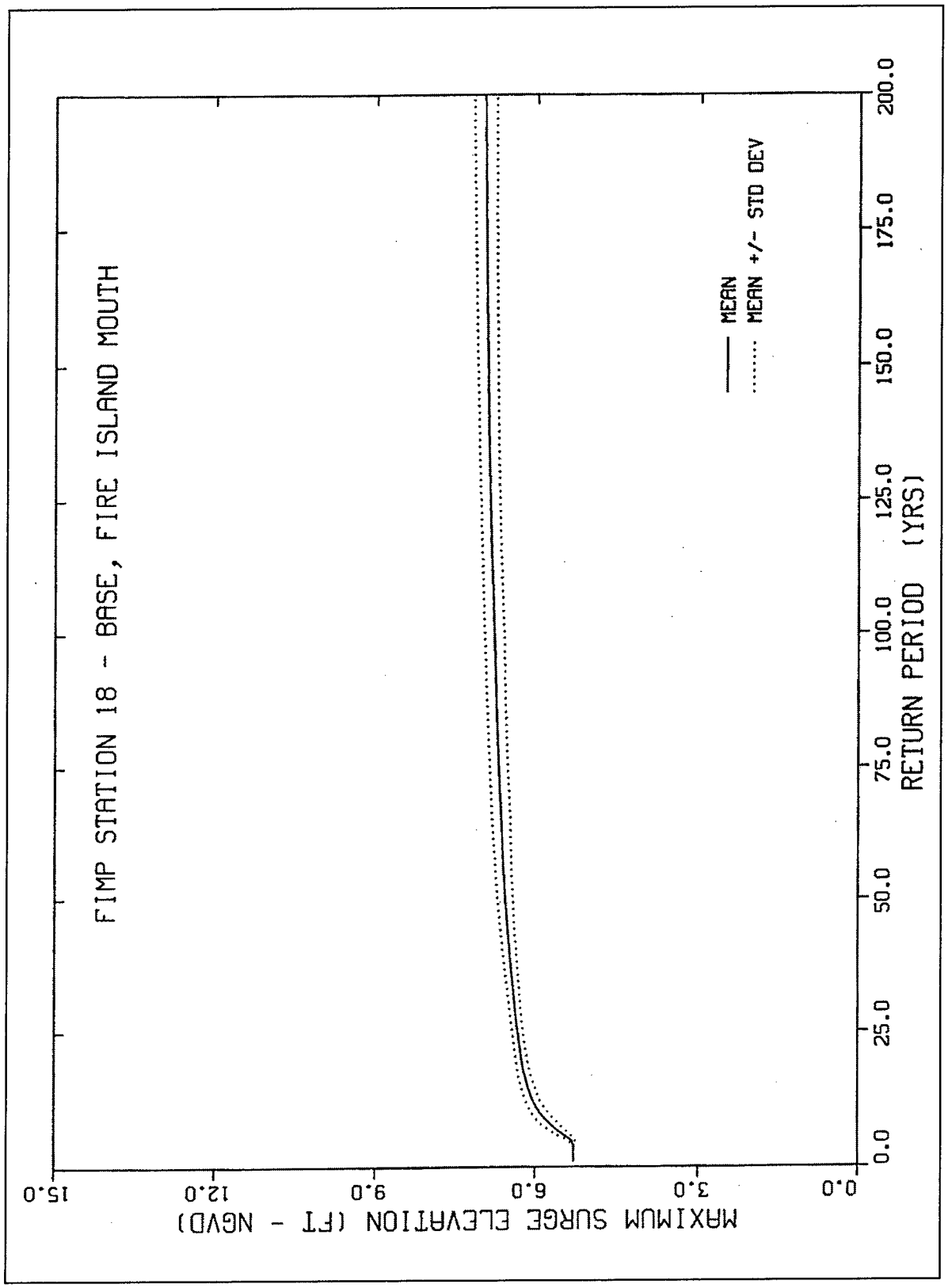

Figure 44. Extratropical mean value and SF for Station 18

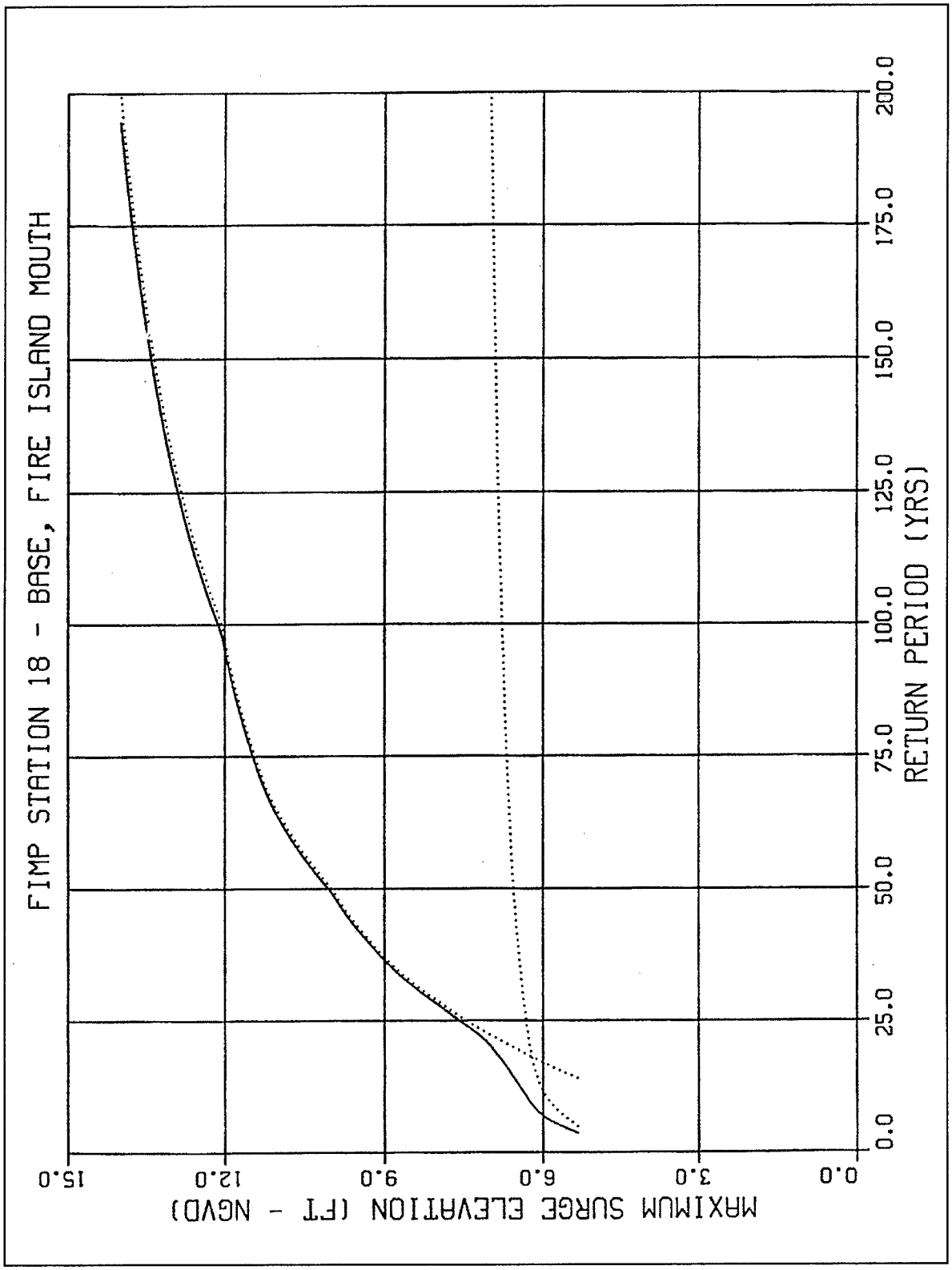

Figure 45. Combined tropical and extratropical frequency relationships for Station 18

Table 39
Summary Surge Frequency Relationship Table for Station 18

FIMP Station 18 - Base, Fire Island Mouth			
Return Period - Years	Tropical (SD)	Extropic (SD)	Combined (SD)
2.00	0.00 (0.00)	5.29 (0.00)	5.29 (0.00)
5.00	0.00 (0.00)	3.90 (0.00)	5.65 (0.00)
10.00	0.00 (0.00)	5.90 (0.16)	6.28 (0.16)
15.00	5.53 (0.88)	6.14 (0.12)	6.62 (1.01)
20.00	6.59 (0.99)	6.25 (0.11)	6.99 (1.10)
25.00	7.46 (1.22)	6.32 (0.10)	7.59 (1.32)
44.00	9.61 (1.52)	6.52 (0.13)	9.66 (1.66)
50.00	10.10 (1.61)	6.57 (0.15)	10.07 (1.76)
100.00	12.08 (1.93)	6.78 (0.18)	12.14 (2.11)
150.00	13.42 (2.22)	6.91 (0.20)	13.48 (2.42)
200.00	14.10 (2.59)	6.98 (0.21)	14.16 (2.80)
250.00	14.62 (2.98)	7.03 (0.21)	14.71 (3.19)

Summary

The REFIMP project effectively evaluated the performance of three configurations of protective dunes along the south coast of Long Island, NY. The study made use of the CEDARS database to identify specific events but used the ADCIRC model (with breaching capabilities) to generate response vectors in the form of maximum storm-surge elevations in the back-bay regions. These responses were used to generate frequency relationships that were effective in evaluating the storm protection afforded by dunes of varying minimum elevation.

The hydrodynamic and stochastic modeling approaches used in the revisited FIMP study represent a great improvement over the techniques employed in the original study. The unstructured grid of the ADCIRC model allows for a single simulation of the study area through specification of a continental scale computational domain. The EST approach was demonstrated to generate results that are consistent with prototype observations, that are easier and faster to implement than the JPM, and that provide an approximate error component necessary for risk-based design criteria.

Example 4: American Samoa Storm-Surge/Runup Frequency Analysis

The American Samoa storm-surge study was conducted for the U.S. Army Engineer Division, Pacific Ocean, to develop stage-frequency relationships for the coasts of five islands within the Territory of American Samoa (Militello and Scheffner 1998). The Islands are located in the South Pacific Ocean at approximately 170 W longitude and 14 S latitude and lie east-northeast of Australia and northeast of New Zealand as shown in Figure 46. This low-latitude location is favorable for tropical storm and hurricane formation and passage. During the period 1987 through 1991, extensive damage from three hurricanes was incurred. Storm damage included village damage and destruction, road washout, harbor destruction, and crop damage (Sea Engineering, Inc., and Belt Collins Hawaii 1994). Development of the storm-surge hydrographs has provided information for planning and mitigation strategies for reduction of the impact of future storms in the study area.

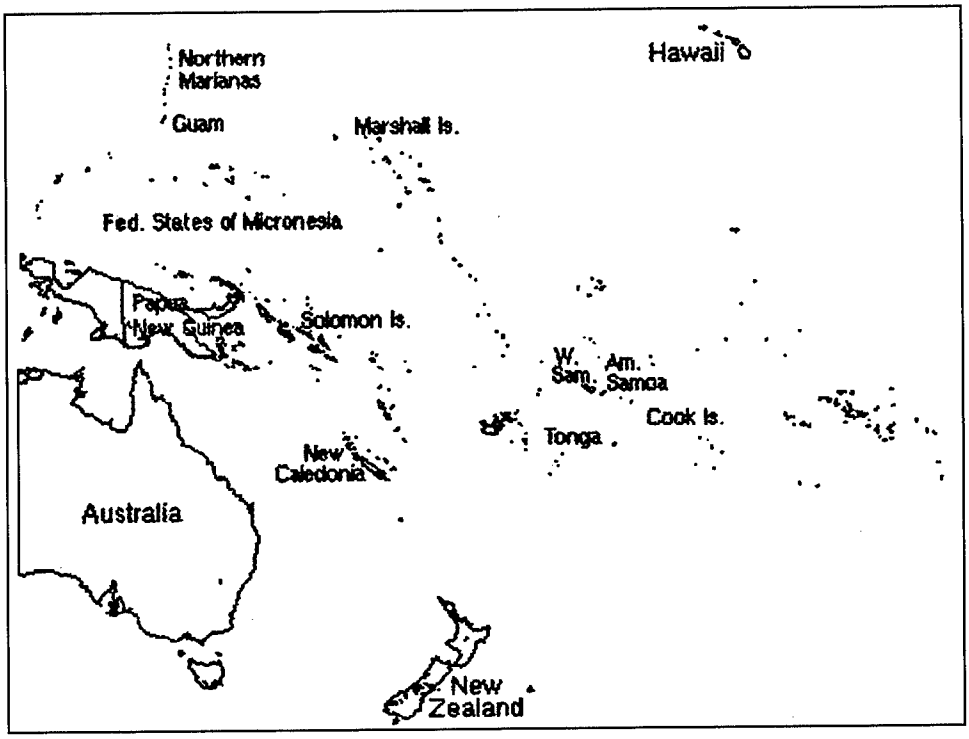

Figure 46. Location map of study area

The islands Tutuila, Aunuu, Ofu, Olosega, and Tau comprise the area of study (see Figure 47) and together cover an area of 77 square miles (199 sq km). Tutuila is the largest of the five islands. The Manu'a Group, consisting of Ofu, Olosega, and Tau, are located 60 miles (97 km) east of Tutuila and Aunuu. All five islands are volcanic, with typically narrow coastal areas and steep mountains. Fringing coral reefs are common around the islands and can extend to 2,000 ft (610 m) out from the shoreline (Sea Engineering, Inc., and Belt

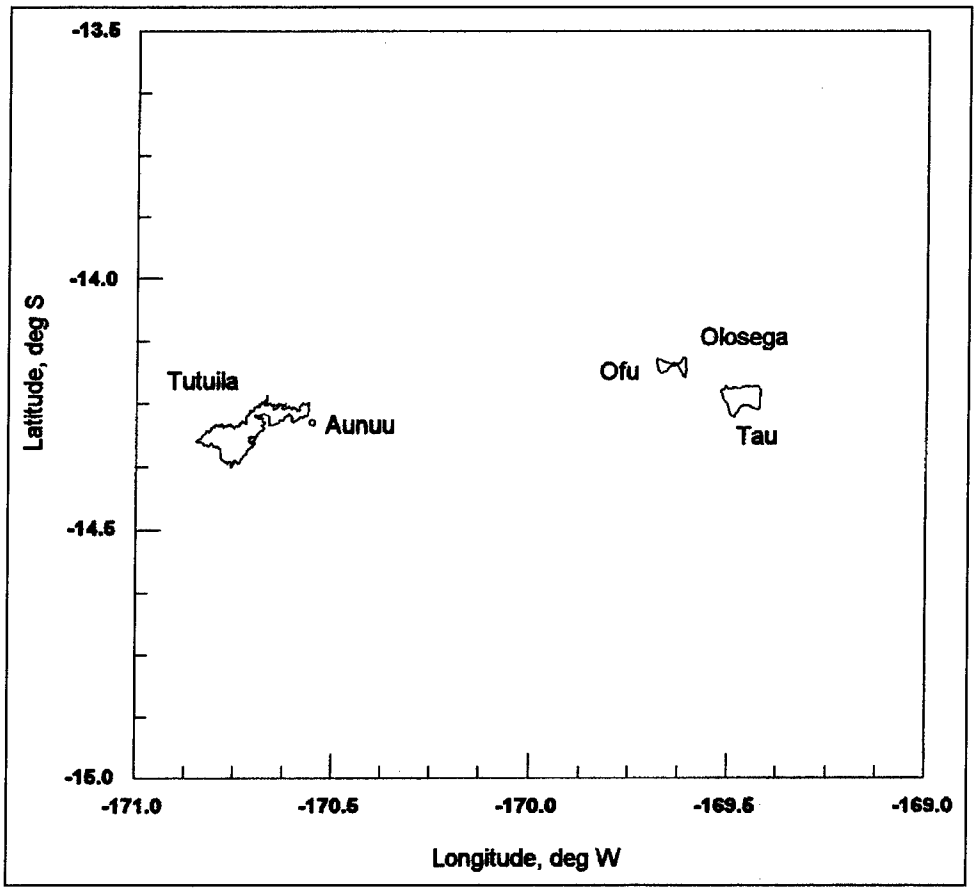

Figure 47. Site map showing the five islands of study

Collins Hawaii 1994). These reefs are typically very shallow, and some are exposed at low tide.

Pago Pago Harbor is the largest embayment of the study site and is located on the southern side of Tutuila (see Figure 48). The harbor is deep, with typical depths of 200 ft (60 m) along its main axis. Tuna canneries, a wharf, and government buildings are located on the harbor shores. Smaller embayments exist on Tutuila, and most are located on the north shore of the island. Aunuu and the Manu'a Group lack natural embayments, although small harbors (Aunuu Small Boat Harbor, Ofu Harbor, and Tau Small Boat Harbor) have been constructed by the U.S. Army Corps of Engineers.

The following discussion summarizes the procedures and selected results of a hurricane stage-frequency analysis for the island coastlines of the U.S. Territory of American Samoa. The steps taken to calculate the stage-frequency relationships were as follows: (a) development of a hurricane database for the western south Pacific Ocean and selection of a representative subset of storms called the "training set," (b) application of a planetary boundary layer model to calculate wind and atmospheric pressure fields for each storm in the training set, (c) simulation of storm surge by application of the long-wave, finite-element

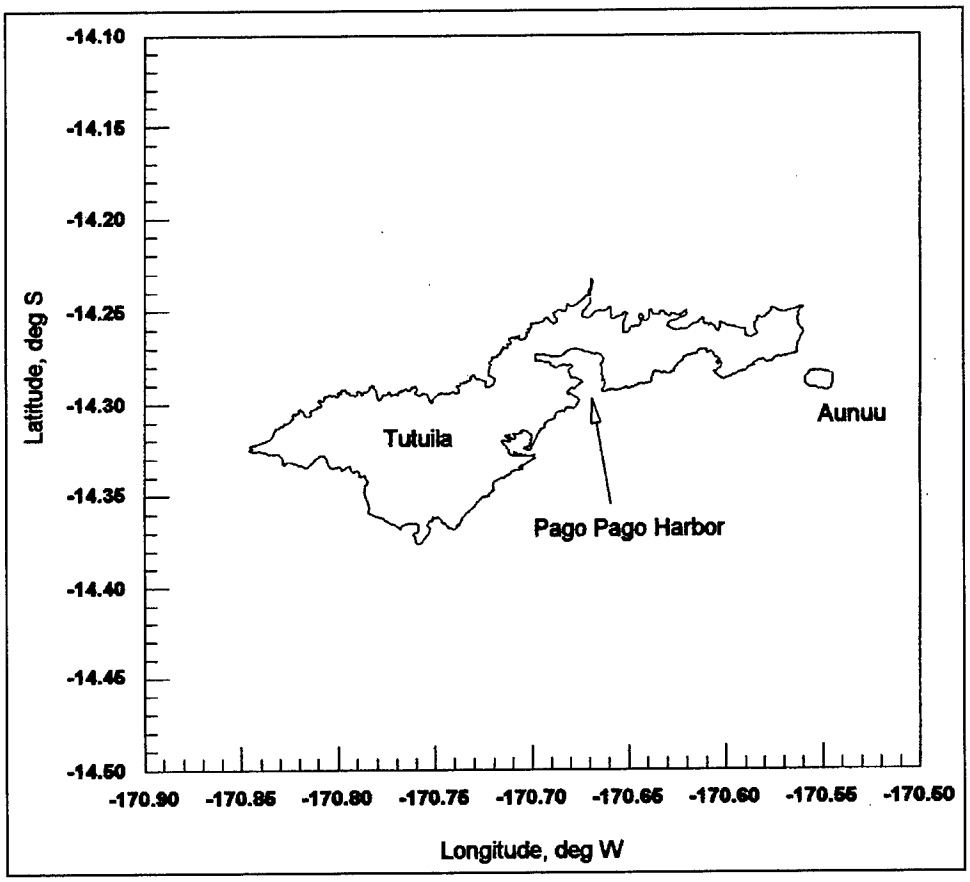

Figure 48. Islands of Tutuila and Aunuu

hydrodynamic model ADCIRC, (d) calculation of ponding level, setup, and runup for each storm at profiles, and (e) development of frequency-of-occurrence relationships for maximum water elevation by application of the EST.

Storm-event selection

The HURDAT database for the South Pacific Ocean contains hurricane and tropical storm information covering a large area including Australia and New Zealand. A subset of storms was selected from the database to comprise the training set for American Samoa. An initial criterion for inclusion in the training set was that the storm track had to pass within a 200-mile radius of any station given in a station list. The station list consisted of 88 stations near the island coasts. Of the 622 storms contained in the HURDAT database for the South Pacific Ocean for 1958 through 1995, 31 storms met the 200-mile radius criterion. These storms were further examined to determine whether they impacted the coasts of the study site. All storms in the training set were found to produce wave-induced setup and runup on the coast, so no storms were eliminated from the training set. Furthermore, because of the location of the American Samoa Islands, historical storms approached the Islands from all sides

providing sufficient representative storms for all coasts. The set of historical storms included in the training set is given in Table 40.

Table 40
Historical Storms Included in the Training Set

Hurricane		Starting Time		Ending Time	
Number	Name	Date	Time, GMT[1]	Date	Time, GMT
18		02/10/59	0000	02/15/59	0000
20		02/13/59	0000	02/16/59	0000
21		02/23/59	0000	03/02/59	0000
28		01/16/60	0000	01/20/60	0000
33		03/17/60	0000	03/23/60	0000
49		03/12/61	0000	03/20/61	0000
60		02/17/62	0000	02/19/62	0000
64		12/21/62	0000	12/21/62	0000
82		03/07/63	1200	03/07/63	0000
96		01/20/64	0000	01/28/64	0000
97		01/24/64	0000	01/26/64	0000
127		01/24/66	0000	02/10/66	0000
146		12/14/67	0000	12/20/67	0000
179		02/11/70	1200	02/24/70	1200
231		01/29/73	0000	02/01/73	1200
274		01/24/75	0000	02/05/75	1200
335		02/13/78	1200	03/01/78	0000
352		02/20/79	0000	02/23/79	1200
390		02/20/81	0000	02/24/81	0000
393		03/01/81	0000	03/03/81	1200
414		02/28/82	0000	03/03/82	1200
500		01/15/87	0000	01/20/87	0600
504		02/03/87	0000	02/05/87	1200
510		02/27/87	0000	03/07/87	0000
513		04/19/87	1800	04/26/87	1200
525	Gina	01/06/89	0600	01/10/89	0000
543	Ofa	01/28/90	0000	02/09/90	1200
562	Val	12/04/91	0600	12/13/91	1200
575	Gene	03/13/92	1800	03/19/92	0000
586	Lin	01/29/93	0000	02/04/93	0000
588	Mick	02/03/93	0000	02/09/93	1200

[1] Greenwich mean time.

Storm wind and atmospheric pressure conditions

The Planetary Boundary Layer (PBL) numerical model (Cardone, Greenwood, and Greenwood 1992) was selected for simulation of hurricane-

generated wind and atmospheric pressure fields. Wind and pressure fields calculated by the PBL are applied as forcing for the hydrodynamic and wave models for computation of storm surge and storm waves, respectively. The PBL model applies the vertically averaged primitive equations of motion for predicting hurricane wind velocities. The model includes parameterization of the momentum, heat, and moisture fluxes together with surface drag and roughness formulations. The PBL model requires a set of time-series "snapshots" for input. The snapshots consist of meteorological storm parameters that define the storm at various stages in its development or at particular times during its life. These parameters were obtained from the HURDAT database or calculated from information contained in the database.

After all snapshots have been processed, hourly wind and atmospheric pressure fields are interpolated to produce a smooth transition from one snapshot to the next. Hourly wind and pressure fields were interpolated from the PBL grid onto the hydrodynamic grid and stored for use by the hydrodynamic model. Similarly, storm wind fields were saved for application in the wave model.

Tidal and storm conditions

Simulations of the long-wave hydrodynamic processes in the study area were conducted by application of the two-dimensional, finite-element model ADCIRC (Luettich, Westerink, and Scheffner 1992). Tidal elevations were not included in the statistical calculations, but were conducted for verification of the hydrodynamic model. The computational grid developed for this study is a large-domain circular grid with a radius of 4 deg (276 miles) and center at 170 deg W longitude and 14.25 deg S latitude. The American Samoa islands are located in the central region of the grid. The large scale of the grid has two main advantages. First, the water-level forcing boundaries are far from the region of interest such that island shorelines are free from boundary effects. Second, because hurricanes are large-scale atmospheric phenomena, a large-domain grid is preferred to maximize the interaction of the horizontal storm area with the computational grid, as well as the storm track.

The grid developed for this study is shown in Figure 49. Grid resolution is coarser in the open regions with increasing resolution toward the shore. Grid parameters and range of scale of element sizes contained in the grid are given in Table 41. The grid around the islands of Western Samoa was not specified to be as detailed as the region surrounding the islands of American Samoa. Reefs, shallow areas, and embayments of the American Samoa islands are finely resolved so that the hydrodynamics can be accurately calculated in these regions. Details of the grid for Tutuila and Aunuu islands are shown in Figure 50, and Figure 51 shows detail of Pago Pago Harbor. Detail of the grid for Ofu, Olosega, and Tau islands are shown in Figure 52.

Tidal elevations specified at the open-water boundary were calculated from tidal amplitudes and phases contained in the LeProvost World Tidal Constituent Database (LeProvost et al. 1994), which provides constituent data at 1-deg

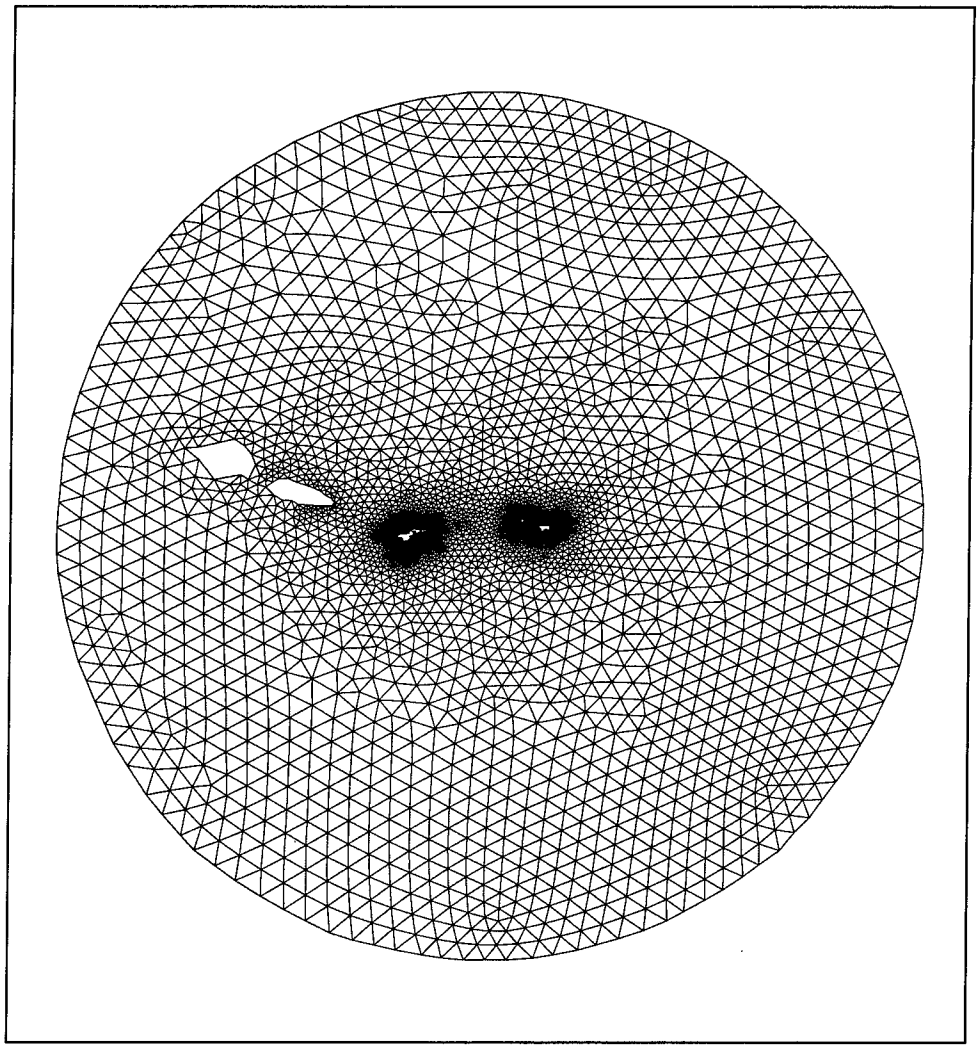

Figure 49. Computational grid for American Samoa

Table 41
Storm-Surge Grid Parameters

Parameter	Value
Maximum element area	81,628,823,171 ft^2 (7,583,565,680 m^2)
Minimum element area	14,973 ft^2 (1,391 m^2)
Ratio of maximum to minimum element areas	5,451,880
Number of elements	41,667
Number of nodes	22,072
Center longitude and latitude	170 W, 14.25 S
Circular grid diameter	4 deg

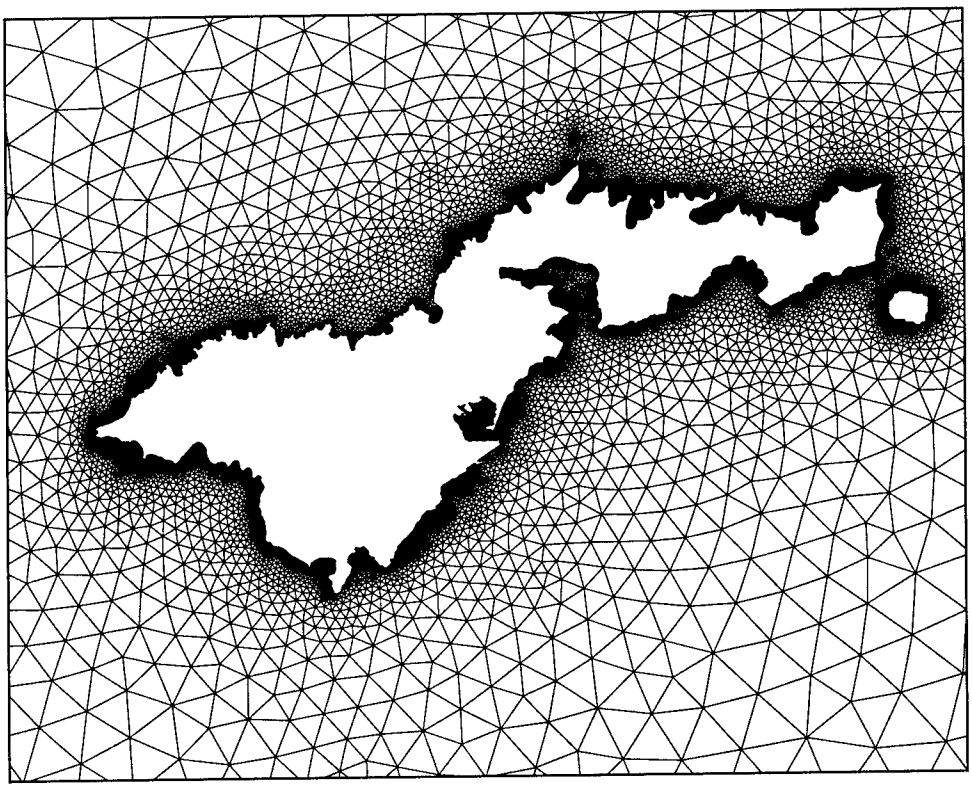

Figure 50. Computational grid showing detail for Tutuila and Aunuu islands

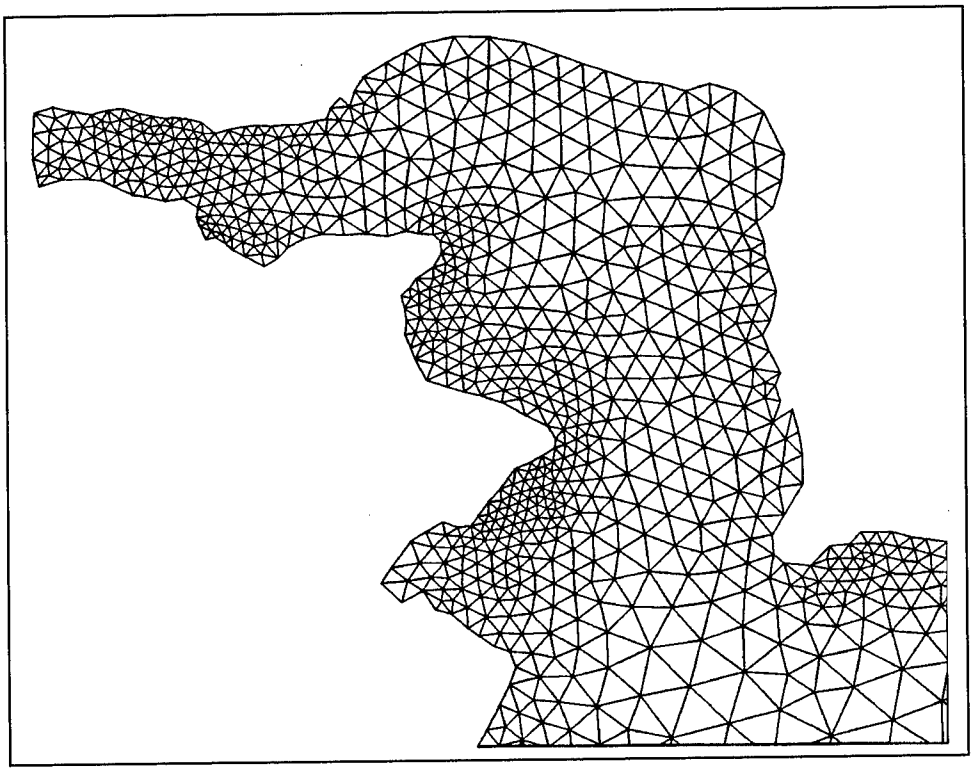

Figure 51. Computational grid showing detail for Pago Pago Harbor

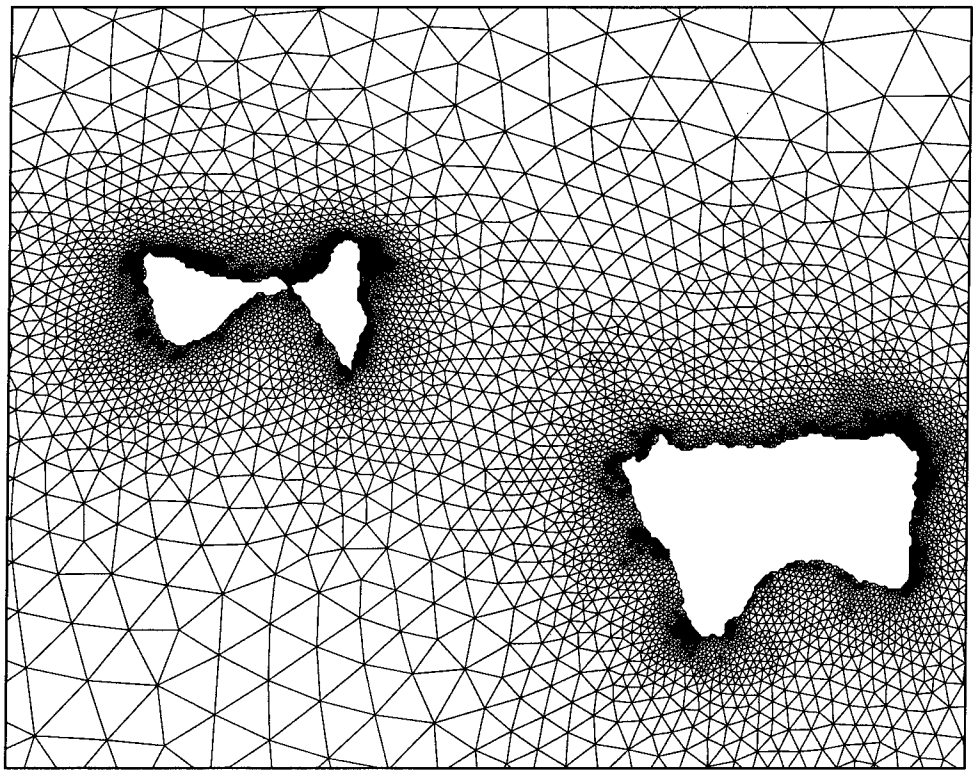

Figure 52. Computational grid showing detail for Ofu, Olosega, and Tau islands

increments in latitude and longitude. A bilinear interpolation algorithm was applied to calculate tidal amplitudes and phases at 118 open boundary nodes. The four tidal constituents applied at the open boundaries were M_2, S_2, N_2, and O_1.

Surge induced by storms was calculated by forcing the hydrodynamic model with wind and pressure fields simulated by the PBL model. Tides were not included in the storm-surge simulations. For each storm, the hydrodynamic model was run for the entire time that the storm was located within the computational grid. These simulations calculated the wind-induced setup and setdown as well as water-level variations owing to atmospheric pressure distribution. Water level was stored at 15-min intervals at 88 numerical gauge locations around the islands shown in Figures 53 through 56.

Wave conditions

Deep-water wave fields were calculated by application of the Wave Information Studies Wave (WISWAVE) model (Resio and Perrie 1989). Application of the wave model required sufficient resolution of a rectangular grid such that calculation points could be distributed around and near to the islands so that representative wave conditions would be captured for all sides of the islands. To meet this requirement, a grid with constant spacing of 0.083 deg

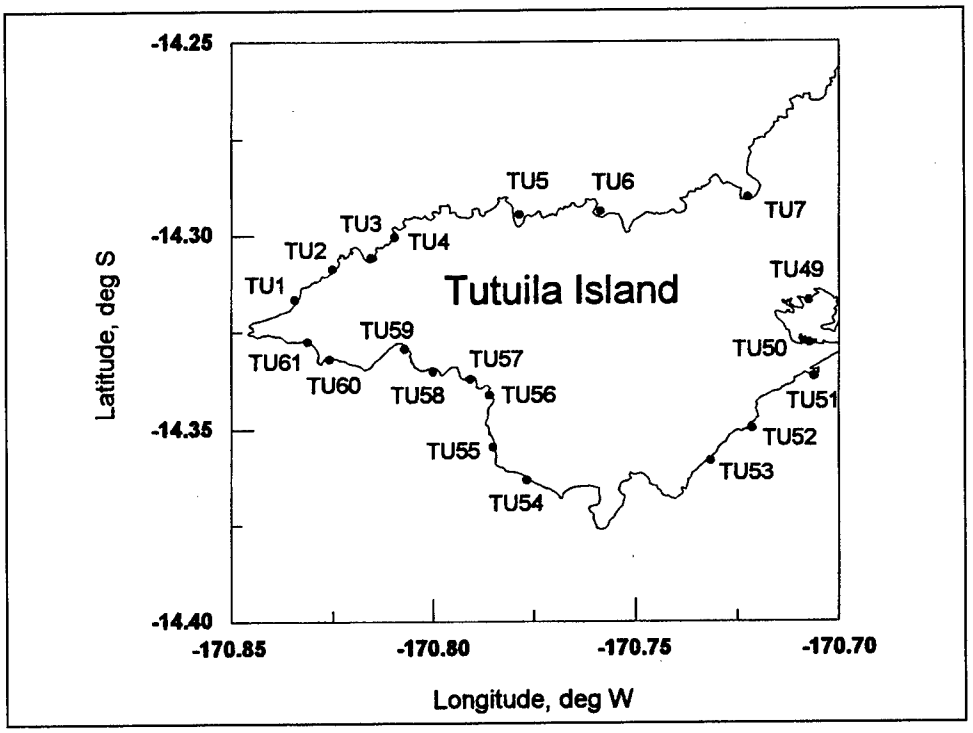

Figure 53. Numerical gauge locations for western Tutuilla Island

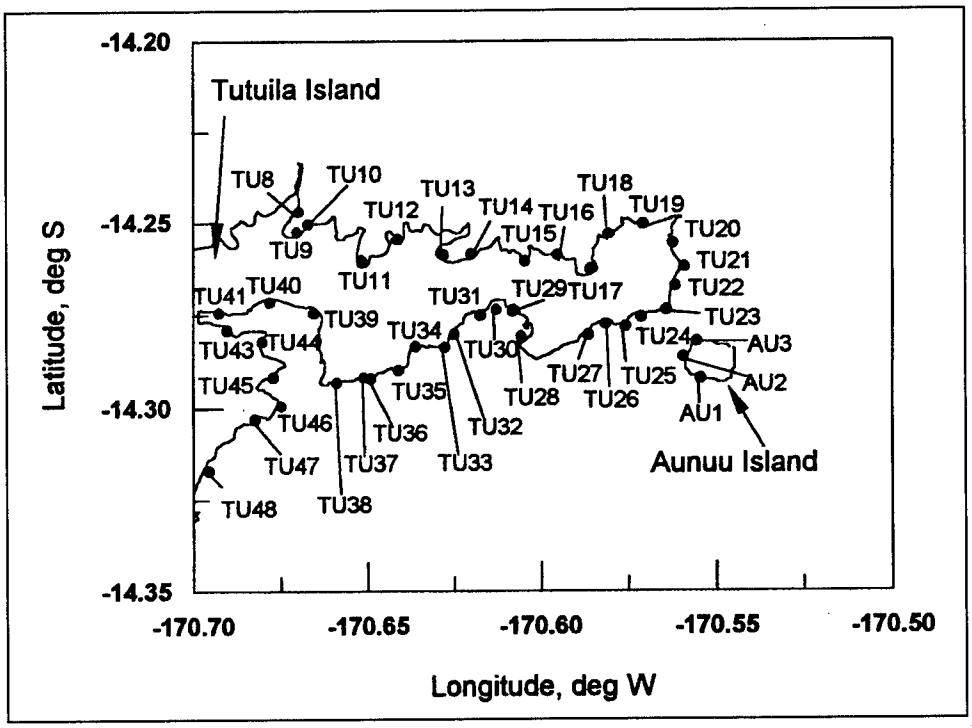

Figure 54. Numerical gauge locations for eastern Tutuilla Island and Anunuu Island

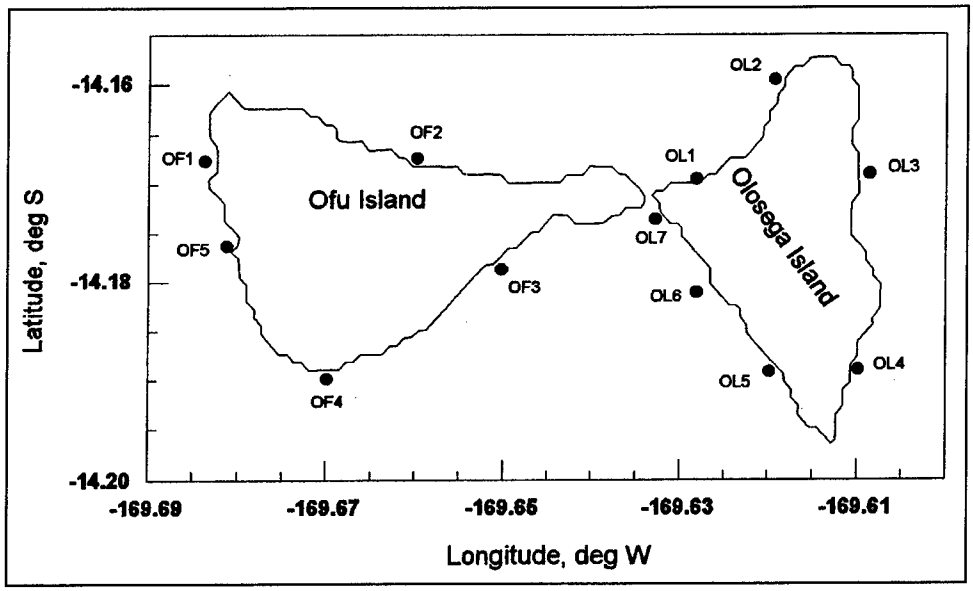

Figure 55. Numerical gauge locations for Ofu Island and Olosega Island

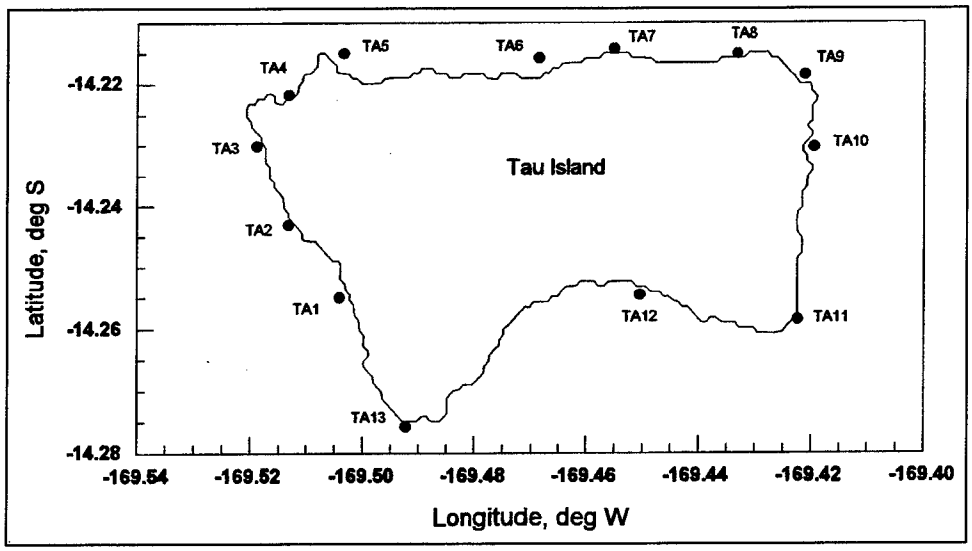

Figure 56. Numerical gauge locations for Tau Island

was developed. Grid bathymetry was taken from that specified in the storm-surge grid (described below) and interpolated onto the wave grid. The method of kriging was applied for the interpolation. The islands of Western Samoa and American Samoa were specified as land in the grid for accurate calculation of wave sheltering and refraction. Details of the grid are given in Table 42.

Wind speed applied as forcing for the wave model was calculated by the PBL model. Wind speed and direction were calculated for each point on the wave grid at 1-hr intervals. Deepwater wave parameters calculated by the wave model

Table 42
WISWAVE Grid Parameters

Parameter	Value
Longitude limits	-173.987 W , -165.961 W
Latitude limits	18.254 S, 10.238 S
Cell side length	0.083 deg
Total number of nodes	9,604
Number of nodes in north-south direction	98
Number of nodes in east-west direction	98

were stored at 32 stations surrounding the American Samoa Islands for each of the 31 storms in the training set. A list of these stations is given in Table 43. The duration of the wave simulations corresponded to the time coverage of each storm. Wave parameters were stored at 1-hr intervals.

Spectral transformation of waves during propagation from one depth to another was calculated by application of the WAVTRAN model, which takes into account shoreline orientation and wave sheltering (Jensen 1983; Gravens et al. 1991). The wave transformation calculation is dependent on the shoreline orientation because the bottom contours are assumed parallel to the shoreline. If wave sheltering is included, waves coming from directions specified by a sheltered angle band are deleted from the spectrum.

Estimates were made of the general shoreline orientation closest to the 88 numerical gauge locations specified around the islands. In addition, estimates of sheltering angle bands were made based on shoreline geometry (bays, coves), existence of land points, and islands. For many of the numerical gauge locations, two-sided wave sheltering was applied.

For numerical gauge locations located within Pago Pago Harbor, WAVTRAN was applied multiple times to calculate wave parameters within the harbor. Pago Pago Harbor is protected from waves by the presence of Taema Bank, which is located approximately 1.5 n.m. (2.8 km) from the harbor mouth. Typical depth over the bank is approximately 30 ft (9 m), which will cause shoaling and breaking of storm waves. Waves were transformed over the bank and propagated into the harbor.

Model verification

The ADCIRC model was verified by comparison of output to both tidal constituents and gauge data for a storm. Water-level measurements were available from one gauge within the study area located in the upper reach of Pago Pago Harbor, Tutuila Island. The position of the gauge is 14.2783 S, 170.6817 W. Because measurements were only available at one location, the model could not be tested for accuracy at other locations in the study area. However, because the inner regions of bays and harbors are relatively difficult to

calibrate in comparison to deeper coastal and open-ocean regions, it is expected that water-level calculations in other regions of the model domain are accurate if calculated water level in the harbor is accurate.

Calibration of the storm-surge model was conducted by driving the model with four tidal constituents and comparing the results of a harmonic analysis of the water level at the Pago Pago Harbor gauge to that calculated by NOS. Table 44 gives the tidal constituents at Pago Pago Harbor as determined by NOS and calculated by ADCIRC. The simulated water-level constituents at the gauge location compare favorably with those calculated from measurements. The maximum error in amplitude is 0.38 in. (0.96 cm) for the M_2 and N_2 constituents, and the maximum error in phase is 7.4 deg for the S_2 constituent.

The storm-surge model was validated by comparison of measured and calculated time-series water levels at the Pago Pago Harbor gauge for the period when Hurricane Val passed through the study area. Comparison of measured and calculated water level during the passage of Hurricane Val is shown in Figure 57. The calculated water level does not reach the elevation of the measured water level, and this error may stem from two sources. Wave setup is not contained in the calculated water level, which would result in underestimation of surge shown in the figure. A second source of error is in representation of the eye of the storm. Hurricane Val passed directly over the island of Tutuila as shown in Figure 58 (dots denote storm position recorded in the HURDAT database). Minor error in location of the storm eye could result in incorrect wind and pressure calculations near Pago Pago Harbor, giving rise to a difference in calculated water level and measured water level.

Response vector generation

Response vectors for stage-frequency analysis of hurricane-induced storm surge include the wind- and pressure-induced water level, wave setup, ponding level, and runup. The combination of these processes through time gives a time series of water stage throughout a storm. Time series of wind- and pressure-induced water level were output directly from ADCIRC. Wave-related processes were calculated for 375 profiles distributed along the coasts of the American Samoa Islands.

Wave processes that contribute to elevated water level during storms are ponding of water on reefs, setup, and runup. Wave setup on reefs owes to overtopping of waves onto the reef platform. As waves break on the reef, water is deposited causing elevated water level. The method of Seelig (1983) was applied to calculate ponding level on the reef, which is a function of the still-water level (astronomical tide and storm surge), deep-water significant wave height, and wave period. Contributions to the ponding level do include waves breaking on the reef, but do not include setup from reformed waves.

Table 43
Deepwater Wave Stations

Station Number	Latitude, deg S	Longitude, deg W
1	14.45	170.93
2	14.37	170.93
3	14.29	170.93
4	14.20	170.93
5	14.20	170.84
6	14.20	170.76
7	14.20	170.68
8	14.20	170.60
9	14.20	170.51
10	14.20	170.43
11	14.29	170.43
12	14.37	170.43
13	14.37	170.51
14	14.37	170.60
15	14.37	170.68
16	14.45	170.68
17	14.45	170.76
18	14.45	170.84
19	14.29	169.68
20	14.20	169.68
21	14.12	169.68
22	14.12	169.60
23	14.12	169.52
24	14.12	169.44
25	14.20	169.44
26	14.29	169.44
27	14.20	169.35
28	14.29	169.35
29	14.29	169.52
30	14.29	169.60
31	14.20	169.77
32	14.12	169.77

Table 44
Tidal Constituents in Pago Pago Harbor

Constituent	NOS Amplitude in. (cm)	NOS Phase deg	ADCIRC Amplitude in. (cm)	ADCIRC Phase deg	Amplitude Error[1], in. (cm)	Phase Error[2] deg
M_2	14.80 (37.58)	180.0	14.42 (36.62)	178.1	-0.38 (-0.96)	-1.9
S_2	2.43 (6.17)	165.5	2.10 (5.33)	158.1	-0.33 (-0.84)	-7.4
N_2	4.22 (10.73)	161.6	3.85 (9.77)	162.4	-0.38 (-0.96)	0.8
O_1	1.14 (2.90)	68.3	1.08 (2.73)	65.6	-0.07 (-0.17)	-2.7

[1] Amplitude Error = Modeled Amplitude = NOS Calculated Amplitude.
[2] Phase Error = Modeled Phase - NOS Calculated Phase.

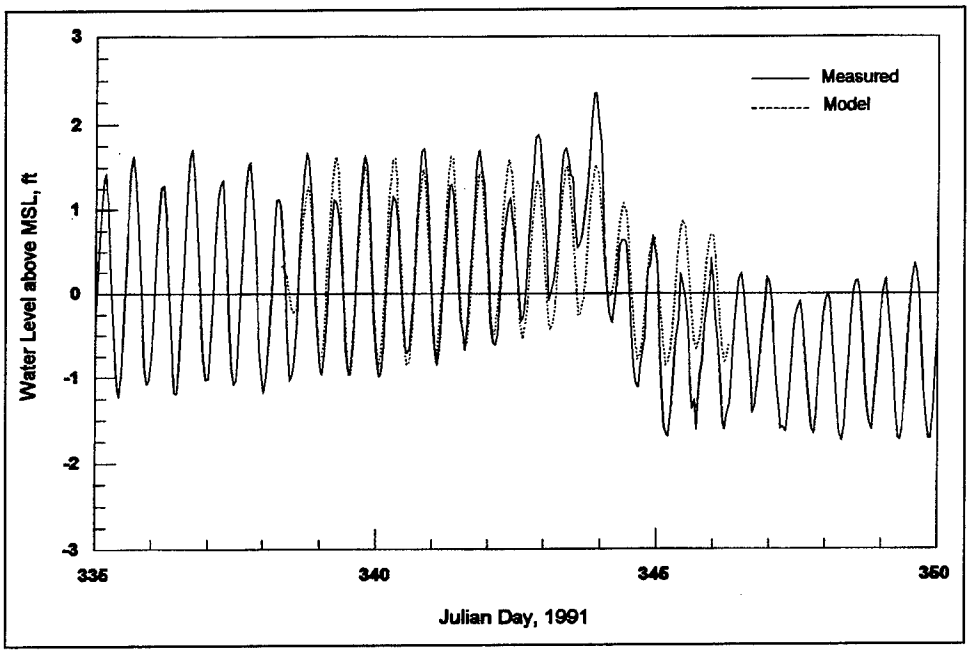

Figure 57. Measured and modeled water level in Pago Pago Harbor for Hurricane Val

The remaining wave parameters calculated for profiles were setup from waves that reformed on the reef and wave runup. The computational method presented in the *Shore Protection Manual* (1984) was applied for the runup calculations for this study. The composite slope method, developed by Saville (1958), was applied to account for changes in grade along a given profile.

Time series of total water elevation were calculated for each storm at each profile. The total water elevation was calculated by linearly adding the wind- and pressure-induced water level, ponding level, wave setup, and wave runup. Peak total water level for each storm was computed and applied as input for the frequency-of-occurrence calculations.

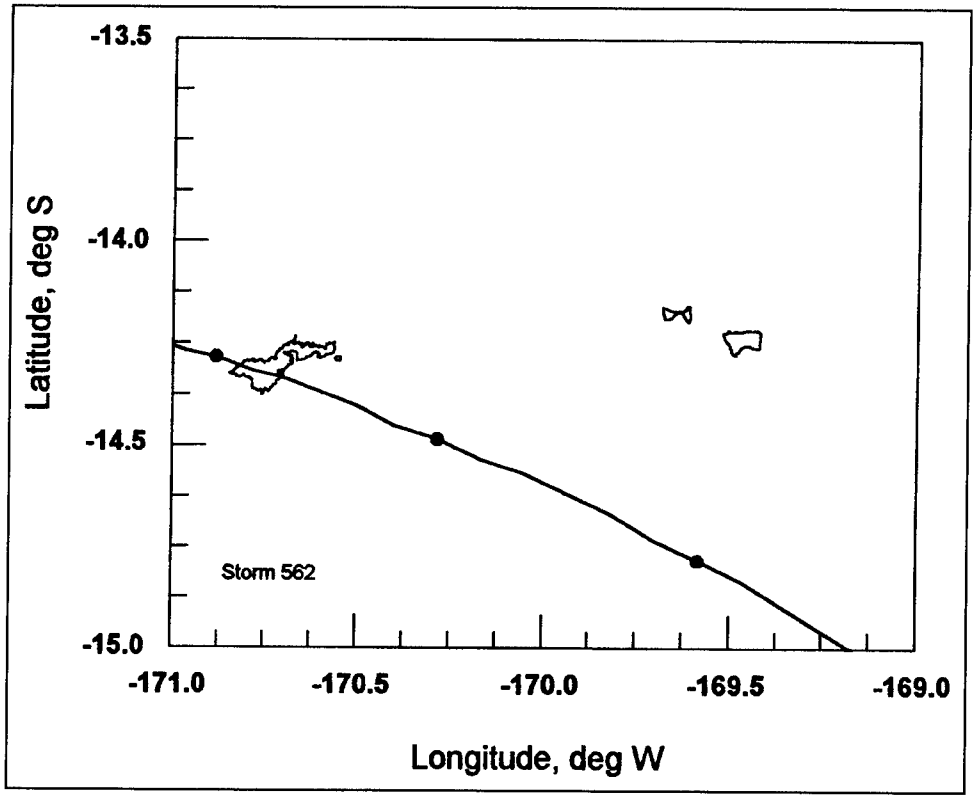

Figure 58. Storm track for Hurricane Val (storm number 562)

Maximum water-elevation calculations, which include wave runup, were compared with debris-line water elevations surveyed by the Federal Emergency Management Agency for Typhoon Ofa. The observed values were supplied for villages on Tutuila Island. Time series of water levels were computed at villages for Typhoon Ofa, and the minimum and maximum values of water level, referenced to MSL, were extracted from the time series. Table 45 shows the comparisons of measured and calculated minimum and maximum water level for 18 villages. Calculated water elevations underpredicted the observed water elevations at 15 villages and overpredicted at 3 villages. On average, the calculated water elevations underpredicted observed values by 5.5 ft for the 18 villages.

The underprediction of water elevations at several of the villages stems, in part, from oversimplification of wave processes over the reef and in situations where the shoreline is curved. Presently, little is known about runup on fringing reefs. The composite-slope method for calculating runup was developed for sloping beaches with structures. The accuracy of the composite-slope method for fringing reef applications has not been established and may introduce error into the runup calculations. Additionally, one-dimensional models were applied to a two-dimensional problem. Waves propagating over reefs will be transformed. In bays and coves with arcuate shorelines and reef edges, the transformation will be complex. In this application, waves were assumed to

Table 45
Observed and Calculated Water Level for Typhoon Ofa

Village	Observed Water Level (FEMA), ft msl	Minimum Calculated Water Level, ft msl	Maximum Calculated Water Level, ft msl
Masefau	5	3.6	3.9
Masausi	16	2.9	2.9
Sailele	16	6.3	6.3
Aoa	12.5	6.2	6.2
Oneona	22	7.4	7.4
Amouli	12	12.2	12.9
Aloa	11	9.5	14.3
Lauagae	22	7.0	8.8
Fagalii	22	11.4	15.3
Poloa	15	13.8	13.8
Amanaue	13	13.4	19.1
Fagamalo	21	6.9	8.6
Maloate	21	10.8	10.8
Afao	17	12.5	12.5
Utomea	17	12.9	12.9
Fagasa	8	5.5	6.1
Vatia	7.5	2.5	2.5
Afono	8.5	3.6	3.6

propagate straight in from the bay mouth or ocean, but in a prototype system, refraction and other processes will modify the waves.

Frequency-of-occurrence computations

Stage-frequency relationships were calculated for 375 profiles along the coast of the American Samoa Islands by application of the EST. These relationships were computed for maximum water level at intervals of 5, 10, 25, 50, and 100 years. Input for the EST included the maximum water level calculated for each of the 31 storms in the training set. The maximum water level was calculated as the linear superposition of the storm surge, ponding level, setup, and runup.

Because the American Samoa Islands are located in a region of tropical storm and hurricane formation and propagation, the Islands can experience storms or waves from any direction. All coastlines of the Islands are subject to storm waves and may experience significant inundation, with the exception of

protected areas such as Pago Pago Harbor. The arcuate shape of many of the coves, particularly on Tutuila, provides sheltering from waves in specific angle bands.

Examples of stage-frequency relationship values for four profiles on the island of Tutuila are given. Table 46 gives the profile number and the nearest numerical gauge (Figures 53 and 54). Example profiles were taken from each side of Tutuila to give information representative of different storm and wave approaches. Maximum expected water-level values and standard deviations are given in Tables 47 through 50 for the example profiles. Figures showing stage-frequency relationships for the example profiles are shown in Figures 59 through 62.

Table 46
Identification Information for Example Profiles

Location on Tutuila	Profile Number	Nearest Numerical Gauge
North coast	49	TU12
East coast	99	TU22
South coast	303	TU54
West coast	8	TU2

Table 47
Return Period, Maximum Water Level, and Water-Level Standard Deviation for Profile Tutuila 012

Return Period, years	Maximum Water Level, ft	Water-Level Standard Deviation, ft
2	3.3	1.4
5	9.4	0.7
10	11.5	0.8
25	13.8	1.0
50	15.3	1.3
75	16.1	1.3
100	16.4	1.3

Summary

A set of hurricane-induced stage-frequency histograms were developed for the Territory of American Samoa. The subject study area consists of the five volcanic islands, Tutuila, Aunuu, Ofu, Olosega, and Tau. Calculation of surge, wind and pressure field, and wave parameters were performed for 31 historical storms through application of four numerical models. Wave-induced setup and runup were calculated at 375 profile locations.

Table 48
Return Period, Maximum Water Level, and Water-Level Standard Deviation for Profile Tutuila 022

Return Period, years	Maximum Water Level, ft	Water-Level Standard Deviation, ft
2	2.8	1.1
5	7.3	0.8
10	10.7	1.5
25	15.5	2.1
50	18.2	2.2
75	19.5	1.9
100	20.1	2.0

Table 49
Return Period, Maximum Water Level, and Water-Level Standard Deviation for Profile Tutuila 054

Return Period, years	Maximum Water Level, ft	Water-Level Standard Deviation, ft
2	1.6	0.7
5	4.2	0.5
10	6.0	1.1
25	9.6	1.5
50	11.5	1.4
75	12.2	1.1
100	12.6	1.2

Table 50
Return Period, Maximum Water Level, and Water-Level Standard Deviation for Profile Tutuila 002

Return Period, years	Maximum Water Level, ft	Water-Level Standard Deviation, ft
2	4.6	1.8
5	10.3	0.7
10	12.1	0.7
25	13.9	0.9
50	15.2	1.1
75	16.0	1.2
100	16.3	1.4

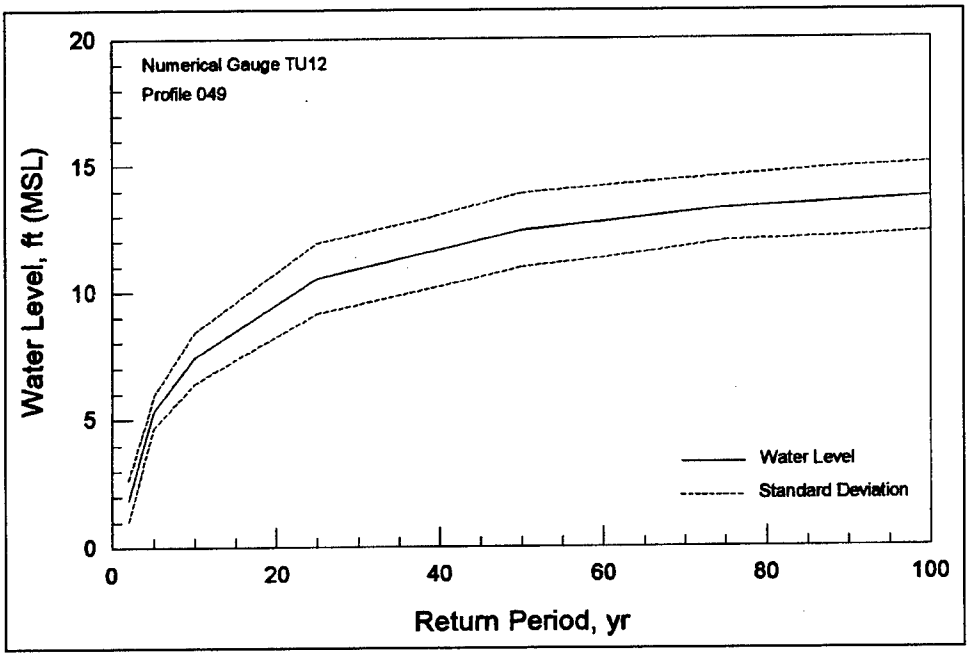

Figure 59. Stage-frequency plot for Profile 049, Tutuila

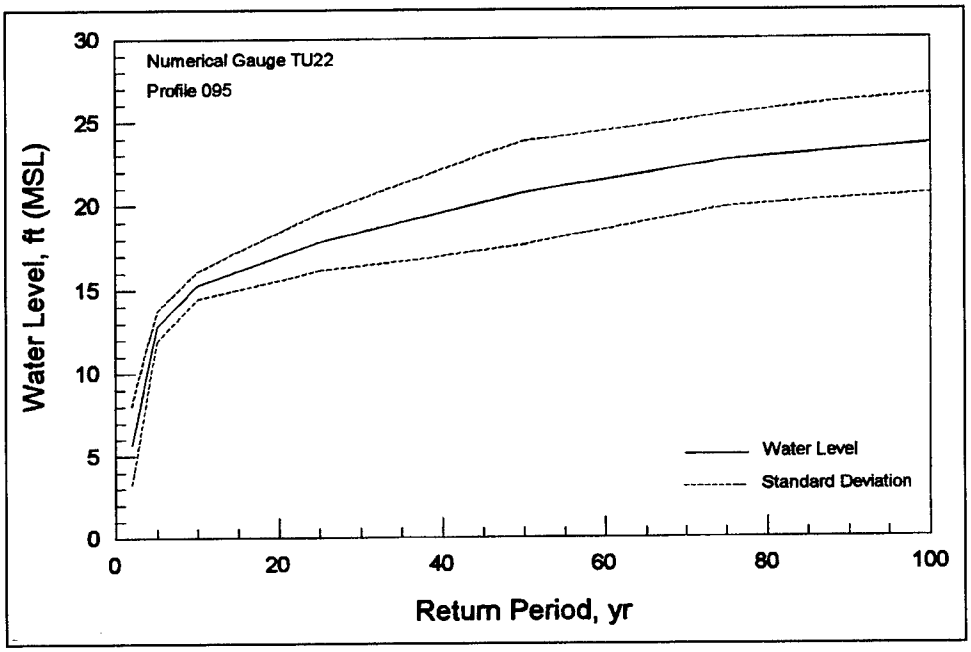

Figure 60. Stage-frequency plot for Profile 095, Tutuila

Storm surge (wind- and atmospheric pressure-induced) was simulated for 31 historical storms and referenced to MSL. Because the islands of American Samoa are volcanic cones with steep sides, shallow shelf areas (such as on the east coast of the United States) do not exist around the islands, so the storm surge does not shoal. Consequently, the storm surge (without consideration of

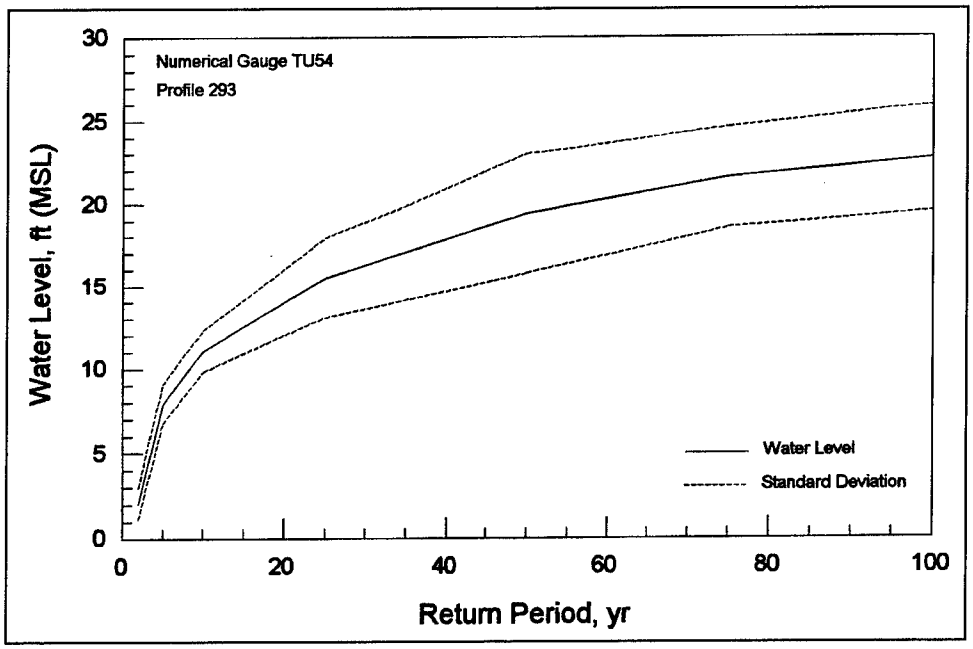

Figure 61. Stage-frequency plot for Profile 293, Tutuila

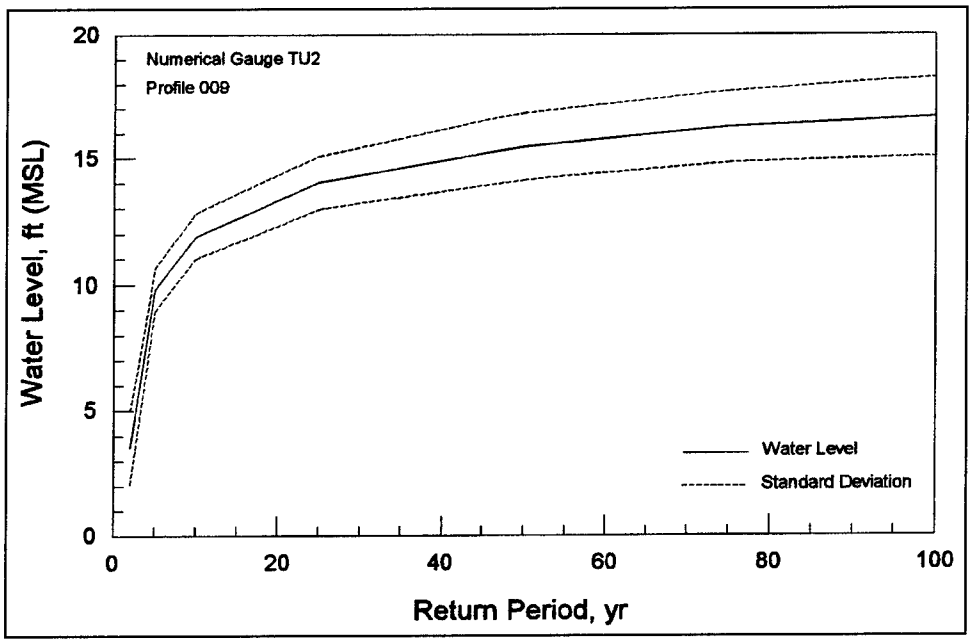

Figure 62. Stage-frequency plot for Profile 009, Tutuila

waves) is small and contributes little to coastal inundation during severe storms. Wave ponding on the reefs, wave setup, and runup cause high inundation levels during storm events.

The EST was applied to calculate stage-frequency relationships based on historical storm parameters and calculated response to the storms. These

relationships were calculated from the maximum water levels computed for each storm, which included storm surge, wave setup, ponding level, and runup. Stage-frequency values and their standard deviations were calculated for 2-, 5-, 10-, 25-, 50-, 75-, and 100-year return periods at 375 profiles.

Example 5: Computation of Storm-Surge Effects for Scour in Estuaries

Introduction

Bridge crossings in tidal waters are subjected to foundation scour resulting from sediment transport and stream instability. Computer hydrodynamic modeling is the most reliable method for predicting the currents at affected bridge piers. These models require storm-surge data and usually an extensive set of simulations in order to generate accurate results. The objective here is to provide a simple method for determining design conditions for surge elevation and flood velocity at a proposed site. This method is specifically directed towards facilitating computations of storm-induced velocities for each potential site in a coastal area. The key features emphasized are the adaptation of a relatively new statistical analysis procedure, EST, to establish better flood-frequency relationships.

Indian River Inlet and the two adjacent bays in Delaware are used for the example estuary in this study. The bays are relatively shallow, and two jetties confine the entrance to the Atlantic Ocean. Within the jetties, significant scour has occurred at the existing bridge causing the placement of stone for bridge pier protection. The tide range at the site is classified as mesotidal. The U.S. Army Corps of Engineers obtained the bathymetric data used in the model.

This procedure is compared with a simple stochastic approach that has been developed by the Corps of Engineers (COE) for estimating frequency-indexed currents impacting bridges. The COE method is used to select what events to simulate and how the results should be analyzed. It was applied to estimate probability-exceedance curves at Brunswick Harbor, Georgia (Cialone, Butler, and Amein 1993).

Data requirements

Three principal models are available to predict storm-surge elevations. FEMA uses the numerical model SURGE to estimate the peak storm-surge elevation, S_{tot} (surge and tide, S_p+H_t), and depth-averaged velocities, based on frequency of occurrence (10-, 50-, 100-, 500-year return period). NOAA uses the numerical model SLOSH to compute the peak storm-surge elevation, S_{tot}, based on hurricane severity (Classes 1 through 5). Neither SLOSH nor SURGE provides hydrographs that are available. The COE surge database (Scheffner

et al. 1994) contains hydrographs for 134 actual hurricanes over 104 years and is, therefore, not linked to a specific design storm or return period.

The process of determining scour velocity involves the acquisition of surge and tide values and tropical-storm parameters in order to determine the storm-surge hydrograph that will be used as input to the hydrodynamic model of the estuary. The most important factor in storm modeling is the intensity of the hurricane, which is directly related to its central pressure P_o. The pressure at a distance r from the storm center can be expressed as :

$$P_r = P_o + (P_r - P_o)e^{-(R/f)} \tag{40}$$

where R is the radius at which the wind speed is greatest (Cialone, Butler, and Amein 1993). Since surge intensity varies with central pressure deficit, the hypothetical time evolution of surge height is given by:

$$S(t) = S_p\,(1-e^{-(D/t)}) + H_t(t) \tag{41}$$

where

$D = R/f$ = storm duration

R = radius of maximum wind

f = forward speed

t = time

H_t = height of tide

S_p = known stage for selected return period

The hydrodynamic storm-surge simulations used for this study were from the finite element model, ADCIRC-2DDI. The ADCIRC model is an advanced hydrodynamic model based upon the generalized wave-continuity equation. It is described in detail in Westerink et al. (1992). Storm-surge computations were made for the 104-year period, 1886 through 1989, and water-surface elevations were recorded at 686 coastal (later referred to as WIS stations) and near-coastal stations (later referred to as ADCIRC stations). The WIS stations were defined by the COE in their hindcast studies for the Gulf of Mexico and the Atlantic Ocean. The 340 Atlantic and Gulf of Mexico WIS stations are located at every 0.25 deg of latitude and longitude along the coastline in water depth averaging between 10 and 20 m. There are 346 ADCIRC stations, located on a shore perpendicular line joining the shoreline to the nearest WIS stations. The WIS and ADCIRC stations are positions for which computed data are stored and do not represent sites where actual field measurements are made. All storm-surge values from the ADCIRC model were simulated without tides and are relative to MSL. Therefore, peak values do not reflect the stage of the tide and the time of historical occurrence, which is why peak values have to be combined with

different tidal phases in order to yield proper results. This database is referenced as the ADCIRC report.

Tropical storm data (R, f) can be obtained from the NOAA technical report NWS-38 (National Weather Service (NWS) 1987). This report compiles a probability distribution of the radius of maximum wind (R) and the forward speed (f), identified with a given percentile of occurrence. Five discrete probability levels are given in NWS-38 to portray R (5, 16.67, 50, 83.3, and 95 percent) and six for f (5, 20, 40, 60, 80, and 95 percent). Research relating R and f to return periods is currently under investigation at the U.S. Army Engineer Research and Development Center. The NOAA report (NWS 1987) also includes actual historical values of R and f for the 85-year period, 1900-1984.

Other site-specific data needed for this analysis include bathymetry, friction and transition loss coefficients, and local winds, which may play an important part in the simulation of storm impacts. Tide data may be obtained either from the current NOAA tide tables or other sources.

Methodology

In this section, a method to determine the velocity-frequency relationship is systematically evaluated. In the following sections, the method is applied to the case of Indian River Inlet in Delaware. The specific data required are also discussed.

Empirical Simulation Technique. The EST method is inspired from a probabilistic bootstrap approach, and it was previously used for computing surge-frequency relationships (Grace 1994). Bootstrap techniques are commonly employed when a sparse data set is used. For example, in the case of Indian River, less than 20 hurricanes have affected the coastline at this site over the entire recorded history (more than 110 years) that is maintained in the National Hurricane Database. Therefore, the existing database does not have the statistical stability or robustness that 110 samples over a 110-year period would provide. The primary goal of the EST is to resample and interpolate a historical database, in order to generate a larger set of data, statistically similar to the historical data. The EST is a statistical procedure designed to develop joint-probability relationships among the various parameters of a multiparameter system. In the EST method, it is first necessary to establish a database of the input and response parameters associated with historical events at the station of interest. In this application, the input parameters chosen are the storm and surge parameters. The response parameters are the results of the simulations, particularly the peak flood and ebb velocities at the nodes of interest. These responses are computed with the hydrodynamic estuary model, using as input either a hydrograph obtained with Equation 41 or the historical hydrographs available from ADCIRC. Then, expansion of the historical data, by slightly perturbing historical events, will produce a training set of storms. This phase should include expected high return-period events.

The EST will then perform N simulations of a T-year sequence. For each simulation the following steps are required (Edge et al. 1998):

a. For each year, the number of storms (s) to occur that year are selected based upon a Poisson distribution (cumulative probability of occurrence), given by:

$$P\ (s,\ \lambda)\ =\ \frac{\lambda^s e^{-\lambda}}{s!} \tag{42}$$

where

s = number of storms per year

λ = number of events/record length in years

$P(s, \lambda)$ = probability of experiencing s storms per year

In the Indian River, the data set used in this example consists of 15 storms over 104 years (λ = 0.144 storms/year); then the probability of 0 hurricanes per year is $P(0)$ = 0.8657, and $P(1)$ = 0.1248 (Poisson). Therefore, if the random number is <0.8657, no storms are simulated this year. If the random number is between 0.8657 and (0.8657+0.1248), one storm is simulated.

b. Randomly select s (s determined above) of the storms from the training set population and then determine input and responses by means of the nearest neighbor interpolation technique (Borgman et al. 1992). This technique is briefly described below.

Let V_j be the selected storm vector (composed of the storm parameters) and U_k (k=1, K, chosen) the K nearest storm vectors (from Euclidean distance, weighing the components according to judged importance), then the new simulated event is:

$$W\ =\ V_j\ +\ \Sigma_{k=1}^{k}\ 2(N_k\ -\ 0.5)\ \cdot\ (U_k\ -\ V_k) \tag{43}$$

where N_k are K independent uniform random numbers on the interval [0, 1.0] generated by the computer. Therefore, $2(N_k - 0.5)$ varies on the segment [-1,1].

c. According to the distance between the new simulated storm W and the storms of the neighborhood (V_j and U_k), the corresponding response variables (surge) of each neighbor are weighed and yield a new simulated surge value for the storm W.

d. The above steps are repeated for the second and subsequent years of the simulation .

The EST procedure ultimately results in N repetitions of T years of simulated event responses. The EST is not simply a resampling of historical events technique, but rather an approach intended to simulate the vector distribution contained in the training set population. In summary, the EST approach is to select a sample storm based on a random number selection between 0 and 1 and then perform a random walk from the selected event to the nearest neighbor vector. The walk is based on independent uniform random numbers on [-1,1] and has the effect of simulating responses that are not identical but similar to the historical events.

The calculation of frequency-of-occurrence relationship for the responses can then be performed. First, an empirical estimate of the cumulative probability distribution function for the response is defined as suggested by Gumbel (1954):

$$P(X \leq X_r) = \frac{r}{(n + 1)} \tag{44}$$

Then, consider that the cumulative probability for an n-year return event is given by:

$$F(n) = 1 - \left(\frac{1}{n}\right) \tag{45}$$

where $F(n)$ is the cumulative probability of occurrence for an event with a recurrence interval of n-years. The frequency-of-occurrence relationships of the response will be obtained by linearly interpolating a response from Equation 44 that corresponds to the probability distribution function associated with a return period specified in Equation 45.

COE procedure. The procedure proposed by the COE is based upon developing a set of storm parameters (radius of maximum winds, R, and forward speed, f), combined with tidal possibilities, in order to approximate the full probable spectrum of conditions that may occur at a site. Cialone, Butler, and Amein (1993) give a complete description of the method. The initial step is to select values for R and f, which represent maximum and minimum storm duration, D, determined by dividing estimates of the maximum and minimum R by the minimum and maximum f, respectively. A more conservative estimate could be made by selecting more extreme values for R and f, but of course it would require more simulations. Four tidal possibilities are also selected: high tide, midfalling tide, low tide, and midrising tide. It is assumed that the time of landfall is completely independent of the tidal position. The peak surge value (S_p) is computed from either sources, NOAA, FEMA, or the COE database. Then, Equation 42 is used to determine the hydrograph shape, and the hydrodynamic model is run for the two durations combined with four tidal positions, which results in eight storm-plus-tide events for each return period. Finally, for each storm-tide combination, the hydrodynamic estuary model is used to compute the velocity at specified locations (nodes) for statistical analysis. The eight peak flood and ebb velocities obtained from the model are

ranked from one to eight, and the cumulative probability, $P(X \leq X_r)$, is then given by the Gumbel distribution in Equation 44.

Application to Indian River

Indian River is located on the south coast of Delaware. Figure 63 is a vicinity map of Indian River Inlet and the adjacent bays. Indian River and Rehoboth Bays share the Indian River Inlet to the sea. The inlet is spanned by State Highway 14. Two piers support the bridge, and the inlet is extended seaward by jetties. The narrowest part of the inlet is approximately 500 ft wide and over 1,200 ft long. Depths in the inlet average 40 ft, but exceed 80 ft locally. Some of the problems and previous studies of Indian River Inlet are discussed in Butler and Lillycrop (1993).

Hydrographic survey data for the inlet and the two bays were obtained in 1988 by the Coastal Engineering Research Center (CERC) and the Philadelphia District of the Corps of Engineers.[1] These data were used to develop the finite element grid for the RMA-2V model. RMA-2V is a two-dimensional, depth-averaged, free surface, finite element model for solving hydrodynamic problems (Thomas and McAnally 1990). There are several one-, two-, and three-dimensional numerical codes that could be used to develop the hydrodynamics in the bay system at Indian River. In fact, several models have been used for evaluating the hydrodynamics of the inlet, including DYNLET, WIFM II, CH3D, and RMA-10. However, for the purpose of this analysis, it was decided that an irregular grid, two-dimensional model would give the best results. The RMA-2V model was selected for use because there was a convenient preprocessor and postprocessor for the model that was available at the time of the study. The finite element mesh, which is shown in Figure 64, consists of 797 quadratic elements and 2,160 nodes. The model was set up using three areas where Manning's n and eddy viscosity could be independently specified. These are the areas offshore of the inlet, the inlet, and the two bays. A 30-hr simulation period (15 hr before and 15 hr after the peak storm surge) was used in all cases, with 30-min time-steps. Figure 64 also shows the nodes in the inlet for which the results are computed.

The COE ADCIRC database was used to obtain storm data for the Indian River site. The closest ADCIRC station from the Indian River was determined as Station 388, just a few kilometers from the ideal input point. A total of 18 storm events were identified from the ADCIRC report that impacted Station 388 for the 104-year period, 1886 through 1989. However, three storms had to be removed from the set because tropical parameters were not available from the NOAA Report NWS 38 for these storms. This report lists parameters for the 85-year period, 1900-84. It was assumed for this study that the historical database is 104 years long. The 15 events are shown in Table 51. For example,

---

[1] Personal Communication, 1994, M. Cialone, U.S. Army Engineer Research and Development Center, Vicksburg, MS.

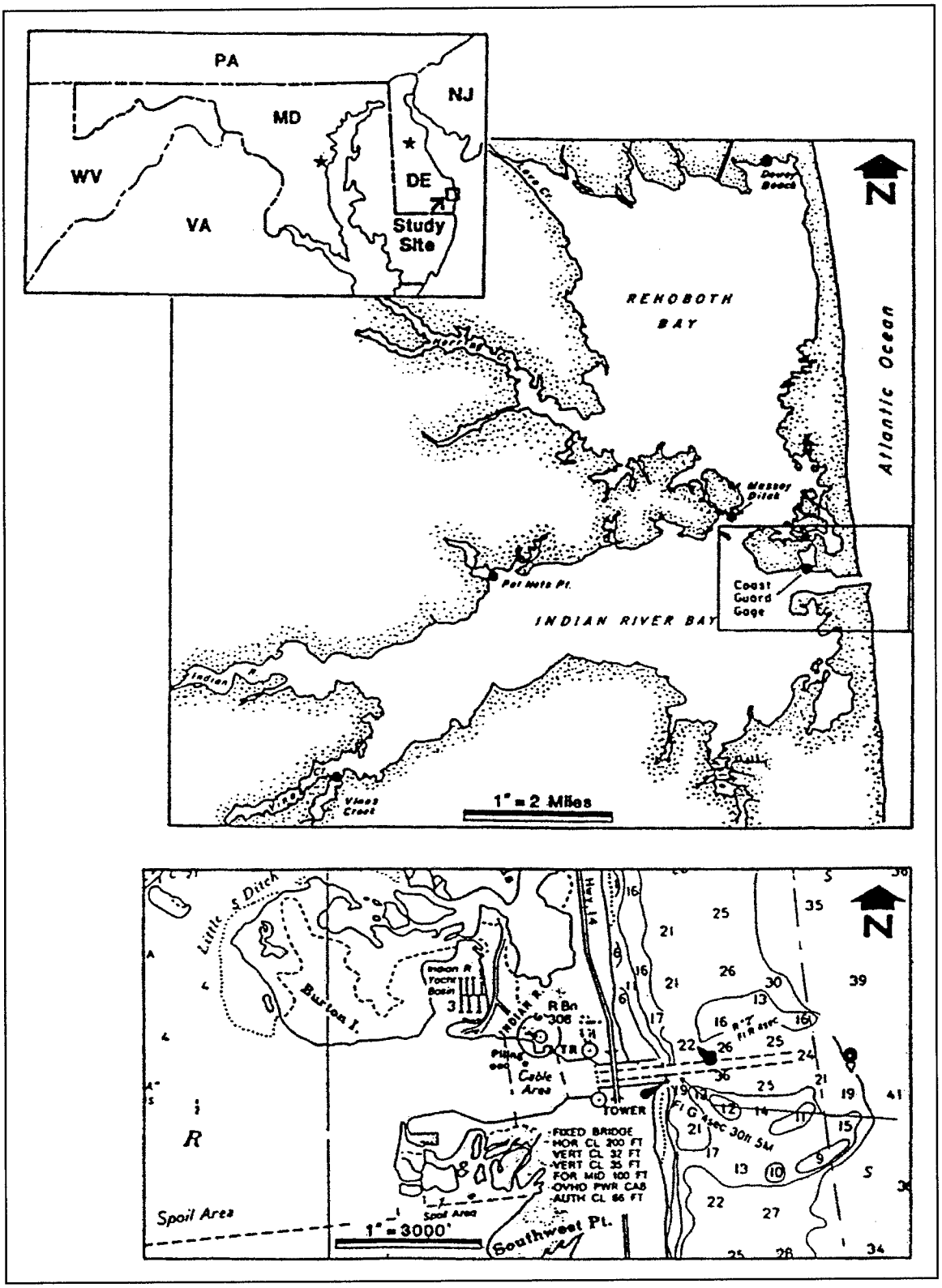

Figure 63. Indian River site map (Edge et al. 1998)

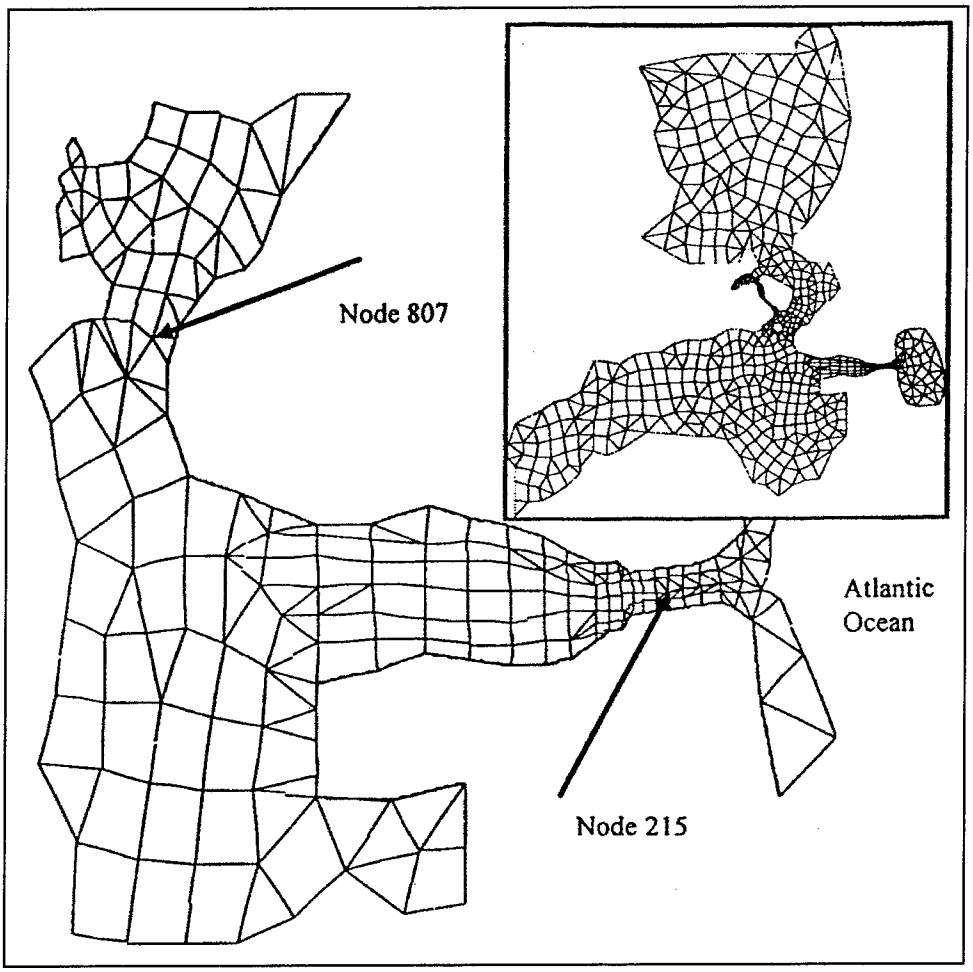

Figure 64. Indian River two-dimensional model finite element mesh (Edge et al. 1998)

Hurricane Camille (Hurdat No. 672), which occurred during August 1969, had a radius of maximum winds of 8 nautical miles, a forward speed of 16 knots, a duration of 0.5 hr (8/16), and a resulting surge of 0.6 m. Surge-frequency data were simply determined with the program ACES (Automated Coastal Engineering System) using the values in Table 51, and they are presented in Table 52.

Data from Tables 51 and 52 were used to develop hydrographs for the EST and COE methods. In this application, however, only the 25-, 50-, 100-, 200-year return period data were investigated.

For the COE and EST simulations, four tidal possibilities were selected: high tide, midfalling tide, low tide, and midrising tide. The NOAA tide tables provided information on the mean tide range at the Indian River as approximately $H_t/2 = 0.58$ m.

Table 51
Tropical Events Impacting Station 388 off the Indian River

Hurdat Storm No.	Given Name	Date (month/day/year)	Surge m	Radius of max. winds *R*, n.m.	Forward Speed *f*, kts	Duration *d* = *R*/*f*, hr
327	Not named	08/17/1933	1.0	39	18	2.2
332	Not named	09/08/1933	1.1	40	9	4.4
353	Not named	08/29/1935	1.3	6	9	0.7
370	Not named	09/08/1936	1.0	34	16	2.1
386	Not named	09/10/1938	0.8	45	47	1.0
436	Not named	09/09/1944	1.7	17	23	0.7
440	Not named	10/12/1944	0.4	29	13	2.2
541	Hazel	10/05/1954	0.5	25	26	1.0
545	Connie	08/03/1955	1.4	38	7	5.4
552	Ione	09/10/1955	0.4	22	9	2.4
597	Donna	08/29/1960	0.4	26	26	1.0
657	Doria	09/08/1967	1.1	20	9	2.2
672	Camille	08/14/1969	0.6	8	16	0.5
712	Agnes	06/14/1972	0.6	20	11	1.8
748	Belle	08/06/1976	0.3	25	21	1.2

Note: From Scheffner et al. (1994) and National Weather Service (1987).

Table 52
Extremal Surge Analysis Using the Weibull Extreme Probability Distribution

Return Period, years	25	50	100	200	300	400	500
Surge, m	1.0	1.3	1.6	1.9	2.0	2.2	2.3

The surge data used in this example are only the peak values determined from the ADCIRC hurricane database. Alternatively, the peak values could have been obtained also from FEMA or NOAA data for the site. Two different sets of hydrographs were developed for the EST method. First, hydrographs were represented by Equation 41, which was a conservative procedure compared with the other two methods. Then, hydrographs were also directly extracted from the ADCIRC database. Among the 15 storms, storm Hurdat numbers 386, 545, and 748 were not present in the data set. A theoretical shape therefore substituted for each of these three storms. Figure 65 shows the difference between the theoretical and the historical hydrographs for the four largest storms at Indian River. The effects of these differences upon the computed velocities are explained later.

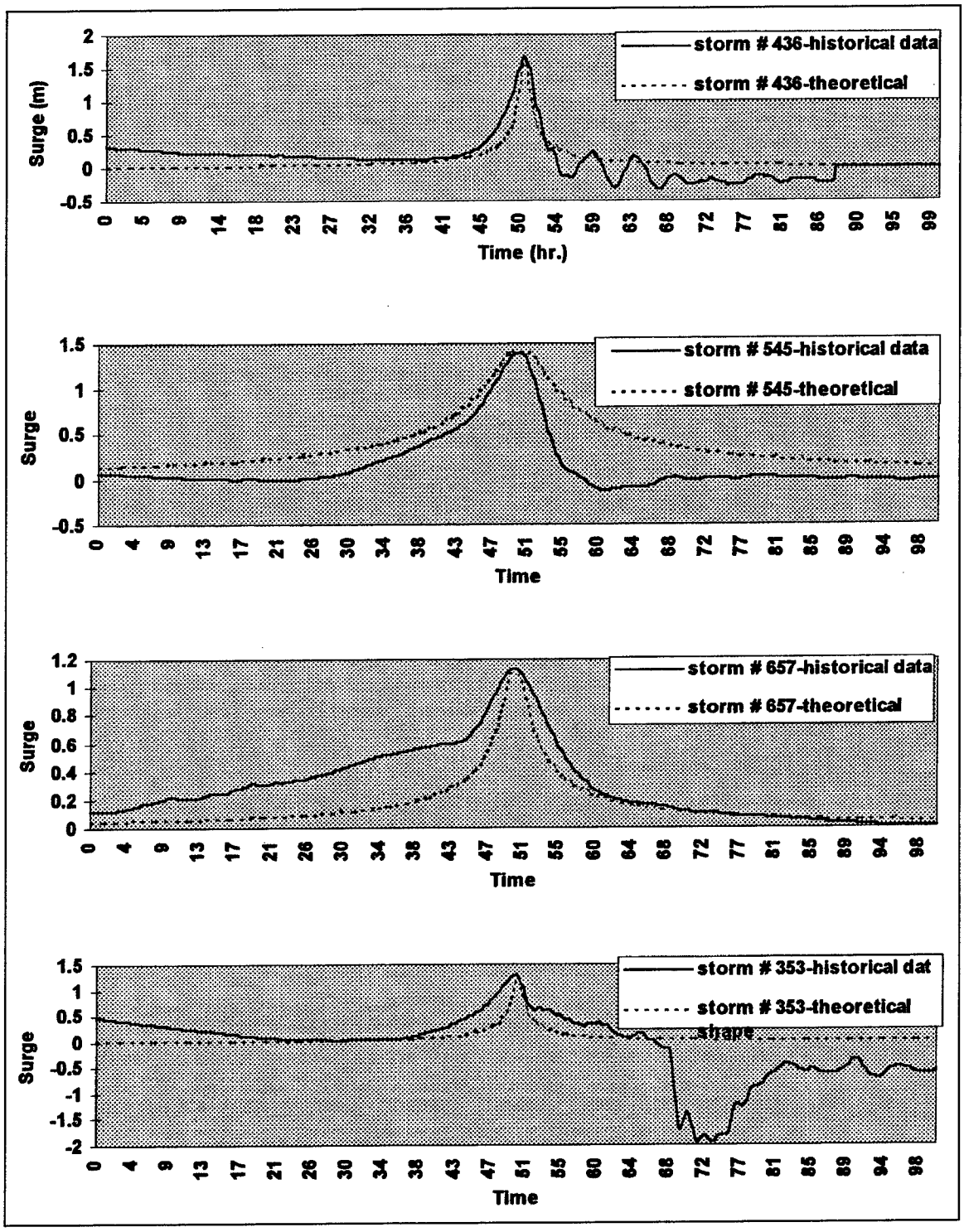

Figure 65. Difference between theoretical and historical hydrograph shape

The EST method required running simulations for all 15 events and four combined tides, hence a total of 60 hydrodynamic simulations. In this application, the input parameters chosen are, for each storm event, the radius of maximum winds R, the forward speed f, the central pressure P_o, the distance between the landfall point and the site considered, the direction of propagation, the peak surge, and the tide phase. The response parameters are peak flood and ebb velocities, the results of the Resource Management Associates (RMA) hydrodynamic simulation.

An example input file to the EST for the first 12 sets of input and response vectors in the Indian River case is given in Table 53 below. In the first event of Storm 327, 1 represents the tidal phase (1, 2, 3, and 4 for high tide, midfalling, low, and midrising tide, respectively), and 158 is the distance in nautical miles between the landfall point and the station (which is at 2,430 n.m. from the Mexican border). In the next column, 1.0 m is the peak surge value at that station; 145° is the angle of propagation in degrees clockwise form North; 966.5 mb is the minimum central pressure; 39 n.m. is the radius of maximum winds; and 18 knots is the forward speed. The response vector is 1.91 m/sec for the peak flood velocity at Node 215.

Table 53
Example EST Input

Storm	Hurdat No.	Tidal Phase	Distance to Landfall, n.m.	Surge Max., m	Direction of Storm, deg	P_o, mb	R, n.m.	f, knots	Peak Flood Velocity, m/sec
1	327	1	158	1.0	145	966.5	39	18	1.91
2	327	2	158	1.0	145	966.5	39	18	1.34
3	327	3	158	1.0	145	966.5	39	18	1.33
4	327	4	158	1.0	145	966.5	39	18	1.78
5	332	1	229	1.1	220	956.7	40	9	1.85
6	332	2	229	1.1	220	956.7	40	9	1.54
7	332	3	229	1.1	220	956.7	40	9	1.46
8	332	4	229	1.1	220	956.7	40	9	1.66
9	353	1	1,005	1.3	130	892.3	6	9	2.35
10	353	2	1,005	1.3	130	892.3	6	9	1.26
11	353	3	1,005	1.3	130	892.3	6	9	1.36
12	353	4	1,005	1.3	130	892.3	6	9	2.25

The statistical procedure consisted of 100 simulations of a 208-year period. This time frame was chosen to limit the extreme value extrapolation to a return period of twice the length of the record (104 *2 = 208). The longer record provides more accurate estimates at all lesser return periods.

The COE method required extreme values for the radius of maximum wind and the forward speed that were also obtained from National Weather Service (1987). The 20 and 80 percentile of occurrence for f and the 16.67 and 83.3 percentile of occurrence for the R were chosen (Figure 66). Note that the data are given in nautical miles measured from the U.S.-Mexico border as provided in the original report. Therefore, two different values of D were computed, D_{max} and D_{min}. Table 54 summarizes the values used in the analysis.

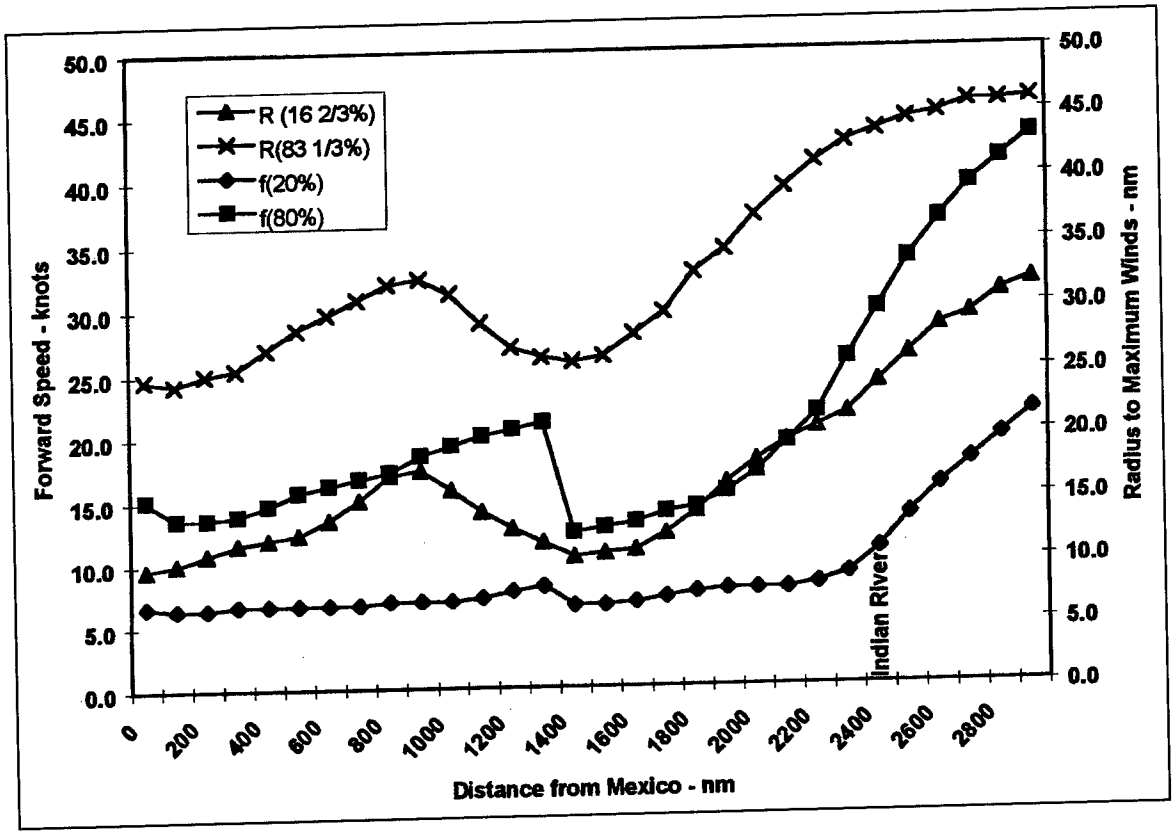

Figure 66. Storm parameters (NOAA NWS 38)

Table 54
Extreme Values for *R* and *f* from National Weather Service (1987)

R (16.67 %) = 23.7 n.m.	R (83.3 %) = 42.9 n.m.
f (20 %) = 10.4 knots	f(80 %) = 30.0 knots
D_{max} = 42.9/10.4 = 4.1 hr	D_{min} = 23.7/30.0 = 0.8 hr

Surge height values were obtained from Table 52. The COE method required (2 durations * 4 tides * 4 stages) = 32 hydrodynamic simulations. Table 55 shows the probability of the percent of surge-plus-tide events with velocities at the node that are equal or less than the values of velocity indicated (for flood and ebb conditions). One interpretation of these results is for a 100-year stage of

Table 55
Peak Flood and Ebb Velocities at Node 215 and Exceedance Probabilities at Four Stages for the COE Method at the Indian River, Delaware

	Stage 1: 1 m. Return period = 25 years			Stage 2: 1.3 m. Return period = 50 years		
Rank	Flood velocity (m/s)	Ebb velocity (m/s)	Cumulative Probability	Flood velocity (m/s)	Ebb velocity (m/s)	Cumulative Probability
1	1.17	-1.41	11 = 1/9 %	1.21	-1.49	11
2	1.25	-1.42	22 = 2/9 %	1.33	-1.49	22
3	1.43	-1.61	33 = 3/9 %	1.50	-1.72	33
4	1.49	-1.63	44 = 4/9 %	1.63	-1.73	44
5	1.63	-1.76	56 = 5/9 %	1.78	-1.92	56
6	1.80	-1.81	67 = 6/9 %	2.02	-1.97	67
7	1.95	-1.82	78 = 7/9%	2.23	-2.05	78
8	2.02	-1.86	89 = 8/9 %	2.32	-2.08	89
	Stage 3: 1.6 m. Return period = 100 years			**Stage 4: 1.9 m. Return period = 200 years**		
Rank	Flood velocity (m/s)	Ebb velocity (m/s)	Cumulative Probability	Flood velocity (m/s)	Ebb velocity (m/s)	Cumulative Probability
1	1.58	-1.55	11	1.65	-1.60	11
2	1.59	-1.58	22	1.91	-1.65	22
3	1.65	-1.83	33	1.91	-1.91	33
4	1.77	-1.83	44	1.92	-1.93	44
5	1.94	-2.06	56	2.08	-2.16	56
6	2.23	-2.07	67	2.42	-2.17	67
7	2.50	-2.26	78	2.74	-2.44	78
8	2.62	-2.30	89	2.87	-2.51	89

1.6 m, the range of velocities expected are from 1.58 to 2.61 m/sec with the expectation that a current exceeding 1.93 m/sec would occur less than 44 (100 minus 56) percent of the time.

Results of all simulations for the observed nodes are plotted on Figure 67 for the flood and ebb velocities. Values from the EST method were averaged from 100 simulations, and the 80-percent confidence interval was computed. The COE method yields mean velocities at the observed nodes with an 80-percent confidence interval. Figure 67 was obtained using theoretical hydrograph shapes for each method.

Figure 68 shows a comparison between the EST procedures for historical and theoretical data. The largest difference is for the flood velocity at Node 215 in the estuary, where results obtained from the theoretical hydrographs are

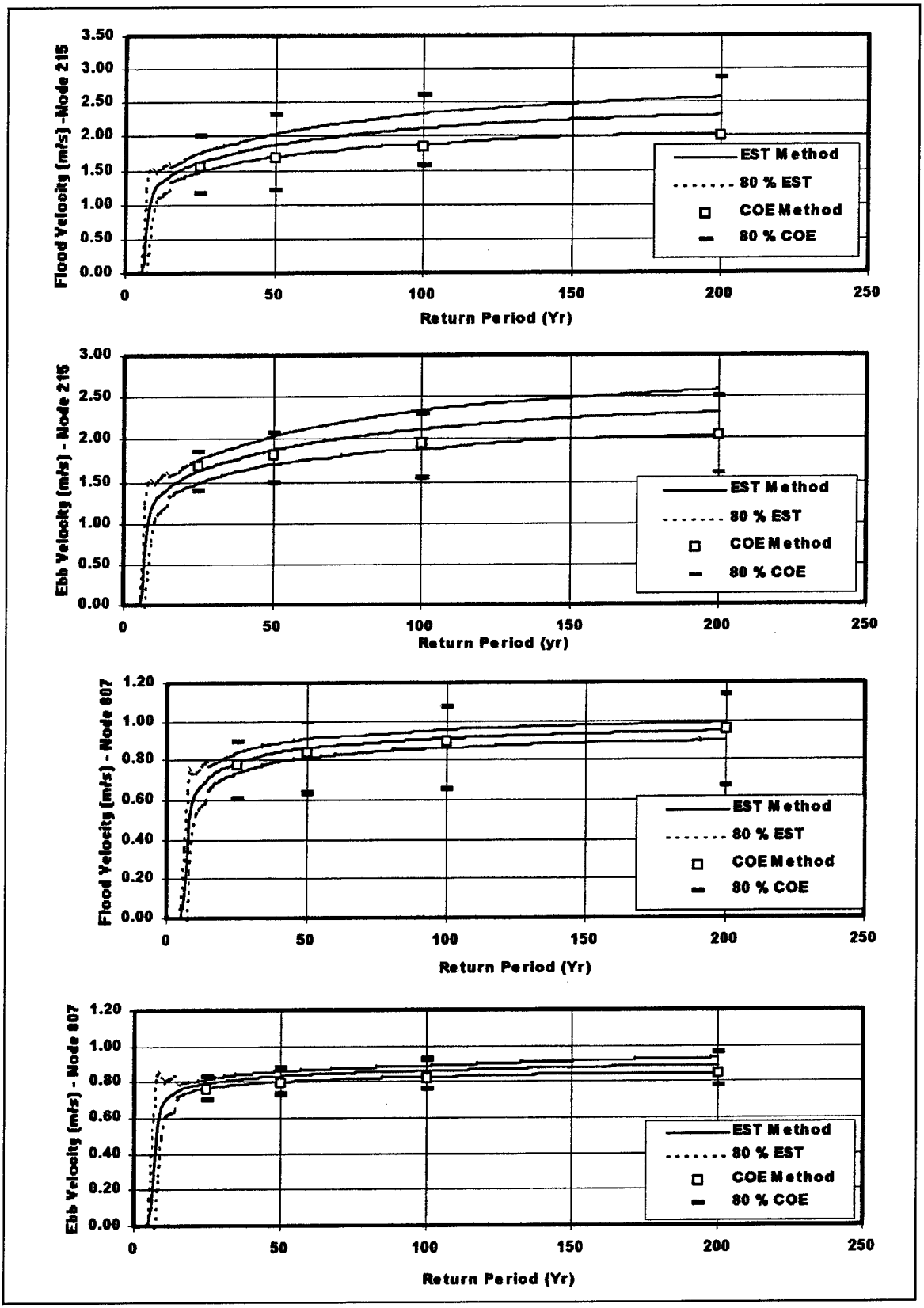

Figure 67. Comparison of velocity versus return period for the EST and the COE methods

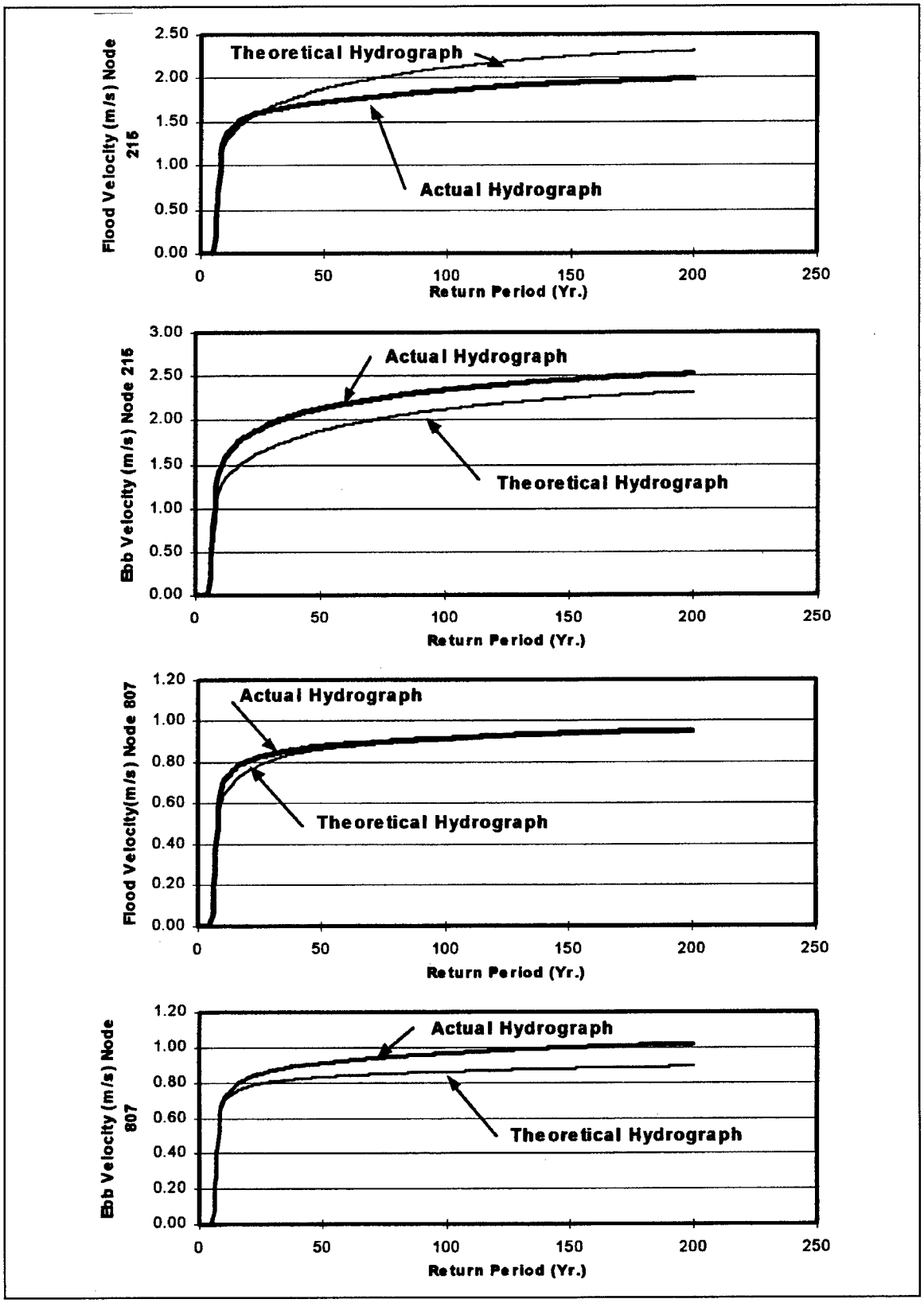

Figure 68. Velocity versus return period - comparison between theoretical and historical hydrograph shape input for the EST

overestimated. In this case, the velocity with a 200-year return period is 17 percent larger. Also, ebb velocities are underestimated in both cases, giving an error close to 10 percent.

There are several factors that could explain these discrepancies. As seen in Figure 65, theoretical hydrographs are symmetrical, whereas the historical data usually are not, particularly after the peak. Most of the time, a negative surge appears after the peak, which tends to increase the negative slope and therefore the resulting ebb velocities. Second, the storm duration (represented by the width of the peak) appears to be in most cases lower in the historical data than in the theoretical data. Therefore, the slope and resulting velocities, especially the flood velocities (positive slope), are lowered. Node 807 inside the bay shows excellent correlation for the flood velocity, probably because of the damping of the system that responds to the main characteristics of the hydrograph only, as this node is far from the boundary conditions.

Summary and conclusion

The EST method is presented to determine the effect of tropical storms on currents in an estuary. The method is applied for the Indian River Inlet-Bay system in Delaware. The empirical simulation technique method is an effective way to accommodate a sparse data set of base data as it recreates and extends the historical database many (100) times. The EST approach also accounts for a random occurrence of the storm surge with the astronomical tide. This method does not require the assumptions generally needed with the joint probability method. By using actual data, including input (storm and tide characteristics) and output (velocities), there are no requirements for developing or guessing joint probability distributions. The COE method also accounts for the random occurrence of the storm surge with the tide, but it yields a very wide confidence interval; it would require many more simulations in order to reduce the confidence interval to that provided by the EST method.

The EST approach is compared with several other methods for determining storm-induced velocities in an estuary in Edge et al. (1998). Edge et al. show that for simpler problems, other approaches may be easier to apply, but that the empirical simulation technique is the most logical and dependable method for most problems. For a major bridge crossing, the additional effort required by the EST method appears to be warranted. For situations in which a larger confidence band can be allowed, the other methods should produce satisfactory results.

6 Summary and Conclusions

This report describes theory and implementation of the EST, a bootstrap-based resampling with replacement and parameter interpolation scheme that generates multiyear life-cycle simulations of storm events and storm impacts. The approach is applicable to any periodic event for which some effect can be attributed. The EST utilizes historical data to develop descriptive input vector storm parameters and response vectors to generate multiple repetitions of multiple years of storm activity generated. Because the approach uses historical or historically based data, each simulation reflects the joint probability inherent in the original database of historic events and does not rely on assumed parametric relationships. Therefore, life-cycle simulations are site specific, do not depend on fixed parametric relationships, and do not assume parameter independence.

This report provides detailed information on how to apply the EST to a frequency study involving tropical and/or extratropical storm-event damages or responses. Five examples are provided to illustrate the versatility of the approach and demonstrate the steps necessary for applying the EST and post-processing the life-cycle simulations to generate frequency relationships. Each example is provided in great detail to describe the actual mechanics of constructing input vector space and the corresponding response or responses. Examples are shown to be either complex requiring mainframe computers or relatively simple requiring existing databases of surge and wave information in conjunction with PC-based response models. In each case study, the models used to generate the responses are described and referenced. Because a variety of applications are covered in the examples, the potential user should be able to modify or extend one to suit a particular application.

The EST is shown in this report to be capable of computing realistic life-cycle simulations such that postprocessing yields accurate frequency-of-occurrence relationships. Because the approach produces multiple simulations, the postprocessing also produces an estimate of error or variability currently defined as ± one standard deviation. This error estimate represents ideal input for developing risk-based design criteria. Additionally, because the EST is a nonparametric approach, it is conceptually superior to other frequency-based simulation procedures such as the JPM. Therefore, the recommendation of this study is that the EST approach should be used for frequency studies because it is

(a) accurate and defendable and (b) provides a necessary error estimate for risk analyses.

References

Ackers, P., and White, R. W. (1973). "Sediment transport: New approach and analysis," *Journal of the Hydraulics Division*, American Society of Civil Engineers, 99(HY11), 2041-2060.

Bijker, E. W. (1967). "Some considerations about scales for coastal models with movable bed," Delft Hydraulics Laboratory, Publication No. 50, Delft.

Borgman, L. E., Miller, M. C., Butler, H. L., and Reinhard, R. D. (1992). "Empirical simulation of future hurricane storm histories as a tool in engineering and economic analysis." *ASCE Proc. Civil Engineering in the Oceans V. College Station, TX. 2-5 November* 1992.

Borgman, L. E., and Scheffner N. W. (1991). "The simulation of time sequences of wave height, period, and direction," Technical Report DRP-91-2, U.S. Army Engineer Waterways Experiment Station, Vicksburg, MS.

Butler, H. L., and Lillycrop, W. J. (1993). "Indian River Inlet: Is there a solution?" *Hydraulic Engineering 93, Proceedings of the 1993 Conference.* American Society of Civil Engineers, Vol. 2, 1218-1223.

Cardone, V. J., Greenwood, C. V., and Greenwood, J. A. (1992). "Unified program for the specification of hurricane boundary layer winds over surfaces of specified roughness," Contract Report CERC-92-1, U.S. Army Engineer Waterways Experiment Station, Vicksburg, MS.

Cialone, M., Butler, H. L., and Amein, M. (1993). "DYNLET1 Application to Federal Highway Administration Projects," Miscellaneous Paper CERC-93-6, U.S. Army Engineer Waterways Experiment Station, Vicksburg.

Clausner, J. E., Scheffner, N. W., and Allison, M. C. (1995). "Assessment of remaining capacity of the Mud Dump site," Letter Report for New York District, U.S. Army Engineer Waterways Experiment Station, Vicksburg, MS.

Edge, B. L., Scheffner, N. W., Fisher, J. S., and Vignet, S. N. (1998). "Determination of velocity in an estuary for bridge scour computations," *Journal of the Hydraulics Division, ASCE* 124(6).

Friedman, J. H. (1991). "Multivariate adaptive regression splines," *Annals of Statistics* 19(1), 1-141.

Grace, P. J. (1994). "Application of an Empirical Simulation Technique to Lake Okeechobee storm surges," Master of Engineering Project, Texas A&M University.

Gravens, M. B. (1992). "User's guide to the shoreline modeling system (SMS)," Instruction Report CERC-92-1, U.S. Army Engineer Waterways Experiment Station, Vicksburg, MS.

Gravens, M. B., Kraus, N. C., and Hanson, H. (1991). "GENESIS: Generalized model for simulating shoreline change; Report 2, Workbook and system user's manual," Technical Report CERC-89-18, U.S. Army Engineer Waterways Experiment Station, Vicksburg, MS.

Gumbel, E. J. (1954). "Statistical theory of extreme value and some practical application," National Bureau of Standards Applied Math. Series 33, U.S. Gov. Publ. Washington, DC.

Harris, D. L. (1963). "Characteristics of the hurricane storm surge," U.S. Dept. of Commerce, Weather Bureau, Technical Paper No. 48, Washington DC.

Hench, J. L., Luettich, R. A., Westerink, J. J., and Scheffner, N. W. (1994). "ADCIRC: An advanced three-dimensional circulation model for shelves, coasts and estuaries; Report 6, Development of a tidal constituent database for the eastern North Pacific," Technical Report DRP-92-6, U.S. Army Engineer Waterways Experiment Station, Vicksburg, MS.

Hubertz, J. M., Brooks, R. M., Brandon, W. A., and Tracy, B. A. (1993). "Hindcast wave information for the U.S. Atlantic Coast," WIS Report 30, Coastal Engineering Research Center, U.S. Army Engineer Waterways Experiment Station, Vicksburg, MS.

Jarvinen, B., and Gebert, J. (1986). "Comparison of observed versus slosh model computed storm surge hydrographs along the Delaware and New Jersey shorelines for Hurricane Gloria, September 1985," NOAA Technical Memorandum NWS NHC 32.

Jarvinen, B. R., Neumann, C. J., and Davis, M. A. S. (1988). "A tropical cyclone data tape for the North Atlantic Basin, 1886-1983: Contents, limitations, and uses," (Second Printing) NOAA Technical Memorandum NWS NHC 22.

Jensen, R. E. (1983). "Methodology for the calculation of a shallow-water wave climate," WIS Report 8, U.S. Army Engineer Waterways Experiment Station, Vicksburg, MS.

Larson, M., and Kraus, N. C. (1989.) "SBEACH: Numerical model for simulating storm-induced beach change; Report 1, Empirical foundation and model development," Technical Report CERC-89-9, U.S. Army Engineer Waterways Experiment Station, Vicksburg, MS.

Larson, M., Kraus, N. C., and Byrnes, M. R. (1990). "SBEACH: Numerical model for simulating storm-induced beach change; Report 2, Numerical formulation and model tests," Technical Report CERC-89-9, U.S. Army Engineer Waterways Experiment Station, Vicksburg, MS.

LeProvost, C. Genco, M. L., Lyard, F., Vincent, P., and Cenceill, P. (1994). "Spectroscopy of the world ocean tides from a hydrodynamic finite element model," *Journal of Geophysical Research* 99(C12), 24, 777-24, 797.

Luettich, R. A., Westerink, J. J., and Scheffner, N. W. (1992). "ADCIRC: An advanced three-dimensional circulation model for shelves, coasts and estuaries; Report 1: Theory and methodology of ADCIRC-2DDI and ADCIRC-3DL," Technical Report DRP-92-6, U.S. Army Engineer Waterways Experiment Station, Vicksburg, MS.

McDowell, S. (1993). "Comparison of baseline bathymetric suveys: New York Mud Dump site," Report by Science Applications International Corporation, submitted to U.S. Army Engineer District, New York, New York.

McDowell, S., May, B., and Pabst, D. (1994). "The December 1992 storm at the New York Mud Dump site," *Proceedings of Dredging '94*, ASCE, New York.

Militello, A., and Scheffner, N. W. (1998). "Hurricane-induced stage-frequency relationships for the territory of American Samoa," Technical Report CHL-98-33, U.S. Army Engineer Waterways Experiment Station, Vicksburg, MS.

National Weather Service. (1987). "Hurricane climatology for the Atlantic and Gulf Coasts of the United States," NOAA Technical Report NWS 38.

Park, J.-G., Borgman, L. E., and Anderson-Sprecher, R. (1996). "Studies for the extended bootstrap/empirical simulation in one-, two-, and three-dimensions," Report prepared for the U.S. Army Engineer Waterways Experiment Station Coastal Engineering Research Center by L. E. Borgman, Inc., Laramie, WY.

Ravindra. Ph.D. thesis in preparation, University of Wyoming, Laramie, WY.

Resio, D. T., and Perrie, W. (1989). "Implications of an f^{-4} equilibrium range for wind-generated waves," *Journal of Physical Oceanography* 19, 193-204.

Saville, T., Jr. (1958). "Wave runup on composite slopes." *Proceedings of the sixth conference on coastal engineering*. American Society of Civil Engineers, Council on Waves.

Scheffner, N. W., and Borgman, L. E. (1992). "A stochastic time series representation of wave data," *ASCE Journal of Waterways, Ports, Coastal and Ocean Engineering* 118(4).

Scheffner, N. W., Mark, D. J., Blain, C. A., Westerink, J. J., and Luettich, R. A. (1994). "ADCIRC: An advanced three-dimensional circulation model for shelves, coasts and estuaries; Report 5, A tropical storm data base for the east and Gulf of Mexico coasts of the United States," Technical Report DRP-92-6, U.S. Army Engineer Waterways Experiment Station, Vicksburg, MS.

Scott, D. (1992). *Multivariate density estimation*. John Wiley and Sons, Inc., New York.

Sea Engineering, Inc., and Belt Collins Hawaii. (1994). "American Samoa shoreline inventory Update II," Prepared for U.S. Army Engineer Division, Pacific Ocean, Fort Shafter, HI.

Seelig, W. N. (1983). "Laboratory study of reef-lagoon system hydraulics," *Journal of Waterway, Port, Coastal and Ocean Engineering* 109(4), 380-391.

Shore Protection Manual. (1984). 4th ed., 2 Vol., U.S. Army Engineer Waterways Experiment Station, U.S. Government Printing Office, Washington, DC.

Sommerfeld, B. G., Mason, J. M., Larson, M., and Kraus, N. C. (1993). "Beach Morphology Analysis Package (BMAP)." *Beach nourishment engineering and management considerations*. D. K. Stauble and N. C. Kraus, ed., *Proceedings Coastal Zone '93*, American Society of Civil Engineers, Reston, VA, 162-175.

Taylor, J. R. (1989). *Empirical model building*. John Wiley & Sons, Inc., New York.

Thomas, W. A., and McAnally, W. H., Jr. (1990). "User's manual for the generalized computer program system: Open-channel flow and sedimentation, TABS-2," U.S. Army Engineer Waterways Experiment Station, Vicksburg, MS.

U.S. Army Corps of Engineers. (1994). "Risk based analysis for evaluation of hydrology/hydraulics and economics in flood damage reduction studies," EC 1105-2-205, Washington, DC.

U.S. Environmental Protection Agency/U.S. Army Corps of Engineers (USACE). (1991). "Evaluation of dredged material proposed for ocean disposal (testing manual)," EPA-503/8-91/001, Office of Water, U.S. Environmental Protection Agency, Washington, DC.

Westerink, J. J., Luettich, R. A., Jr., Baptista, A. M., Scheffner, N. W., and Farrar, P. (1992). "Tide and storm surge predictions using finite-element model," *Journal of Hydraulic Engineering*, American Society of Civil Engineers, Vol. 118(10), 1373-1390.

Westerink, J. J., Luettich, R. A., and Scheffner, N. W. (1993). "ADCIRC: An advanced three-dimensional circulation model for shelves, coasts and estuaries; Report 3, Development of a tidal constituent data base for the western North Atlantic and Gulf of Mexico," Technical Report DRP-92-6, U.S. Army Engineer Waterways Experiment Station, Vicksburg, MS.

REPORT DOCUMENTATION PAGE

Form Approved
OMB No. 0704-0188

1. AGENCY USE ONLY *(Leave blank)*	2. REPORT DATE	3. REPORT TYPE AND DATES COVERED
	December 1999	Final report

4. TITLE AND SUBTITLE
Use and Application of the Empirical Simulation Technique: User's Guide

5. FUNDING NUMBERS

6. AUTHOR(S)
Norman W. Scheffner, Leon E. Borgman, James E. Clausner, Billy L. Edge, Peter J. Grace, Adele Militello

7. PERFORMING ORGANIZATION NAME(S) AND ADDRESS(ES)
U.S. Army Engineer Research and Development Center, Coastal and Hydraulics Laboratory, 3909 Halls Ferry Road, Vicksburg, MS 39180-6199; University of Wyoming, Laramie, WY 32070; Texas A&M University, College Station, TX 77843-3136; U. S. Army Engineer District, Jacksonville, P.O. Box 4970, Jacksonville, FL 32202-0019

8. PERFORMING ORGANIZATION REPORT NUMBER
Technical Report CHL-99-21

9. SPONSORING/MONITORING AGENCY NAME(S) AND ADDRESS(ES)
U.S. Army Corps of Engineers
Washington, DC 20314-1000

10. SPONSORING/MONITORING AGENCY REPORT NUMBER

11. SUPPLEMENTARY NOTES

12a. DISTRIBUTION/AVAILABILITY STATEMENT
Approved for public release; distribution is unlimited.

12b. DISTRIBUTION CODE

13. ABSTRACT ***(Maximum 200 words)***

This report describes theory and implementation of the Empirical Simulation Technique (EST) procedure for simulating multiple life-cycle sequences of nondeterministic multiparameter systems such as storm events and their corresponding environmental impacts. The EST is based on a "Bootstrap" resampling-with-replacement, interpolation, and subsequent smoothing technique in which random sampling of a finite length database is used to generate a larger database. Parameters describing this expanded database result in the generation of life-cycle simulations of storm-event activity with corresponding impacts. Because the approach is universally valid for effects because of any periodic event forcing, five detailed examples are provided to describe application of the EST for various storm-related impacts. These include vertical erosion of subaqueous disposal mounds, dune and beach recession, maximum storm-surge elevation, combined storm surge and runup on beaches, and maximum velocities associated with bridge pier scour. Each example provides detailed descriptions of the construction of input and response vector space and provides a summary of EST application and study results.

14. SUBJECT TERMS
Empirical Simulation Technique
Frequency analysis
Frequency-of-occurrence
Life-cycle simulation
Stochastic modeling

15. NUMBER OF PAGES
189

16. PRICE CODE

17. SECURITY CLASSIFICATION OF REPORT	18. SECURITY CLASSIFICATION OF THIS PAGE	19. SECURITY CLASSIFICATION OF ABSTRACT	20. LIMITATION OF ABSTRACT
UNCLASSIFIED	UNCLASSIFIED		